Targeting HIV-1 RNA with ribozymes and small interfering RNAs for therapeutic applications

Robert Scarborough

Department of Microbiology and Immunology

McGill University, Montréal, Québec, Canada

August 2015

A thesis submitted to McGill University in partial fulfilment of the requirements of the degree of doctor of philosophy

ABSTRACT

Human immunodeficiency virus (HIV) infection can now be treated with combination therapy to prevent the development of acquired immune deficiency syndrome. However, current therapies cannot clear an infection and different approaches are now being considered to cure HIV. Combination antiviral gene therapy has the potential to be used in cell transplant to provide long-term control of HIV replication in the absence of medication and small RNA therapies are among the top candidates for this approach. HIV RNA is an attractive target for RNA therapies that act through an antisense-based mechanism, such as ribozymes and small interfering RNAs (siRNAs). Although several potential therapeutic RNAs have been described, the characteristics that make both a safe and efficacious design are still being elucidated.

This thesis examines the potential for two classes of RNA molecules to be used in HIV therapy. Novel methods were developed to identify target sites in HIV RNA for modified hepatitis delta virus ribozymes (HDV-Rzs) and a highly conserved site was identified that was accessible to both an HDV-Rz hand an siRNA. Variations in siRNA length were also examined to optimize the format of an siRNA targeting this site for further development as both a drug and gene therapeutic for HIV. Due to the sequence and structural diversity of HIV RNA, antisense target sites that are both accessible and conserved across different strains are rare. This work describes a novel target site with great potential for the development of antisense-based RNA therapies. The results presented also contribute to our understanding of RNA-based therapy design and development for HIV-1 infection or other human afflictions.

RESUMÉ

L'infection par le virus de l'immunodéficience humain (VIH) peut actuellement être traitée par les thérapies combinées pour prévenir le développement du syndrome d'immunodéficience acquise. Cependant, de telles thérapies ne peuvent éliminer l'infection par le VIH, et de nouvelles approches sont envisagées pour atteindre l'objectif de guérison. La thérapie génique antivirale combinée, a le potentiel d'être utilisée en transplantation cellulaire pour controler durablement la réplication du VIH en absence de médication; les petits ARNs sont des candidats idéaux pour cette approche thérapeutique. L'ARN du VIH est une cible idéale pour les thérapies basées sur l'ARN antisens, telles que les ribozymes (Rz) et les petits ARN interférants (siARN). Plusieurs ARN ont été identifiés comme étant des candidats pour la thérapie génique, mais les critères de conception nécessaires à un produit final sécuritaire et efficace restent inconnus.

Cette thèse examine le potentiel de deux classes de molécules d'ARN d'être utilisées en thérapie contre le VIH. Nous avons développé de nouvelles méthodes pour identifier les sites au sein de l'ARN du VIH à cibler avec des Rz dérivés du Rz du virus de l'hépatite delta (HDV-Rz) et nous avons identifié un site extrêmement conservé et accessible à un HDV-Rz et un siARN. Nous avons conçu des expériences qui permettront d'optimiser le format d'un siARN ciblant le site que nous avons identifié, afin de poursuivre son développement comme médicament et comme thérapie génique contre le VIH. La diversité de séquence et de structure de l'ARN du VIH font en sorte que les sites cibles des molécules agissant par antisens ne sont que rarement accessibles et conservées parmi plusieurs souches de virus. Notre travail décrit un nouveau site cible ayant

un grand potentiel pour le développement de thérapies basées sur l'ARN antisens. Les résultats présentés contribuent aussi à notre compréhension de la conception des thérapies basées sur l'ARN antisens en fournissant de précieuses informations sur le développement des Rz et des siARN optimisés pour traiter l'infection par le VIH ainsi que d'autres maladies infectieuses chez l'humain.

ACKNOWLEDGEMENTS

First and foremost I would like to thank my supervisor, Dr. Anne Gatignol, for her guidance and support in the execution of the work presented in this thesis. Anne tirelessly reviewed and re-reviewed all of the material presented here and has given me the opportunity to develop my scientific planning skills through countless hours of discussion and assistance. From her expertise in HIV and RNA biology, she has helped guide me in attaining a strong knowledge base in these fields, and given me extensive instruction on the preparation of manuscripts, presentations, patents and grant proposals. Anne's dedication to the study of HIV biology and treatment has been an inspiration to me from the beginnings of my time as a Master student in her lab, through to the completion of my PhD. I will be forever grateful to her for accepting me into her lab and supporting me through my time in graduate studies.

I would also like to thank all of the past and present members of Dr. Gatignol's laboratory who I have had the pleasure to work with. First, I would like to thank Dr. Sébastien Lainé, who initiated the project that became the topic for my PhD thesis. Second, I would like to thank Aïcha Daher for training me in the various techniques required to execute the experiments described in this thesis and for always coming up with the best approaches to troubleshoot problems encountered with experimental designs. Aïcha has been a great mentor and has become a wonderful friend. I would also like to recognize the contributions of Carlos Melendez-Pena, Jean-Francois Gelinas, Guerline Clerzius, Lucile Sinck, Eileen Shaw and Samantha Burugu for their support during different times in my graduate studies, as well as my productive

undergraduate summer student Etienne Boudrias-Dalle and par excellence honors student Kelsey Adams, for their assistance in producing some of the data presented in this thesis. Last, but certainly not least, I would like to thank Dr. Sylvanne Daniels for providing guidance and support throughout a large portion of my graduate studies, for our coffee breaks and after work fiascos, and for her ever prominent smile and cheerful persona.

I would also like to thank Dr. Jean-Pierre (JP) Perreault for his guidance and support as an advisor and major collaborator on the work presented in this thesis. JP welcomed me into his lab for training, connected me with his students and was an integral partner in the development of my project. I would also like to acknowledge all of the members from JPs lab who assisted in the design and execution of experiments, including Julie Motard, Dominique Lévesque and especially Michel Lévesque. Michel and I exchanged countless emails and collaborated on several experiments. Without his help and expertise, none of this could have been possible. Acknowledgement are also due to Ian Chute from Dr. Rodney Ouellette's laboratory, who collaborated with Michel and I on the design and execution of micro-array experiments presented in this thesis. I would also like to thank my other thesis advisory committee members, Drs Shan-Lu Liu and Andrew Mouland for their helpful suggestions and support in guiding me through my PhD project.

Finally, I would like to acknowledge the support provided by all of my friends and family, in particular the Scarborough family (Jayne, Bob, Cindy and Shawn) the Switzer-Tiihonen family (Robyn, Susan, Silas, and Elias), Erin Balaban, Sarah Moses and Vincent Fleifel.

PREFACE

This thesis follows the "Manuscript-based thesis" format in accordance with McGill University's "Guidelines for preparation of a thesis". The work presented in this thesis represents a significant contribution to knowledge and is the result of independent scholarship. Parts of this thesis have been published in scientific journals and references to these publications as well as the contribution of authors are described in the preface of each applicable chapter.

Results from Chapters 2, 3 and 4 were included in a provisional US patent application (Ref: 61/869,852, filed August 26, 2013) and a full international patent cooperation treaty (PCT) application (Ref: 782/11168.396, filed on August 25, 2014). The application was published on March 5, 2015 as follows:

Publication number: **WO2015027334 A1**
Publication type: Application
Application number: PCT/CA2014/050814
Inventors: Anne GATIGNOL, **Robert Scarborough**
Applicant: The Royal Institution For The Advancement Of Learning / McGill University

Manuscripts not included in this thesis, for which the candidate made significant contributions before or during the course of his thesis work, include:

Daniels SM, Sinck L, Ward NJ, Melendez-Pena CE, **Scarborough RJ**, Azar I, Rance E, Daher A, Pang KM, Rossi JJ, and Gatignol A. 2015. ***HIV-1 RRE RNA acts as an RNA silencing suppressor by competing with TRBP-bound siRNAs.*** RNA Biol 12(2):123-35.

Lainé S, **Scarborough RJ**, Lévesque D, Didierlaurent L, Soye KJ, Mougel M, Perreault JP, and Gatignol A. 2011. ***In vitro and in vivo cleavage of HIV-1 RNA by new SOFA-HDV ribozymes and their potential to inhibit viral replication.*** RNA Biol 8 (2):343-53.

MacFarland R, Hard ML, **Scarborough R**, Badel K, and Calandra G. 2010. ***A pharmacokinetic study of plerixafor in subjects with varying degrees of renal impairment.*** Biol Blood Marrow Transplant 16 (1):95-101.

Bodart V, Anastassov V, Darkes MC, Idzan SR, Labrecque J, Lau G, Mosi RM, Neff KS, Nelson KL, Ruzek MC, Patel K, Santucci Z, **Scarborough R**, Wong RS, Bridger GJ, Macfarland RT, and Fricker SP. 2009. ***Pharmacology of AMD3465: a small molecule antagonist of the chemokine receptor CXCR4.*** Biochem Pharmacol 78 (8):993-1000.

Daniels SM, Melendez-Pena CE, **Scarborough RJ**, Daher A, Christensen HS, El Far M, Purcell DF, Laine S, and Gatignol A. 2009. ***Characterization of the TRBP domain required for dicer interaction and function in RNA interference.*** BMC Mol Biol 10:38.

Nyunt MM, Becker S, MacFarland RT, Chee P, **Scarborough R**, Everts S, Calandra GB, and Hendrix CW. 2008. ***Pharmacokinetic effect of AMD070, an Oral CXCR4 antagonist, on CYP3A4 and CYP2D6 substrates midazolam and dextromethorphan in healthy volunteers.*** J Acquir Immune Defic Syndr 47 (5):559-65.

TABLE OF CONTENTS

LIST OF FIGURES AND TABLES

LIST OF ABBREVIATIONS

ADAR1	Adenosine deaminase acting on RNA 1
Ago	Argonaute
AIDS	Acquired immune deficiency syndrome
APOBEC	Apolipoprotein B mRNA editing complex
ARV	Antiretroviral
AZT	Azidothymidine
bRN-P	Bacterial RNase P
BST	Bone marrow stromal cell antigen
CA	Capsid
cART	Combination antiretroviral therapy
CD	Cluster of differentiation
CDC	Centers for Disease Control
CDK9	Cyclin dependent kinase 9
cDNA	Complementary DNA
CMV	Cytomegalovirus
CRF	Circulating recombinant form
DIS	Dimerization initiation signal
DSE	Distal sequence elements
dNTP	Deoxy-nucleotide tri-phosphate
dsiRNA	Dicer substrate small interfering RNA
dsRNA	Double-stranded RNA
EGS	External guide sequence
eIF	Eukaryotic initiation factor
Env	Envelope
ESCRT	Endosomal sorting complexes required for transport
FDA	Food and drug administration
GALT	Gut associated lymphatic tissue

Gp	Glycoprotein
HDAC	Histone deacetylase
HDV	Hepatitis delta virus
HH	Hammerhead
HIV	Human immunodeficiency virus
Hp	Hairpin
HR	Heptad repeat
hRN-P	Human RNase P
HSC	Hematopoietic stem cell
IL	Interleukin
IN	Integrase
INsTI	Integrase strand transfer inhibitor
IRES	Internal ribosome entry site
LEDGF	Lens epithelium-derived growth factor
LTR	Long terminal repeat
MA	Matrix
MHC	Major histocompatibility complex
miRNA	MicroRNA
MMLV	Moloney murine leukemia virus
MSCV	Mouse stem cell virus
NC	Nucleocapsid
Nef	Negative factor
NNRTI	Non-nucleoside reverse transcriptase inhibitor
NRTI	Nucleoside reverse transcriptase inhibitor
NtRTI	Nucleotide RT inhibitor
ORF	Open reading frame
PACT	PKR activator
PI	Protease inhbitor
PIC	Pre-integration complex
PKR	RNA activated protein kinase

Pol	Polymerase
PPT	Polypurine tract
PR	Protease
Pre-miRNA	Precursor micro RNA
Pri-miRNA	Primary micro RNA
PSE	Proximal sequence elements
pTEF	Positive transcription elongation factor
R	Repeat
R5	HIV-1 strains that use the CCR5 co-receptor for entry
RISC	RNA-induced silencing complex
RNA enzyme	RNase
RNAi	RNA interference
RNase	Ribonuclease
RRE	Rev response element
RT	Reverse transcriptase
Rz	Ribozyme
shRNA	Short hairpin RNA
siRNA	Small interfering RNA
SIV	Simian immunodeficiency virus
SLII	Stem loop II
snoRNA	Small nucleolar RNA
snRNA	Small nuclear RNA
SOFA	Specific on off adaptor
SU	Surface unit
SV40	Simian virus 40
TAR	Transactivation response RNA
TDF	Tenofovir disoprovil fumarate
Tk	Thymidine kinase
TM	Transmembrane
TRBP	TAR RNA binding protein

tRNA	Transfer RNA
UTR	Untranslated region
VA	Virus associated
Vif	Viral infectivity factor
Vpr	Viral protein r
Vpu	Viral protein u
X4	HIV-1 strains that use the CXCR4 co-receptor for entry
ZFN	Zinc finger nucleases

Chapter 1

INTRODUCTION

1.1 Preface

This chapter provides a literature review of three topics relevant to the research presented in this thesis. Section **1.2** reviews the discovery, origins and replication cycle of human immunodeficiency virus (HIV) as well as its pathogenic mechanisms that result in acquired immune deficiency syndrome (AIDS). Current and experimental therapies for HIV-1 infection are described in section **1.3** and the development of small RNAs for HIV-1 therapy is described in section **1.4**. All of the material presented in this chapter is a result of independent scholarship. Parts of section **1.4.1**, describing the development of ribozyme therapies for HIV infection, have been published in the following book chapter:

Scarborough RJ and Gatignol A. (2015). "HIV and Ribozymes."
Adv Exp Med Biol. 848:97-116.
In: Gene Therapy for HIV and Chronic Infections.
Editors: Berkhout B, Ertl MD, Hildegund CJ and Weinberg MS.

1.2 HIV/AIDS

Human immunodeficiency virus (HIV) is a member of the genus *Lentivirus* within the *Retroviridae* family of retroviruses. Similar to other retroviruses, HIV has an RNA genome that replicates via a proviral DNA intermediate, integrated into the chromosomes of its host cell. According to the UNAIDS 2013 report on the global AIDS epidemic (http://www.unaids.org), an estimated 32.2 to 38.8 million people were living with HIV and 1.9 to 2.7 million new infections occurred in 2012. In most cases, infection with HIV results in an asymptomatic phase lasting several years, followed by the development of a fatal acquired immune deficiency syndrome (AIDS). This section summarizes the discovery, origins and distribution of HIV species and subtypes (section **1.2.1**) and provides an overview of the HIV-1 replication cycle (section **1.2.2**) and its pathogenesis (section **1.2.3**).

1.2.1 HIV discovery, origins and distribution

In September 1982, the United States Centers for Disease Control (CDC) recommended the name AIDS [1] to describe a set of common symptoms first documented in the summer of 1981 [2]. Early in 1983, evidence that the disease was caused by an infectious agent that could be transmitted through sexual contact, from mother to child and through blood products was available [3, 4]. In May of 1983, Barré-Sinoussi et al. reported a new retrovirus isolated from patients with symptoms and risk factors indicative of infection with this agent and called it lymphadenopathy associated virus [5]. In 1984, the groups of Gallo [6, 7] and Levy [8] provided further evidence that this new retrovirus was the cause of AIDS, calling it human T-lymphotropic retrovirus III, and AIDS-associated retrovirus, respectively. A consensus on the

name HIV for this new retrovirus was established in 1986 [9]. Also in 1986, a similar but antigenically distinct virus was discovered in two AIDS patients in Western Africa [10]. This virus was later classified as HIV-2, while the originally identified species is classified as HIV-1 [11].

HIV-1 and HIV-2 entered the human population by zoonotic transmission(s) from closely related simian immunodeficiency viruses (SIVs) that infect other primates. HIV-1 is closely related to SIVs that infect chimpanzees (SIVcpz) and gorillas (SIVgor) [11], while HIV-2 is related to SIVs that infect sooty mangabeys (SIVsmm) [12] and laboratory macaques (SIVmac) [13-15]. A schematic of HIV evolution is illustrated in Figure 1.1, based on phylogenetic relationships between HIVs and SIVs [11]. While both HIV-1 and HIV-2 can cause AIDS, infection with HIV-2 results in a longer asymptomatic phase and has a lower transmission frequency compared to HIV-1, in part because of lower plasma virus levels in infected individuals [16]. While HIV-2 represents a significant part of the HIV/AIDS epidemic, the work presented in this thesis focuses on HIV-1, the most prevalent and widely distributed species.

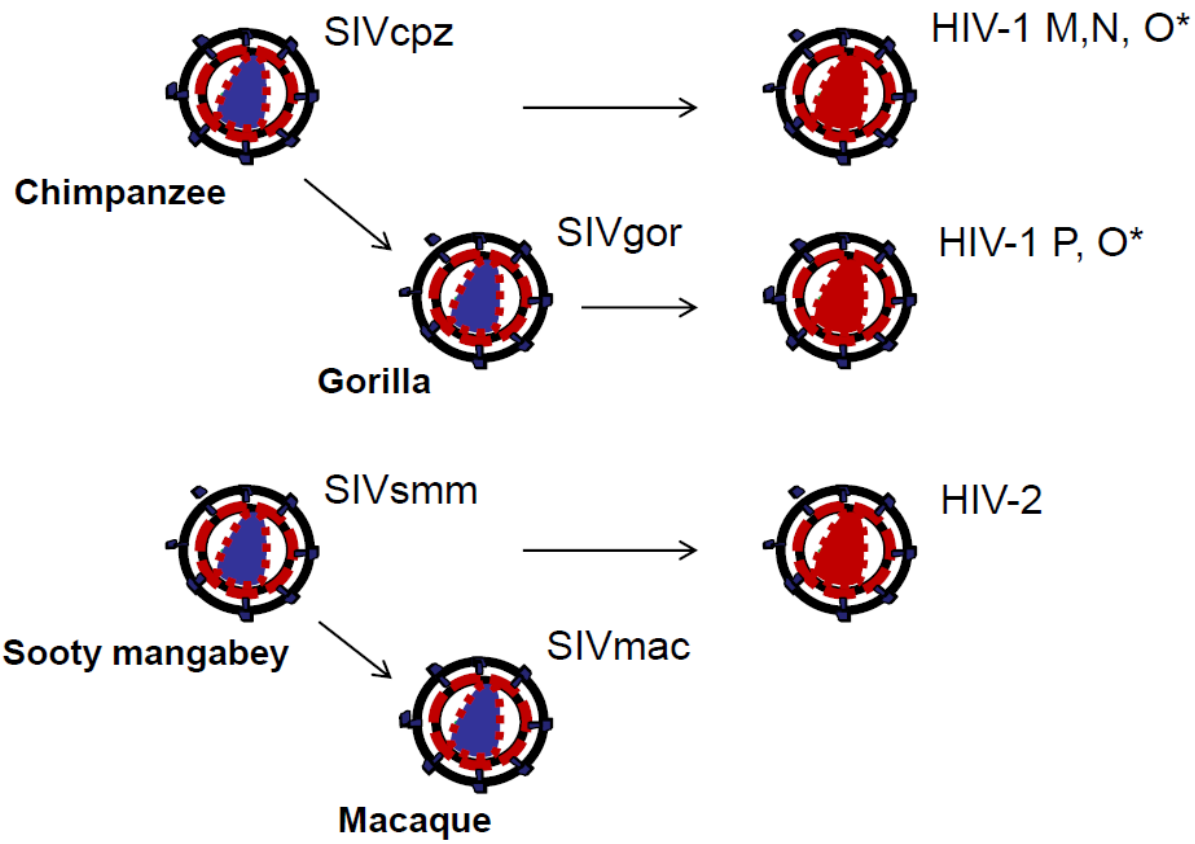

Figure 1.1. HIV-1 and HIV-2 evolution from SIVs

Predicted lines of evolution for HIV-1 (groups M, N, O and P) and HIV-2 from SIVs are illustrated. Each SIV is shown with its species abbreviation in the upper right hand corner of the virus and the species it infects in the lower left hand corner. As the origins of HIV-1 group O were unclear, it is shown with an asterisk in both of its potential lines of evolution. Adapted from [11].

HIV-1 is thought to have evolved from four separate zoonotic transmissions from chimpanzees and gorillas giving rise to Groups M (Major), O (Outlier), N (Non-M, non-O) and P (Figure 1.1). Group M is responsible for the pandemic, group O represents less than 1% of global infections and Groups N and P have only been identified in a small number of individuals [11]. Since its entry into the human population, HIV-1 group M has spread to nearly every country and has diverged into several different genetic subtypes (A-D, F-H, J and K) [17]. As co-infection with these subtypes can result in viral recombination events (reviewed in [18]), several circulating

recombinant forms (CRFs) have also been identified. CRFs are named according to their sequence of classification and the two subtypes they are derived from, for example, CRF01_AE was the first CRF classified and is made up of recombined A and E subtype sequences. The predicted global distribution of HIV-1 group M subtypes and CRFs from data obtained between 2004 and 2007 [19] is presented in Figure 1.2.

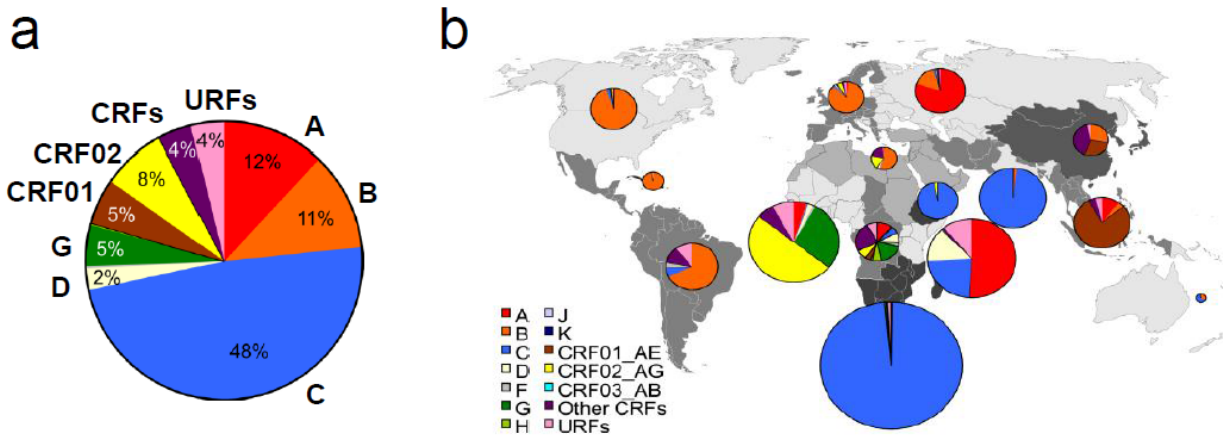

Figure 1.2. Distribution of HIV-1 Group M subtypes and circulating recombinant forms.

a) The total global distribution of HIV-1 group M subtypes, circulating recombinant forms (CRFs) and unique recombinant forms (URFs) are shown based on data obtained from 2004-2007 (Modified from [19]). **b)** From the same data, the distribution of HIV-1 subtypes by global regions is shown with the relative proportion of infections illustrated by the size of the pie charts (From [19]).

The prevalence of different subtypes and CRFs varies greatly in different geographical regions (Figure 1.2 **b**). For example, subtype B accounts for most infections in North America and Europe, whereas in countries located in Southern Africa, with the highest HIV-1 infection numbers, subtype C is the most prevalent [19]. Since resources for HIV research have historically been available in countries affected by subtype B, most scientific studies have been conducted using strains from this subtype. Inter-subtype differences have been described

(reviewed in [17]), therefore certain aspects of HIV-1 biology presented in sections **1.2.2** and **1.2.3** may not apply to all subtypes. Going forward, there is a clear need for more data on some of the most prevalent non-B subtypes (Figure 1.2), to better understand diversity in HIV-1 biology.

1.2.2 HIV-1 replication cycle

HIV-1 gains access to its target cells through receptor-mediated fusion of the viral and host cell membranes, which releases the viral RNA genome into the cytoplasm (Figure 1.3). The replication cycle then proceeds with reverse transcription of the RNA genome into a double-stranded DNA genome, which is integrated into the host cell's chromosomes. Once integrated, the DNA genome, or provirus, is transcribed from the HIV-1 long terminal repeat (LTR) promoter as a single transcript. The full-length transcript is used both for new HIV-1 RNA genomes, and for the translation of the HIV-1 Gag and Gag-Pol polyproteins. Other HIV-1 proteins are translated from alternatively spliced transcripts and, along with a dimer of full-length HIV-1 RNA genomes, they assemble at the host cell's outer membrane to produce new infectious viruses. The general steps of the replication cycle are outlined in Figure 1.3 and details on the different steps are presented in sections **1.2.2.1** to **1.2.2.5**.

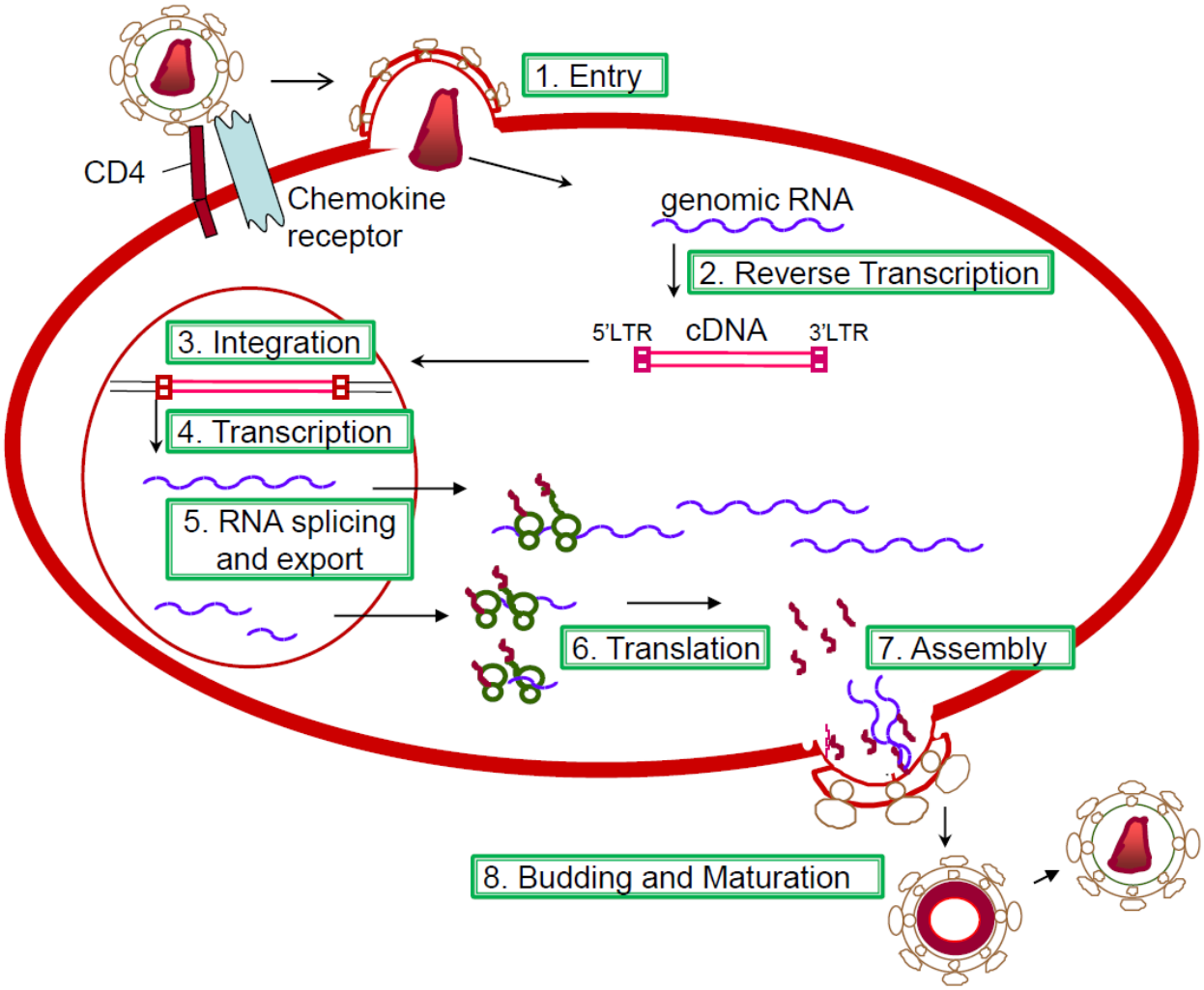

Figure 1.3. HIV-1 replication cycle

The basic steps of the HIV-1 replication cycle are illustrated in green boxes, from entry to budding and maturation. Adapted from [20].

1.2.2.1 Viral architecture and accessory proteins

HIV-1 viruses are contained within a lipid membrane obtained from their host cell. On the surface they harbour several heterotrimers of HIV-1 envelope (Env) surface unit (SU) and transmembrane (TM) proteins, often called glycoproteins (gp) gp120 and gp41, respectively . The viral membrane also contains several cellular proteins derived from its previous host cell.

While none have been identified as being required for infection, several have been shown to act as partners of viral attachment and entry into new host cells (reviewed in [21]).

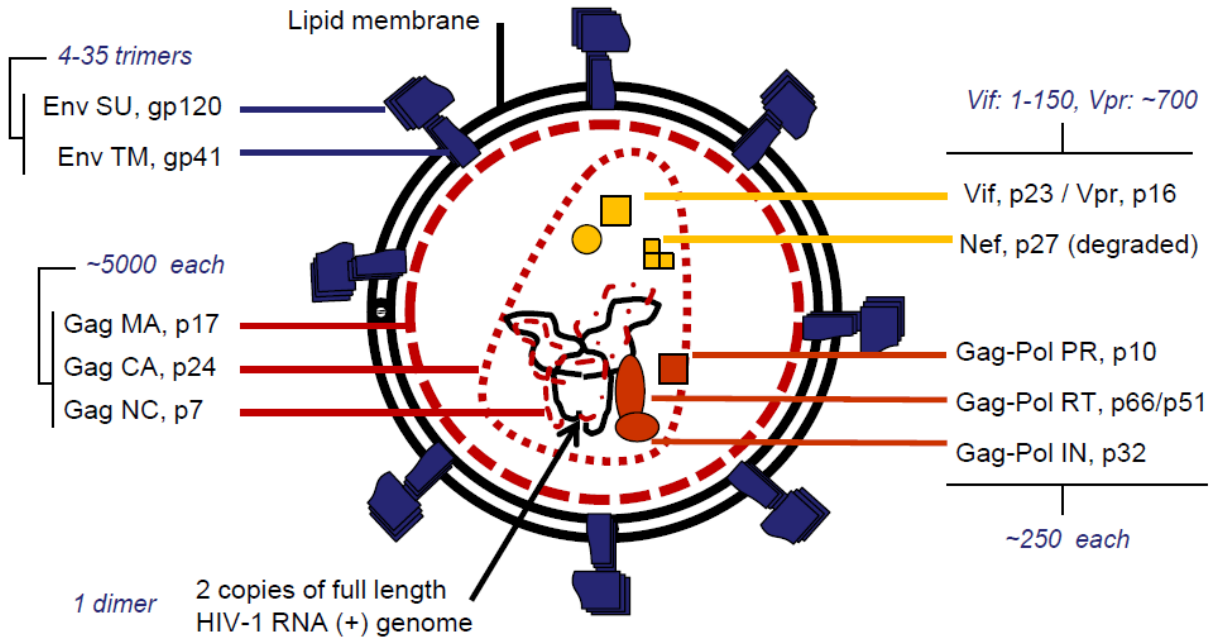

Figure 1.4. Architecture of an infectious HIV-1 virus.

The structure and approximate number of each viral protein and RNA are illustrated for an infectious HIV-1 virus. Approximate numbers of viral proteins are from a review table [22] and abbreviations are described in the text. The viral structure is adapted from [23].

Inside the lipid membrane, the processing products of the HIV-1 Gag polyprotein define the architecture of the virus. The matrix (MA) product lines the inner viral membrane, the capsid (CA) product encases the viral genome and proteins in an icosahedral shell, and the nucleocapsid (NC) product coats two dimerized copies of the viral genomic RNA (Figure 1.4). HIV-1 viruses contain approximately 5,000 copies of each of these processing products [22] and they are critical to the architecture of an infectious viral particle (reviewed in [24]).

An infectious virus also contains the three HIV-1 enzymes, protease (PR), reverse transcriptase (RT) and integrase (IN). These enzymes are processing products of the Gag-Pol polyprotein and are present at approximately 250 copies each [22] (Figure 1.4). Additional viral proteins present in an HIV-1 virus are the accessory proteins, viral infectivity factor (Vif), viral protein r (Vpr) and degradation products of negative factor (Nef). While these proteins do not directly participate in HIV-1 replication, they interact with cellular proteins to provide a suitable host cell environment for replication to occur.

The Vif accessory protein directs the polyubiquitination of human apolipoprotein B mRNA editing complex 3 proteins, particularly APOBEC3G, a cytidine deaminase that catalyzes the conversion of cytidine to uridine. This function of Vif is critical for preventing editing of viral DNA by these proteins during reverse transcription. The Vpr accessory protein can also direct the polyubiquitination of cellular proteins; however, the identity and mechanisms of these proteins are still being elucidated [25]. Other roles identified for Vpr include inducing cell cycle arrest at the G2/M phase and participating in the translocation of viral DNA into the nucleus [22].

Although originally named for negative effects on viral replication, the accessory protein Nef is in fact a pro-viral protein [26]. The first pro-viral effect identified for Nef was its ability to down-regulate cell surface expression of the cluster of differentiation 4 (CD4) protein [27], which counteracts restriction of virus release mediated through interactions between CD4 and gp120 on budding viruses. Nef can also down-regulate cell surface expression of major histocompatibility complex I (MHC I) [28] and MHC II [29] molecules on an infected cell,

which helps infected cells evade cell-mediated immunity. In addition to assisting in viral replication, Nef is also considered a major pathogenicity factor of HIV-1 infection [30].

Another accessory protein, which is not present in an infectious virus, is the viral protein u (Vpu). An important function identified for Vpu was its ability to direct the polyubiquitination of bone marrow stromal cell antigen 2 (BST-2/tetherin), which was shown to be a major restriction factor for virus release at the cell surface [31, 32]. The replication steps described in sections **1.2.2.2** to **1.2.2.5** can occur in the absence of accessory proteins in certain laboratory conditions; however, they are all critical components of viral replication in a natural setting .

1.2.2.2 Entry, uncoating and reverse transcription

Viral entry is initiated by binding of the HIV-1 Env SU gp120 subunit to the human CD4 receptor on a target cell (Figure 1.3). Although entry is often depicted as occurring at the cell surface with a free virus, it can also occur through direct cell to cell transmission [33, 34]. Binding induces a conformational change in gp120 that allows it to bind to a chemokine co-receptor and HIV-1 variants are often classified as chemokine receptor CCR5 (R5), CXCR4 (X4), or dual tropic (R5/X4), based on their ability to use one or both of these co-receptors for entry. Transmitted viruses are almost exclusively R5, and R5 viruses are most prevalent in early and chronic infection. In certain individuals, particularly those infected with HIV-1 subtype B, disease progression is preceded by a switch to X4 and R5/X4 virus [35]. While the mechanisms and consequences of co-receptor switching are poorly understood [36], this phenomenon has major implication for existing and novel therapies that target the CCR5 co-receptor.

Following binding of gp120 to CD4 and a chemokine co-receptor, the Env TM gp41 subunit rearranges so that its N-terminal domain, referred to as the fusion peptide, inserts itself within the host cell membrane. gp41 then undergoes conformational changes to form a six helix bundle, which provides the energy for membrane fusion [33]. These events lead to the fusion of the viral membrane with its new host cell membrane, and entry of the capsid into the cytoplasm. Through complex steps involving both cellular and viral factors, the capsid and nucleocapsid proteins are uncoated (reviewed in [37]) and at the same time, the genomic RNA is reverse transcribed into complementary DNA (cDNA) (Figure 1.3).

Reverse transcription is common to all retroviruses and for HIV-1 it is accomplished by a heterodimer of the full length RT enzyme (p66) and a truncated inactive RT subunit (p51) [38]. The primer for HIV-1 reverse transcription is human transfer RNA lysine 3 ($tRNA^{Lys3}$), which is incorporated into viral particles and binds to the 5' end of the genomic RNA. Using this primer, RT catalyzes RNA-dependent DNA synthesis of the 5' repeat (R) region from the genomic RNA. Through the RNase H activity of RT, the 5' R region of the viral genome is degraded and the newly synthesized DNA template is transferred to the 3' R region, located at the 3' end of the viral genome, in a process referred to as first strand transfer. Using this DNA intermediate as a primer, RT then catalyzes RNA-dependent DNA synthesis of the full-length antisense or minus (-) strand of HIV-1 DNA. The RNase H domain of RT then degrades most of the viral genomic RNA, except for two polypurine tracts (PPTs) located at its 3' end (3'-PPT) and central region (cPPT). Both PPTs serve as primers for DNA-dependent DNA synthesis of the sense or plus (+) strand of HIV-1 DNA. Through a second strand-transfer reaction, DNA synthesized from the 3'-PPT is used as a primer for synthesis of the 5' end of the (+) strand DNA. Elongation of the 5'

end proceeds through the cPPT, displacing the original strand and terminating at ~ 80-100 nts from the cPPT. This process results in a linear double-stranded DNA product with a DNA flap in the discontinuous (+) strand, which is important for nuclear localization of the proviral DNA. Prior to integration, the flap is removed and the (+) strand is made continuous by cellular enzymes [39].

1.2.2.3 Integration and transcription

Following reverse transcription, the LTR ends of the linear double-stranded cDNA product (or provirus) are processed by the viral enzyme IN, to yield 3' hydroxyl groups at each end. This process marks the transition of the viral genome from the reverse transcription complex to the pre-integration complex (PIC) [40]. In addition to IN, the HIV-1 PIC contains other viral proteins (MA and Vpr) and a cellular protein (lens epithelium-derived growth factor, LEDGF), which all contain nuclear localization signals. Along with the DNA flap in the (+) strand DNA, these proteins help translocate the PIC from the cytoplasm to the nucleus; however, the mechanisms and relative contribution of each component are poorly understood [41]. Once inside the nucleus, IN makes a staggered cut in the host cell's DNA and simultaneously transfers the processed 3' ends of the viral DNA to the 5' phosphates of the target site, in what is called the strand transfer step. The host cell's DNA repair machinery then completes integration by joining the 5' ends of the viral DNA to the host cell DNA, resulting in an integrated provirus, which can be transcribed to direct the production of new virus [40].

Once integrated into the cellular DNA, the provirus becomes organized into nucleosomes, which serve as a barrier to transcription. Following nucleosome remodelling by cellular factors, basal RNA polymerase II-mediated transcription occurs from the LTR promoter. However, only small amounts of full-length transcripts are produced, multiply-spliced and exported to the cytoplasm. For efficient transcription, the HIV-1 protein Tat is required. Tat is produced from multiply-spliced transcripts and localizes to the nucleus to trans-activate HIV-1 transcription. Once in the nucleus, Tat binds to the positive transcription elongation factor pTEFb, composed of cyclin T1 and the cyclin dependent kinase 9 (CDK9). The complex then binds to the 5' transactivation response RNA (TAR) on initiated transcripts followed by a transfer to the transcription initiation complex where CDK9 phosphorylates RNA polymerase II. This function of Tat is critical for efficient transcription and for a productive infection [42].

1.2.2.4 RNA splicing, transport and translation

Following transcription of HIV-1 RNA, the full length transcript is alternatively spliced by the cellular machinery to yield over 40 different mRNAs, which can be grouped into singly-spliced or doubly-spliced variants [43]. In the early phase, doubly-spliced viral RNAs exit the nucleus through the mRNA export factor TAP/NXF1. These RNAs are then translated into Tat, Rev and Nef. Because of their associations with the spliceosomal machinery and other nuclear factors, the full-length and singly-spliced transcripts cannot efficiently exit the nucleus. In the late phase, the Rev protein enters the nucleus and binds to the Rev response element (RRE) present in the Env coding RNA sequence of the full-length and singly-spliced transcripts. Rev helps overcome the restriction in export by linking these transcripts to export through the CRM1/Exportin 1 pathway

[44, 45]. The full-length, and representatives of singly- and doubly-spliced transcripts coding for each viral protein and polyprotein are illustrated in Figure 1.5.

HIV-1 mRNAs are predominantly translated by cellular cap-dependent mechanisms; however, translation from an internal ribosome entry site (IRES) can also occur [46]. The 5' untranslated region (5'UTR) of HIV-1 transcripts contains many highly structured regions such as the TAR element, the primer binding site and the dimerization site. These regions act as barriers to cap-dependent translation initiation and are overcome through the recruitment of cellular proteins, including the TAR RNA binding protein (TRBP), the autoantigen La and Staufen [47]. Another barrier to translation results as part of the immune response to HIV-1 infection and an important player in translational inhibition is the interferon-induced RNA activated protein kinase (PKR). PKR shuts down both viral and cellular translation by phosphorylating the alpha subunit of the translation elongation initiation factor, eIF2α. HIV-1 uses several different mechanisms to overcome this inhibition, including inactivation of PKR by the viral protein Tat [48], replication in cells with high levels of PKR inhibitors such as TRBP [49] and adenosine deaminase acting on RNA 1 (ADAR1) [50], and by changing the function of the PKR activator (PACT) into a PKR inhibitor [51].

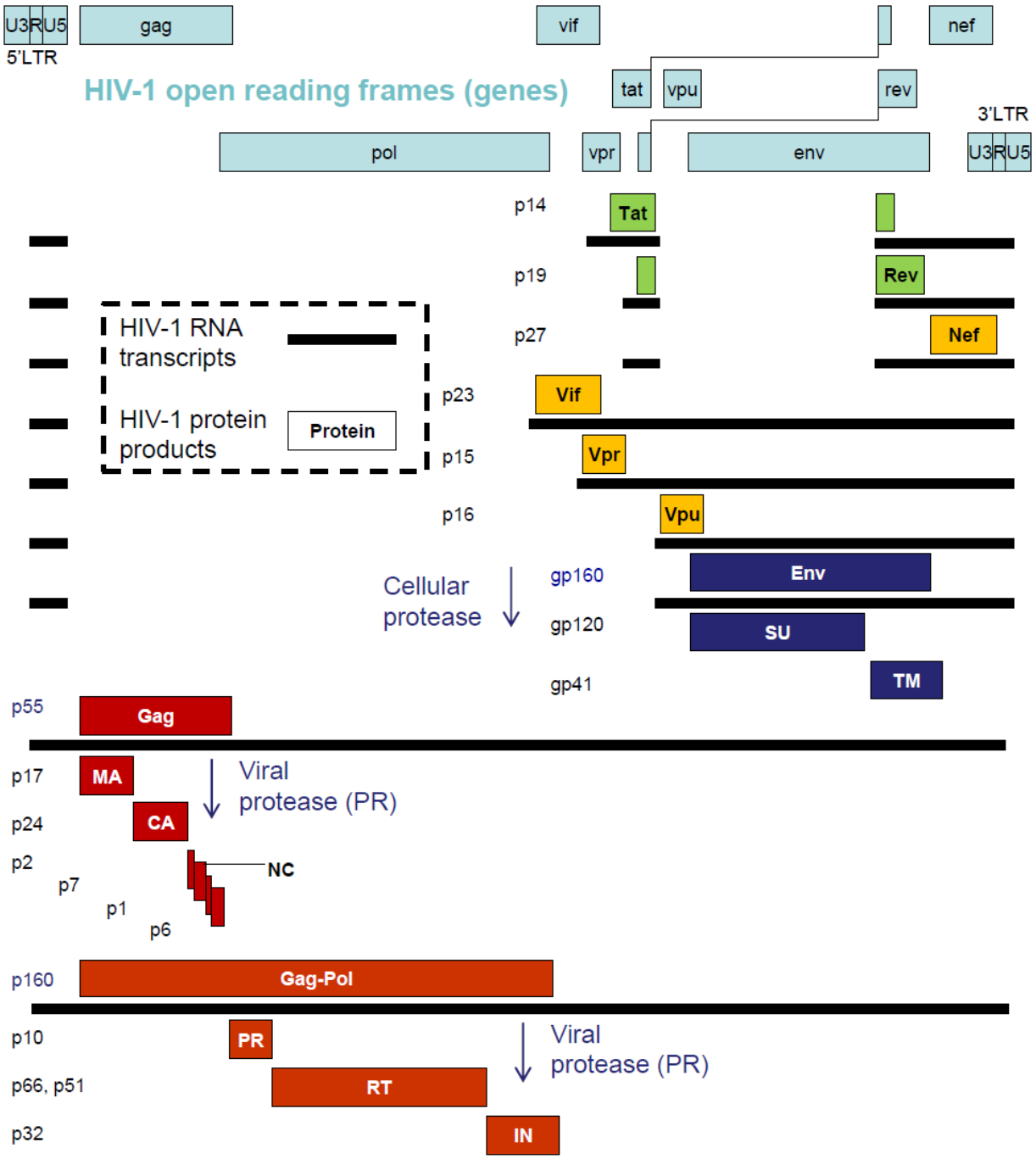

Figure 1.5. HIV-1 open reading frames, RNA transcripts and protein products.

The open reading frames (ORFs) for each HIV-1 protein and polyprotein are illustrated in blue boxes. Representatives of the full-length and spliced transcripts of HIV-1 RNA are illustrated below the ORFs with their protein products and processing products shown. Adapted from [52].

The protein products of HIV-1 translation are illustrated in Figure 1.5 over their respective transcripts. For the full-length transcript, sequence and structural elements in the RNA can coordinate a frame-shift during translation that allows for the alternative translation of the Gag and Gag-Pol polyproteins [53]. These precursor proteins are then cleaved by the HIV-1 PR protein, predominantly after viral assembly and budding. The other precursor or polyprotein is the Env gp160, which is cleaved by the cellular protease Furin prior to assembly to produce the Env TM (gp41) and SU (gp120) proteins [54].

1.2.2.5 Assembly, budding and maturation

The assembly of the viral RNA and proteins occurs at the plasma membrane and is orchestrated by the Gag polyprotein, which alone can assemble into virus-like particles. The MA domain of Gag is responsible for its interaction with cell membranes and as Gag accumulates at assembly sites, it multimerizes through several Gag-Gag interactions [23]. The Env glycoprotein complex of gp41 and gp120 traffics to cell membranes from the Golgi through the cellular secretory pathway and the membrane-bound heterotrimers are recruited to an assembling virus through interactions with the MA domain of Gag. The NC domain of Gag binds to HIV-1 RNA, primarily in a structured region at the 5' end of the genome called the packaging element (psi, ψ) and sequences within the RRE region of the Env coding sequence. Upon multimerization of Gag at the plasma membrane, its RNA binding specificity changes, and this change is thought to help in the selective incorporation of viral genomic RNA over cellular RNAs into budding virions [55]. The C-terminal p6 domain of Gag binds to the cellular endosomal sorting factors TSG101 [56] and ALIX [57], which are members of the endosomal sorting complexes required for

transport (ESCRT) machinery. The multimerization of Gag forms a growing spherical lattice that eventually buds out of the cell with the help of the ESCRT machinery [58].

Following budding, the virus matures through the activation of the PR domain of the Gag-Pol polyprotein, which is incorporated into virions through interactions between its Gag domain and the multimerized Gag lattice. The PR cleaves Gag-Pol into free PR, IN and RT as well as the Gag polyproteins into MA, CA and NC proteins. This process triggers major changes to the structure of the virus including the assembly of the icosahedral capsid and stabilization of the genomic RNA by the NC (reviewed in [58]). The final result is a mature viral particle (Figure 1.4) that can transfer the RNA genome into a new host cell and continue the replication cycle (Figure 1.3).

1.2.3 HIV-1 pathology

A typical HIV-1 infection can be divided into three distinct phases based on characteristic measurements of plasma viral RNA levels and peripheral blood $CD4^+$ T cell counts (Figure 1.6). A lot is known about the pathogenic consequences of HIV-1 infection; however, the precise mechanisms by which HIV-1 affects the immune system remain an area of debate and ongoing research. This section provides an overview of the clinical manifestations of HIV-1 infection during primary infection (section **1.2.3.1**), chronic infection (section **1.2.3.2**) and AIDS (section **1.2.3.3**)

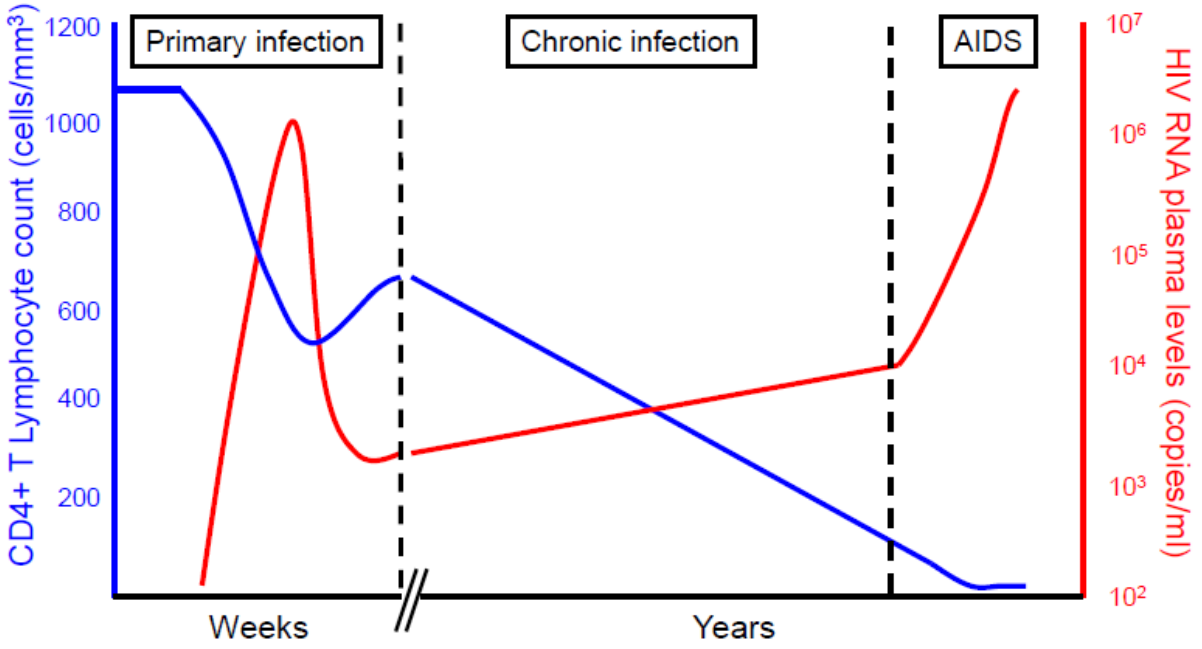

Figure 1.6. Clinical phases of HIV-1 infection (Viral load and $CD4^+$ T cell counts).

The three phases of a typical HIV-1 infection are shown with their characteristic peripheral blood $CD4^+$ T lymphocyte counts and plasma RNA levels (viral load). During primary infection, several non-specific symptoms may be present, the chronic phase is typically asymptomatic and AIDS produces an array of HIV-1 specific illnesses that eventually lead to death. Adapted from [59].

1.2.3.1 Primary infection

Primary infection is often accompanied by symptoms including fever, lymphadenopathy, and other 'flu-like' manifestations. During this phase, the virus disseminates from its point of entry to the gut associated lymphatic tissue (GALT). This tissue contains the highest number of HIV-1 target cells and is thought to be the main site of HIV-1 replication both during primary infection and throughout the chronic phase [60]. Once an infection is established in the GALT, HIV-1 disseminates to a wide range of body compartments, particularly to other lymphoid tissues. As plasma viral levels increase, there is a massive depletion of $CD4^+$ T cells both in the lymphatic tissue and the peripheral blood [60] (Figure 1.6).

The first immune responses to infection involve the release of inflammatory cytokines from dendritic cells, including interferon-α and interleukin-15 [61]. An early antibody response is also mounted prior to peak viremia and this response can be used to diagnose HIV-1 infection. Functionally, these antibodies fail to neutralize the virus and it is not until several weeks after the spike in plasma viremia that neutralizing antibodies emerge [61]. $CD8^+$ T cell responses to HIV-1 appear just before the peak in viremia and are likely responsible for the initial control of HIV-1 replication since their appearance is followed shortly by a decrease in plasma viral levels. Another factor that contributes to the decrease in plasma viral levels is the extensive direct and indirect depletion of $CD4^+$ T cells, which limits the number of HIV-1 target cells available for production of new virus [61].

Following the appearance of neutralizing antibodies to HIV-1, the acute phase of infection ends, and viral levels stabilize at what is often referred to as the viral set point [60]. Although this set point gradually increases over the course of chronic infection, it remains relatively constant compared to the drastic changes that occur in primary infection and AIDS (Figure 1.6). Sequential rounds of viral escape from HIV-1 specific immune responses and the evolution of new responses greatly contribute to this set point, and its level is positively correlated with disease progression [62]. Several recent clinical studies have suggested that initiation of antiviral therapy during primary infection may help minimize damage to the immune system as well as limit the size of drug resistant viral reservoirs (described in section **1.3.2.1**) [63]. Results from the "Mississippi baby" [64] and the VISCONTI cohort [65] have also shown that very early treatment can lead to long-lasting control of HIV replication in the absence of therapy. Although primary infection is challenging to identify, these results should encourage the early

identification and prompt initiation of treatment whenever possible, as such action may help improve the long term management of infection and could work synergistically with experimental therapies designed to clear HIV-1 reservoirs.

1.2.3.2 Chronic infection

Once a viral set point is achieved, the chronic phase of HIV-1 infection begins (Figure 1.6). During this phase, progressive damage to lymphoid tissue occurs as a result of both continued HIV-1 replication in theses tissues and chronic immune activation. Although the mechanisms are not fully understood, the high level of HIV-1 replication that occurs in the GALT is associated with an increase in intestinal epithelial permeability, which results in increased translocation of microbes and their products across the intestinal barrier [66]. Along with HIV-1 antigens, this increased exposure to other microbial components contributes to chronic immune activation, which is preset throughout the chronic phase [60]. Architectural changes in peripheral lymph nodes also occur, and may contribute to a loss of immune cell homeostasis, damaging diverse cellular components of the immune system [67].

One of the consequences of chronic immune activation and dysregulation of immune cell tissues is an increase in immune cell turnover, not only in $CD4^+$ T cells but also in other cell types such as $CD8^+$ T cells, B cells and NK cells. Over several years, diverse immune cell populations fail to regenerate and function properly, eventually leading to a breakdown in the immune system [60]. Although the relative contribution of direct and indirect effects of viral replication to the

progressive destruction of the immune system are not completely understood, the overall consequence of the chronic phase is the development of AIDS.

1.2.3.3 AIDS

AIDS is characterized by low peripheral blood $CD4^+$ T cell counts and rapidly increasing plasma HIV-1 RNA levels (Figure 1.6). During AIDS, the immune system collapses and the infected person is unable to control common microbial infections including those that are usually non-pathogenic (referred to as opportunistic infections). Due predominantly to unchecked replication of oncogenic viruses, such as herpes and papilloma viruses, a variety of AIDS-defining malignancies also develop [68].

AIDS can be reversed and prevented by inhibiting HIV-1 replication with antiretroviral therapies. As the chronic phase is characterized by a progressive loss of immune function, early initiation and compliance with therapy can prevent not only AIDS but also many non-AIDS related morbidities associated with HIV-1 infection. While effective therapies are available, access to medication and medical expertise remain barriers to the elimination of AIDS in some of the most affected populations. In populations with access to therapy, drug toxicities and the emergence of drug resistance are major challenges in the long term care of HIV-1 infected individuals.

1.3 HIV-1 therapy

Advances in our understanding of HIV-1 biology (section **1.2**) enabled the development of antiretrovirals (ARVs) targeting HIV-1 replication. The first ARV was azidothymidine (AZT), a

nucleoside analogue targeting the HIV-1 RT enzyme. AZT was approved by the United States Food and Drug Administration (US FDA) in 1987 and since then 27 additional ARVs have been approved for therapy (Table 1.1) [69, 70]. The standard of care for HIV-1 infection includes a combination of ARVs from at least two different classes, sometimes referred to as combination ARV therapy (cART). This therapy approach is required to prevent the development of drug resistant virus, which emerges when any single ARV is used alone. cART has transformed HIV-1 from a fatal disease into a chronic manageable disease; however, it is unable to cure an infection and ARVs must be administered chronically to prevent disease progression to AIDS.

Soon after the first effective cART regimens were implemented in 1995/1996 it was shown that replication-competent HIV-1 persists even after prolonged suppression [71] and that latently infected resting $CD4^+$ T cells can serve as an HIV-1 reservoir during therapy [72]. In 1999 it was estimated that it would take over 60 years to clear HIV-1 from that reservoir [73] and it is now clear that cART regimens must be administered indefinitely to inhibit HIV-1 replication and prevent disease progression to AIDS. To attain an HIV-1 cure, either elimination of all drug resistant viral reservoirs (sterilizing cure) or resistance to HIV-1 replication in the absence of cART (functional cure) must be achieved [74]. In this section, current HIV-1 therapies (section **1.3.1**) and three prominent approaches to attain an HIV-1 cure (section **1.3.2**) are described.

1.3.1 Current HIV-1 therapy

Currently available ARVs target viral entry, reverse transcription, integration and proteolytic cleavage of the Gag and Gag-Pol polyproteins. The steps they inhibit in the HIV-1 replication

cycle are illustrated in Figure 1.7 and a list of molecules approved by the US FDA for treatment of HIV-1 is provided in Table 1.1. Details on each class of molecules are described in sections **1.3.1.1** to **1.3.1.4,** according to their chronological approval by the US FDA.

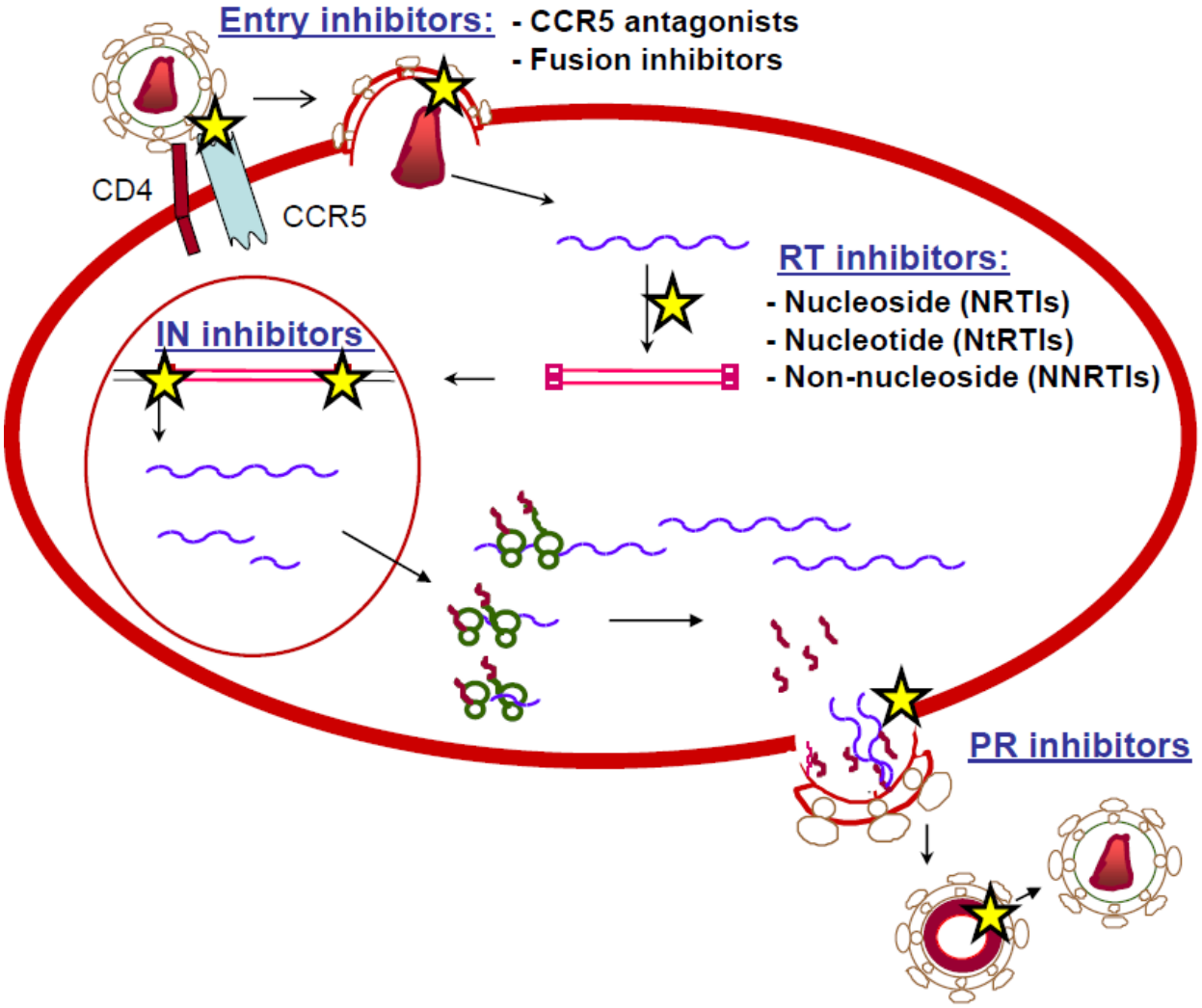

Figure 1.7. Targets of US FDA approved inhibitors in the HIV-1 replication cycle

The different sites of action for HIV-1 entry, reverse transcriptase (RT), integrase (IN) and protease (PR) inhibitors are illustrated with yellow stars in the HIV-1 replication cycle (adapted from [20]). Sub-classes of entry and RT inhibitors are also illustrated.

Table 1.1. List of US FDA approved anti-HIV-1 drugs

Abbreviation	Generic name	Trade name	Year of FDA approval
Nucleoside Reverse Transcriptase Inhibitors (NRTIs)			
AZT/ZDV	Zidovudine	Retrovir	1987
ddI	Didanosine	Videx	1991
ddC	Zalcitabine	HIVID	1992
d4T	Stavudine	Zerit	1994
3TC	Lamivudine	Elpivir	1995
ABC	Abacavir	Ziagen	1998
FTC	Emtricitabine	Emtriva	2003
Nucleotide Reverse Transcriptase Inhibitors (NtRTIs)			
TDF	Tenofovir	Viread	2001
Non-Nucleoside Reverse Transcriptase Inhibitors (NNRTIs)			
NVP	Nevirapine	Viramune	1996
DLV	Delavirdine	Rescriptor	1997
EFV	Efavirenz	Sustiva	1998
ETR	Etravirine	Intelence	2008
RPV	Rilpivirine	Edurant	2011
Protease Inhibitors (PIs)			
SQV	Saquinavir	Invirase	1995
RTV	Ritonavir	Norvir	1996
IDV	Indinavir	Crixivan	1996
NFV	Nelfinavir	Viracept	1997
APV	Amprenavir	Agenerase	1999
LPV/RTV	Lopinavir+Ritonavir	Kaletra	2000
ATV	Atazanavir	Reyataz	2003
FOS-APV	Fosamprenavir	Lexiva	2003
TPV	Tipranavir	Aptivus	2005
DRV	Darunavir	Prezista	2006
Entry Inhibitors			
T-20	Enfuvirtide	Fuzeon	2003
MVC	Maraviroc	Celsentri	2007
Integrase Inhibitors / Integrase Strand Transfer Inhibitors (InIs / InSTIs)			
RAL	Raltegravir	Isentress	2007
EVG	Elvitegravir	Vitekta	2012
DTG	Dolutegravir	Tivicay	2013

Table adapted from: http://www.avert.org/antiretroviral-drugs.htm

1.3.1.1 HIV-1 Reverse Transcriptase inhibitors

The first several ARVs were nucleoside reverse transcriptase (RT) inhibitors (NRTIs) and seven have been approved by the US FDA for the treatment of HIV-1 infection (Figure 1.7**,** Table 1.1). NRTIs mimic deoxy-nucleotide tri-phosphates (dNTPs) and compete with these substrates for inclusion in either the (+) or (-) strand of HIV-1 DNA during reverse transcription (section **1.2.2.2**). All NRTIs lack a 3' hydroxyl group in their sugar moiety, so once incorporated into a DNA chain they terminate elongation since they cannot form new phosphodiester bonds with incoming dNTPs [69]. Resistance to NRTIs can result from mutations in RT that selectively exclude a particular NRTI from its binding site. Other mutations can increase the rate of excision of NRTIs from the RT complex after they are incorporated [75].

Unlike other ARVs, NRTIs are delivered in an inactive form, which must be sequentially phosphorylated by cellular kinases to convert the nucleoside analogue into its active dNTP analogue. Nucleotide RT inhibitors (NtRTI) are similar to NRTIs except that they by-pass at least the first phosphorylation reaction required to generate an active tri-phosphate drug metabolite [76]. So far, only one NtRTI has been approved by the US FDA for HIV-1 therapy (Table 1.1), with others in various stages of development [75]. Since the beginning of the epidemic, N(t)RTIs have been a cornerstone of HIV-1 therapy and they remain an essential component of cART regimens with the NtRTI tenofovir disoprovil fumarate (TDF) being among the most commonly prescribed of all ARVs [77].

Another class of RT inhibitors are the non-nucleoside RT inhibitors (NNRTIs) and five NNRTIs have been approved by the US FDA for HIV-1 therapy (Figure 1.7**,** Table 1.1). NNRTIs all bind

to the same site in RT, in close proximity to the DNA polymerase active site. When bound by an NNRTI, the conformation of the RT active site changes such that it can no longer bind its natural substrate (dNTPs) and its DNA polymerase activity is inhibited. In addition to this inhibition, NNRTI binding also affects the RNase H activity of RT [78] and both mechanisms likely contribute to the potent inhibition of HIV-1 replication provided by this class of molecules. Amino-acid substitutions in the NNRTI binding site of RT can lead to NNRTI resistance. These resistant viruses do not usually have major deficiencies in their ability to replicate and are therefore able to persist in HIV-1 infected populations more easily than other drug resistant viruses [69]. Despite the low barrier to resistance, NNRTIs are commonly used in first line cART regimens due to their excellent safety and efficacy profiles [76].

1.3.1.2 HIV-1 Protease inhibitors

Protease inhibitors (PIs) comprise the largest class of ARVs, with ten molecules approved by the US FDA for HIV-1 therapy (Figure 1.7**,** Table 1.1). All PIs bind to the active site of HIV-1 PR and block its ability to catalyze the cleavage of the polyproteins Gag and Gag-Pol, a critical step towards the maturation of infectious viruses (section **1.2.2.5**). Biochemical data on the structure of the PR enzyme and computational approaches were used to design many PIs and they are one of the first successful examples of structure assisted, or rational, drug design [79]. All PIs, with the exception of one (tipranavir), contain a hydroxyethelene core that mimics the peptide bonds of the Gag and Gag-Pol PR cleavage sites [80]. Primary resistance mutations to PIs are generally located in the active site of the enzyme and these mutations often confer cross-resistance to other PIs. In contrast to NNRTI resistance mutations, these primary resistance mutations have major

effects on the replicative fitness of the virus and secondary mutations in PR as well as mutations in the Gag and Gag-Pol cleavage sites are required to maintain resistance and PR function under drug pressure [69].

The addition of the PIs to HIV-1 therapy in 1995 and 1996 lead to the first dual class cART regimens. Treatment with some of the first PIs resulted in adverse effects on the metabolic system and affected the metabolism of co-administered drugs [76]. Newer PIs have been designed to improve the tolerability of this class of ARVs and they are commonly used in cART.

1.3.1.3 HIV-1 entry inhibitors

The first entry inhibitor approved by the US FDA for cART was enfuvirtide, a 36-amino acid peptide analogue of the C terminal heptad repeat domain (HR2) in the HIV-1 Env TM gp41 protein (Figure 1.4). By mimicking this domain, enfuvirtide inhibits conformational changes in the gp41 protein that are required to form the six-helix bundle and promote fusion of the viral and host cell membranes (section **1.2.2.2**, Figure 1.7). Resistance to enfuvirtide can emerge from mutations in the N-terminal heptad repeat domain (HR1), which interacts with HR2 to promote fusion [81]. Unlike all other FDA approved ARVs, enfuvirtide is not a small molecule, and instead of being administered orally as a pill or capsule, it must be administered by sub-cutaneous injection [76]. When approved in 2003, only three classes of ARVs were available and enfuvirtide was valuable for patients experiencing cART failure due to multi-drug resistance [69]. With the approval of the orally available entry co-receptor inhibitor Maraviroc, and the HIV-1 IN inhibitors (section **1.3.1.4**), use of enfuvirtide in salvage therapy is likely to fall into

disuse. However, the development of small molecule inhibitors of gp41 and viral fusion could lead to new ARVs targeting the fusion step of viral entry [82].

The only orally available entry inhibitor is Maraviroc, approved by the US FDA in 2007. Maraviroc is a small molecule antagonist of the CCR5 chemokine receptor and acts allosterically to alter the conformation of the receptor such that it can no longer interact with both its agonists and the HIV-1 Env SU gp120 protein [69] (Figure 1.7). It is the only ARV that targets a cellular protein instead of a viral protein and part of the rationale behind the development of this class of ARVs came from the identification of an HIV-1 resistant population with a homozygous 32 amino acid deletion in their CCR5 gene (CCR5Δ32/Δ32) [83]. As this population had no apparent health problems, it was thought that antagonists of this receptor could be used safely in cART regimens and clinical data on Maraviroc has so far supported this assumption [84]. In contrast, treatment of HIV-1 infected subjects with the CXCR4 antagonist AMD3100 produced leukocytosis in all study participants [85] and is now used as a potent hematopoietic stem cell (HSC) mobilizer for HSC transplant [86, 87]. Despite the potential safety issues of targeting the CXCR4 co-receptor, treatment with CXCR4 co-receptor antagonists would be useful for people infected with dual tropic or X4 tropic virus, and progress has been made in the development of new molecules for these populations [88, 89].

Pre-existing resistance to Maraviroc due to X4 or dual tropic viruses can be determined to exclude these populations from therapy; however, the sensitivity of available tests may miss some individuals with low levels of these viruses. So far, clinical and pre-clinical studies have not identified co-receptor switching under Maraviroc drug pressure, suggesting that unless

already present, resistance will not develop through this mechanism [84]. However, resistance can develop through mutations in the viral envelope proteins that permit viruses to use both the free and the inhibitor bound CCR5 co-receptor for entry [69].

1.3.1.4 HIV-1 integrase inhibitors

The first HIV-1 IN inhibitor, Raltegravir, was approved by the US FDA in 2007 [69] and since then two others, Elvitegravir and Dolutegravir, have been approved for HIV-1 therapy [70] (Table 1.1). All of the available IN inhibitors target the strand transfer activity of HIV-1 IN, required to insert the proviral DNA into the host cell's chromosomes (Figure 1.7). Often called integrase strand transfer inhibitors (InSTIs), these molecules bind only to complexes of HIV-1 IN and proviral DNA. Through interactions with IN and the viral DNA, InSTIs sequester magnesium ions away from the IN active site, preventing its catalytic activities in the strand transfer reaction [69]. Resistance to InSTIs can emerge from mutations in the IN active site near amino acids that interact with magnesium ions [69]. As with the PIs, these primary mutations have major effects on the replicative fitness of the drug resistant virus, and secondary mutations are required to restore IN activity. Although limited data is available on this class of inhibitors, early clinical results suggest that the genetic barrier to InSTI resistance is as high or even higher than that of commonly used PIs [70]. While more long-term data on the safety and efficacy of InSTIs is needed, results from studies so far suggest that this class will become a major part of successful cART regimens.

1.3.2 HIV-1 cure research

While there is a lot of hope that either a sterilizing cure (complete elimination) or a functional cure (control of HIV-1 replication in the absence of cART) can be accomplished, a broadly applicable clinical approach has yet to be described [74]. To eliminate HIV-1 from an infected person, all replication-competent cART-resistant reservoirs must be eliminated and approaches in development to accomplish this are described in section **1.3.2.1.** Therapies designed to stimulate immune control of HIV-1 replication in the absence of cART are described in section **1.3.2.2,** and the transplantation of HIV-1 resistant target cells to control HIV-1 replication is described in section **1.3.2.3.**

1.3.2.1 Elimination of cART resistant viral reservoirs

With the advent of cART, it was estimated that two to three years of a completely suppressive regimen would be sufficient to eliminate the virus [90]. This was based on the observation that following initiation of cART there were two phases of decay in plasma viremia. The first phase of decay was rapid and could be accounted for by the loss of free virions (half life ~ 6 hours) and replication in productively infected cells (half life ~ 1.6 days). The second phase of decay was attributed to longer-lived infected cells (half life ~ 1-4 weeks) [90]. Unfortunately, HIV-1 was found to persist past this second phase of decay in an inactive but replication competent form. The major cellular reservoir for this source of virus was identified as resting $CD4^+$ T cells [72], and has since been more precisely defined as resting central memory or transitional memory $CD4^+$ T cells, depending on the level of peripheral blood $CD4^+$ T cell counts [91]. These cells can be generated when an infected activated $CD4^+$ T cell reverts into a resting memory state.

Although a rare event, this population of cells is established early in infection and because of its long life span, is thought to be the major barrier to elimination in cART-treated individuals. Since these cells can intermittently be activated to produce virus during therapy, they may be responsible for low levels of virus detected by highly sensitive assays and are certainly a major source of viral rebound once therapy is stopped [92].

Experimental approaches to eliminate HIV-1 reservoirs have primarily focused on activating HIV-1 replication in latently infected $CD4^+$ T cell populations. The goal is to make these cell populations susceptible to the pathological effects of viral replication and HIV-1 specific immune clearance. Both interleukin-2 (IL-2) [93, 94] and IL-2 together with anti-CD3 antibodies [95-97] have been evaluated in clinical studies in an attempt to reactivate latent virus by inducing general T cell activation; however, a decrease in the viral reservoir could not be observed and general T cell activation was highly toxic. To more directly reactivate HIV-1 transcription (section **1.2.2.3**) several classes of molecules have been proposed including histone deacetylase (HDAC) inhibitors, histone methyltransferase inhibitors, DNA methyltransferase inhibitors, Protein kinase C activators and pTEF-b activators (reviewed in [98]). In 2005 it was reported that the HDAC inhibitor, valproic acid, could reduce the size of the latent reservoir in resting $CD4^+$ T cells [99]; however, subsequent studies reported no significant reduction [100, 101]. A recent study using another HDAC inhibitor, vorinistat, reported that while an increase in transcription from latency occurred in most patients, a significant reduction in latently infected $CD4^+$ T cells could not be observed [102].

As different mechanisms of latency may be susceptible to different classes of compounds, it has been suggested that combinations may provide a more effective reactivation strategy for clinical trials [103]. There is also evidence that reactivation of latently infected $CD4^+$ T cells does not result in their death and that additional interventions such as HIV-1 specific antigen stimulation of $CD8^+$ T cells prior to reactivation will be required to eliminate this latent cell population in the clinic [104]. A further incompletely understood barrier to elimination is whether other cell types such as myeloid cells can serve as reservoirs for latent HIV-1 and whether or not these cells, if they exist, will be equally affected by "shock and kill" therapy approaches designed to clear latently infected $CD4^+$ T cells [105]. Although little progress has been made in the clinic, it is hoped that a better understanding of viral latency and an increase in the number of approaches evaluated in clinical trials can eventually lead to the elimination of HIV-1 from an infected individual.

1.3.2.2 Immune therapies to control HIV-1 replication

In the absence of complete elimination, therapies designed to stimulate better immune control of HIV-1 replication have the potential to provide a functional cure for HIV-1 infection [106]. The goal of many of these therapies is to simulate a phenotype observed in a small sub-population of HIV-1 infected individuals known as elite controllers. These individuals are able to maintain undetectable plasma viral levels in the absence of cART, and for most elite controllers, this is a result of enhanced HIV-1 immune responses [107]. Both genetic and immunological studies of this patient population have suggested that $CD8^+$ T cell responses to HIV-1 play a major role in providing control of HIV-1 replication; however, the various factors involved are not completely

understood [107]. Studies on this population have already helped guide the design of some immune-based strategies, and a better understanding of elite controllers is likely to provide new approaches.

Several cytokines have been evaluated as candidates for immune therapy in clinical trials, including IL-2, IL-7 and IL-12 (reviewed in [106]). While providing some beneficial clinical effects in combination with cART on $CD4^+$ T cell counts, the use of these agents alone is unlikely to induce a lasting control of HIV-1 replication and their chronic use is limited due to various side effects. Nevertheless, in combination with different HIV-1 antigen delivery mechanisms, certain immune stimulants may enhance the production of HIV-1 specific immune responses and they are likely to play an important role in developing effective therapeutic vaccination approaches to control HIV-1 replication in the absence of cART [106].

Several approaches to stimulate superior HIV-1 specific immune responses through delivery of HIV-1 antigens have been evaluated. Collectively called therapeutic vaccinations, methods have included direct delivery of HIV-1 peptides, delivery of HIV-1 antigens from DNA or viral vectors and delivery of cells expressing viral antigens (reviewed in [106]). Transplantation of $CD8^+$ T cells, genetically modified to direct them towards HIV-1 antigens, is also under investigation [108]. While a successful approach remains elusive, a better understanding of the mechanisms that contribute to the elite controller phenotype and advances in the delivery of HIV-1 antigens and genetically modified cells could provide the first broadly applicable functional cure for HIV-1 infection.

1.3.2.3 HIV-1 resistant cell transplant to control HIV-1 replication

Although no person with an established HIV-1 infection has been cured through elimination (section **1.3.2.1**) or superior immune control (section **1.3.2.2**), one infected man has attained a functional cure through HIV-1 resistant cell transplant. Timothy Brown, also known as the Berlin patient, received an allogeneic (genetically non-identical) hematopoietic stem cell (HSC) transplant from an individual with the homozygous CCR5Δ32/Δ32 deletion, a genotype that renders cells resistant to infection by HIV-1 R5 tropic viruses [83] (described in section **1.3.1.3**). The treatment was prescribed to treat both relapsed acute myeloid leukemia and, potentially, HIV-1 infection [109]. Timothy has been off cART therapy since his transplant and remains the only individual who has been functionally cured of HIV-1. Unfortunately, the high risk associated with allogeneic HSC transplant and the low incidence of known CCR5Δ32/Δ32 carriers makes the protocol used in this case inaccessible to the vast majority of HIV-1 infected individuals.

The idea of using HIV-1 resistant cell transplant to treat HIV-1 infection had been proposed early in the HIV-1 epidemic (1988) [110]. The first clinical trials were completed in the late 1990s using transplant of $CD4^+$ T cells transduced with a gene directing the production of a protein-based or RNA-based antiviral agent. Since then, several clinical trials have been conducted to evaluate the safety and efficacy of diverse genes, or combinations of genes, for use in both $CD4^+$ T cell and HSC transplant therapy (Table 1.2).

Table 1.2. Completed and ongoing HIV-1 resistant cell transplant trials

Antiviral gene	Ex vivo manipulation	Status	Year	Ref
Proteins and peptides				
Dominant negative mutant HIV-1 Rev protein (Rev M10)	Gold particle transfected $CD4^+$ T cells	Completed	1996	[111]
	Murine retrovirus transduced $CD4^+$ T cells	Completed	1998	[112]
	Murine retrovirus transduced HSCs	Completed	2005	[113]
Dominant negative HIV-1 Rev protein	Murine retrovirus transduced syngeneic $CD4^+$ T cells	Completed	2005	[114]
	Murine retrovirus transduced HSCs	Completed	2002, 2009	[115], [116]
gp41 peptide, fusion inhibitor (C46)	Murine retrovirus transduced $CD4^+$ T cells	Completed	2007	[117]
Zinc finger nuclease proteins targeting the CCR5 gene	Adenovirus transduced $CD4^+$ T cells	Ongoing[1]: NCT-00842634 01252641 01044654	2014	[118]
RNA				
Ribozyme targeting HIV-1 tat/vpr RNA (Rz2, OZ-1)	Murine retrovirus transduced $CD4^+$ T cells	Completed	1998	[119]
	Murine retrovirus transduced syngeneic $CD4^+$ T cells	Completed	2005	[120]
	Murine retrovirus transduced HSCs	Completed	1999, 2004	[121], [122]
	Murine retrovirus transduced HSCs, Phase II	Completed	2009	[123]
Ribozyme targeting HIV-1 5'UTR and tat/rev RNA	Murine retrovirus transduced HSCs	Completed	2003	[124]
Antisense RNA targeting HIV-1 env RNA (VRX496)	Lentivirus (HIV) transduced $CD4^+$ T cells	Completed	2006	[125]
	Lentivirus (HIV) transduced $CD4^+$ T cells	Ongoing[1]: NCT-00295477 00131560	2013	[126]
RRE-decoy targeting HIV-1 Rev	Murine retrovirus transduced HSCs	Completed	1999	[127]
Combinations				
1. siRNA: tat/rev 2. ribozyme: CCR5 3. TAR-decoy : Tat	Lentivirus (HIV) transduced HSCs	Ongoing[1]: NCT-01961063	2010	[128]
1. siRNA: CCR5 2. gp41 peptide (C46)	Lentivirus (HIV) transduced HSCs and $CD4^+$ T cells	Ongoing[1]: NCT-01734850	-	-

[1] ClinicalTrials.gov identifier numbers are provided for ongoing studies, information on the status of these studies is available at clinicaltrials.gov.

Protein-based genes that have advanced to clinical trials include trans-dominant HIV-1 Rev proteins, designed to inhibit the export of singly-spliced and full-length HIV-1 RNA to the cytoplasm (section **1.2.2.4**) and a gp41 peptide inhibitor of viral fusion, with a similar mechanism as the entry inhibitor enfurvitide, available for cART therapy (section **1.3.1.3**) (Table 1.2). A potential limitation of these and other protein-based genes is that they may be processed and presented to the adaptive immune system, which could lead to both selective clearance of the HIV-1 resistant cells and chronic immune activation [108]. Another protein-based approach currently under evaluation is the ex-vivo delivery of Zinc finger nucleases (ZFNs) designed to modify the CCR5 gene [118] (Table 1.2). In contrast to other antiviral genes that are inserted into the chromosomes of transplanted cells with retroviral vectors, ZFNs are expressed transiently from an adenoviral vector. Their expression permanently alters a sequence in the CCR5 gene to phenotypically mimic the CCR5Δ32/Δ32 genotype of the donor used for the Berlin patient, Timothy Brown. Although this approach would be applicable to the majority of HIV-1 infected individuals exclusively harbouring HIV-1 R5 tropic viruses, very few gene editing agents have entered clinical trials, and the safety of this approach has not been extensively evaluated. Newer gene editing technologies, such as the CRISPR (clustered regularly interspaced short palindromic repeats)-associated protein-9 nuclease (Cas9) in combination with a guide RNA targeting the CCR5 gene have also been evaluated in preclinical studies and may offer more specificity over the protein directed ZFN approach [129].

RNA-based genes that have advanced to clinical trials include antisense RNAs, ribozymes, small interfering RNAs (siRNAs) and RNA decoys (Table 1.2). A major advantage of RNA-based genes over protein-based genes is that RNAs do not have the potential to elicit adaptive immune

responses [108]. The small size of their transcriptional units (promoter plus RNA coding sequence) also make it easier to design transfer vectors delivering combinations of antiviral genes [130] and five out of the six genes that have advanced to combination delivery trials are RNA-based (Table 1.2). Results from the Berlin patient suggest that it is possible to functionally cure HIV-1 infection and the development of antiviral RNAs is likely to contribute to the identification of a safe and efficacious protocol to provide a broadly applicable functional cure.

1.4 RNA Inhibitors of HIV-1 replication

Several steps in the HIV-1 replication cycle have been exploited for the development of therapeutic RNAs (Figure 1.8). The HIV-1 Tat and Rev proteins have been targeted by RNA decoys that mimic either the TAR or RRE RNA elements of HIV-1 RNA. TAR or RRE decoys inhibit the transactivation of transcription (section **1.2.2.3**) or RNA export (section **1.2.2.4**) mediated by the Tat or Rev proteins, respectively. Using in vitro selection, several RNA aptamers have also been designed to specifically target diverse HIV-1 proteins such as the RT enzyme (reviewed in [131]). In addition to RNAs targeting viral proteins, therapeutic RNAs have also been designed to target either HIV-1 RNA or the mRNA of a protein that assists in viral replication. These molecules are collectively called antisense RNAs [132] and both ribozymes (section **1.4.1**) and siRNAs (section **1.4.2**) are among the most promising antisense-based agents for use in HIV-1 gene or drug therapy.

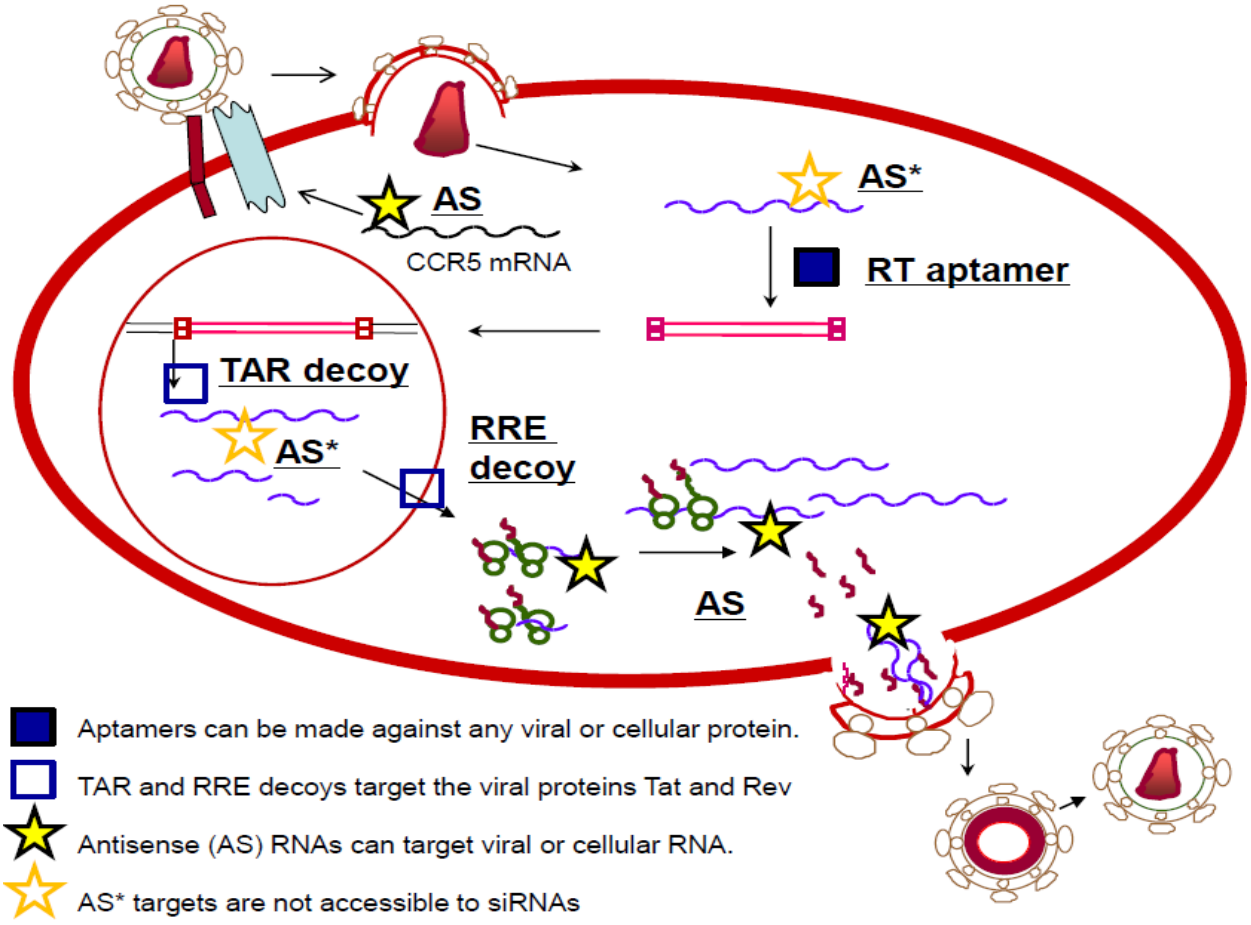

Figure 1.8. Small RNA targets in the HIV-1 replication cycle

The site of action for an RNA aptamer targeting the HIV-1 reverse transcriptase (RT) enzyme is illustrated with a solid box. However, any viral or cellular protein can be targeted by RNA aptamers. TAR and RRE RNA decoys are illustrated with open boxes. These RNAs act to sequester the viral proteins Tat and Rev, and prevent them from transactivating transcription and exporting viral RNA from the nucleus, respectively. Antisense (AS) molecules include simple antisense RNAs, ribozymes and small interfering (si) RNAs. Because they need a large protein complex that is localized to the cytoplasm, AS targets in the incoming viral RNA and in the nucleus may not be accessible to siRNAs (AS*). Adapted from [20].

1.4.1 Ribozymes targeting HIV-1

Ribozymes are catalytic RNAs found in the genomes of diverse organisms. A thorough understanding of their mechanisms (section **1.4.1.1**) has led to the development of therapeutic

ribozymes targeting diverse human afflictions including HIV-1 infection. Ribozyme motifs used to design anti-HIV-1 RNAs as well as their target sites in HIV-1 RNA and the CCR5 co-receptor mRNA are described in sections **1.4.1.2** and **1.4.1.3**. Alternative promoter strategies used to express ribozymes in human cells and different RNA conjugates used to enhance their activity are described in sections **1.4.1.4** and **1.4.1.5**. Clinical results with anti-HIV-1 ribozymes are summarized in section **1.4.1.6**.

1.4.1.1 Natural ribozyme mechanisms

The first demonstration that an RNA molecule could function as an enzyme was provided in 1982 by Kruger and colleagues [133]. They showed that a segment of tetrahymena ribosomal precursor mRNA mediated the RNA cleavage and ligation reactions involved in intron self-splicing. These catalytic RNAs were called ribozymes and several self-splicing group I and II intron ribozymes have since been identified in the genomes of diverse species [134]. In 1983, a second class of ribozymes was identified, when it was shown that the RNA component of bacterial ribonuclease P (RNase P) complexes was responsible for mediating the cleavage of precursor tRNAs [135]. It has since been confirmed that this ribozyme is the catalytic moiety in all RNase P complexes and a variety of substrates in addition to precursor tRNAs have been identified [136]. Another ubiquitous ribozyme is found in the ribosome, where ribosomal RNA catalyzes the peptidyl transferase reaction required to link amino acids together during protein synthesis [137].

The most diverse group of ribozymes identified to date are the small self-cleaving ribozymes [138]. Ribozymes from this group include hammerhead (HH) and hairpin (Hp) ribozymes, initially identified in the tobacco ringspot virus satellite RNA, and the hepatitis delta virus (HDV) ribozyme, identified in the HDV satellite RNA of the hepatitis B virus [139]. Both HH [140, 141] and HDV-like [142, 143] ribozymes have since been identified in the genomes of a wide range of organisms where they mediate diverse functions in RNA biogenesis and regulation. Additional small self-cleaving ribozymes that have been described include the varakud satellite [144], glmS [145], CoTC [146] and the recently identified twister [147] ribozymes.

1.4.1.2 Design of therapeutic anti-HIV-1 ribozymes

Among the first ribozymes designed to inhibit HIV-1 replication were a HH [148] and a Hp [149] ribozyme targeting HIV-1 RNA. Since the natural motifs are self-cleaving (in cis), modifications were made so that they could specifically and efficiently cleave a target RNA in trans [150-152] (Figure 1.9 **a,b**). The vast majority of anti-HIV ribozymes have been based on the HH and Hp motifs and only ribozymes from these two classes have reached clinical trials (section **1.4.1.6**). Another small self-cleaving ribozyme motif that has proven amenable to the development of therapeutic ribozymes is the HDV ribozyme [153-157] (Figure 1.9 **c**) and data obtained prior to and during the execution of this thesis have shown that they have the potential to inhibit HIV-1 production and replication [158, 159]. In addition to small self-cleaving ribozymes, the endogenous activity of human RNase P (hRN-P) has been exploited to inhibit HIV-1 replication by introducing a sequence-specific antisense RNA (external guide sequence,

EGS) that binds to its target in such a way that it resembles RNase P substrates [160-162] (Figure 1.9 **d**). A modification to this approach has also been used to express bacterial RNase P (bRN-P) linked to an EGS to cleave a target in HIV-1 RNA [163]. The potential for using Group II intron ribozymes for targeted intron insertion into HIV-1 DNA has also been explored [164, 165], and future studies may identify new approaches to harness the activity of natural ribozyme motifs to inhibit HIV-1 replication.

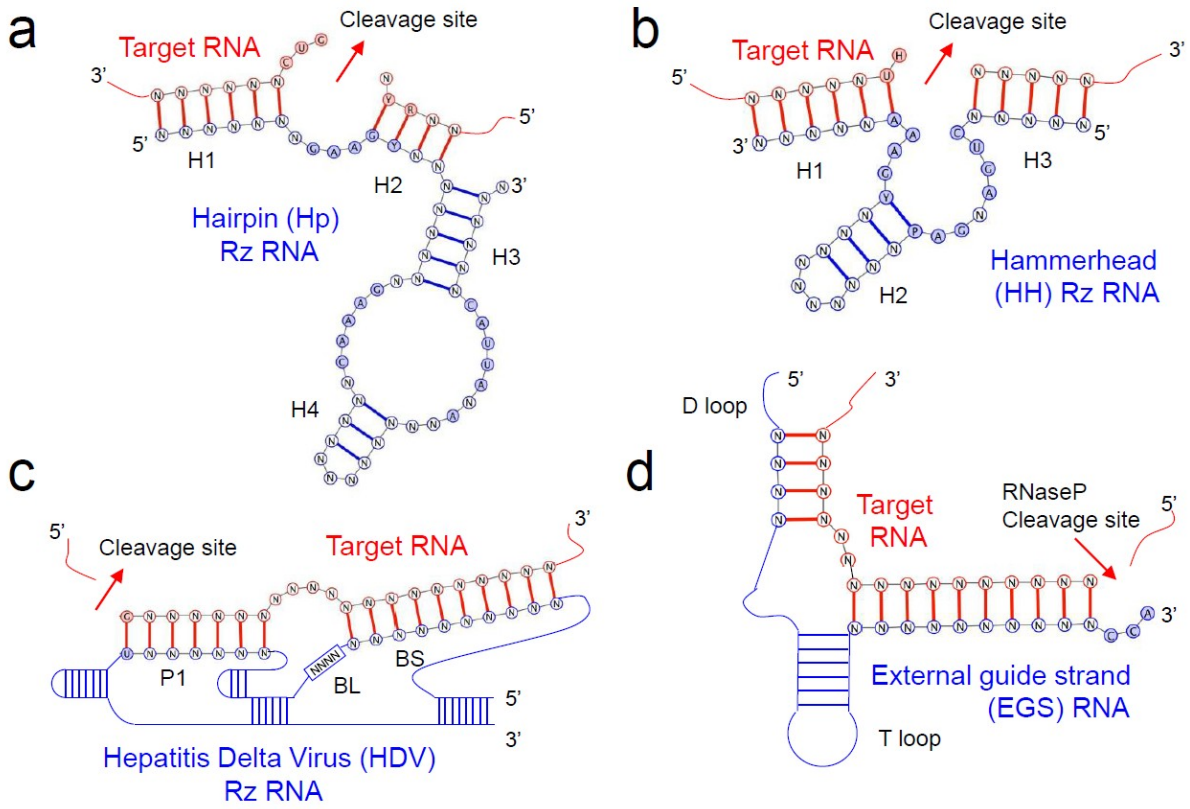

Figure 1.9. Schematic of ribozymes designed to target HIV-1 replication.

Base pairing between a ribozyme (Rz) or external guide strand (EGS) with its target RNA is shown as red bars, internal Rz or EGS base pairing is shown as blue bars. Nucleotides in the target RNA, Rz or EGS that are commonly conserved are shaded and named according to IUPAC conventions for nucleotides. The cleavage site in the target RNA is indicated with a filled red arrow. RNA secondary structures were drawn using VARNA [166]. **a) Hairpin (Hp) Rz:** In complex with its target RNA, a typical Hp Rz forms four helices (H); H1 can be lengthened to increase specificity [152]. **b) Hammerhead (HH) Rz:** In complex with its target RNA, a typical HH Rz forms three helices (H); H1 and H3 can be lengthened to increase specificity [152]. **c) Hepatitis delta virus (HDV) Rz:** In complex with its target RNA, the specific on/off adaptor (SOFA) HDV Rz forms the P1 stem of the HDV Rz and an additional biosensor (BS) stem. The BS stem can be lengthened to increase specificity and the length of the spacer (SP) in the target RNA can be changed to facilitate Rz design. An internal blocker (BL) sequence can replace the target RNA in the P1 stem, preventing it from non-specifically cleaving unintended 7 base targets [167, 168]. **d) RNase P EGS:** In complex with its target RNA, a typical EGS forms a T loop and D loop, which resemble corresponding structures in a tRNA. This structure directs cleavage by human RNase P at the indicated position in the target [160].

1.4.1.3 Anti HIV-1 ribozyme target sites

The first target site exploited for the design of anti-HIV ribozymes was a sequence in HIV-1 RNA coding for the Gag polyprotein [148]. This landmark study demonstrated that a trans-cleaving ribozyme could be used to inhibit HIV-1 gene expression when delivered from a DNA vector, and it launched a number of efforts to identify ribozymes suitable for gene therapy clinical trials. The first to reach the clinic were two Hp ribozymes targeting sequences in the 5'UTR and Pol coding sequence of HIV-1 RNA [119] (Table 1.2). Originally described in 1992 [149], the target site in the 5'UTR was attractive because of its high sequence conservation, its importance in HIV-1 replication and its presence in all spliced and unspliced HIV-1 transcripts (Figure 1.10). As HIV-1 RNA is structured [169], many potential ribozyme target sites are inaccessible and several approaches have been described to identify optimal cleavage sites. In one of the first studies to screen HIV-1 RNA for accessible ribozyme target sites, Bramlage and colleagues probed the 5'UTR using HH ribozymes with randomized binding arms [170]. Using an in vitro screen, two target sites were identified with cleavage sites upstream of genome positions 569 and 615 according to the numbering in the HIV-1 strain HXB2 (GenBank K03455). The 569 target remains one of the most popular sites for HH ribozymes, and for Hp ribozymes, with a cleavage site upstream of position 566 (Figure 1.10/Table 1.3). While a good correlation between the in vitro cleavage of the HIV-1 5'UTR and its accessibility in a cellular environment was reported [170], this is not the case for many other HIV-1 RNA sequences [171, 172], making cellular screens more appropriate for target site identification.

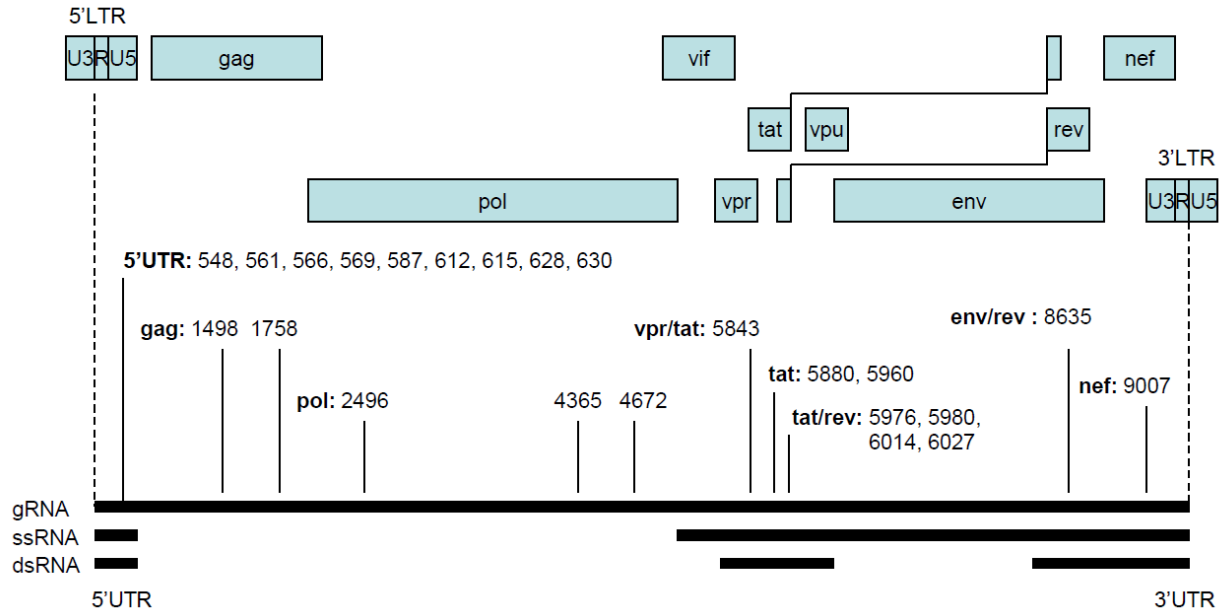

Figure 1.10. Positions of ribozyme target sites in HIV-1 RNA.

Untranslated and protein-coding regions (light blue boxes) of HIV-1 are shown above the three groups of HIV-1 RNA transcripts (black lines). Ribozyme target sites are illustrated based on their position directly after their cleavage site in reference strain HXB2 (GenBank: K03455). Approximate locations with respect to the full length genomic (g) RNA are shown. The regions present in singly-spliced (ss) and doubly-spliced (ds) transcripts are illustrated below the gRNA.

Table 1.3. Study results for different ribozyme target sites in HIV-1 RNA

Target[1]	Rz	RNA conj.	Prom.	~ % inhibition of HIV-1 expression[2]	Activity on HIV-1 replication[3]	Rz effect[4]	Ref.
UTR: 548	HH	sno-RNA	U6	~100% in 293T cells	Partial in CEM cells (pHIV7)	Strong	[173]
UTR: 561	hRNaseP	-	$tRNA^{Val}$	ND	Complete in M4C8 cells (stbl. transf.)	Strong	[160]
				ND	Partial in M4C8 cells (pLNL6)	Strong	[161]
UTR: 566 (Hp) 569 (HH)	Hp	-	β-actin	~70% in HeLa cells	ND	Strong	[149]
			$tRNA^{Val}$	~95% in HeLa cells	ND	Strong	[174]
			VA1	~85% in HeLa cells	ND	Strong	
			$tRNA^{Val}$, VA1	ND	Partial in HSC derived macrophages (pLNL6), VA1-Rz > $tRNA^{Val}$-Rz	ND	[175]
			$tRNA^{Val}$	ND	Partial in Jurkat cells (pLNL6)	ND	[176]
				ND	Partial in PBMCs (pLNL6)	ND	[177]
				ND	Partial in PBMC derived $CD4^+$ T cells (pLNL6)	ND	[178]
		RRE-SLII	$tRNA^{Val}$	ND	Partial in Molt 4/8 cells (stbl. transf.)	ND	[179]
				ND	Partial in Molt 4/8 cells (pLNL6), Hp-SLII > Hp	ND	[180]
	HH	-	U6	~40% in 293 cells	ND	Weak	[181]
		sno-RNA	U6	ND	Complete in CEM cells (pBabe)	Strong	[182]
		α–TAR	U6	ND	Partial in U87-CD4-CXCR4 cells (co-transf.)	Weak	[183]
	HH, Hp	3' cisRz	CMV	~ 40% (HH), 50% (Hp) in HeLa cells	Complete in HUT78 cells (stbl. transf.), HH = Hp	ND	[184]
		α–DIS	U6	~90% (HH), 60% (Hp) in 293T cells	ND	ND	[185]
UTR: 587	HH	-	Tk-TAR	ND	Partial in MT-4 cells (pMoTN)	ND	[186]
UTR: 612 (HH) 615 (Hp)	Hp	α–TAR	U6	ND	Complete in U87-CD4-CXCR4 cells (co-transf.)	Weak	[183]
	HH, Hp	α–DIS, DIS	U6	~ 55% (HH-αDIS), 80% (Hp-DIS) in 293T cells	ND	ND	[185]
UTR: 628	HH	$tRNA^{Lys3}$	U6	No effect in 293 cells, effects on infectivity of produced virus	ND	Weak	[187], [188]
UTR: 630	HH	3' cisRz	CMV	~ 10% in Hela cells (stbl. transf.)	ND	ND	[184]
Gag: 1498	HDV	-	H1	~ 50% in 293T cells	Partial in Jurkat cells (stbl. transf.)	Strong	[159]
Gag: 1758	HH	-	β–Actin	ND	Partial in Hela $CD4^+$ cells (stbl. transf.)	ND	[148]
Pol: 2496	Hp	-	VA1, MMLV-LTR	ND	Partial in Jurkat cells (pLNL6), VA1 > MMLV LTR	ND	[189]

Table 1.2. (cont'd): Study results for different ribozyme target sites in HIV-1 RNA

Target[1]	Rz	RNA conj.	Prom.	~ % inhibition of HIV-1 expression[2]	Activity on HIV-1 replication[3]	Rz effect[4]	Ref.
Pol: 4365		Sno RNA	U6	~100% in 293T cells	Partial in CEM cells (pHIV7)	Strong	[173]
Pol: 4672	HH	3' cisRz	CMV	~ 50% in Hela cells (stbl. transfection)	ND	ND	[184]
		-	MMLV-LTR	ND	Partial in HuT78 cells (pLN-LCo)	Strong	[190]
Vpr/Tat: 5843	HH	-	SV40	ND	Complete in SupT1 cells (stbl. transf.)	ND	[191]
		-	MMLV-LTR	ND	Partial in PBLs (pLNL6)	ND	[192]
		-	MMLV-LTR	ND	Partial in CEM T4 cells (pLNL6)	Strong	[193]
	HDV	-	CMV	~ 60% in Hela cells	ND	ND	[158]
Tat: 5880	HH	-	MMLV-LTR	ND	Partial in Jurkat cells (pBNSP1)	None	[194]
		U1sn RNA	U1	ND	Partial in Jurkat cells (stabl trans)	Strong	[195]
Tat: 5880	HH	-	MMLV-LTR	ND	Partial in CEM cells for both Rzs (pLN)	Strong	[196]
Tat/Rev: 6027	HH×2	-	MMLV-LTR, CMV, $tRNA^{Met}$	ND	Complete in CEM for all promoters (pLN)	Strong	[197]
		-	MMLV-LTR	ND	Partial in bone marrow cultures (pLN)	ND	[198]
Tat/Rev: 6014	bRNaseP	-	U6	~ 90% in 293 T cells	Partial in H9 cells (pLXSN)	Strong	[163]
Tat/Rev: 5960, 5976, 5980	HDV	-	CMV	~ 60% for all in Hela cells	ND	ND	[158]
Env/ Rev: 8635	Hp	-	$tRNA^{Val}$	ND	Complete in Molt 4/8 cells (pLNL6)	Strong	[199]
		RRE SLII	$tRNA^{Val}$		Partial in Molt 4/8 cells (pLNL6)	ND	[180]
Nef: 9007	HH	3' cisRz	CMV (3'cis HH Rz)	ND	Partial in HUT78 cells (stabl. transf.)	ND	[200]

Abbreviation: RNA conjugate (conj.), promoter (prom.), reference (ref.), not determined (ND).

[1] The HIV-1 RNA region (illustrated in Figure 1.10) followed by the nt position directly after the Rz cleavage site in HIV-1 reference strain HXB2 (GenBank K03455) is given.

[2] Results for studies with Rzs co-transfected with an HIV-1 molecular clone into cells that support expression of HIV-1, but not infection. Studies with cells stably transfected with Rz DNA are indicated (stbl. transf.).

[3] Results are reported for Rzs in cells that support HIV-1 infection. Methods of expressing Rzs are indicated in brackets, viral vectors used to transduce cells are indicated by the gene transfer plasmid used (ie. pHIV7).

[4] The Rz effect is reported for studies that compared inhibition by the Rz to an inactivated Rz or antisense control.

The first cellular screen conducted to identify target sites in HIV-1 RNA that were accessible to inhibition by ribozymes, used a randomized library based on small nucleolar RNA (snoRNA)-linked HH ribozymes [182]. Two novel target sites were identified in the HIV-1 5'UTR and Pol coding sequence (positions 548 and 4365, Figure 1.10/Table 1.3) and the corresponding ribozymes were able to strongly inhibit both HIV-1 production in an adherent cell line and virus replication in transduced $CD4^+$ T cells [173]. For other antisense molecules, several cellular screens have been conducted to identify the best antiviral candidates from libraries of molecules targeting highly conserved sequences in HIV-1 RNA [201-204]. Using this approach, Müller-Kuller and colleagues identified a target site in the Pol coding sequence of HIV-1 RNA (position 4672, Figure 1.10/Table 1.3) that was particularly accessible to the antiviral activity of a HH ribozyme [190]. In this thesis we have used a similar approach to identify a target site in the Gag coding sequence of HIV-1 RNA (position 1498, Figure 1.10/Table 1.3) [168] that was accessible to the antiviral activities of both an HDV ribozyme and a short hairpin RNA (shRNA) [159]. While several target sites in HIV-1 RNA have been identified as being accessible to different ribozymes (summarized in Table 1.3), cellular screens have been useful in identifying better target sites for previously described HH [173, 190] and HDV [159] ribozymes, and are likely to play an important role in the identification of new candidates.

In addition to HIV-1 RNA, the mRNAs for cellular factors that assist in HIV-1 replication have been the target for several antisense technologies, and one ribozyme screen has been used to identify novel target genes [205]. Most attention has been given to the β-chemokine receptor, CCR5, which serves as the co-receptor for the commonly transmitted R5-tropic HIV-1 strains and is the target for the entry inhibitor Maraviroc (section **1.3.1.3**). For the design of ribozymes,

it is important that they exclusively target the CCR5 gene and not the other highly similar β-chemokine receptor genes. The first ribozymes designed to target this gene were two HH ribozymes with cleavage occurring upstream of positions 77 [206] and 359 [207], according to a published sequence (GenBank U54994.1) (Table 1.4). Using sequence alignments, the cleavage at position 77 was shown to be highly specific for the CCR5 gene and used to design a HH ribozyme with activity against HIV-1 replication [208, 209]. In combination with an shRNA and an HIV-1 trans-activation response (TAR) RNA decoy, this ribozyme has been evaluated in advanced preclinical studies [210, 211] and in the first clinical study [128]. Potential ribozyme target sites have been identified in other regions of the CCR5 gene (summarized in Table 1.4) and, with the characterization of new cellular co-factors of HIV-1 replication [212], may soon be identified in other human genes.

Table 1.4. Study results for different ribozyme target sites in CCR5 mRNA

Target[1]	Rz	Prom.	~ % inhibition of cell surface CCR5 expression[2]	Inhibition of HIV-1 replication[3]	Rz effect[4]	Ref.
69, 445, 952	Hp	$tRNA^{Val}$	~80% in PM1 cells (pAMFT), target 69	Complete in PM1 cells (pAMFT), all targets	strong	[213]
72, 208, 304	HH×3	MMLV-LTR	Reduced in HOS-R5 cells in tandem (pLN)	ND	ND	[214]
77	HH	CMV	~ 60% from pCCR5 in HEK293 cells (co-transf.)	ND	strong	[206]
	HH	VA1	~ 70% in HOS-R5 cells (stbl transf.)	Partial in PM-1 cells (pBabe) and HOS-R5 cells (stbl transf.)	weak	[208]
			~ 50% in HOS-R5 cells (pGINa)	Partial in HSC derived macrophages (pG1Na)	weak	[209]
			Reduced in SupT1, PM1 and monocyte derived macrophages (pSV)	Partial in PM-1, SupT1, macrophage and microglial cells (pSV)	ND	[215]
			ND	Partial in HSC derived monocytes (pHIV-7: sh-Rz, sh-Rz-TAR)	ND	[210]
			ND	Partial in HSC derived thymocytes (pHIV-7: sh-Rz-TAR)	ND	[211]
359	HH	In vitro	ND	ND	ND	[207]
seven sites	HH×7	MSCV-LTR	~ 90% in PM1 cells	Complete in PM1 cells (pMGIN)	ND	[216]

Abbreviations: promoter (prom.), reference (ref.), not determined (ND).
[1] Target sites are grouped by their nt position directly after their cleavage site in the CCR5 gene (GenBank: U54994.1).
[2] Results are reported for reduction in CCR5 expression relative to control cells. Methods of expressing Rzs are indicated in brackets, viral vectors used to tranduce cells are indicated by the gene transfer plasmid used (ie. pAMFT).
[3] Results are reported for inhibition of HIV-1 replication, methods of expressing Rzs are given as in [2].
[4] The Rz effect is reported for studies that compared inhibition by the Rz to an inactivated Rz or antisense control.

1.4.1.4 Ribozyme expression strategies

The first ribozyme designed to target HIV-1 replication in human cells was expressed from the human RNA polymerase II (Pol II) β-actin promoter [148]. Other RNA Pol II promoters that have been used include elements from the simian virus 40 (SV40), cytomegalovirus (CMV) and the long terminal repeat (LTR) of moloney murine leukemia virus (MMLV) or mouse stem cell virus (MSCV) (Table 1.3 and Table 1.4). One limitation of RNA Pol II promoters is that the ribozyme must be expressed within a larger transcript and this may affect both its ability to bind

and cleave its target. Nevertheless, several HH and Hp ribozymes have been shown to be catalytically active when expressed from these promoters as a larger transcript (Table 1.3) and most clinical trials have used them to express ribozymes in patient cells (section **1.4.1.6**). Because they are expressed within an RNA transcript with both a 5' cap and a 3' poly(A) tail (Figure 1.11 **a**), ribozymes expressed from RNA Pol II promoters are transported to the cytoplasm. In the cytoplasm, ribozymes can target incoming HIV-1 RNA, new HIV-1 transcripts made from proviral DNA or the mRNAs for cellular factors involved in viral replication [152]. To reduce the effect of steric interference by the poly(A) tail, ribozyme expression vectors have been designed with a self-cleaving HH ribozyme positioned at the 3' end of the HIV-1 specific ribozyme [184, 200] (Figure 1.11 **b**). Ribozymes expressed in this manner were able to inhibit both HIV-1 gene expression and viral integration into the host cell genome [184], suggesting that the poly(A) tail is dispensable for their ability to target incoming HIV-1 RNA in the cytoplasm. To design an expression vector that responds to the presence of HIV-1 infection, a herpes thymidine kinase (Tk) RNA Pol II promoter has been engineered to express the HIV-1 TAR RNA element [186] (Figure 1.11 **c**). In the HIV-1 LTR, this structure binds to the HIV-1 Tat protein and enhances the recruitment of RNA Pol II transcription elongation factors [42] (section **1.2.2.3**). Due to enhanced ribozyme expression in cells infected by HIV-1, a HH ribozyme expressed from the Tk-TAR promoter was more effective at inhibiting HIV-1 replication compared to the same ribozyme expressed from the Tk, CMV or SV40 promoters [186]. Similar HIV-1 specific expression strategies have been used for other anti-HIV RNAs, including shRNAs [217] and microRNAs (miRNAs) [218] using either the HIV-1 LTR itself, or the TAR RNA expressed in the context of another RNA Pol II promoter.

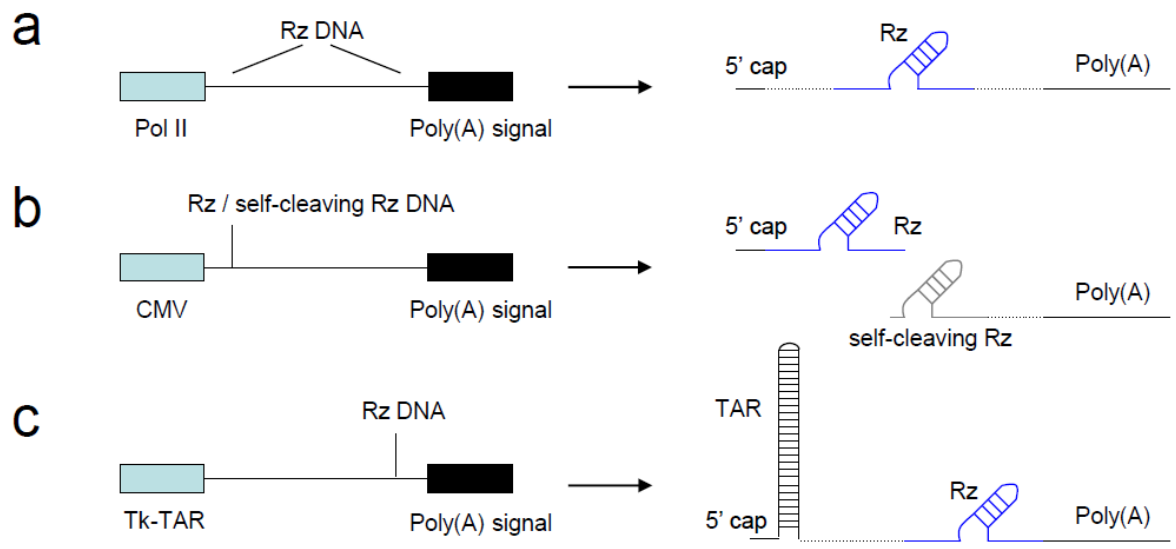

Figure 1.11. RNA Polymerase II promoter strategies for anti-HIV riboyzmes.

Promoters and poly(A) signals are shown as light blue and black boxes, respectively. Rz containing transcripts are shown with a 5' methylated cap and 3' poly(A) tail. Major double-stranded regions are illustrated, not to scale. **a) General Pol II promoter:** The Rz DNA can be inserted anywhere between the promoter and poly(A) signal. The resulting Rz transcript (blue) will be embedded in the Pol II transcript (dotted line). **b) Pol II - 3' self-cleaving Rz:** The addition of a self-cleaving Rz (grey) directly after the intended Rz (blue) can produce a Pol II promoted transcript with a defined 3' end. A CMV promoter strategy is illustrated [184]. **c) Pol II – TAR:** Modification of Pol II promoters using the HIV-1 TAR RNA enable high levels of transcription in the presence of the HIV-1 protein Tat. A modified thymidine kinase (tk) TAR RNA promoter strategy is illustrated [186].

RNA Pol III promoters exclusively express small non-coding RNAs and can be grouped in three main types according to the promoter structure [219]. Type II promoters share structurally related intragenic A and B boxes and include the virus associated (VA) 1 RNA promoter as well as most tRNA promoters [220]. Both tRNA and VA1 promoters have been used to express anti-HIV ribozymes appended to the 3' ends of the RNA transcripts and some VA1 promoters have been designed to express ribozymes within the VA1 RNA (Figure 1.12 **a**). As with RNA Pol II promoters, an advantage of the type II RNA Pol III promoters is that the RNA transcript may be localized to the cytoplasm through tRNA and VA1 RNA export pathways. Several effective anti-

HIV ribozymes expressed from tRNA promoters have been described (Table 1.3 and Table 1.4) and one has been tested in a clinical trial [119]. The design of these promoters can affect the localization of ribozymes. Some studies showed a predominantly nuclear distribution ($tRNA^{Met}$) [181, 221] and others a predominantly cytoplasmic distribution ($tRNA^{Val}$) [222]. Depending on the desired cellular localization, careful design of these promoters may be required to achieve an optimal therapeutic effect. Since VA1 RNA transcripts are predominantly cytoplasmic [223, 224], ribozymes expressed together with the VA1 RNA are expected to have a cytoplasmic distribution. To limit cellular toxicity of the VA1 RNA, ribozymes expressed within the VA1 transcript have been inserted to replace stem loop IV [208] (Figure 1.12 **a**, bottom transcript), which is known to bind the cellular p68 kinase PKR [225]. Although careful consideration of the potential VA1 RNA mediated effects is warranted, several effective ribozymes have been designed using this promoter (Table 1.3 and Table 1.4) with one advancing to clinical trials [128].

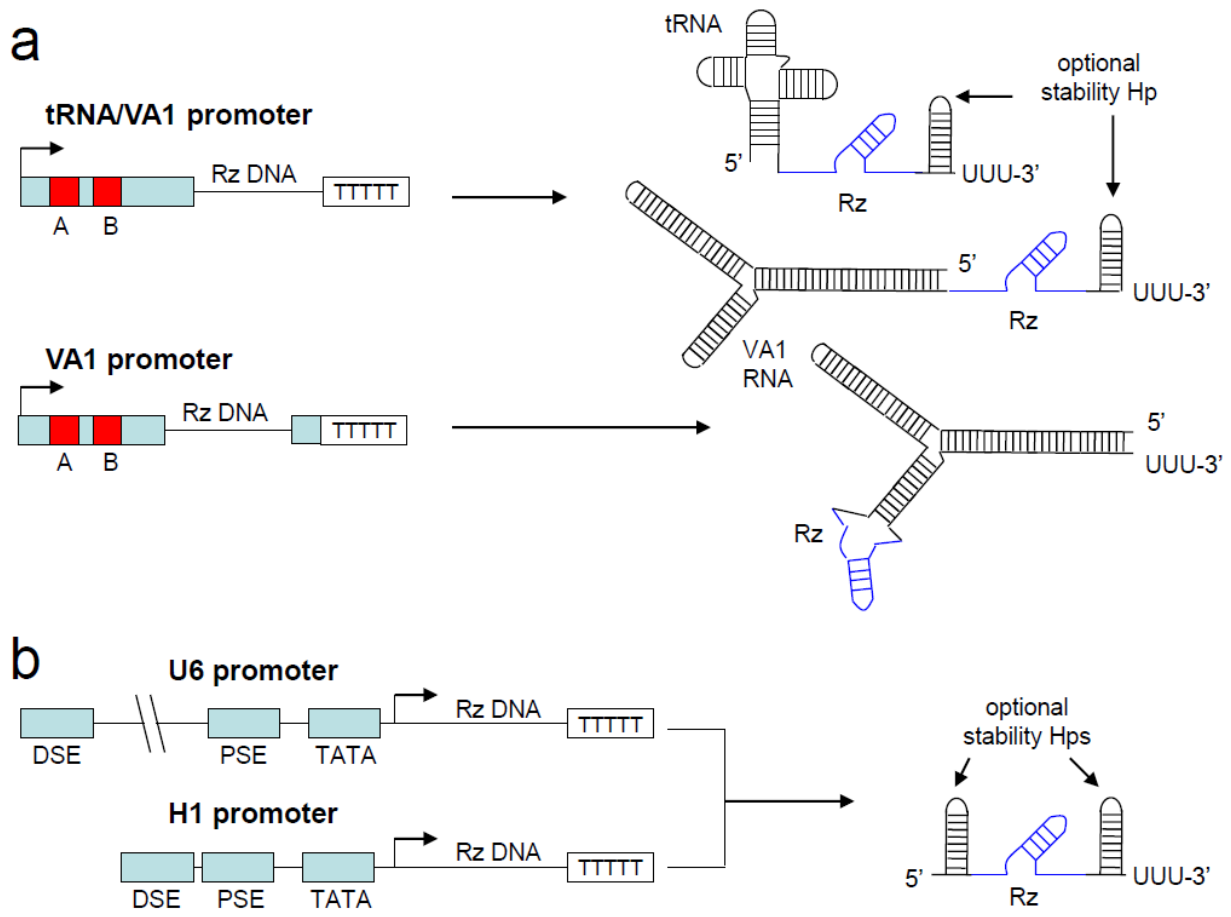

Figure 1.12. RNA Polymerase III promoter strategies for anti-HIV ribozymes.

Promoters are shown as light blue boxes and the Pol III termination sequence of 5 thymidines (T) is outlined. Examples of Rz-containing transcripts are shown with predominantly double-stranded regions illustrated, not to scale. Optional stability hairpins (Hp) are shown in some transcripts. These can be added at the transcription initiation site and/or directly before the termination signal, to protect single stranded ends from degradation by exonucleases. **a) Type II promoters:** tRNA or VA1 promoters with conserved A and B boxes highlighted in red are shown [220]. Examples of Rz transcripts (blue) expressed from these promoters are illustrated with respect to their placement in a tRNA or VA1 gene. In the bottom transcript, the Rz is expressed within VA1 RNA at the end of a stem loop [208]. **b) Type III promoters:** Distal and proximal sequence elements (DSE, PSE) as well as TATA boxes are shown for the human U6 [219] and H1 [226] promoters. The first 27 nt of the U6 transcript have been used to serve as a stability hairpin at the 5' end (called U6 + 27 promoter) [181].

Type III RNA Pol III promoters do not include intragenic regions and can be used to express any RNA with the addition of 2-4 uridines (U) at the 3' end (Figure 1.12 **b**). Examples of type III promoters include the human U6 small nuclear (sn) and H1 RNase P RNA promoters [219]. Advantages of the U6 and H1 promoters for the expression of anti-HIV-1 RNAs include their precise transcription start and end sites, high transcriptional activity in different cell types and small size [227]. U6 or H1 promoters have been used to express HDV ribozymes [159], RNase P-EGS ribozymes [163] and several HH and Hp ribozymes with different RNA conjugates added to enhance their inhibition of HIV-1 expression or replication (Table 1.3).

1.4.1.5 Ribozyme-RNA conjugates

Several studies have explored the possibility of conjugating ribozymes to different RNA structures in order to enhance their antiviral activity. The first conjugation used for this purpose was a Hp ribozyme fused to stem loop II (SLII) of the HIV-1 Rev response element (RRE) [179] (Figure 1.13**a**). The rationale behind this approach was that the SLII-RRE could serve both as a decoy RNA for the HIV-1 Rev protein and as a means to localize the ribozyme to singly-spliced and unspliced HIV-1 transcripts, which must interact with Rev to exit the nucleus. Using a similar approach, the TAR RNA has been conjugated to HH and Hp ribozymes to provide an additional decoy effect for the HIV-1 Tat protein and to localize ribozymes to their target sites in the 5'UTR of HIV-1 RNA [183, 228]. The HIV-1 dimerization initiation signal (DIS) has also been used to localize ribozymes to the 5'UTR, while also acting to directly inhibit the process of HIV-1 RNA dimerization [185] (Figure 1.13 **b**).

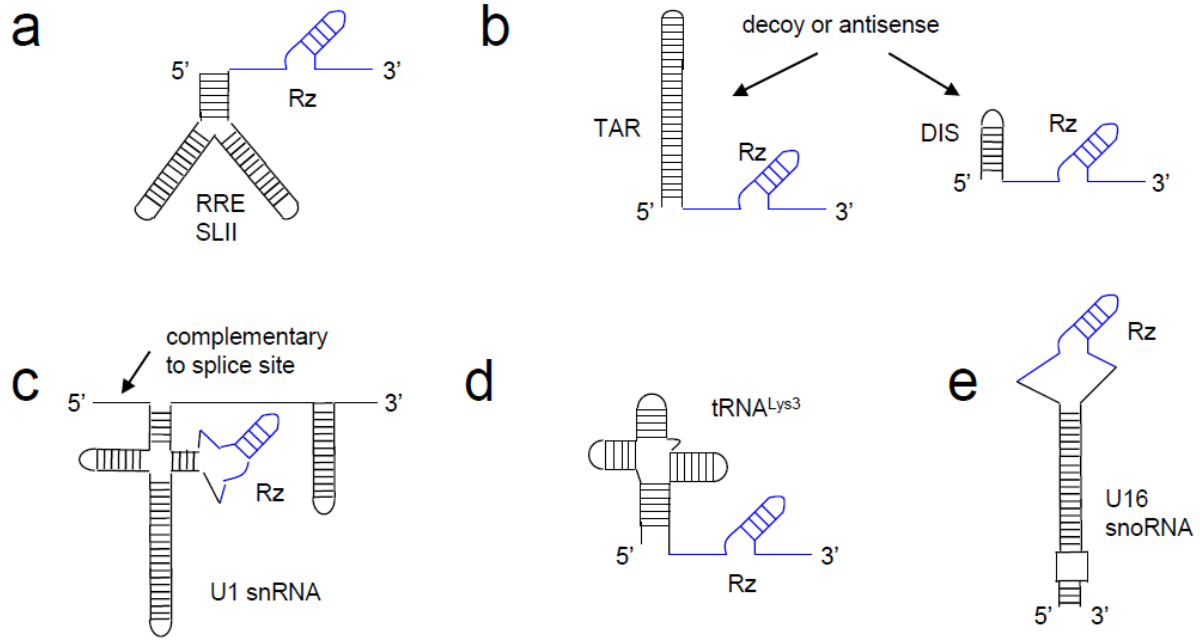

Figure 1.13. Ribozyme RNA conjugates.

Predominantly double-stranded regions of Rzs conjugated to different RNA structures are illustrated (not to scale). Depending on the Rz and its expression strategy, different RNA may be appended to the 5' or 3' ends. **a) HIV-1 Rev Response Element (RRE) stem loop II (SLII):** Acts as a decoy for HIV-1 Rev and localizes its Rz conjugate to HIV-1 transcripts that bind to Rev [179]. **b) HIV-1 trans activation response (TAR) and dimerization initiation signal (DIS):** Act as decoys for HIV-1 Tat and HIV-1 RNA dimerization, respectively. Through hybridization with their corresponding structures in HIV-1 RNA, both sense and antisense molecules can localize their Rzs to targets in the 5'UTR [183, 185]. **c) Human U1 small nuclear (sn) RNA:** Can be modified to recruit the splicing machinery to a complementary target sequence in HIV-1 RNA and localizes a Rz to that splice site [195]. **d) tRNA^{Lys3}:** Localizes a Rz to the tRNA^{Lys3} primer binding site located within the 5'UTR [188]. **e) U16 small nucleolar (sno) RNA**: Localizes a Rz to the nucleolus [182].

Human RNA motifs have also been used to enhance the antiviral effects of ribozymes. One of the first human RNAs used for this purpose was the spliceosomal U1 snRNA (Figure 1.13 **c**), modified to target the HIV-1 Rev 5' splice site and to localize a HH ribozyme to an adjacent region [195]. The tRNA^{Lys3} molecule, which binds to the 5'UTR and serves as the primer for HIV-1 reverse transcription [229] has also been used to localize ribozymes to HIV-1 RNA.

Ribozymes targeting a site adjacent to the primer binding site (position 628, Figure 1.10/Table 1.3) and conjugated to $tRNA^{Lys3}$ (Figure 1.13 **d**) were not able to inhibit HIV-1 expression, but reduced the infectivity of HIV-1 virions, suggesting that they localize with HIV-1 RNA in viral particles [187, 188]. HH ribozymes conjugated to the human U16 snoRNA (Figure 1.13 **e**) have been shown to localize to the nucleolus [182] and provide strong antiviral effects against both HIV-1 production and replication [173, 182]. Based on these results, it has been suggested that HIV-1 RNA traffics through the nucleolus [182] and co-localization in this compartment may be particularly beneficial for ribozymes targeting HIV-1 RNA.

1.4.1.6 Anti-HIV ribozymes in the clinic

The first study to evaluate the clinical potential of anti-HIV ribozymes used two Hp ribozymes targeting the 5'UTR and Pol coding sequence of HIV-1 RNA (positions 569 and 2469, Figure 1.10/Table 1.3) [119]. The ribozymes were inserted into a single MMLV vector (LNL6) and expressed from the vector LTR (position 2469) or a $tRNA^{Val}$ promoter (position 569). Following ex vivo transduction of patient-derived $CD4^+$ T cells, ribozyme expressing cells could be detected for a short term post-infusion in a single patient [230]. Only the ribozyme expressed from the $tRNA^{Val}$ promoter could be detected in this patient, leading to speculation that the $tRNA^{Val}$ promoter may be better suited for sustained ribozyme expression compared to the MMLV LTR in a clinical setting [231]. A similar clinical protocol used the MMLV LTR to express a single HH ribozyme targeting the overlapping vpr/tat coding sequence (position 5843, Figure 1.10/Table 1.3). In this trial, cells were isolated from HIV-1 negative donors and transplanted into their sero-discordant, HIV-1 positive identical twins [232]. Four pairs of sero-

discordant twins were evaluated and the recipients were followed from 29 to 44 months post-transplantation. Although expression of the ribozyme was detected in cells from all patients throughout the study period, the number of ribozyme expressing cells was low and the study was not set up to evaluate the antiviral efficacy of the ribozyme [120].

In addition to $CD4^+$ T cells, hematopoietic stem cells (HSC) have been used in an effort to express ribozymes and other anti-HIV-1 RNAs in all major HIV-1 target cells [130]. The first ribozymes evaluated for use in HSC transplant were two HH ribozymes targeting the tat and overlapping tat/rev coding sequences of HIV-1 RNA (positions 5880 and 6027, Figure 1.10/Table 1.3). The ribozymes were expressed in tandem from the MMLV LTR and transduced ex vivo into patient derived HSCs. Two trials were conducted with and without marrow ablation prior to autologous transplant [124]. Although ribozyme expression could be observed in patient cells, it did not occur at a high enough frequency to evaluate an antiviral effect in either trial. A similar trial using autologous HSC transplant without marrow ablation [121, 122] was conducted for the tat/vpr ribozyme vector evaluated for use in $CD4^+$ T cell transplant [120, 232] (position 5843, Figure 1.10/Table 1.3). A phase II clinical study was next performed with this ribozyme and for the first time a moderate antiviral effect for an anti-HIV ribozyme was observed [123]. Although improvements in the efficacy of the ribozyme therapy are needed, results from this trial have so far shown that expression of an anti-HIV ribozyme is safe and the study remains active for follow-up evaluation (ClinicalTrials.gov NCT01177059). Recently, a HH ribozyme targeting the HIV-1 entry co-receptor gene CCR5 (position 77, Table 1.4), has advanced to clinical trials in combination with other antiviral agents. This ribozyme has been introduced into patient HSCs, in combination with an shRNA and snoRNA-linked TAR decoy, using a lentiviral vector (HIV-

7) [128] (Table 1.2). A safety/efficacy study to further evaluate this therapy is ongoing (ClinicalTrials.gov NCT01961063).

1.4.2 RNA interference molecules targeting HIV-1

RNA interference (RNAi) is a process by which small double-stranded RNAs (dsRNAs) use cellular proteins to degrade or repress a target RNA. First described in 1998 [233], RNAi plays major roles in both cellular defence against pathogens and post-transcriptional gene regulation (section **1.4.2.1**). The development of different RNAi technologies as therapeutic agents is described in section **1.4.2.2** and mechanisms of toxicity that have been characterized for them are described in section **1.4.2.3**. Progress in the development of RNAi based therapies for HIV-1 infection is summarized in section **1.4.2.4**.

1.4.2.1 Natural RNA interference mechanisms

Nearly all eukaryotic cells can use the RNAi pathway to target foreign dsRNA, and in many organisms it is a major defence mechanism against pathogens [234]. Defence is accomplished through the processing of dsRNA regions of pathogenic RNA into small or short interfering RNAs (siRNAs). siRNAs then associate with cellular proteins to form an RNA-induced silencing complex (RISC), which can cleave the sequence of foreign RNA from which the siRNA was derived. A general illustration of this process is provided in Figure 1.14. In most cells, the RNA enzyme (RNase) responsible for generating the siRNAs is called Dicer and the RNase responsible for target cleavage is an argonaute (Ago) protein [235].

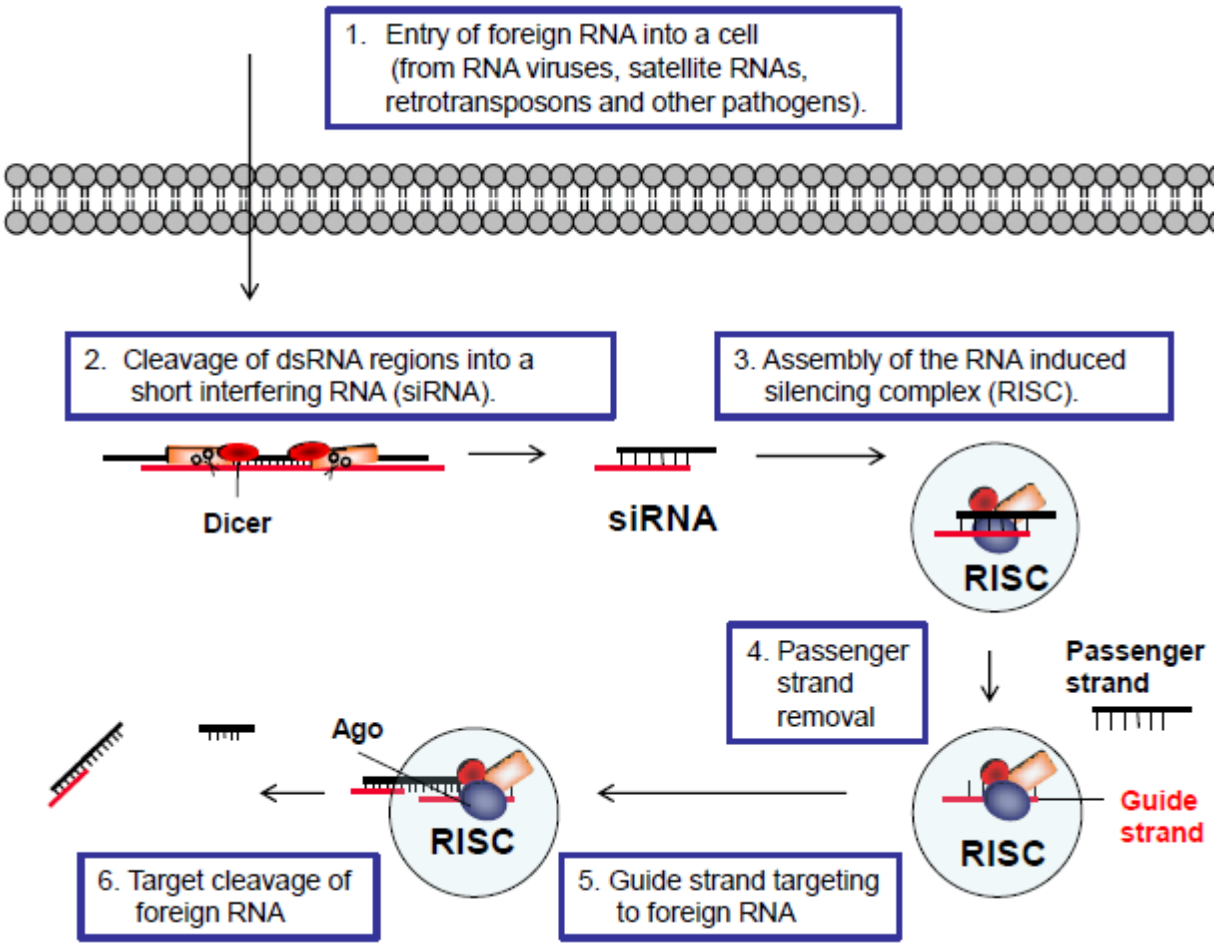

Figure 1.14. General steps of the RNAi defence pathway.

1. Pathogenic RNAs such as viral RNA, satellite RNA and retrotransposons gain access to the cytoplasm of a cell. **2.** Double-stranded RNA (dsRNA) regions of the pathogenic RNAs are recognized by a complex including the Dicer enzyme, which processes these regions into small interfering RNAs (siRNA). **3.** siRNAs are then loaded into the RNA-induced silencing complex (RISC).**4.** The passenger strand is removed from the RISC complex. **5.** The guide strand directs the RISC complex to its complementary target in the pathogenic RNA. **6.** The target sequence is cleaved by an argonaute (Ago) protein in the RISC. Adapted from [235].

Although well defined as a defence mechanism in plants and invertebrates [234], the role of RNAi in defence against mammalian pathogens has been debated. A review of several studies speculated that RNAi is not a functional immune response to mammalian viruses, as no virus-derived siRNAs were conclusively found from a variety of independent studies [236]. This view

has been challenged, with recent data providing evidence that antiviral RNAi is indeed functional in certain mammalian cell types, and that it exists alongside protein-based immunity to foreign RNAs [237]. Given the variety of protein-based RNA immune sensors available in mammalian cells, RNAi immunity may be restricted to certain cell types and pathogens. In addition, many mammalian pathogens may have evolved mechanisms to evade RNAi immunity, contributing to the small amount of evidence provided to support its existence [238].

In 2001, a role for the RNAi pathway in post-transcriptional gene regulation mediated by small dsRNAs called microRNAs (miRNAs) was first described using cells from *Caenorhabditis elegans* (*C. elegans*) [239-241] and it has since been characterized in nearly all eukaryotic organisms. Most mammalian genes are targets of this regulation [242] and to date, 2588 mature human miRNA sequences have been deposited in the miRBase database (http://www.mirbase.org/) [243]. Like siRNAs (Figure 1.14), miRNAs use the RNAi pathway to target sequences in RNA that are complementary to their guide strand. In human cells, they are derived from primary (pri-) miRNAs, which are expressed predominantly from their own RNA Pol II promoters, but can also be found in introns of other genes or expressed from RNA Pol III promoters [244]. Pri-miRNAs form a hairpin structure, which is cleaved by the RNase Drosha in complex with the RNA binding protein DGCR8, to produce a 60 to 80 nt precursor (pre-) miRNA with a two nucleotide 3' overhang at the base of the hairpin stem (Figure 1.15). Nuclear export occurs via Exportin 5 [245] and once in the cytoplasm, pre-miRNAs form a complex with the RNase Dicer and the RNA binding protein TRBP [246]. This complex directs the cleavage of the hairpin loop to produce a mature miRNA with a two nt 3' overhang on each strand. An argonaute (Ago) protein is then recruited to form the miRNA RISC (miRISC). Because of their

imperfect complementarity with their targets in different messenger RNAs (mRNAs), miRNAs typically direct translational repression or targeted degradation (Figure 1.15), as opposed to target cleavage directed by siRNAs (Figure 1.14).

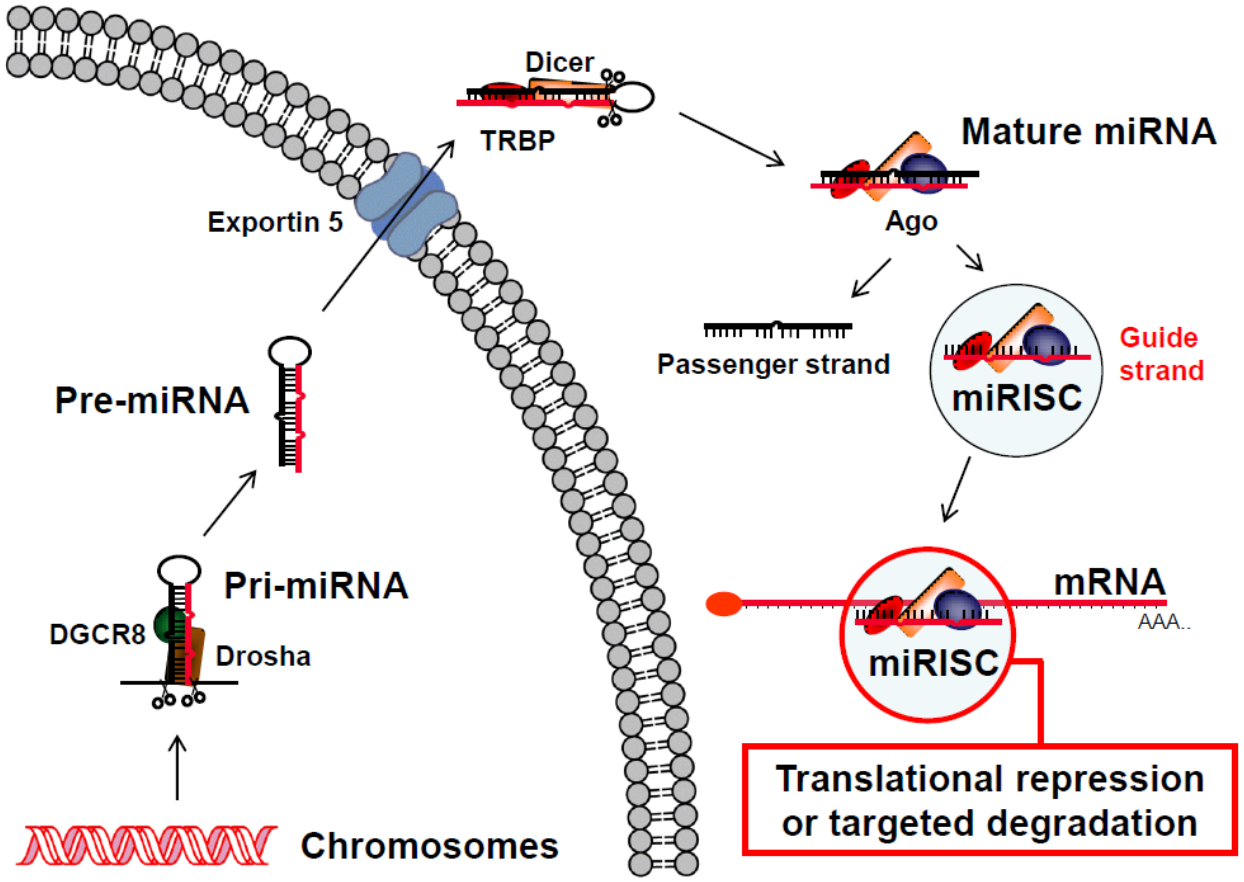

Figure 1.15. Human miRNA pathway

The general steps of the human miRNA pathway are illustrated starting with expression of a primary microRNA (Pri-miRNA) from a cell's chromosomes (bottom, left). The Pri-miRNA is recognized by the endonuclease Drosha in complex with the RNA binding protein DGCR8. Drosha cleaves the Pri-miRNA into a pre-miRNA with a 3' overhang. The pre-miRNA is then exported to the cytoplasm by the Exportin 5 transporter complex and recognized by the endonuclease Dicer in complex with the RNA binding protein TRBP. Dicer cleaves the loop off of the pre-miRNA to generate a mature miRNA. Following recruitment of additional proteins, including an Argonaute (Ago) protein, the passenger strand of the miRNA is removed and the miRISC complex targets complementary sequences in mRNA transcripts for translational repression or targeted degradation (bottom, right). Adapted from [235].

In addition to their role in cellular gene regulation, both viral and cellular derived miRNAs have been described as playing important roles in the regulation of mammalian viruses (reviewed in [247]). For example, Ouellet et al. identified two functional miRNAs derived from the HIV-1 TAR element [248] and Huang et al. demonstrated that several cellular miRNAs contribute to HIV-1 latency in resting $CD4^+$ T cells [249].

As models of RNAi evolve and new pathways are identified, unraveling the intricacies of its role in immunity and gene regulation will remain an important focus of research for several years to come. Our understanding of these mechanisms has also provided several new classes of potential therapeutic molecules that use the RNAi pathway to target pathogenic RNAs or modify pathogenic gene expression.

1.4.2.2 RNA interference therapeutics

Although the delivery of dsRNAs could elicit an RNAi response in cells from diverse organisms, a similar induction of mammalian RNAi could not initially be observed in several different cell lines [250, 251]. Following the identification of siRNAs as the processing products of dsRNA and effectors of the RNAi pathway in *Drosophila* [252, 253] and *C. elegans* [254] (Figure 1.14), Elbashir et al. and Caplan et al. showed that the delivery of these siRNAs to a variety of mammalian cell lines could elicit a potent RNAi response [255, 256]. Results also suggested that the failure to observe effective inhibition using longer dsRNAs was due to activation of dsRNA immune responses, masking RNAi effects in mammalian cells. These findings gave rise to the application of siRNAs as both research tools and potential therapeutic molecules.

The most commonly used siRNA design is often called the canonical siRNA. Canonical siRNAs are the major product of Dicer cleavage, consisting of two 21 nt RNA strands that form 19 base pairs with a 2 nt overhang at the 3' end of each strand (Figure 1.16 **a**). In this format, the siRNA does not need to be cleaved by Dicer and can enter the RISC directly. Two thymidine residues are often used for the 2 nt overhangs, initially chosen by Elbashir et al. to cut costs of synthesis and for the theoretical possibility that the DNA modifications may protect siRNAs from nucleases [255]. Although present in both strands, it had been observed that the efficiency of an siRNA was not dependent on base pairing between the guide strand overhangs and the target RNA [257]. In a study comparing different nts in the guide strand overhang, Strapps et al. found that, although similar in efficiency at early time points, a distinct disadvantage of thymidine residues compared to RNA nts was evident at later time points [258]. Since the design of efficacious siRNA drug therapies requires the most stable and potent molecules, the results of this study highlight the importance of the overhang nts to therapeutic design, and additional studies are warranted to determine what the ideal canonical siRNA format should be for any particular target sequence.

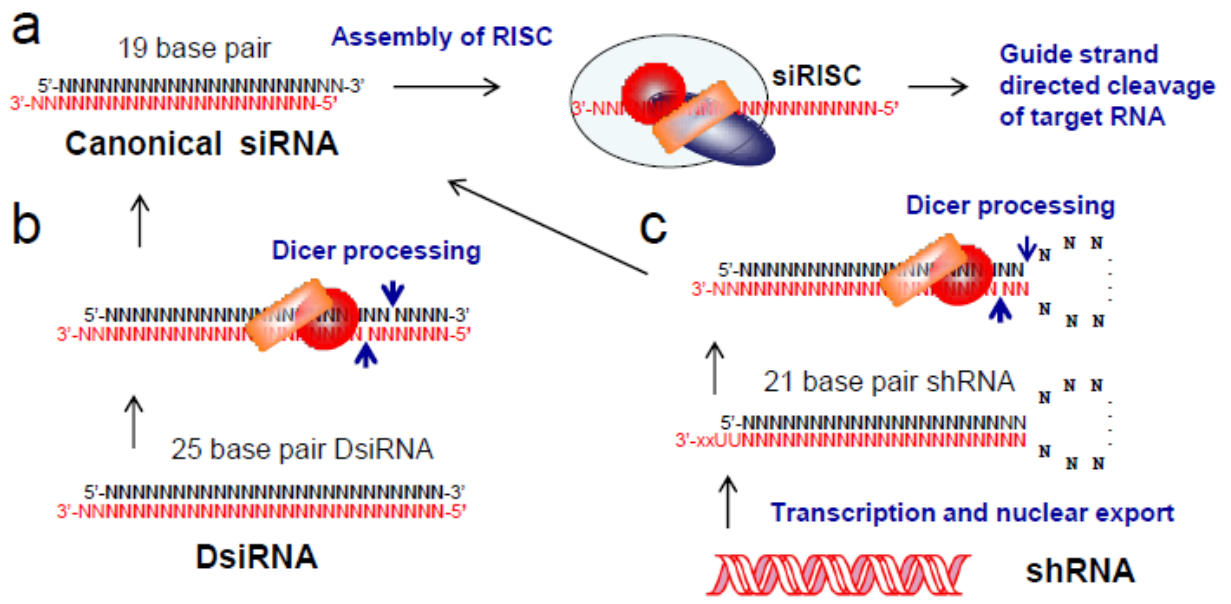

Figure 1.16. Designs of therapeutic RNAi molecules.

a) The structure of a canonical siRNA, representing the major Dicer cleavage product is illustrated. This format can enter directly into the RNA induced silencing complex (RISC) to direct the cleavage of its specified target RNA. **b)** A typical Dicer substrate siRNA (dsiRNA) is illustrated at the bottom. This format must first be processed by Dicer to generate a canonical siRNA that can enter the RISC. **c)** DNA coding for an shRNA and its transcriptional product are illustrated for a typical shRNA. As with the dsiRNA, the shRNA must be processed by Dicer to generate a canonical siRNA that can enter the RISC.

In addition to modifications in the overhangs, several non-canonical siRNA formats have been evaluated, including one or two blunt ends, various strand lengths and different nt modifications (reviewed in [259]). Results published in 2005 suggested that longer siRNAs that must first be cleaved by Dicer (termed Dicer substrate siRNAs, dsiRNA) were more effective compared to their sequence-matched canonical siRNAs [260]. Any siRNA format that must first be cleaved by Dicer can be considered a dsiRNA, and a commonly used design consists of a 27 nt guide strand and 25 nt passenger strand [261, 262] (Figure 1.16 **b**). It has been postulated that by recruiting the Dicer complex, dsiRNAs can more efficiently mediate RNAi [260, 263] and recent data demonstrated that the dsiRNA design results in better RISC assembly as well as guide

strand accumulation and loading into Ago proteins [263]. The authors of this study summarized that out of eleven dsiRNAs evaluated by their group, nine were more effective compared to their sequence-matched canonical siRNAs. Another group reported that dsiRNAs are more stable in human serum compared to canonical siRNAs [264] and they have been evaluated in preclinical mouse models of nociception [265], rheumatoid arthritis [266], human metapneumovirus infection [267], hepatitis C virus infection [268] and HIV-1 infection [269]. In contrast with reports that dsiRNAs are more potent compared to canonical designs, Foster et al. concluded that there is no difference in potency between canonical siRNAs and dsiRNAs [270] and evidence has been provided that in certain cell types, the dsiRNA designs have higher potential to elicit innate immune responses [270, 271]. Other results have reported that siRNAs with lengths shorter than the canonical siRNA can also elicit RNAi and may limit potential mechanisms of toxicity such as stimulation of innate immune responses [272, 273]. While there are conflicting results regarding the optimal length and format of therapeutic siRNAs, it is likely that the optimal design for any particular target site will require empirical data to identify the safest and most efficacious molecule for therapeutic development.

Shortly after the first descriptions of effective gene silencing by synthetic siRNAs in mammalian cells, Brummelkamp et al. showed that siRNAs could also be delivered to mammalian cells from DNA vectors expressing short hairpin RNAs (shRNAs) [274] (Figure 1.16 **c**). This enabled the development of therapeutic shRNAs for use in gene therapy, and several have been designed as antiviral genes for use in cell transplant therapies for HIV-1 infection (section **1.3.2.3**). The structure of an shRNA closely resembles a pre-miRNA (Figure 1.15), and it is exported from the nucleus and processed by Dicer in a similar manner. shRNAs are generally expressed from RNA

Pol III promoters, described in section **1.4.1.4** for ribozyme expression strategies. Transcription starts at the 5' end of the intended passenger strand and terminates at the 3' end of the intended guide strand, resulting in a guide strand overhang of two to four uridines [275] (Figure 1.16 **c**).

As with siRNAs, several alternative shRNA formats have been evaluated including alternative loop sequences and different stem lengths (reviewed in [275]). Although they are usually expressed from DNA vectors, shRNAs can also be delivered as pre-synthesized RNAs, and some data suggest that they may be more potent compared to their sequence-matched canonical siRNAs [276, 277]. In a detailed analysis of different stem lengths, McIntyre and colleagues concluded that there was no clear relationship between stem length and suppressive activity [278], suggesting that empirical data is required for a particular target site to identify the optimal shRNA format.

1.4.2.3 Mechanisms of RNAi therapeutic toxicity

As of 2012, twenty-two si/shRNA therapeutics had advanced to clinical trials for the treatment of at least sixteen different diseases, including HIV-1 infection (reviewed in [279]). Through the development process, several potential mechanisms of toxicity have been identified, and the parameters of si/shRNA design that need to be considered to develop safer therapeutics are still being defined. While siRISC-directed cleavage requires perfect complementarity between the siRNA guide strand and its target RNA, the siRNA guide and passenger strands can target partially complementary regions in human mRNA transcripts through miRISC pathways [280, 281]. The sequence requirements for miRISC pathways are not fully understood, which presents

a major limitation in terms of designing therapeutics with low potential to induce off-target gene silencing. Although they are likely to be refined, certain algorithms that include an analysis of potential off-targeting through siRISC and miRISC pathways have been developed to assist in the identification of therapeutic target sites [282, 283] (https://sispotr.icts.uiowa.edu/, http://gyanxet-beta.com). In addition to avoiding complementary sequences in unintended human mRNAs through computational approaches, the potential for siRNA candidates to affect gene expression can also be evaluated using genomic and proteomic assays in human cells.

Unlike ribozymes (section **1.4.1**), si/shRNAs require human proteins to mediate their effects and high levels of si/shRNAs have been shown to affect the activity of RNAi proteins [284]. Disturbances in the RNAi pathway can be evaluated with proteomic and genomic assays. Effects on the RNAi machinery can also be minimized by using sub-saturating levels of potent molecules. Although early studies suggested that siRNAs under 30 base pairs could inhibit a specific RNA without triggering an innate immune response [255, 285], several examples have shown that many siRNAs do trigger immune responses in diverse cell and animal models (reviewed in [286, 287]). To mitigate these effects, immunostimulatory sequences that have been identified can be avoided and modifications to particular nts in an siRNA sequence can be used to prevent immune stimulation. However, in both cases, trial and error may be required to identify siRNAs that retain potent activity against their intended targets and have low potential to elicit immune responses [286]. Although several siRNAs with good preclinical safety and efficacy have advanced to clinical trials [279], the design of siRNAs with low potential to disturb cellular pathways and elicit immune responses is likely to play an important role in the development of the next generation of siRNA molecules for therapeutic applications.

1.4.2.4 RNAi therapy for HIV-1 infection

As of 2011, over 750 si/shRNAs had been designed to target HIV-1 RNA, covering every coding and non-coding region [288]. Although several candidate therapies have been characterized, many of the target sites identified are poorly conserved and would not be suitable for the development of broadly applicable gene or drug therapies. In 2006, ter Brake et al. screened HIV-1 RNA for highly conserved shRNA target sites by calculating sequence homology in 20 nt windows among all complete HIV-1 sequences available in the Los Alamos HIV-1 database (170 at the time of analysis). Nineteen target regions were identified with high sequence conservation and out of 86 shRNAs, 21 were shown to have strong effects against HIV-1 production [203]. Four of these shRNAs were shown to be efficacious and safe in transduced T cells [289, 290] and three were proposed for combination therapy based on an evaluation of their effects in a humanized mouse model [291].

In 2007, a second genome-wide screen for highly conserved siRNA target sites in HIV-1 RNA was published by Naito et al. [201]. Similar to the ter Brake et al. study [203], they calculated sequence conservation in 21 nt windows using all complete sequences available on the LosAlamos HIV-1 database (495 at the time of analysis). They identified 216 target sequences with greater than 70% conservation and selected 41 based on activity predictions from different algorithms available at the time [292-294]. siRNAs targeting 39 of these sequences were shown to be active against HIV-1 production; however, whether these results can be extrapolated to the development of shRNA therapies is unclear. In 2009, McIntyre et al. published a new set of sequence conservation estimates using all full-length and partial gene sequences available on the Los Alamos HIV-1 database in addition to 150 proprietary subtype B sequences. The authors

designed 96 shRNAs based on their conservation estimates and ranked them according to these estimates and the activity of the shRNAs against HIV-1 production. One of the top shRNAs identified in the McIntyre et al. data set has since been evaluated in a humanized mouse model in combination with an shRNA targeting mRNA of the HIV-1 entry co-receptor, CCR5 [295].

Although several highly conserved target sites have been identified in HIV-1 RNA, the methods used to screen si/shRNAs targeting them have so far employed only one concentration of inhibitor, and a large proportion of the candidates evaluated were described as active inhibitors (from 24% in the ter Brake et al. study to 95% in the Naito et al. study) [201-203]. In a recent screen for highly accessible target sites in HIV-1 RNA, Low et al. demonstrated that concentration dependent studies can be used to distinguish potent shRNAs from among different active inhibitors [296]. They also provided evidence that a predicted secondary structure for HIV-1 NL4-3 RNA [169] could be used to identify potent shRNAs.

Evidence that sh/siRNAs targeting HIV-1 RNA can be used to safely inhibit HIV-1 replication in mouse models has been provided [211, 269, 291, 295, 297] and one candidate targeting the overlapping tat/rev coding sequence of HIV-1 RNA has advanced to a clinical trial [128] (Table 1.2). Results from different genome-wide screens suggest that sh/siRNAs targeting highly conserved and accessible target sites in HIV-1 RNA are rare and that better clinical candidates can be identified by evaluating both of these parameters.

In addition to genome-wide screens of HIV-1 RNA, three large-scale siRNA screens have been conducted to identify human genes that play a role in HIV-1 replication [298-300]. Although

many potential new target genes for si/shRNA therapy were identified, only three genes (MED7, MED8, and RELA) were found in common between the studies and well characterized co-factors of HIV-1 replication, such as LEDGF/p75, were not identified in any of them [212]. In 2011, Eekels et al. tested several shRNAs targeting 30 human genes that were previously shown to contribute to HIV-1 replication [301]. From these genes they identified TRBP, ALIX and AGT6 as being most suitable for long term inhibition of HIV-1 replication with minimal toxicity in shRNA-transduced T cell lines. An advantage of targeting mRNAs of cellular proteins involved in HIV-1 replication is that it would be very difficult for HIV-1 to develop resistance to the knockdown of a critical factor used for its replication. The major limitation is that targeting cellular genes can result in multiple and unpredictable side effects and a thorough examination will be required to determine whether down-regulating a particular HIV-1 co-factor can be tolerated in long-term therapy. As with drug therapies (section **1.3.1.3**) and ribozyme therapies (section **1.4.1.3**), the CCR5 entry co-receptor remains the most attractive HIV-1 co-factor for targeting by sh/siRNAs, and one CCR5 shRNA has recently advanced to a clinical trial (NCT-01734850) (Table 1.2).

1.5 Objectives

The general objective of this thesis was to design and evaluate anti-HIV RNAs that could be used in combination with other antiviral genes in HSC transplant therapy for HIV-1 infection. Before the start of this project, a previous post-doctoral fellow (Dr. Lainé) in Dr. Gatignol's lab had collaborated with Dr. Perreault's lab at Sherbrooke University to generate several potential anti-HIV ribozymes based on the SOFA-HDV-Rz motif. To complete the characterization of

these ribozymes, I worked in collaboration with members of Dr. Perreault's lab to generate some of the templates required for in vitro cleavage experiments and performed several experiments to characterize their activity in cell culture. Data on these ribozymes were published in 2011 [158], and showed for the first time that SOFA-HDV-Rzs could be used to target HIV-1 RNA. A limitation of these ribozymes was that, although highly active in vitro, they had weak activity in cell culture and were not significantly more active compared to their catalytically inactive antisense controls (unpublished data). Since improved HH ribozymes had been identified by screening HIV-1 RNA for accessible target sites in human cells [173, 190] (section **1.4.1.3**), the first specific objective of the work presented in this thesis was to identify more effective SOFA-HDV-Rzs by screening different regions of HIV-1 RNA for accessible and conserved target sites.

Objective 1: Identify highly conserved and accessible SOFA-HDV-Rz target sites in HIV-1 RNA

Since the SOFA-HDV-Rz binds to its target site in two adjacent regions, conservation estimates at the nt level were considered to be more appropriate for identifying highly conserved target sites in HIV-1 RNA compared to published estimates reported in 20-23 nt windows for the identification of si/shRNA target sites [201, 202] (section **1.4.2.4**). Methods developed to calculate sequence conservation at the nt level and use this data to identify highly conserved SOFA-HDV-Rz target sites in HIV-1 RNA are provided in a step-by-step protocol in Chapter 2. The methods developed to generate a library of SOFA-HDV-Rz candidates and compare their ability to inhibit HIV-1 production are also provided in Chapter 2. In agreement with previous ribozyme screens [173, 190], results presented in Chapter 3 demonstrated that among several

potential target sites in HIV-1 RNA, very few were accessible to inhibition by SOFA-HDV-Rzs. One target site starting at position 1498 in HIV-1 strain NL4-3 was identified that was particularly accessible to a SOFA-HDV-Rz. Based on these results, the next objective was to further evaluate the clinical potential of this target site for both ribozyme and shRNA therapy.

Objective 2: Evaluate the clinical potential of a SOFA-HDV-Rz and shRNA targeting a sequence in HIV-1 RNA coding for the Gag polyprotein

Based on its high sequence conservation, particular susceptibility to a SOFA-HDV-Rz and its position in a predominantly single-stranded region in a published secondary structure of HIV-1 RNA [169], it was hypothesized that the Gag 1498 target site could be used to design an shRNA with good clinical potential for HIV-1 therapy. Results presented in Chapter 3 demonstrate that, within their respective classes, both a ribozyme and shRNA directed against the Gag 1498 target site have an excellent efficacy and safety profile for further development as anti-HIV-1 therapies. The ability of the shRNA to potently inhibit HIV-1 production in diverse strains, with minimal off-target effects on human mRNAs, provided further evidence that this target site may be ideal for the development of RNAi therapies.

Objective 3: Optimize the design of siRNA and shRNA molecules targeting a sequence in HIV-1 RNA coding for the Gag polyprotein for further development as HIV-1 therapies.

Results from different studies have suggested that empirical data for a particular target site may be required to identify the optimal length and format of both therapeutic siRNAs and shRNAs (section **1.4.2.2**). For this final objective, shRNAs and siRNAs targeting the Gag 1498 site with different lengths were evaluated for effects on HIV-1 production and their potential to elicit

immune responses. The results generated for this objective are summarized in Chapter 4 and showed that the optimal length differs for siRNAs and shRNAs targeting the Gag 1498 site, providing further evidence that empirical data are necessary to identify the best format for therapeutic development.

1.6 REFERENCES

1. Greene, WC (2007). A history of AIDS: looking back to see ahead. *European journal of immunology* **37 Suppl 1**: S94-102.
2. CDC (1981). Kaposi's sarcoma and Pneumocystis pneumonia among homosexual men--New York City and California. *MMWR Morbidity and mortality weekly report* **30**: 305-308.
3. Jaffe, HW (2008). The early days of the HIV-AIDS epidemic in the USA. *Nature immunology* **9**: 1201-1203.
4. CDC (1983). Prevention of acquired immune deficiency syndrome (AIDS): report of inter-agency recommendations. *MMWR Morbidity and mortality weekly report* **32**: 101-103.
5. Barre-Sinoussi, F, Chermann, JC, Rey, F, Nugeyre, MT, Chamaret, S, Gruest, J*, et al.* (1983). Isolation of a T-lymphotropic retrovirus from a patient at risk for acquired immune deficiency syndrome (AIDS). *Science* **220**: 868-871.
6. Popovic, M, Sarngadharan, MG, Read, E, and Gallo, RC (1984). Detection, isolation, and continuous production of cytopathic retroviruses (HTLV-III) from patients with AIDS and pre-AIDS. *Science* **224**: 497-500.
7. Gallo, RC, Salahuddin, SZ, Popovic, M, Shearer, GM, Kaplan, M, Haynes, BF*, et al.* (1984). Frequent detection and isolation of cytopathic retroviruses (HTLV-III) from patients with AIDS and at risk for AIDS. *Science* **224**: 500-503.
8. Levy, JA, Hoffman, AD, Kramer, SM, Landis, JA, Shimabukuro, JM, and Oshiro, LS (1984). Isolation of lymphocytopathic retroviruses from San Francisco patients with AIDS. *Science* **225**: 840-842.
9. Coffin, J, Haase, A, Levy, JA, Montagnier, L, Oroszlan, S, Teich, N*, et al.* (1986). What to call the AIDS virus? *Nature* **321**: 10.
10. Clavel, F, Guetard, D, Brun-Vezinet, F, Chamaret, S, Rey, MA, Santos-Ferreira, MO*, et al.* (1986). Isolation of a new human retrovirus from West African patients with AIDS. *Science* **233**: 343-346.
11. Sharp, PM, and Hahn, BH (2011). Origins of HIV and the AIDS pandemic. *Cold Spring Harb Perspect Med* **1**: a006841.
12. Hirsch, VM, Olmsted, RA, Murphey-Corb, M, Purcell, RH, and Johnson, PR (1989). An African primate lentivirus (SIVsm) closely related to HIV-2. *Nature* **339**: 389-392.

13. Apetrei, C, Kaur, A, Lerche, NW, Metzger, M, Pandrea, I, Hardcastle, J*, et al.* (2005). Molecular epidemiology of simian immunodeficiency virus SIVsm in U.S. primate centers unravels the origin of SIVmac and SIVstm. *J Virol* **79**: 8991-9005.
14. Chakrabarti, L, Guyader, M, Alizon, M, Daniel, MD, Desrosiers, RC, Tiollais, P*, et al.* (1987). Sequence of simian immunodeficiency virus from macaque and its relationship to other human and simian retroviruses. *Nature* **328**: 543-547.
15. Guyader, M, Emerman, M, Sonigo, P, Clavel, F, Montagnier, L, and Alizon, M (1987). Genome organization and transactivation of the human immunodeficiency virus type 2. *Nature* **326**: 662-669.
16. Campbell-Yesufu, OT, and Gandhi, RT (2011). Update on human immunodeficiency virus (HIV)-2 infection. *Clinical infectious diseases : an official publication of the Infectious Diseases Society of America* **52**: 780-787.
17. Hemelaar, J (2013). Implications of HIV diversity for the HIV-1 pandemic. *The Journal of infection* **66**: 391-400.
18. Blackard, JT, Cohen, DE, and Mayer, KH (2002). Human immunodeficiency virus superinfection and recombination: current state of knowledge and potential clinical consequences. *Clinical infectious diseases : an official publication of the Infectious Diseases Society of America* **34**: 1108-1114.
19. Hemelaar, J, Gouws, E, Ghys, PD, and Osmanov, S (2011). Global trends in molecular epidemiology of HIV-1 during 2000-2007. *AIDS* **25**: 679-689.
20. Gorry, PR, Ong, C, Thorpe, J, Bannwarth, S, Thompson, KA, Gatignol, A*, et al.* (2003). Astrocyte infection by HIV-1: mechanisms of restricted virus replication, and role in the pathogenesis of HIV-1-associated dementia. *Curr HIV Res* **1**: 463-473.
21. Ott, DE (2008). Cellular proteins detected in HIV-1. *Reviews in medical virology* **18**: 159-175.
22. Swanson, CM, and Malim, MH (2008). SnapShot: HIV-1 proteins. *Cell* **133**: 742, 742.e741.
23. Adamson, CS, and Freed, EO (2007). Human immunodeficiency virus type 1 assembly, release, and maturation. *Adv Pharmacol* **55**: 347-387.
24. Briggs, JA, and Krausslich, HG (2011). The molecular architecture of HIV. *J Mol Biol* **410**: 491-500.
25. Collins, DR, and Collins, KL (2014). HIV-1 accessory proteins adapt cellular adaptors to facilitate immune evasion. *PLoS pathogens* **10**: e1003851.
26. Foster, JL, and Garcia, JV (2007). Role of Nef in HIV-1 replication and pathogenesis. *Adv Pharmacol* **55**: 389-409.
27. Guy, B, Kieny, MP, Riviere, Y, Le Peuch, C, Dott, K, Girard, M*, et al.* (1987). HIV F/3' orf encodes a phosphorylated GTP-binding protein resembling an oncogene product. *Nature* **330**: 266-269.
28. Schwartz, O, Marechal, V, Le Gall, S, Lemonnier, F, and Heard, JM (1996). Endocytosis of major histocompatibility complex class I molecules is induced by the HIV-1 Nef protein. *Nature medicine* **2**: 338-342.
29. Stumptner-Cuvelette, P, Morchoisne, S, Dugast, M, Le Gall, S, Raposo, G, Schwartz, O*, et al.* (2001). HIV-1 Nef impairs MHC class II antigen presentation and surface expression. *Proc Natl Acad Sci U S A* **98**: 12144-12149.
30. Foster, JL, and Garcia, JV (2008). HIV-1 Nef: at the crossroads. *Retrovirology* **5**: 84.

31. Neil, SJ, Zang, T, and Bieniasz, PD (2008). Tetherin inhibits retrovirus release and is antagonized by HIV-1 Vpu. *Nature* **451**: 425-430.
32. Mitchell, RS, Katsura, C, Skasko, MA, Fitzpatrick, K, Lau, D, Ruiz, A*, et al.* (2009). Vpu antagonizes BST-2-mediated restriction of HIV-1 release via beta-TrCP and endo-lysosomal trafficking. *PLoS pathogens* **5**: e1000450.
33. Klasse, PJ (2012). The molecular basis of HIV entry. *Cellular microbiology* **14**: 1183-1192.
34. Fais, S, Capobianchi, MR, Abbate, I, Castilletti, C, Gentile, M, Cordiali Fei, P*, et al.* (1995). Unidirectional budding of HIV-1 at the site of cell-to-cell contact is associated with co-polarization of intercellular adhesion molecules and HIV-1 viral matrix protein. *AIDS* **9**: 329-335.
35. Gorry, PR, and Ancuta, P (2011). Coreceptors and HIV-1 pathogenesis. *Current HIV/AIDS reports* **8**: 45-53.
36. Harouse, JM, Gettie, A, Tan, RC, Blanchard, J, and Cheng-Mayer, C (1999). Distinct pathogenic sequela in rhesus macaques infected with CCR5 or CXCR4 utilizing SHIVs. *Science* **284**: 816-819.
37. Arhel, N (2010). Revisiting HIV-1 uncoating. *Retrovirology* **7**: 96.
38. Esposito, F, Corona, A, and Tramontano, E (2012). HIV-1 Reverse Transcriptase Still Remains a New Drug Target: Structure, Function, Classical Inhibitors, and New Inhibitors with Innovative Mechanisms of Actions. *Molecular biology international* **2012**: 586401.
39. Abbink, TE, and Berkhout, B (2007). HIV-1 reverse transcription: close encounters between the viral genome and a cellular tRNA. *Adv Pharmacol* **55**: 99-135.
40. Krishnan, L, and Engelman, A (2012). Retroviral integrase proteins and HIV-1 DNA integration. *J Biol Chem* **287**: 40858-40866.
41. Levin, A, Loyter, A, and Bukrinsky, M (2011). Strategies to inhibit viral protein nuclear import: HIV-1 as a target. *Biochimica et Biophysica Acta (BBA) - Molecular Cell Research* **1813**: 1646-1653.
42. Gatignol, A (2007). Transcription of HIV: Tat and cellular chromatin. *Adv Pharmacol* **55**: 137-159.
43. Tazi, J, Bakkour, N, Marchand, V, Ayadi, L, Aboufirassi, A, and Branlant, C (2010). Alternative splicing: regulation of HIV-1 multiplication as a target for therapeutic action. *The FEBS journal* **277**: 867-876.
44. Lever, AM (2007). HIV-1 RNA packaging. *Adv Pharmacol* **55**: 1-32.
45. Neville, M, Stutz, F, Lee, L, Davis, LI, and Rosbash, M (1997). The importin-beta family member Crm1p bridges the interaction between Rev and the nuclear pore complex during nuclear export. *Curr Biol* **7**: 767-775.
46. Brasey, A, Lopez-Lastra, M, Ohlmann, T, Beerens, N, Berkhout, B, Darlix, JL*, et al.* (2003). The leader of human immunodeficiency virus type 1 genomic RNA harbors an internal ribosome entry segment that is active during the G2/M phase of the cell cycle. *J Virol* **77**: 3939-3949.
47. Burugu, S, Daher, A, Meurs, EF, and Gatignol, A (2014). HIV-1 translation and its regulation by cellular factors PKR and PACT. *Virus Res* **193**: 65-77.

48. Cai, R, Carpick, B, Chun, RF, Jeang, KT, and Williams, BR (2000). HIV-I TAT inhibits PKR activity by both RNA-dependent and RNA-independent mechanisms. *Archives of biochemistry and biophysics* **373**: 361-367.
49. Daher, A, Longuet, M, Dorin, D, Bois, F, Segeral, E, Bannwarth, S*, et al.* (2001). Two dimerization domains in the trans-activation response RNA-binding protein (TRBP) individually reverse the protein kinase R inhibition of HIV-1 long terminal repeat expression. *J Biol Chem* **276**: 33899-33905.
50. Clerzius, G, Gélinas, JF, Daher, A, Bonnet, M, Meurs, EF, and Gatignol, A (2009). ADAR1 interacts with PKR during human immunodeficiency virus infection of lymphocytes and contributes to viral replication. *J Virol* **83**: 10119-10128.
51. Clerzius, G, Shaw, E, Daher, A, Burugu, S, Gelinas, JF, Ear, T*, et al.* (2013). The PKR activator, PACT, becomes a PKR inhibitor during HIV-1 replication. *Retrovirology* **10**: 96.
52. Peterlin, BM, and Trono, D (2003). Hide, shield and strike back: how HIV-infected cells avoid immune eradication. *Nat Rev Immunol* **3**: 97-107.
53. Karn, J, and Stoltzfus, CM (2012). Transcriptional and posttranscriptional regulation of HIV-1 gene expression. *Cold Spring Harb Perspect Med* **2**: a006916.
54. Hallenberger, S, Bosch, V, Angliker, H, Shaw, E, Klenk, HD, and Garten, W (1992). Inhibition of furin-mediated cleavage activation of HIV-1 glycoprotein gp160. *Nature* **360**: 358-361.
55. Kutluay, SB, Zang, T, Blanco-Melo, D, Powell, C, Jannain, D, Errando, M*, et al.* (2014). Global changes in the RNA binding specificity of HIV-1 gag regulate virion genesis. *Cell* **159**: 1096-1109.
56. Garrus, JE, von Schwedler, UK, Pornillos, OW, Morham, SG, Zavitz, KH, Wang, HE*, et al.* (2001). Tsg101 and the vacuolar protein sorting pathway are essential for HIV-1 budding. *Cell* **107**: 55-65.
57. Fisher, RD, Chung, HY, Zhai, Q, Robinson, H, Sundquist, WI, and Hill, CP (2007). Structural and biochemical studies of ALIX/AIP1 and its role in retrovirus budding. *Cell* **128**: 841-852.
58. Sundquist, WI, and Krausslich, HG (2012). HIV-1 assembly, budding, and maturation. *Cold Spring Harb Perspect Med* **2**: a006924.
59. Fauci, AS, Pantaleo, G, Stanley, S, and Weissman, D (1996). Immunopathogenic mechanisms of HIV infection. *Annals of internal medicine* **124**: 654-663.
60. Moir, S, Chun, TW, and Fauci, AS (2011). Pathogenic mechanisms of HIV disease. *Annual review of pathology* **6**: 223-248.
61. Cohen, MS, Shaw, GM, McMichael, AJ, and Haynes, BF (2011). Acute HIV-1 Infection. *New England Journal of Medicine* **364**: 1943-1954.
62. Mellors, JW, Rinaldo, CR, Jr., Gupta, P, White, RM, Todd, JA, and Kingsley, LA (1996). Prognosis in HIV-1 infection predicted by the quantity of virus in plasma. *Science* **272**: 1167-1170.
63. Henrich, TJ, and Gandhi, RT (2013). Early treatment and HIV-1 reservoirs: a stitch in time? *The Journal of infectious diseases* **208**: 1189-1193.
64. Persaud, D, Gay, H, Ziemniak, C, Chen, YH, Piatak, M, Jr., Chun, TW*, et al.* (2013). Absence of detectable HIV-1 viremia after treatment cessation in an infant. *The New England journal of medicine* **369**: 1828-1835.

65. Saez-Cirion, A, Bacchus, C, Hocqueloux, L, Avettand-Fenoel, V, Girault, I, Lecuroux, C*, et al.* (2013). Post-treatment HIV-1 controllers with a long-term virological remission after the interruption of early initiated antiretroviral therapy ANRS VISCONTI Study. *PLoS pathogens* **9**: e1003211.
66. Lackner, AA, Mohan, M, and Veazey, RS (2009). The gastrointestinal tract and AIDS pathogenesis. *Gastroenterology* **136**: 1965-1978.
67. Costiniuk, CT, and Angel, JB (2012). Human immunodeficiency virus and the gastrointestinal immune system: does highly active antiretroviral therapy restore gut immunity[quest]. *Mucosal Immunol* **5**: 596-604.
68. Boshoff, C, and Weiss, R (2002). Aids-related malignancies. *Nat Rev Cancer* **2**: 373-382.
69. Arts, EJ, and Hazuda, DJ (2012). HIV-1 antiretroviral drug therapy. *Cold Spring Harb Perspect Med* **2**: a007161.
70. Grobler, JA, and Hazuda, DJ (2014). Resistance to HIV integrase strand transfer inhibitors: in vitro findings and clinical consequences. *Current opinion in virology* **8c**: 98-103.
71. Wong, JK, Hezareh, M, Gunthard, HF, Havlir, DV, Ignacio, CC, Spina, CA*, et al.* (1997). Recovery of replication-competent HIV despite prolonged suppression of plasma viremia. *Science* **278**: 1291-1295.
72. Finzi, D, Hermankova, M, Pierson, T, Carruth, LM, Buck, C, Chaisson, RE*, et al.* (1997). Identification of a reservoir for HIV-1 in patients on highly active antiretroviral therapy. *Science* **278**: 1295-1300.
73. Finzi, D, Blankson, J, Siliciano, JD, Margolick, JB, Chadwick, K, Pierson, T*, et al.* (1999). Latent infection of CD4+ T cells provides a mechanism for lifelong persistence of HIV-1, even in patients on effective combination therapy. *Nature medicine* **5**: 512-517.
74. Deeks, SG, Autran, B, Berkhout, B, Benkirane, M, Cairns, S, Chomont, N*, et al.* (2012). Towards an HIV cure: a global scientific strategy. *Nat Rev Immunol* **12**: 607-614.
75. Cihlar, T, and Ray, AS (2010). Nucleoside and nucleotide HIV reverse transcriptase inhibitors: 25 years after zidovudine. *Antiviral research* **85**: 39-58.
76. De Clercq, E (2007). The design of drugs for HIV and HCV. *Nature reviews Drug discovery* **6**: 1001-1018.
77. De Clercq, E (2010). Antiretroviral drugs. *Curr Opin Pharmacol* **10**: 507-515.
78. Hang, JQ, Li, Y, Yang, Y, Cammack, N, Mirzadegan, T, and Klumpp, K (2007). Substrate-dependent inhibition or stimulation of HIV RNase H activity by non-nucleoside reverse transcriptase inhibitors (NNRTIs). *Biochem Biophys Res Commun* **352**: 341-350.
79. Wlodawer, A, and Vondrasek, J (1998). Inhibitors of HIV-1 protease: a major success of structure-assisted drug design. *Annual review of biophysics and biomolecular structure* **27**: 249-284.
80. Wensing, AM, van Maarseveen, NM, and Nijhuis, M (2010). Fifteen years of HIV Protease Inhibitors: raising the barrier to resistance. *Antiviral research* **85**: 59-74.
81. Matthews, T, Salgo, M, Greenberg, M, Chung, J, DeMasi, R, and Bolognesi, D (2004). Enfuvirtide: the first therapy to inhibit the entry of HIV-1 into host CD4 lymphocytes. *Nature reviews Drug discovery* **3**: 215-225.
82. Yu, F, Lu, L, Du, L, Zhu, X, Debnath, AK, and Jiang, S (2013). Approaches for identification of HIV-1 entry inhibitors targeting gp41 pocket. *Viruses* **5**: 127-149.

83. Liu, R, Paxton, WA, Choe, S, Ceradini, D, Martin, SR, Horuk, R, *et al.* (1996). Homozygous defect in HIV-1 coreceptor accounts for resistance of some multiply-exposed individuals to HIV-1 infection. *Cell* **86**: 367-377.
84. Perry, CM (2010). Maraviroc: a review of its use in the management of CCR5-tropic HIV-1 infection. *Drugs* **70**: 1189-1213.
85. Hendrix, CW, Collier, AC, Lederman, MM, Schols, D, Pollard, RB, Brown, S, *et al.* (2004). Safety, pharmacokinetics, and antiviral activity of AMD3100, a selective CXCR4 receptor inhibitor, in HIV-1 infection. *Journal of acquired immune deficiency syndromes (1999)* **37**: 1253-1262.
86. Keating, GM (2011). Plerixafor: a review of its use in stem-cell mobilization in patients with lymphoma or multiple myeloma. *Drugs* **71**: 1623-1647.
87. MacFarland, R, Hard, ML, Scarborough, R, Badel, K, and Calandra, G (2010). A pharmacokinetic study of plerixafor in subjects with varying degrees of renal impairment. *Biology of blood and marrow transplantation : journal of the American Society for Blood and Marrow Transplantation* **16**: 95-101.
88. Nyunt, MM, Becker, S, MacFarland, RT, Chee, P, Scarborough, R, Everts, S, *et al.* (2008). Pharmacokinetic effect of AMD070, an Oral CXCR4 antagonist, on CYP3A4 and CYP2D6 substrates midazolam and dextromethorphan in healthy volunteers. *Journal of acquired immune deficiency syndromes (1999)* **47**: 559-565.
89. Bodart, V, Anastassov, V, Darkes, MC, Idzan, SR, Labrecque, J, Lau, G, *et al.* (2009). Pharmacology of AMD3465: a small molecule antagonist of the chemokine receptor CXCR4. *Biochemical pharmacology* **78**: 993-1000.
90. Perelson, AS, Essunger, P, Cao, Y, Vesanen, M, Hurley, A, Saksela, K, *et al.* (1997). Decay characteristics of HIV-1-infected compartments during combination therapy. *Nature* **387**: 188-191.
91. Chomont, N, El-Far, M, Ancuta, P, Trautmann, L, Procopio, FA, Yassine-Diab, B, *et al.* (2009). HIV reservoir size and persistence are driven by T cell survival and homeostatic proliferation. *Nature medicine* **15**: 893-900.
92. Ruelas, DS, and Greene, WC (2013). An integrated overview of HIV-1 latency. *Cell* **155**: 519-529.
93. Chun, TW, Engel, D, Mizell, SB, Hallahan, CW, Fischette, M, Park, S, *et al.* (1999). Effect of interleukin-2 on the pool of latently infected, resting CD4+ T cells in HIV-1-infected patients receiving highly active anti-retroviral therapy. *Nature medicine* **5**: 651-655.
94. Stellbrink, HJ, van Lunzen, J, Westby, M, O'Sullivan, E, Schneider, C, Adam, A, *et al.* (2002). Effects of interleukin-2 plus highly active antiretroviral therapy on HIV-1 replication and proviral DNA (COSMIC trial). *Aids* **16**: 1479-1487.
95. Prins, JM, Jurriaans, S, van Praag, RM, Blaak, H, van Rij, R, Schellekens, PT, *et al.* (1999). Immuno-activation with anti-CD3 and recombinant human IL-2 in HIV-1-infected patients on potent antiretroviral therapy. *Aids* **13**: 2405-2410.
96. van Praag, RM, Prins, JM, Roos, MT, Schellekens, PT, Ten Berge, IJ, Yong, SL, *et al.* (2001). OKT3 and IL-2 treatment for purging of the latent HIV-1 reservoir in vivo results in selective long-lasting CD4+ T cell depletion. *Journal of clinical immunology* **21**: 218-226.

97. Kulkosky, J, Nunnari, G, Otero, M, Calarota, S, Dornadula, G, Zhang, H*, et al.* (2002). Intensification and stimulation therapy for human immunodeficiency virus type 1 reservoirs in infected persons receiving virally suppressive highly active antiretroviral therapy. *The Journal of infectious diseases* **186**: 1403-1411.
98. Xing, S, and Siliciano, RF (2013). Targeting HIV latency: pharmacologic strategies toward eradication. *Drug discovery today* **18**: 541-551.
99. Lehrman, G, Hogue, IB, Palmer, S, Jennings, C, Spina, CA, Wiegand, A*, et al.* (2005). Depletion of latent HIV-1 infection in vivo: a proof-of-concept study. *Lancet* **366**: 549-555.
100. Sagot-Lerolle, N, Lamine, A, Chaix, ML, Boufassa, F, Aboulker, JP, Costagliola, D*, et al.* (2008). Prolonged valproic acid treatment does not reduce the size of latent HIV reservoir. *Aids* **22**: 1125-1129.
101. Archin, NM, Cheema, M, Parker, D, Wiegand, A, Bosch, RJ, Coffin, JM*, et al.* (2010). Antiretroviral intensification and valproic acid lack sustained effect on residual HIV-1 viremia or resting CD4+ cell infection. *PLoS One* **5**: e9390.
102. Elliott, JH, Wightman, F, Solomon, A, Ghneim, K, Ahlers, J, Cameron, MJ*, et al.* (2014). Activation of HIV Transcription with Short-Course Vorinostat in HIV-Infected Patients on Suppressive Antiretroviral Therapy. *PLoS pathogens* **10**: e1004473.
103. Archin, NM, and Margolis, DM (2014). Emerging strategies to deplete the HIV reservoir. *Current opinion in infectious diseases* **27**: 29-35.
104. Shan, L, Deng, K, Shroff, NS, Durand, CM, Rabi, SA, Yang, HC*, et al.* (2012). Stimulation of HIV-1-specific cytolytic T lymphocytes facilitates elimination of latent viral reservoir after virus reactivation. *Immunity* **36**: 491-501.
105. Kumar, A, Abbas, W, and Herbein, G (2014). HIV-1 latency in monocytes/macrophages. *Viruses* **6**: 1837-1860.
106. Vanham, G, and Van Gulck, E (2012). Can immunotherapy be useful as a "functional cure" for infection with Human Immunodeficiency Virus-1? *Retrovirology* **9**: 72.
107. Walker, BD, and Yu, XG (2013). Unravelling the mechanisms of durable control of HIV-1. *Nat Rev Immunol* **13**: 487-498.
108. Hoxie, JA, and June, CH (2012). Novel cell and gene therapies for HIV. *Cold Spring Harb Perspect Med* **2**: a007179.
109. Allers, K, Hutter, G, Hofmann, J, Loddenkemper, C, Rieger, K, Thiel, E*, et al.* (2011). Evidence for the cure of HIV infection by CCR5Delta32/Delta32 stem cell transplantation. *Blood* **117**: 2791-2799.
110. Baltimore, D (1988). Gene therapy. Intracellular immunization. *Nature* **335**: 395-396.
111. Woffendin, C, Ranga, U, Yang, Z, Xu, L, and Nabel, GJ (1996). Expression of a protective gene-prolongs survival of T cells in human immunodeficiency virus-infected patients. *Proc Natl Acad Sci U S A* **93**: 2889-2894.
112. Ranga, U, Woffendin, C, Verma, S, Xu, L, June, CH, Bishop, DK*, et al.* (1998). Enhanced T cell engraftment after retroviral delivery of an antiviral gene in HIV-infected individuals. *Proc Natl Acad Sci U S A* **95**: 1201-1206.
113. Podsakoff, GM, Engel, BC, Carbonaro, DA, Choi, C, Smogorzewska, EM, Bauer, G*, et al.* (2005). Selective survival of peripheral blood lymphocytes in children with HIV-1 following delivery of an anti-HIV gene to bone marrow CD34(+) cells. *Mol Ther* **12**: 77-86.

114. Morgan, RA, Walker, R, Carter, CS, Natarajan, V, Tavel, JA, Bechtel, C*, et al.* (2005). Preferential survival of CD4+ T lymphocytes engineered with anti-human immunodeficiency virus (HIV) genes in HIV-infected individuals. *Hum Gene Ther* **16**: 1065-1074.
115. Kang, EM, de Witte, M, Malech, H, Morgan, RA, Phang, S, Carter, C*, et al.* (2002). Nonmyeloablative conditioning followed by transplantation of genetically modified HLA-matched peripheral blood progenitor cells for hematologic malignancies in patients with acquired immunodeficiency syndrome. *Blood* **99**: 698-701.
116. Hayakawa, J, Washington, K, Uchida, N, Phang, O, Kang, EM, Hsieh, MM*, et al.* (2009). Long-term vector integration site analysis following retroviral mediated gene transfer to hematopoietic stem cells for the treatment of HIV infection. *PLoS One* **4**: e4211.
117. van Lunzen, J, Glaunsinger, T, Stahmer, I, von Baehr, V, Baum, C, Schilz, A*, et al.* (2007). Transfer of autologous gene-modified T cells in HIV-infected patients with advanced immunodeficiency and drug-resistant virus. *Mol Ther* **15**: 1024-1033.
118. Tebas, P, Stein, D, Tang, WW, Frank, I, Wang, SQ, Lee, G*, et al.* (2014). Gene editing of CCR5 in autologous CD4 T cells of persons infected with HIV. *The New England journal of medicine* **370**: 901-910.
119. Wong-Staal, F, Poeschla, EM, and Looney, DJ (1998). A controlled, Phase 1 clinical trial to evaluate the safety and effects in HIV-1 infected humans of autologous lymphocytes transduced with a ribozyme that cleaves HIV-1 RNA. *Hum Gene Ther* **9**: 2407-2425.
120. Macpherson, JL, Boyd, MP, Arndt, AJ, Todd, AV, Fanning, GC, Ely, JA*, et al.* (2005). Long-term survival and concomitant gene expression of ribozyme-transduced CD4+ T-lymphocytes in HIV-infected patients. *J Gene Med* **7**: 552-564.
121. Amado, RG, Mitsuyasu, RT, Symonds, G, Rosenblatt, JD, Zack, J, Sun, LQ*, et al.* (1999). A phase I trial of autologous CD34+ hematopoietic progenitor cells transduced with an anti-HIV ribozyme. *Hum Gene Ther* **10**: 2255-2270.
122. Amado, RG, Mitsuyasu, RT, Rosenblatt, JD, Ngok, FK, Bakker, A, Cole, S*, et al.* (2004). Anti-human immunodeficiency virus hematopoietic progenitor cell-delivered ribozyme in a phase I study: myeloid and lymphoid reconstitution in human immunodeficiency virus type-1-infected patients. *Hum Gene Ther* **15**: 251-262.
123. Mitsuyasu, RT, Merigan, TC, Carr, A, Zack, JA, Winters, MA, Workman, C*, et al.* (2009). Phase 2 gene therapy trial of an anti-HIV ribozyme in autologous CD34+ cells. *Nature medicine* **15**: 285-292.
124. Michienzi, A, Castanotto, D, Lee, N, Li, S, Zaia, JA, and Rossi, JJ (2003). RNA-mediated inhibition of HIV in a gene therapy setting. *Ann N Y Acad Sci* **1002**: 63-71.
125. Levine, BL, Humeau, LM, Boyer, J, MacGregor, RR, Rebello, T, Lu, X*, et al.* (2006). Gene transfer in humans using a conditionally replicating lentiviral vector. *Proc Natl Acad Sci U S A* **103**: 17372-17377.
126. Tebas, P, Stein, D, Binder-Scholl, G, Mukherjee, R, Brady, T, Rebello, T*, et al.* (2013). Antiviral effects of autologous CD4 T cells genetically modified with a conditionally replicating lentiviral vector expressing long antisense to HIV. *Blood* **121**: 1524-1533.
127. Kohn, DB, Bauer, G, Rice, CR, Rothschild, JC, Carbonaro, DA, Valdez, P*, et al.* (1999). A clinical trial of retroviral-mediated transfer of a rev-responsive element decoy gene into CD34(+) cells from the bone marrow of human immunodeficiency virus-1-infected children. *Blood* **94**: 368-371.

128. DiGiusto, DL, Krishnan, A, Li, L, Li, H, Li, S, Rao, A*, et al.* (2010). RNA-based gene therapy for HIV with lentiviral vector-modified CD34(+) cells in patients undergoing transplantation for AIDS-related lymphoma. *Sci Transl Med* **2**: 36ra43.
129. Saayman, S, Ali, SA, Morris, KV, and Weinberg, MS (2015). The therapeutic application of CRISPR/Cas9 technologies for HIV. *Expert Opin Biol Ther* **15**: 819-830.
130. Rossi, JJ, June, CH, and Kohn, DB (2007). Genetic therapies against HIV. *Nat Biotechnol* **25**: 1444-1454.
131. Shum, KT, Zhou, J, and Rossi, JJ (2013). Aptamer-based therapeutics: new approaches to combat human viral diseases. *Pharmaceuticals (Basel)* **6**: 1507-1542.
132. Haasnoot, J, and Berkhout, B (2009). Nucleic acids-based therapeutics in the battle against pathogenic viruses. *Handb Exp Pharmacol* **189**: 243-263.
133. Kruger, K, Grabowski, PJ, Zaug, AJ, Sands, J, Gottschling, DE, and Cech, TR (1982). Self-splicing RNA: autoexcision and autocyclization of the ribosomal RNA intervening sequence of Tetrahymena. *Cell* **31**: 147-157.
134. Edgell, DR, Chalamcharla, VR, and Belfort, M (2011). Learning to live together: mutualism between self-splicing introns and their hosts. *BMC Biol* **9**: 22.
135. Guerrier-Takada, C, Gardiner, K, Marsh, T, Pace, N, and Altman, S (1983). The RNA moiety of ribonuclease P is the catalytic subunit of the enzyme. *Cell* **35**: 849-857.
136. Esakova, O, and Krasilnikov, AS (2010). Of proteins and RNA: the RNase P/MRP family. *RNA* **16**: 1725-1747.
137. Cech, TR (2000). Structural biology. The ribosome is a ribozyme. *Science* **289**: 878-879.
138. Ferre-D'Amare, AR, and Scott, WG (2010). Small self-cleaving ribozymes. *Cold Spring Harb Perspect Biol* **2**: a003574.
139. Cech, TR (2002). Ribozymes, the first 20 years. *Biochem Soc Trans* **30**: 1162-1166.
140. de la Pena, M, and Garcia-Robles, I (2010). Ubiquitous presence of the hammerhead ribozyme motif along the tree of life. *RNA* **16**: 1943-1950.
141. Garcia-Robles, I, Sanchez-Navarro, J, and de la Pena, M (2012). Intronic hammerhead ribozymes in mRNA biogenesis. *Biol Chem* **393**: 1317-1326.
142. Webb, CH, Riccitelli, NJ, Ruminski, DJ, and Luptak, A (2009). Widespread occurrence of self-cleaving ribozymes. *Science* **326**: 953.
143. Webb, CH, and Luptak, A (2011). HDV-like self-cleaving ribozymes. *RNA Biol* **8**: 719-727.
144. Saville, BJ, and Collins, RA (1990). A site-specific self-cleavage reaction performed by a novel RNA in Neurospora mitochondria. *Cell* **61**: 685-696.
145. McCown, PJ, Roth, A, and Breaker, RR (2011). An expanded collection and refined consensus model of glmS ribozymes. *RNA* **17**: 728-736.
146. Teixeira, A, Tahiri-Alaoui, A, West, S, Thomas, B, Ramadass, A, Martianov, I*, et al.* (2004). Autocatalytic RNA cleavage in the human beta-globin pre-mRNA promotes transcription termination. *Nature* **432**: 526-530.
147. Roth, A, Weinberg, Z, Chen, AG, Kim, PB, Ames, TD, and Breaker, RR (2013). A widespread self-cleaving ribozyme class is revealed by bioinformatics. *Nat Chem Biol* **10**: 56-60.
148. Sarver, N, Cantin, EM, Chang, PS, Zaia, JA, Ladne, PA, Stephens, DA*, et al.* (1990). Ribozymes as potential anti-HIV-1 therapeutic agents. *Science* **247**: 1222-1225.

149. Ojwang, JO, Hampel, A, Looney, DJ, Wong-Staal, F, and Rappaport, J (1992). Inhibition of human immunodeficiency virus type 1 expression by a hairpin ribozyme. *Proc Natl Acad Sci U S A* **89**: 10802-10806.
150. Duarte, EA, Leavitt, MC, Yamada, O, and Yu, M (1997). Hairpin ribozyme gene therapy for AIDS. *Methods Mol Biol* **74**: 459-468.
151. Citti, L, and Rainaldi, G (2005). Synthetic hammerhead ribozymes as therapeutic tools to control disease genes. *Curr Gene Ther* **5**: 11-24.
152. Rossi, JJ (2000). Ribozyme therapy for HIV infection. *Adv Drug Deliv Rev* **44**: 71-78.
153. Bergeron, LJ, and Perreault, JP (2005). Target-dependent on/off switch increases ribozyme fidelity. *Nucleic Acids Res* **33**: 1240-1248.
154. Bergeron, LJ, Reymond, C, and Perreault, JP (2005). Functional characterization of the SOFA delta ribozyme. *RNA* **11**: 1858-1868.
155. Motard, J, Rouxel, R, Paun, A, von Messling, V, Bisaillon, M, and Perreault, JP (2011). A novel ribozyme-based prophylaxis inhibits influenza A virus replication and protects from severe disease. *PLoS One* **6**: e27327.
156. Lévesque, MV, Lévesque, D, Brière, FP, and Perreault, JP (2010). Investigating a new generation of ribozymes in order to target HCV. *PLoS One* **5**: e9627.
157. Robichaud, GA, Perreault, JP, and Ouellette, RJ (2008). Development of an isoform-specific gene suppression system: the study of the human Pax-5B transcriptional element. *Nucleic Acids Res* **36**: 4609-4620.
158. Lainé, S, Scarborough, RJ, Lévesque, D, Didierlaurent, L, Soye, KJ, Mougel, M*, et al.* (2011). In vitro and in vivo cleavage of HIV-1 RNA by new SOFA-HDV ribozymes and their potential to inhibit viral replication. *RNA Biol* **8**: 343-353.
159. Scarborough, RJ, Levesque, MV, Boudrias-Dalle, E, Chute, IC, Daniels, SM, Ouellette, RJ*, et al.* (2014). A Conserved Target Site in HIV-1 Gag RNA is Accessible to Inhibition by Both an HDV Ribozyme and a Short Hairpin RNA. *Mol Ther Nucleic Acids* **3**: e178.
160. Hnatyszyn, H, Spruill, G, Young, A, Seivright, R, and Kraus, G (2001). Long-term RNase P-mediated inhibition of HIV-1 replication and pathogenesis. *Gene Ther* **8**: 1863-1871.
161. Kraus, G, Geffin, R, Spruill, G, Young, AK, Seivright, R, Cardona, D*, et al.* (2002). Cross-clade inhibition of HIV-1 replication and cytopathology by using RNase P-associated external guide sequences. *Proc Natl Acad Sci U S A* **99**: 3406-3411.
162. Jiang, X, Sunkara, N, Lu, S, and Liu, F (2014). Directing RNase P-Mediated Cleavage of Target mRNAs by Engineered External Guide Sequences in Cultured Cells. *Methods Mol Biol* **1103**: 45-56.
163. Zeng, W, Chen, YC, Bai, Y, Trang, P, Vu, GP, Lu, S*, et al.* (2012). Effective Inhibition of Human Immunodeficiency Virus 1 Replication by Engineered RNase P Ribozyme. *PLoS One* **7**: e51855.
164. Guo, H, Karberg, M, Long, M, Jones, JP, 3rd, Sullenger, B, and Lambowitz, AM (2000). Group II introns designed to insert into therapeutically relevant DNA target sites in human cells. *Science* **289**: 452-457.
165. Nazari, R, and Joshi, S (2008). Exploring the potential of group II introns to inactivate human immunodeficiency virus type 1. *J Gen Virol* **89**: 2605-2610.
166. Darty, K, Denise, A, and Ponty, Y (2009). VARNA: Interactive drawing and editing of the RNA secondary structure. *Bioinformatics* **25**: 1974-1975.

167. Lévesque, MV, and Perreault, JP (2012). Target-induced SOFA-HDV ribozyme. *Methods Mol Biol* **848**: 369-384.
168. Scarborough, RJ, Lévesque, MV, Perreault, JP, and Gatignol, A (2014). Design and Evaluation of Clinically Relevant SOFA-HDV Ribozymes Targeting HIV RNA. *Methods Mol Biol* **1103**: 31-43.
169. Watts, JM, Dang, KK, Gorelick, RJ, Leonard, CW, Bess, JW, Jr., Swanstrom, R*, et al.* (2009). Architecture and secondary structure of an entire HIV-1 RNA genome. *Nature* **460**: 711-716.
170. Bramlage, B, Luzi, E, and Eckstein, F (2000). HIV-1 LTR as a target for synthetic ribozyme-mediated inhibition of gene expression: site selection and inhibition in cell culture. *Nucleic Acids Res* **28**: 4059-4067.
171. Dropulic, B, and Jeang, KT (1994). Intracellular susceptibility to ribozymes in a tethered substrate-ribozyme provirus model is not predicted by secondary structures of human immunodeficiency virus type 1 RNAs in vitro. *Antisense Res Dev* **4**: 217-221.
172. Ramezani, A, and Joshi, S (1996). Comparative analysis of five highly conserved target sites within the HIV-1 RNA for their susceptibility to hammerhead ribozyme-mediated cleavage in vitro and in vivo. *Antisense Nucleic Acid Drug Dev* **6**: 229-235.
173. Unwalla, HJ, Li, H, Li, SY, Abad, D, and Rossi, JJ (2008). Use of a U16 snoRNA-containing ribozyme library to identify ribozyme targets in HIV-1. *Mol Ther* **16**: 1113-1119.
174. Yu, M, Ojwang, J, Yamada, O, Hampel, A, Rapapport, J, Looney, D*, et al.* (1993). A hairpin ribozyme inhibits expression of diverse strains of human immunodeficiency virus type 1. *Proc Natl Acad Sci U S A* **90**: 6340-6344.
175. Yu, M, Leavitt, MC, Maruyama, M, Yamada, O, Young, D, Ho, AD*, et al.* (1995). Intracellular immunization of human fetal cord blood stem/progenitor cells with a ribozyme against human immunodeficiency virus type 1. *Proc Natl Acad Sci U S A* **92**: 699-703.
176. Yamada, O, Yu, M, Yee, JK, Kraus, G, Looney, D, and Wong-Staal, F (1994). Intracellular immunization of human T cells with a hairpin ribozyme against human immunodeficiency virus type 1. *Gene Ther* **1**: 38-45.
177. Leavitt, MC, Yu, M, Yamada, O, Kraus, G, Looney, D, Poeschla, E*, et al.* (1994). Transfer of an anti-HIV-1 ribozyme gene into primary human lymphocytes. *Hum Gene Ther* **5**: 1115-1120.
178. Leavitt, MC, Yu, M, Wong-Staal, F, and Looney, DJ (1996). Ex vivo transduction and expansion of CD4+ lymphocytes from HIV + donors: prelude to a ribozyme gene therapy trial. *Gene Ther* **3**: 599-606.
179. Yamada, O, Kraus, G, Luznik, L, Yu, M, and Wong-Staal, F (1996). A chimeric human immunodeficiency virus type 1 (HIV-1) minimal Rev response element-ribozyme molecule exhibits dual antiviral function and inhibits cell-cell transmission of HIV-1. *J Virol* **70**: 1596-1601.
180. Gervaix, A, Li, X, Kraus, G, and Wong-Staal, F (1997). Multigene antiviral vectors inhibit diverse human immunodeficiency virus type 1 clades. *J Virol* **71**: 3048-3053.
181. Good, PD, Krikos, AJ, Li, SX, Bertrand, E, Lee, NS, Giver, L*, et al.* (1997). Expression of small, therapeutic RNAs in human cell nuclei. *Gene Ther* **4**: 45-54.

182. Michienzi, A, Cagnon, L, Bahner, I, and Rossi, JJ (2000). Ribozyme-mediated inhibition of HIV 1 suggests nucleolar trafficking of HIV-1 RNA. *Proc Natl Acad Sci U S A* **97**: 8955-8960.
183. Puerta-Fernandez, E, Barroso-del Jesus, A, Romero-Lopez, C, Tapia, N, Martinez, MA, and Berzal-Herranz, A (2005). Inhibition of HIV-1 replication by RNA targeted against the LTR region. *AIDS* **19**: 863-870.
184. Hotchkiss, G, Maijgren-Steffensson, C, and Ahrlund-Richter, L (2004). Efficacy and mode of action of hammerhead and hairpin ribozymes against various HIV-1 target sites. *Mol Ther* **10**: 172-180.
185. Sánchez-Luque, FJ, Reyes-Darias, JA, Puerta-Fernández, E, and Berzal-Herranz, A (2010). Inhibition of HIV-1 replication and dimerization interference by dual inhibitory RNAs. *Molecules* **15**: 4757-4772.
186. Weerasinghe, M, Liem, SE, Asad, S, Read, SE, and Joshi, S (1991). Resistance to human immunodeficiency virus type 1 (HIV-1) infection in human CD4+ lymphocyte-derived cell lines conferred by using retroviral vectors expressing an HIV-1 RNA-specific ribozyme. *J Virol* **65**: 5531-5534.
187. Westaway, SK, Cagnon, L, Chang, Z, Li, S, Li, H, Larson, GP*, et al.* (1998). Virion encapsidation of tRNA(3Lys)-ribozyme chimeric RNAs inhibits HIV infection. *Antisense Nucleic Acid Drug Dev* **8**: 185-197.
188. Chang, Z, Westaway, S, Li, S, Zaia, JA, Rossi, JJ, and Scherer, LJ (2002). Enhanced expression and HIV-1 inhibition of chimeric tRNA(Lys3)-ribozymes under dual U6 snRNA and tRNA promoters. *Mol Ther* **6**: 481-489.
189. Yu, M, Poeschla, E, Yamada, O, Degrandis, P, Leavitt, MC, Heusch, M*, et al.* (1995). In vitro and in vivo characterization of a second functional hairpin ribozyme against HIV-1. *Virology* **206**: 381-386.
190. Müller-Kuller, T, Capalbo, G, Klebba, C, Engels, JW, and Klein, SA (2009). Identification and characterization of a highly efficient anti-HIV pol hammerhead ribozyme. *Oligonucleotides* **19**: 265-272.
191. Sun, LQ, Wang, L, Gerlach, WL, and Symonds, G (1995). Target sequence-specific inhibition of HIV-1 replication by ribozymes directed to tat RNA. *Nucleic Acids Res* **23**: 2909-2913.
192. Sun, LQ, Pyati, J, Smythe, J, Wang, L, Macpherson, J, Gerlach, W*, et al.* (1995). Resistance to human immunodeficiency virus type 1 infection conferred by transduction of human peripheral blood lymphocytes with ribozyme, antisense, or polymeric trans-activation response element constructs. *Proc Natl Acad Sci U S A* **92**: 7272-7276.
193. Wang, L, Witherington, C, King, A, Gerlach, WL, Carr, A, Penny, R*, et al.* (1998). Preclinical characterization of an anti-tat ribozyme for therapeutic application. *Hum Gene Ther* **9**: 1283-1291.
194. Lo, KM, Biasolo, MA, Dehni, G, Palu, G, and Haseltine, WA (1992). Inhibition of replication of HIV-1 by retroviral vectors expressing tat-antisense and anti-tat ribozyme RNA. *Virology* **190**: 176-183.
195. Michienzi, A, Conti, L, Varano, B, Prislei, S, Gessani, S, and Bozzoni, I (1998). Inhibition of human immunodeficiency virus type 1 replication by nuclear chimeric anti-HIV ribozymes in a human T lymphoblastoid cell line. *Hum Gene Ther* **9**: 621-628.

196. Zhou, C, Bahner, IC, Larson, GP, Zaia, JA, Rossi, JJ, and Kohn, EB (1994). Inhibition of HIV-1 in human T-lymphocytes by retrovirally transduced anti-tat and rev hammerhead ribozymes. *Gene* **149**: 33-39.
197. Zhou, C, Bahner, I, Rossi, JJ, and Kohn, DB (1996). Expression of hammerhead ribozymes by retroviral vectors to inhibit HIV-1 replication: comparison of RNA levels and viral inhibition. *Antisense Nucleic Acid Drug Dev* **6**: 17-24.
198. Bauer, G, Valdez, P, Kearns, K, Bahner, I, Wen, SF, Zaia, JA*, et al.* (1997). Inhibition of human immunodeficiency virus-1 (HIV-1) replication after transduction of granulocyte colony-stimulating factor-mobilized CD34+ cells from HIV-1-infected donors using retroviral vectors containing anti-HIV-1 genes. *Blood* **89**: 2259-2267.
199. Yamada, O, Kraus, G, Leavitt, MC, Yu, M, and Wong-Staal, F (1994). Activity and cleavage site specificity of an anti-HIV-1 hairpin ribozyme in human T cells. *Virology* **205**: 121-126.
200. Larsson, S, Hotchkiss, G, Su, J, Kebede, T, Andang, M, Nyholm, T*, et al.* (1996). A novel ribozyme target site located in the HIV-1 nef open reading frame. *Virology* **219**: 161-169.
201. Naito, Y, Nohtomi, K, Onogi, T, Uenishi, R, Ui-Tei, K, Saigo, K*, et al.* (2007). Optimal design and validation of antiviral siRNA for targeting HIV-1. *Retrovirology* **4**: 80.
202. McIntyre, GJ, Groneman, JL, Yu, YH, Jaramillo, A, Shen, S, and Applegate, TL (2009). 96 shRNAs designed for maximal coverage of HIV-1 variants. *Retrovirology* **6**: 55.
203. ter Brake, O, Konstantinova, P, Ceylan, M, and Berkhout, B (2006). Silencing of HIV-1 with RNA interference: a multiple shRNA approach. *Mol Ther* **14**: 883-892.
204. Sajic, R, Lee, K, Asai, K, Sakac, D, Branch, DR, Upton, C*, et al.* (2007). Use of modified U1 snRNAs to inhibit HIV-1 replication. *Nucleic Acids Res* **35**: 247-255.
205. Waninger, S, Kuhen, K, Hu, X, Chatterton, JE, Wong-Staal, F, and Tang, H (2004). Identification of cellular cofactors for human immunodeficiency virus replication via a ribozyme-based genomics approach. *J Virol* **78**: 12829-12837.
206. Gonzalez, MA, Serrano, F, Llorente, M, Abad, JL, Garcia-Ortiz, MJ, and Bernad, A (1998). A hammerhead ribozyme targeted to the human chemokine receptor CCR5. *Biochem Biophys Res Commun* **251**: 592-596.
207. Goila, R, and Banerjea, AC (1998). Sequence specific cleavage of the HIV-1 coreceptor CCR5 gene by a hammer-head ribozyme and a DNA-enzyme: inhibition of the coreceptor function by DNA-enzyme. *FEBS Lett* **436**: 233-238.
208. Cagnon, L, and Rossi, JJ (2000). Downregulation of the CCR5 beta-chemokine receptor and inhibition of HIV-1 infection by stable VA1-ribozyme chimeric transcripts. *Antisense Nucleic Acid Drug Dev* **10**: 251-261.
209. Bai, J, Gorantla, S, Banda, N, Cagnon, L, Rossi, J, and Akkina, R (2000). Characterization of anti-CCR5 ribozyme-transduced CD34+ hematopoietic progenitor cells in vitro and in a SCID-hu mouse model in vivo. *Mol Ther* **1**: 244-254.
210. Li, MJ, Kim, J, Li, S, Zaia, J, Yee, JK, Anderson, J*, et al.* (2005). Long-term inhibition of HIV-1 infection in primary hematopoietic cells by lentiviral vector delivery of a triple combination of anti-HIV shRNA, anti-CCR5 ribozyme, and a nucleolar-localizing TAR decoy. *Mol Ther* **12**: 900-909.

211. Anderson, J, Li, MJ, Palmer, B, Remling, L, Li, S, Yam, P*, et al.* (2007). Safety and efficacy of a lentiviral vector containing three anti-HIV genes--CCR5 ribozyme, tat-rev siRNA, and TAR decoy--in SCID-hu mouse-derived T cells. *Mol Ther* **15**: 1182-1188.
212. Eekels, JJ, and Berkhout, B (2011). Toward a durable treatment of HIV-1 infection using RNA interference. *Prog Mol Biol Transl Sci* **102**: 141-163.
213. Feng, Y, Leavitt, M, Tritz, R, Duarte, E, Kang, D, Mamounas, M*, et al.* (2000). Inhibition of CCR5-dependent HIV-1 infection by hairpin ribozyme gene therapy against CC-chemokine receptor 5. *Virology* **276**: 271-278.
214. Bai, J, Rossi, J, and Akkina, R (2001). Multivalent anti-CCR ribozymes for stem cell-based HIV type 1 gene therapy. *AIDS Res Hum Retroviruses* **17**: 385-399.
215. Cordelier, P, Kulkowsky, JW, Ko, C, Matskevitch, AA, McKee, HJ, Rossi, JJ*, et al.* (2004). Protecting from R5-tropic HIV: individual and combined effectiveness of a hammerhead ribozyme and a single-chain Fv antibody that targets CCR5. *Gene Ther* **11**: 1627-1637.
216. Nazari, R, Ma, XZ, and Joshi, S (2008). Inhibition of human immunodeficiency virus-1 entry using vectors expressing a multimeric hammerhead ribozyme targeting the CCR5 mRNA. *J Gen Virol* **89**: 2252-2261.
217. Unwalla, HJ, Li, MJ, Kim, JD, Li, HT, Ehsani, A, Alluin, J*, et al.* (2004). Negative feedback inhibition of HIV-1 by TAT-inducible expression of siRNA. *Nat Biotechnol* **22**: 1573-1578.
218. Sanghvi, VR, and Steel, LF (2011). Expression of interfering RNAs from an HIV-1 Tat-inducible chimeric promoter. *Virus Res* **155**: 106-111.
219. Schramm, L, and Hernandez, N (2002). Recruitment of RNA polymerase III to its target promoters. *Genes Dev* **16**: 2593-2620.
220. White, RJ (2011). Transcription by RNA polymerase III: more complex than we thought. *Nat Rev Genet* **12**: 459-463.
221. Bertrand, E, Castanotto, D, Zhou, C, Carbonnelle, C, Lee, NS, Good, P*, et al.* (1997). The expression cassette determines the functional activity of ribozymes in mammalian cells by controlling their intracellular localization. *RNA* **3**: 75-88.
222. Kuwabara, T, Warashina, M, Koseki, S, Sano, M, Ohkawa, J, Nakayama, K*, et al.* (2001). Significantly higher activity of a cytoplasmic hammerhead ribozyme than a corresponding nuclear counterpart: engineered tRNAs with an extended 3' end can be exported efficiently and specifically to the cytoplasm in mammalian cells. *Nucleic Acids Res* **29**: 2780-2788.
223. Strijker, R, Fritz, DT, and Levinson, AD (1989). Adenovirus VAI-RNA regulates gene expression by controlling stability of ribosome-bound RNAs. *EMBO J* **8**: 2669-2675.
224. Svensson, C, and Akusjarvi, G (1990). A novel effect of adenovirus VA RNA1 on cytoplasmic mRNA abundance. *Virology* **174**: 613-617.
225. Katze, MG, DeCorato, D, Safer, B, Galabru, J, and Hovanessian, AG (1987). Adenovirus VAI RNA complexes with the 68 000 Mr protein kinase to regulate its autophosphorylation and activity. *EMBO J* **6**: 689-697.
226. Hannon, GJ, Chubb, A, Maroney, PA, Hannon, G, Altman, S, and Nilsen, TW (1991). Multiple cis-acting elements are required for RNA polymerase III transcription of the gene encoding H1 RNA, the RNA component of human RNase P. *J Biol Chem* **266**: 22796-22799.

227. Unwalla, HJ, and Rossi, JJ (2006). Promoting gene therapy: expression systems for transgenes and posttranscriptional gene silencing. *Biotechnol Genet Eng Rev* **23**: 71-91.
228. Puerta-Fernandez, E, Barroso-del Jesus, A, Romero-Lopez, C, and Berzal-Herranz, A (2003). HIV-1 TAR as anchoring site for optimized catalytic RNAs. *Biol Chem* **384**: 343-350.
229. Kleiman, L (2002). tRNA(Lys3): the primer tRNA for reverse transcription in HIV-1. *IUBMB Life* **53**: 107-114.
230. Buchschacher, GL, Jr., and Wong-Staal, F (2001). Approaches to gene therapy for human immunodeficiency virus infection. *Hum Gene Ther* **12**: 1013-1019.
231. Kruger, M, Beger, C, and Wong-Staal, F (1999). Use of ribozymes to inhibit gene expression. *Methods Enzymol* **306**: 207-225.
232. Cooper, D, Penny, R, Symonds, G, Carr, A, Gerlach, W, Sun, LQ*, et al.* (1999). A marker study of therapeutically transduced CD4+ peripheral blood lymphocytes in HIV discordant identical twins. *Hum Gene Ther* **10**: 1401-1421.
233. Fire, A, Xu, S, Montgomery, MK, Kostas, SA, Driver, SE, and Mello, CC (1998). Potent and specific genetic interference by double-stranded RNA in Caenorhabditis elegans. *Nature* **391**: 806-811.
234. Ding, S-W, and Voinnet, O. Antiviral Immunity Directed by Small RNAs. *Cell* **130**: 413-426.
235. Daniels, SM, and Gatignol, A (2012). The multiple functions of TRBP, at the hub of cell responses to viruses, stress, and cancer. *Microbiology and molecular biology reviews : MMBR* **76**: 652-666.
236. Umbach, JL, and Cullen, BR (2009). The role of RNAi and microRNAs in animal virus replication and antiviral immunity. *Genes Dev* **23**: 1151-1164.
237. Sagan, SM, and Sarnow, P (2013). Molecular biology. RNAi, Antiviral after all. *Science* **342**: 207-208.
238. Jeang, KT (2012). RNAi in the regulation of mammalian viral infections. *BMC Biol* **10**: 58.
239. Lagos-Quintana, M, Rauhut, R, Lendeckel, W, and Tuschl, T (2001). Identification of novel genes coding for small expressed RNAs. *Science* **294**: 853-858.
240. Lee, RC, and Ambros, V (2001). An extensive class of small RNAs in Caenorhabditis elegans. *Science* **294**: 862-864.
241. Lau, NC, Lim, LP, Weinstein, EG, and Bartel, DP (2001). An abundant class of tiny RNAs with probable regulatory roles in Caenorhabditis elegans. *Science* **294**: 858-862.
242. Friedman, RC, Farh, KK, Burge, CB, and Bartel, DP (2009). Most mammalian mRNAs are conserved targets of microRNAs. *Genome research* **19**: 92-105.
243. Kozomara, A, and Griffiths-Jones, S (2014). miRBase: annotating high confidence microRNAs using deep sequencing data. *Nucleic Acids Res* **42**: D68-73.
244. Lee, Y, Kim, M, Han, J, Yeom, KH, Lee, S, Baek, SH*, et al.* (2004). MicroRNA genes are transcribed by RNA polymerase II. *Embo j* **23**: 4051-4060.
245. Lund, E, Guttinger, S, Calado, A, Dahlberg, JE, and Kutay, U (2004). Nuclear export of microRNA precursors. *Science* **303**: 95-98.
246. Daniels, SM, Melendez-Peña, CE, Scarborough, RJ, Daher, A, Christensen, HS, El Far, M*, et al.* (2009). Characterization of the TRBP domain required for dicer interaction and function in RNA interference. *BMC Mol Biol* **10**: 38.

247. Skalsky, RL, and Cullen, BR (2010). Viruses, microRNAs, and host interactions. *Annu Rev Microbiol* **64**: 123-141.
248. Ouellet, DL, Plante, I, Landry, P, Barat, C, Janelle, ME, Flamand, L*, et al.* (2008). Identification of functional microRNAs released through asymmetrical processing of HIV-1 TAR element. *Nucleic Acids Res* **36**: 2353-2365.
249. Huang, J, Wang, F, Argyris, E, Chen, K, Liang, Z, Tian, H*, et al.* (2007). Cellular microRNAs contribute to HIV-1 latency in resting primary CD4+ T lymphocytes. *Nature medicine* **13**: 1241-1247.
250. Ui-Tei, K, Zenno, S, Miyata, Y, and Saigo, K (2000). Sensitive assay of RNA interference in Drosophila and Chinese hamster cultured cells using firefly luciferase gene as target. *FEBS Lett* **479**: 79-82.
251. Caplen, NJ, Fleenor, J, Fire, A, and Morgan, RA (2000). dsRNA-mediated gene silencing in cultured Drosophila cells: a tissue culture model for the analysis of RNA interference. *Gene* **252**: 95-105.
252. Zamore, PD, Tuschl, T, Sharp, PA, and Bartel, DP (2000). RNAi: double-stranded RNA directs the ATP-dependent cleavage of mRNA at 21 to 23 nucleotide intervals. *Cell* **101**: 25-33.
253. Hammond, SM, Bernstein, E, Beach, D, and Hannon, GJ (2000). An RNA-directed nuclease mediates post-transcriptional gene silencing in Drosophila cells. *Nature* **404**: 293-296.
254. Parrish, S, Fleenor, J, Xu, S, Mello, C, and Fire, A (2000). Functional anatomy of a dsRNA trigger: differential requirement for the two trigger strands in RNA interference. *Molecular cell* **6**: 1077-1087.
255. Elbashir, SM, Harborth, J, Lendeckel, W, Yalcin, A, Weber, K, and Tuschl, T (2001). Duplexes of 21-nucleotide RNAs mediate RNA interference in cultured mammalian cells. *Nature* **411**: 494-498.
256. Caplen, NJ, Parrish, S, Imani, F, Fire, A, and Morgan, RA (2001). Specific inhibition of gene expression by small double-stranded RNAs in invertebrate and vertebrate systems. *Proc Natl Acad Sci U S A* **98**: 9742-9747.
257. Elbashir, SM, Lendeckel, W, and Tuschl, T (2001). RNA interference is mediated by 21- and 22-nucleotide RNAs. *Genes Dev* **15**: 188-200.
258. Strapps, WR, Pickering, V, Muiru, GT, Rice, J, Orsborn, S, Polisky, BA*, et al.* (2010). The siRNA sequence and guide strand overhangs are determinants of in vivo duration of silencing. *Nucleic Acids Res* **38**: 4788-4797.
259. Snead, NM, and Rossi, JJ (2012). RNA interference trigger variants: getting the most out of RNA for RNA interference-based therapeutics. *Nucleic Acid Ther* **22**: 139-146.
260. Kim, DH, Behlke, MA, Rose, SD, Chang, MS, Choi, S, and Rossi, JJ (2005). Synthetic dsRNA Dicer substrates enhance RNAi potency and efficacy. *Nat Biotechnol* **23**: 222-226.
261. Rose, SD, Kim, DH, Amarzguioui, M, Heidel, JD, Collingwood, MA, Davis, ME*, et al.* (2005). Functional polarity is introduced by Dicer processing of short substrate RNAs. *Nucleic Acids Res* **33**: 4140-4156.
262. Amarzguioui, M, Lundberg, P, Cantin, E, Hagstrom, J, Behlke, MA, and Rossi, JJ (2006). Rational design and in vitro and in vivo delivery of Dicer substrate siRNA. *Nature protocols* **1**: 508-517.

263. Snead, NM, Wu, X, Li, A, Cui, Q, Sakurai, K, Burnett, JC*, et al.* (2013). Molecular basis for improved gene silencing by Dicer substrate interfering RNA compared with other siRNA variants. *Nucleic Acids Res* **41**: 6209-6221.
264. Kubo, T, Zhelev, Z, Ohba, H, and Bakalova, R (2007). Modified 27-nt dsRNAs with dramatically enhanced stability in serum and long-term RNAi activity. *Oligonucleotides* **17**: 445-464.
265. Dore-Savard, L, Roussy, G, Dansereau, MA, Collingwood, MA, Lennox, KA, Rose, SD*, et al.* (2008). Central delivery of Dicer-substrate siRNA: a direct application for pain research. *Mol Ther* **16**: 1331-1339.
266. Howard, KA, Paludan, SR, Behlke, MA, Besenbacher, F, Deleuran, B, and Kjems, J (2009). Chitosan/siRNA nanoparticle-mediated TNF-alpha knockdown in peritoneal macrophages for anti-inflammatory treatment in a murine arthritis model. *Mol Ther* **17**: 162-168.
267. Darniot, M, Schildgen, V, Schildgen, O, Sproat, B, Kleines, M, Ditt, V*, et al.* (2012). RNA interference in vitro and in vivo using DsiRNA targeting the nucleocapsid N mRNA of human metapneumovirus. *Antiviral research* **93**: 364-373.
268. Kim, M, Shin, D, Kim, SI, and Park, M (2006). Inhibition of hepatitis C virus gene expression by small interfering RNAs using a tri-cistronic full-length viral replicon and a transient mouse model. *Virus Res* **122**: 1-10.
269. Zhou, J, Neff, CP, Liu, X, Zhang, J, Li, H, Smith, DD*, et al.* (2011). Systemic administration of combinatorial dsiRNAs via nanoparticles efficiently suppresses HIV-1 infection in humanized mice. *Mol Ther* **19**: 2228-2238.
270. Foster, DJ, Barros, S, Duncan, R, Shaikh, S, Cantley, W, Dell, A*, et al.* (2012). Comprehensive evaluation of canonical versus Dicer-substrate siRNA in vitro and in vivo. *Rna* **18**: 557-568.
271. Reynolds, A, Anderson, EM, Vermeulen, A, Fedorov, Y, Robinson, K, Leake, D*, et al.* (2006). Induction of the interferon response by siRNA is cell type- and duplex length-dependent. *Rna* **12**: 988-993.
272. Chang, CI, Yoo, JW, Hong, SW, Lee, SE, Kang, HS, Sun, X*, et al.* (2009). Asymmetric shorter-duplex siRNA structures trigger efficient gene silencing with reduced nonspecific effects. *Mol Ther* **17**: 725-732.
273. Chu, CY, and Rana, TM (2008). Potent RNAi by short RNA triggers. *Rna* **14**: 1714-1719.
274. Brummelkamp, TR, Bernards, R, and Agami, R (2002). A system for stable expression of short interfering RNAs in mammalian cells. *Science* **296**: 550-553.
275. Lambeth, LS, and Smith, CA (2013). Short hairpin RNA-mediated gene silencing. *Methods Mol Biol* **942**: 205-232.
276. Siolas, D, Lerner, C, Burchard, J, Ge, W, Linsley, PS, Paddison, PJ*, et al.* (2005). Synthetic shRNAs as potent RNAi triggers. *Nat Biotechnol* **23**: 227-231.
277. McAnuff, MA, Rettig, GR, and Rice, KG (2007). Potency of siRNA versus shRNA mediated knockdown in vivo. *Journal of pharmaceutical sciences* **96**: 2922-2930.
278. McIntyre, GJ, Yu, YH, Lomas, M, and Fanning, GC (2011). The effects of stem length and core placement on shRNA activity. *BMC Mol Biol* **12**: 34.
279. Burnett, JC, and Rossi, JJ (2012). RNA-based therapeutics: current progress and future prospects. *Chem Biol* **19**: 60-71.

280. Birmingham, A, Anderson, EM, Reynolds, A, Ilsley-Tyree, D, Leake, D, Fedorov, Y*, et al.* (2006). 3' UTR seed matches, but not overall identity, are associated with RNAi off-targets. *Nature methods* **3**: 199-204.
281. Jackson, AL, Burchard, J, Schelter, J, Chau, BN, Cleary, M, Lim, L*, et al.* (2006). Widespread siRNA "off-target" transcript silencing mediated by seed region sequence complementarity. *Rna* **12**: 1179-1187.
282. Boudreau, RL, Spengler, RM, Hylock, RH, Kusenda, BJ, Davis, HA, Eichmann, DA*, et al.* (2013). siSPOTR: a tool for designing highly specific and potent siRNAs for human and mouse. *Nucleic Acids Res* **41**: e9.
283. Das, S, Ghosal, S, Kozak, K, and Chakrabarti, J (2013). An siRNA designing tool with a unique functional off-target filtering approach. *Journal of biomolecular structure & dynamics* **31**: 1343-1357.
284. Castanotto, D, Sakurai, K, Lingeman, R, Li, H, Shively, L, Aagaard, L*, et al.* (2007). Combinatorial delivery of small interfering RNAs reduces RNAi efficacy by selective incorporation into RISC. *Nucleic Acids Res* **35**: 5154-5164.
285. Xia, H, Mao, Q, Paulson, HL, and Davidson, BL (2002). siRNA-mediated gene silencing in vitro and in vivo. *Nat Biotechnol* **20**: 1006-1010.
286. Whitehead, KA, Dahlman, JE, Langer, RS, and Anderson, DG (2011). Silencing or stimulation? siRNA delivery and the immune system. *Annual review of chemical and biomolecular engineering* **2**: 77-96.
287. Marques, JT, and Williams, BR (2005). Activation of the mammalian immune system by siRNAs. *Nat Biotechnol* **23**: 1399-1405.
288. Tyagi, A, Ahmed, F, Thakur, N, Sharma, A, Raghava, GP, and Kumar, M (2011). HIVsirDB: a database of HIV inhibiting siRNAs. *PLoS One* **6**: e25917.
289. von Eije, KJ, ter Brake, O, and Berkhout, B (2009). Stringent testing identifies highly potent and escape-proof anti-HIV short hairpin RNAs. *J Gene Med* **11**: 459-467.
290. von Eije, KJ, ter Brake, O, and Berkhout, B (2008). Human immunodeficiency virus type 1 escape is restricted when conserved genome sequences are targeted by RNA interference. *J Virol* **82**: 2895-2903.
291. Centlivre, M, Legrand, N, Klamer, S, Liu, YP, Jasmijn von Eije, K, Bohne, M*, et al.* (2013). Preclinical in vivo evaluation of the safety of a multi-shRNA-based gene therapy against HIV-1. *Mol Ther Nucleic Acids* **2**: e120.
292. Ui-Tei, K, Naito, Y, Takahashi, F, Haraguchi, T, Ohki-Hamazaki, H, Juni, A*, et al.* (2004). Guidelines for the selection of highly effective siRNA sequences for mammalian and chick RNA interference. *Nucleic Acids Res* **32**: 936-948.
293. Reynolds, A, Leake, D, Boese, Q, Scaringe, S, Marshall, WS, and Khvorova, A (2004). Rational siRNA design for RNA interference. *Nat Biotechnol* **22**: 326-330.
294. Amarzguioui, M, and Prydz, H (2004). An algorithm for selection of functional siRNA sequences. *Biochem Biophys Res Commun* **316**: 1050-1058.
295. Ringpis, GE, Shimizu, S, Arokium, H, Camba-Colon, J, Carroll, MV, Cortado, R*, et al.* (2012). Engineering HIV-1-resistant T-cells from short-hairpin RNA-expressing hematopoietic stem/progenitor cells in humanized BLT mice. *PLoS One* **7**: e53492.
296. Low, JT, Knoepfel, SA, Watts, JM, ter Brake, O, Berkhout, B, and Weeks, KM (2012). SHAPE-directed discovery of potent shRNA inhibitors of HIV-1. *Mol Ther* **20**: 820-828.

297. Zhou, J, Neff, CP, Swiderski, P, Li, H, Smith, DD, Aboellail, T*, et al.* (2013). Functional in vivo delivery of multiplexed anti-HIV-1 siRNAs via a chemically synthesized aptamer with a sticky bridge. *Mol Ther* **21**: 192-200.
298. Brass, AL, Dykxhoorn, DM, Benita, Y, Yan, N, Engelman, A, Xavier, RJ*, et al.* (2008). Identification of host proteins required for HIV infection through a functional genomic screen. *Science* **319**: 921-926.
299. Konig, R, Zhou, Y, Elleder, D, Diamond, TL, Bonamy, GM, Irelan, JT*, et al.* (2008). Global analysis of host-pathogen interactions that regulate early-stage HIV-1 replication. *Cell* **135**: 49-60.
300. Zhou, H, Xu, M, Huang, Q, Gates, AT, Zhang, XD, Castle, JC*, et al.* (2008). Genome-scale RNAi screen for host factors required for HIV replication. *Cell host & microbe* **4**: 495-504.
301. Eekels, JJ, Geerts, D, Jeeninga, RE, and Berkhout, B (2011). Long-term inhibition of HIV-1 replication with RNA interference against cellular co-factors. *Antiviral research* **89**: 43-53.

Chapter 2

Design and evaluation of clinically relevant SOFA-HDV ribozymes targeting HIV RNA

This chapter was adapted from the following book chapter:

Scarborough RJ, Lévesque MV, Perreault JP, and Gatignol A. 2014. "Design and Evaluation of Clinically Relevant SOFA-HDV Ribozymes Targeting HIV RNA." Methods Mol Biol 1103:31-43.

In: Therapeutic Applications of Ribozymes and Riboswitches: Methods and Protocols

Editors: Lafontaine D and Dubé A.

2.1 PREFACE

This chapter provides an introduction to, and step-by-step protocols for, the methods developed to identify highly conserved SOFA-HDV ribozyme target sites in HIV-1 RNA with low potential for off-target effects on human RNAs. Methods developed to screen a large number of candidate SOFA-HDV ribozymes for effects on HIV-1 production are also provided.

Contribution of authors: Methods to calculate sequence conservation in HIV-1 RNA and determine the effects of SOFA-HDV ribozymes on HIV-1 production were developed by RJS under the supervision of AG. Methods to design and generate SOFA-HDV ribozyme expression vectors were developed by RJS and MVL under the supervision of JPP and AG. RJS wrote the book chapter and all authors contributed to its review and revision.

2.2 ABSTRACT

Nucleic acid therapies targeting HIV replication have the potential to be used in conjunction with or in place of the standard small molecule therapies. Among the different classes of nucleic acid therapies, several ribozymes (Rzs, RNA enzymes) have been developed to target HIV RNA. The design of Rzs targeting HIV RNA is complicated by the sequence diversity of viral strains and the structural diversity of their target sites. Using the SOFA-HDV Rz as an example, this chapter describes methods that can be used to design ribozymes for controlling HIV replication. We describe how to: 1) identify highly conserved Rz target sites in HIV RNA; 2) generate a set of Rzs with the potential to be used as therapeutics; and 3) screen these Rzs for activity against HIV production.

2.3 INTRODUCTION

The treatment of Human Immunodeficiency Virus (HIV) infection with combination small molecule therapy is effective in preventing the development of Acquired Immune Deficiency Syndrome (AIDS) [1, 2]. Although the emergence of resistant virus can often be managed through the proper administration and monitoring of combination therapy, the cumulative toxicological effects of chronic, changing, and lifelong small molecule therapy will always present a major health problem for HIV infected individuals [3]. Several small RNA therapeutics specifically targeting HIV RNA have been developed. These molecules have the potential to be used either in a combination gene therapy approach [4], or as a complement to current small molecule therapies using appropriate delivery vehicles [5].

Ribozymes (Rzs) represent a small group of catalytic RNA molecules that are widely distributed throughout nature. They can recognize and cleave an RNA target in *trans* through specific base pairing and intrinsic catalytic activity. The ability of engineered Rzs to cleave their targets without the assistance of cellular proteins makes them excellent candidates for therapeutic applications [6]. Rz motifs that have been modified to target HIV RNA include hammerhead, hairpin, and Hepatitis Delta Virus (HDV) Rzs [7-9]. The HDV Rz is found in the RNA genome of HDV, a satellite RNA of the Hepatitis B virus [10]. Modifications around the catalytic core of this motif have been made to generate a *trans*-acting HDV Rz with a specific on/off adaptor (SOFA), providing the necessary target specificity required for their development as therapeutic agents (Figure 2.1 **a**) [11-13]. Several SOFA-HDV Rzs have been identified with activity against viral [8, 14, 15] or cellular RNAs [16-18], and general methods for the identification and screening of SOFA-HDV Rzs have been described [19]. In this chapter we describe specific methods to identify conserved SOFA-HDV Rz target sites in HIV RNA (section **2.5.1**), design SOFA-HDV Rz vectors for transient transfection under the control of an RNA Polymerase III promoter (section **2.5.2**), and screen a large number of SOFA-HDV Rz vectors for activity against HIV production in human cells (section **2.5.3**).

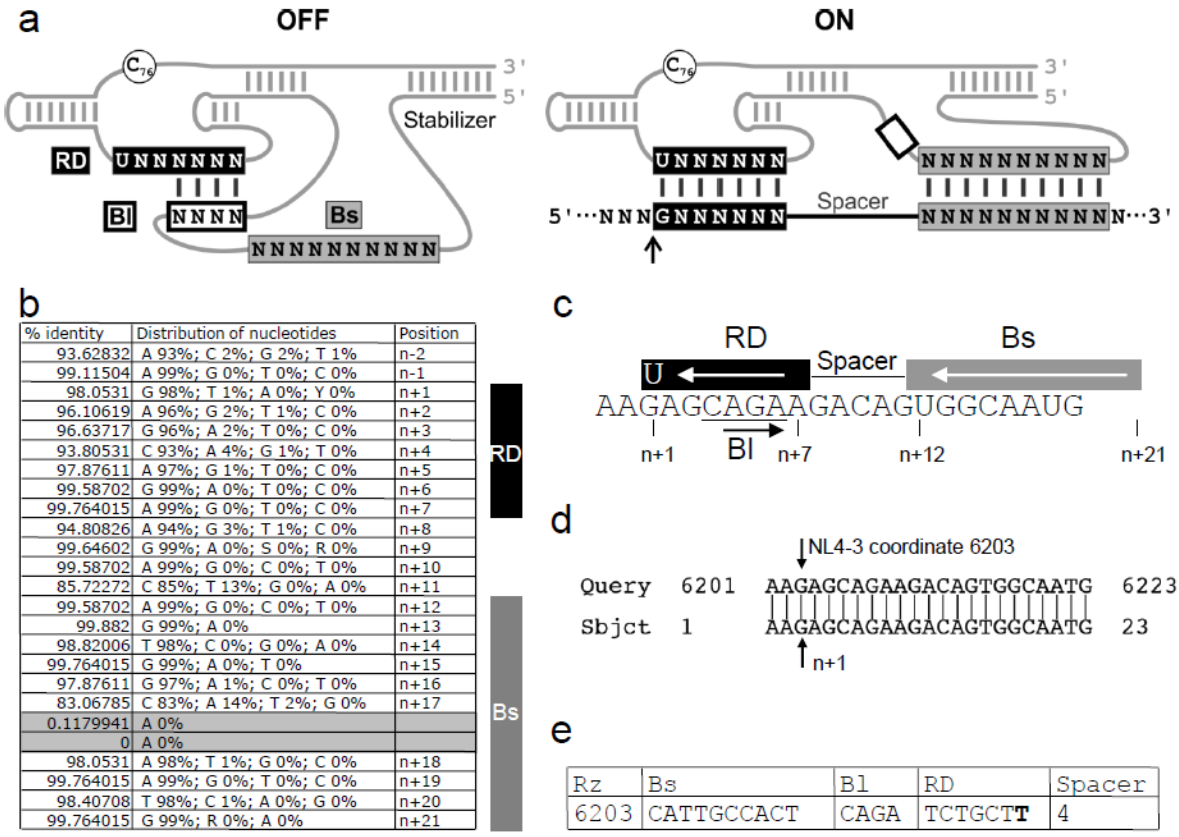

Figure 2.1. SOFA-HDV Rz and design process.

a) Representation of the SOFA-HDV Rz in both OFF (without the target RNA) and ON (with the target RNA) conformation. The key features of the SOFA-HDV Rz are indicated. The recognition domain (RD) is in a black box, the blocker (Bl) is in a white box and the biosensor (Bs) is in a grey box. The catalytic cytosine C76, which can be mutated to generate an inactive ribozyme, is represented by a circle. The stabilizer stem joins the 5' and 3' ends and the spacer is the region between the RD and the Bs binding sites in the target RNA. The arrow points to the cleavage site. **b)** The percentage of sequences in an HIV alignment with identity to the consensus nt (column 1) and the distribution and identities of all nts (column 2) at each position of a potential SOFA-HDV Rz target site (column 3) are shown. Letters other than A, T, C and G in column 2 represent ambiguities (example Y = T or C). **c)** The target site as RNA, including the n-2 and n-1 positions and excluding the low frequency insertions, is shown next to the corresponding SOFA-HDV Rz. The Rz RD and Bs are illustrated as black and grey rectangles respectively. The Bl sequence is underlined. **d)** An example of the nBLAST output of this target site aligned to HIV strain NL4-3 (M19921) is shown. **e)** The DNA sequences for the corresponding Rz are illustrated in a table.

Estimates of HIV sequence conservation at the nucleotide (nt) level have been used to identify conserved hairpin Rz target sites [20] and to characterize small interfering (si)RNA target sites [21]. In section **2.5.1**, we describe an alternative approach to estimate HIV sequence conservation at the nt level. We then explain how to identify SOFA-HDV Rz target sites in HIV RNA, using open access and currently available software. Specifically, the methods describe how to obtain sequence alignments from the Los Alamos HIV database, analyze them using Jalview alignment editor [22], and display them in Microsoft Excel spreadsheets in a manner that is convenient for identifying conserved SOFA-HDV Rz target sites. These methods allow higher cut-off values to be set for essential nts surrounding the SOFA-HDV Rz cleavage site, compared to less essential nts in other regions of the target site.

Several different promoters have been used to express anti-HIV Rzs in cells so that their effects on HIV production can be evaluated. In section **2.5.2** we describe the methods we have used to construct expression vectors with SOFA-HDV Rzs under the control of the human H1 RNA polymerase III promoter using a commercially available vector (psiRNA-hH1GFPzeo, InvivoGen). This vector has previously been used to express SOFA-HDV Rzs targeting cellular RNAs in human cells [16], and contains the GFP::zeo^{R} fusion gene, which can be used to both evaluate the transfection efficiency (GFP) and select for transfected cells in the presence of Zeocin (zeo^{R}). Like the U6 and 7SK promoters, the H1 promoter can be used to express small RNAs with the addition of only 2-4 Us at the 3' end [23]. Rzs expressed from these promoters localize predominantly in the nucleus [24], and have been shown to be more active against HIV production compared to Rzs expressed from tRNA and RNA polymerase II promoters [24, 25]. The procedures described include the sequences of the DNA used for cloning SOFA-HDV Rzs

into the psiRNA-hH1 vector, and methods to quickly generate a large number of constructs for cellular expression.

Several methods have been used to evaluate the activity of small RNA therapeutics targeting HIV RNA. Although HIV infection models are the most clinically relevant, they are not amenable to transient transfection, and require either stable transfection or transduction of the therapeutic RNAs under evaluation. A general method, that has been widely employed to screen anti-HIV RNAs, involves cotransfection of the therapeutic RNA with an HIV molecular clone, followed by an evaluation of virus production in adherent cell culture supernatants. A good correlation has been found between activity in cotransfection experiments and activity in HIV infection models [26, 27]. In section **2.5.3** we describe a simple and cost effective method to screen SOFA-HDV Rzs using an HIV Reverse Transcriptase (RT) assay to estimate the production of infectious virus in cotransfected HEK 293T cell supernatants. The methods are optimized for screening the activity of up to 30 potential Rzs, with appropriate controls, using a microplate scintillation counter.

The methods presented in this chapter outline a specific screening protocol for the identification of SOFA-HDV Rzs targeting HIV RNA with clinical potential. In conjunction with considerations for the design of SOFA-HDV Rzs described previously [19], the procedures outlined provide a guide for the design and evaluation of therapeutic SOFA-HDV Rzs, which may be particularly useful for their development as antivirals. These methods could also be useful for the identification and screening of other antisense based therapeutics targeting HIV RNA.

2.4 MATERIALS

2.4.1 Computer software

1. HIV LosAlamos database, available for online use at http://www.hiv.lanl.gov
2. Jalview Alignment Editor Version 2, available for download at http://www.jalview.org
3. NCBI BLAST, available for online use at http://blast.ncbi.nlm.nih.gov/Blast.cgi
4. Ribosubstrate software, available for online use at http://www.riboculb.org/ribosubstrates

2.4.2 psiRNA-hH1 SOFA-HDV Rz expression vectors

1. psiRNA-hH1GFPzeo (InvivoGen).
2. Zeocin (100 mg/ml, InvivoGen).
3. *BbsI/BpiI*, 10× Green buffer (Fermentas).
4. Transfection grade mini-prep kit (Purelink HiPure miniprep kit, Invitrogen).

2.4.3 Determination of HIV RT activity (Modified from Refs [28, 29])

1. TransIT-LT1 (Mirus).
2. Non-radioactive cocktail: 60 mM Tris-HCl (from 1 M Tris-HCl pH 7.8), 75 mM KCl, 5 mM $MgCl_2$, 1.04 mM EDTA, 1 % Nonidet P-40 (NP-40).
3. Radioactive cocktail: 60 mM Tris-HCl (from 1 M Tris-HCl pH 7.8), 75 mM KCl, 5 mM $MgCl_2$, 1.04 mM EDTA, 10 µg/ml Polyadenylic acid (Roche), 0.33 µg/ml oligo dT (Invitrogen). Added immediately before use: 8 mM DTT ($C_4H_{10}O_2S_2$, EMD Millipore), 5 µl [^{32}P] dTTP (3000 Ci/mmol, Perkin Elmer) for each 500 µl reaction volume.
4. DEAE (Di Ethyl Amino Ethyl) filter mat, printed 96 well grid, 90×120 mm (1450-522, Perkin Elmer).
5. Sample bags 90×120 mm (1450-432, Perkin Elmer).

6. Microplate scintillation counter (Microbeta TriLux, Perkin Elmer).

2.5 METHODS

2.5.1 Identification of conserved SOFA-HDV Rz target sites in HIV RNA

1. In your internet browser, go to the HIV Los Alamos database, select the sequence database.
2. Under the tools dropdown box, select QuickAlign (formerly Epilign and Primalign).
3. Scroll down to "Retrieve alignment(s) based on coordinates" and enter the coordinates of a target region in HIV strain HXB2 (Genbank accession number K03455), select "complete" for Gene/region/protein.
4. Under options select "HIV1" as Organism, "nucleotide" as Sequence type and 'Web alignment (all complete sequences)" as Alignment type. Click submit.
5. The position of the HIV sequence that you entered will be highlighted in an illustration of the HIV genome and a summary table will be provided. Click on the download button with fasta selected as the format. Save this file to your computer.
6. Open Jalview alignment editor. Close all pop-up windows. Under File, select "input alignment" – "from file". Select the fasta file that contains the alignment.
7. A window will open with the alignment, at the bottom of the window a histogram will be shown above the consensus sequence. This histogram represents the percent (%) conservation for each nt in the alignment, in reference to the consensus nt.
8. Under view, scroll down to "Autocalculated Annotation", make sure "show consensus histogram" and "show consensus logo" are selected (*see* **Note 1**).

9. In the File menu of the window that contains the alignment, select “Export Annotations”, choose CSV (Spreadsheet) as format and export to file. Save this file to your computer with a .txt extension (*see* **Note 2**).
10. Open the .txt file with Microsoft Excel. The Text Import Wizard will ask you to select “the original data type”. Select “delimited – characters such as commas or tabs separate each field”. Click next.
11. Select “comma” as delimiters (deselect all other delimiters), click next, click finish.
12. The data from the alignment will open in two rows. Copy these rows, and use paste special (transpose) to convert them into columns. The first column represents the percentage of sequences in the alignment with identity to the consensus nt at each position. The second column represents the distribution of nt identities among the sequences in the alignment at each position (Figure 2.1 **b**).
13. Delete all rows for which the value in column 1 is less than 10% (Figure 2.1 **b**, grey rows). This will remove insertions that occur in <10% of the sequences relative to the consensus sequence (*see* **Note 3**).
14. Set cutoff values for different nts in the Rz target site. The conservation requirements we use for SOFA-HDV Rzs targeting HIV RNA include: 1) the nts upstream from the cleavage site (n-2 and n-1) cannot be G (n-1) or CC at > 5%; 2) at the level of the recognition domain (RD) binding site (n+1 to n+7), the first nt (n+1) must be G at > 95%, and n+2 to n+7 can be any nt at >85%; and 3) the biosensor (Bs) binding site (n+(9-15) to n+(19-25)) can be any nt at >75% (*see* **Note 4**). The RD (black rectangle) and Bs (grey rectangle) binding sites are illustrated next to a potential SOFA-HDV Rz target site (Figure 2.1 **b**).

15. For each conserved target site, record the n-2 to n+(19-25) sequence, excluding low frequency (<10%) insertions (Figure 2.1 **c**, target site shown as RNA).
16. In your internet browser, go to the NCBI BLAST homepage. Choose nucleotide blast from the Basic BLAST programs and enter the accession number of the HIV viral strain that will be used for screening under "Enter Query Sequence" (example: NL4-3, Gene accession number "M19921").
17. Select "Align two or more sequences" under the Query Sequence. Copy and paste the potential target site from step 15 (Figure 2.1 **c**) as DNA into "Enter Subject Sequence". Select "Somewhat similar sequences (blastn)" for Program Selection [30]. Click on "BLAST".
18. Under "Alignments", the potential target site will be aligned to the selected viral strain with its coordinates in that strain (Figure 2.1 **d**). Make sure that the displayed "sbjct" length matches the input length (23 nts for this example) (*see* **Note 5**).
19. Record the corresponding DNA sequences of the SOFA-HDV Rz in a table (Figure 2.1 **e**), where the Bs and RD sequences are the reverse complement of their corresponding target sites (Figure 2.1 **c**), with C replaced by T at the end of the RD (Figure 2.1 **e**, bold). The blocker (Bl) is the four nts at the end of the RD binding site (Figure 2.1 **c**, underlined), and the spacer is the number of nts between the RD and Bs binding sites (Figure 2.1 **c**).
20. Go to the Ribosubstrate homepage, click on "Search for SOFA-HDV Rz substrates". Select "Human NCBI build 36.2 mRNAs" as cDNA bank. Copy and paste the first 6 nts of the RD, and all of the nts of the Bs for a specific Rz (Figure 2.1 **e**) into the respective fields. Select "Wait for results here" and click submit. Eliminate Rzs that have low scores

in “With wobble” or “With wobble and mismatch” tables. We eliminate any Rz that has a score of less than 10 for any human RNA (*see* **Note 6**).

2.5.2 Design of SOFA-HDV Rz vectors for transient transfection

1. For each SOFA-HDV Rz target site identified, design a specific oligonucleotide with the sequence:

   5’-TAATACGACTCACTATAGGGCCAGCTAGTTT(Bs)(Bl)CAGGGTCCACCTCCT CGCGGT(RD)GGGCATCCGTTCGCG-3’,

   using the sequences documented from section **2.5.1** for Bs, Bl and RD (Figure 2.1 **e**).
2. To make double-stranded (ds) DNA coding for each specific SOFA-HDV Rz, design the common reverse oligonucleotide:

   5’-CCAGCTAGAAAGGGTCCCTTAGCCATCCGCGAACGGATGCCC-3’,

   the overlapping regions of the oligonucleotides (step 1 and 2) are underlined (*see* **Note 7**).
3. To make dsDNA coding for each specific SOFA-HDV Rz with an inactivated Rz backbone, design the common inactive reverse oligonucleotide:

   5’-CCAGCTAGAAAGGGTCCCTTA**T**CCATCCGCGAACGGATGCCC-3’,

   the G-T change, which produces a C to A change in the Rz coding sequence, is in bold and the overlapping regions of the oligonucleotides (step 1 and 3) are underlined (*see* **Note 8**).
4. An irrelevant Rz should be designed as a control. For this we use HBV303 [12], which targets a site in HBV RNA and does not have an effect on HIV production compared to

the empty transfection plasmid in experiments described in section **2.4.3** (Figure 2.2). The specific oligonucleotide for this Rz (Step 1) contains the following sequences from 5' to 3': (Bs):GAGACAAGAA, (Bl): GTTT and (RD): AAACCAT (*see* **Note 9**).

5. Design cloning primers A and B:

   (A): 5'-TATAAGTTCTGTATGAGTTCACG**GAAGAC**CGACCT↓CGGGCCAGCTA GTTT-3'

   (B): 5'-CAACAACAGTGTTCGGATGAACTGATGCTAT**GAAGAC**TCCAAA↓AA CCAGCTAGAAAGGGTC-3',

   These primers contain the recognition site for the restriction enzyme *BbsI*/*BpiI* (GAAGAC), which cleaves at 6 nts downstream from its recognition site (indicated with an arrow) generating ends that are compatible for ligation into *BbsI*/*BpiI*-digested-psiRNA-hH1GFPzeo. The sequences that align with the specific forward and reverse SOFA-HDV Rz oligonucleotides are underlined.

6. Prepare a PCR mix with cloning primers A and B (2 μM each), the common reverse oligonucleotide from step 3 or 4 (25 nM), 1× PCR buffer, $MgCl_2$ (1.5 mM), dNTP mix (200 nM each), and Taq DNA Polymerase (1 μl/100 μl). Aliquot 100 μl of the PCR mix into labeled PCR tubes, add 1 μl of each specific SOFA-HDV Rz oligonucleotide from step 2 (2.5 μM) to each tube, and use the following PCR protocol: 94 °C for 2 min followed by 20 cycles [94 °C for 30 sec, 50 °C for 30 sec, 72 °C for 30 sec], and then 72 °C for 2 min.

7. Purify the PCR products using a PCR Purification Kit (Qiagen), digest the eluate (25 μl) and psiRNA-hH1GFPzeo plasmid (12 μg in 25 μl) overnight with *BbsI*/*BpiI* (2 μl) and

10× *BbsI*/*BpiI* buffer (3 µl) at 37 °C. Run the digestion products on an agarose gel, excise the bands and purify using a Gel Extraction Kit (Qiagen). Ligate each extracted PCR product to the extracted psiRNA-hH1GFPzeo vector using 100 ng of PCR product and 100 ng of vector in 10 µl ddH_2O with 1× ligation buffer and 1 µl of T4 ligase. Ligate overnight at 14 °C, warm to 37 °C and transform *E.coli* DH5α subcloning efficiency (40 µl) with each ligation using heat shock (10 min on ice, 30 sec at 42 °C, 2 min on ice). Add 350 µl LB-Miller broth and incubate at 37 °C with agitation for 2 hrs. Plate transformed bacteria onto LB-Miller agar plates containing Zeocin (25 µg/ml), and pre-coated with 30 µl Xgal (2% in DMSO) and 30 µl IPTG (0.1 M) for blue/white colony selection. Incubate the plates upside down at 37 °C overnight.

8. Amplify white colonies from each plate in 4 ml LB-Miller broth + 1 µl of 100 mg/ml Zeocin stock solution, overnight at 37 °C with agitation. Use a mini-prep kit designed for the purification of transfection grade DNA to purify the plasmids (*see* **Note 10**).
9. Confirm that psiRNA-hH1 SOFA-HDV Rz constructs are correct by sequencing using the primer: 5'-TCTACGGGGTCTGACGC-3' (*see* **Note 11**).

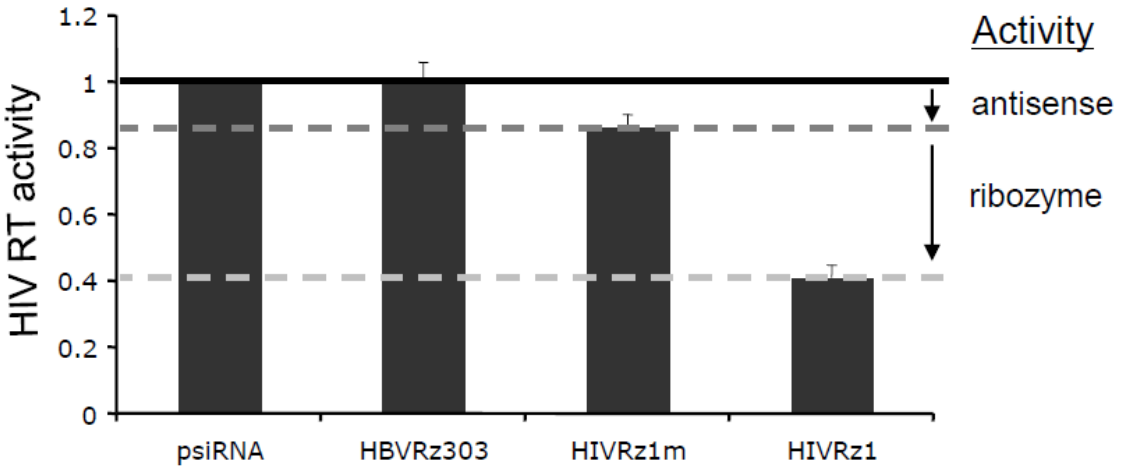

Figure 2.2. Inhibition of HIV production by a SOFA-HDV Rz.

HEK 293T cells were cotransfected with HIV molecular clone pNL4-3 and different Rz constructs. HIV-1 RT activity was measured in the cell supernatant. Data are normalized to cotransfection with the empty Rz expression plasmid (psiRNA) and include the activity of an irrelevant Rz (HBVRz303), a Rz targeting HIV RNA with an inactivated backbone (HIVRz1m) and the same Rz with an active Rz backbone (HIVRz1). The antisense and ribozyme activity of HIVRz1 are indicated.

2.5.3 Screening of SOFA-HDV Rzs for activity against HIV production

1. Plate HEK 293T cells (ATCC) in up to four 24 well plates, 24 hrs prior to transfection. Cells should be at approximately 50% confluency prior to transfection.
2. Prepare HIV molecular clone (example pNL4-3) DNA at a concentration of 10 ng/µl in ddH_2O. Aliquot 7.5 µl into 1.5 ml microcentrifuge tubes, one for each well. Dilute psiRNA-hH1 SOFA-HDV Rz plasmid preparations from section **2.5.2** to 100 ng/µl in ddH_2O, add 7.5 µl of each plasmid to the transfection tubes containing HIV DNA in triplicate. For each set of transfections, include the empty psiRNA-hH1 vector and an

irrelevant psiRNA-hH1 SOFA HDV Rz (example HBV303, section **2.5.2** step 4) in triplicate.

3. Dilute the DNA in 25 µl of media without serum. In a biosafety level 3 (BL3) laboratory, add 2 µl of TransIT-LT1 to each tube, applied under the surface, making sure not to touch the sides of the tube. Let DNA-TransIT complexes form for 20 min. Apply the DNA-TransIT complexes dropwise over each well in the 24 well plate, gently swirl the plate and incubate at 37 °C for 48 hrs.
4. Gently swirl the plates. For each well, transfer 200 µl of supernatant to wells of a 96 well plate in 8 rows of 6 wells (48 samples from two 24 well plates, corresponds to one DEAE paper, step 8). The supernatants can be stored at -80 °C, or immediately used for the determination of HIV RT activity.
5. Prepare 96 well plates with 25 µl of non-radioactive cocktail in 8 rows of 6 wells, one for each set of supernatants that you would like to measure.
6. Using a multichannel pipette, transfer 5 µl of supernatant to the 25 µl of non-radioactive cocktail. Incubate at room temperature for 15 min and remove the plate from the BL3 laboratory to a certified radioactive laboratory (*see* **Note 12**).
7. Pipette 25 µl of radioactive cocktail (DTT and TTP added) to each well containing non-radioactive cocktail and supernatant (*see* **Note 13**), incubate at 37 °C for 2 hrs.
8. Spot 5 µl of the reaction mixture onto DEAE papers (using every other square, 48 samples), and allow the papers to dry (5 min). Wash the papers five times in 2× SSC buffer for 5 min with agitation. Wash twice for 1 min in 95% ethanol and allow the papers to dry (30 min).

9. Seal papers in plastic bags (Perkin Elmer) and measure cpm on a plate reader (Microbeta, Perkin Elmer).
10. For each SOFA-HDV Rz that has activity against HIV production compared to the empty plasmid and irrelevant control (HBV303), generate the inactive version by following steps 6-9 in section **2.5.2** using the common reverse oligonucleotide from **2.5.2** step 3.
11. Repeat steps 1-9 for each active and inactive Rz including the empty plasmid and irrelevant control. This will provide information on the effects of Rz turnover on the inhibition of HIV production (Figure 2.2).

2.6 NOTES

Note 1: In Jalview Version 2.7, data on the identity and percentage of nts other than the consensus nt will be missing if the "show consensus logo" is not selected. A preview of what will be exported can be viewed by scrolling over the histogram at the bottom of the window.

Note 2: Export annotation can also be selected by right clicking on the word "consensus", next to the histogram.

Note 3: Insertions that occur at a low frequency relative to the consensus sequence are common and can be ignored when selecting conserved target sites (we use less than 10% as the cutoff value). Deleting these rows from the data set makes it easier to find and document potential target sites.

Note 4: The conservation cutoffs can be altered depending on the sequence diversity of the target. If using a Pol III promoter for expression of the Rz, target sites that include 4 or more As in the RD or Bs binding sites should be avoided, as this will result in possible Pol III termination signals (TTTT) within the Rz. For the same reason, the Bs binding site should not end with A, as there are 3 Us between the stabilizer and Bs (Figure 2.1 **a**) and the RD binding site should not end with 4 Ts, as it will generate a Bl with 4 Ts [19]. The number of nts between the RD and Bs (called the spacer) can be 1-7 nts (3-5 nts is generally used) and the optimal Bs length is 10 nts [31]. The length of the spacer can be modified to avoid poorly conserved nts in the Bs [19].

Note 5: If the target site from the consensus sequence does not align perfectly with the target site in the HIV viral strain selected, either "no significant similarity found" or the best match with gaps (horizontal line) and mutations (missing vertical line) will be displayed under "alignment". If the discrepancy between the consensus sequence (sbjct) and the query sequence is in the RD or the Bs binding sites, eliminate the target site. If the discrepancy is in the n-2 or n-1 positions, ensure that these are not G (n-1) or CC in the query sequence. If the discrepancy is in the spacer (region between the RD and the Bs binding sites) continue to Step 19.

Note 6: Details on the scoring for the Ribosubstrate software have been described [32]. Hammerhead Rz target sites can also be screened using the Ribosubstrate software.

Note 7: The dsDNA generated from these oligonucleotides can also be used to evaluate the activity of SOFA-HDV Rzs *in vitro* [19].

Note 8: The C76A mutation described here and the C76U or C76G mutations inactivate the catalytic activity of the SOFA-HDV Rz. They are generated by mutation in the reverse oligonucleotide. The inactive SOFA-HDV Rzs are used to evaluate the antisense activity of specific Rzs [19].

Note 9: For the design of SOFA-HDV Rzs with different targets, ensure that the irrelevant Rz selected does not have activity against that target. The selection of irrelevant Rzs has been described [19].

Note 10: It is very important that the DNA for each SOFA-HDV Rz construct is purified in the same way, as differences in the plasmid preparation may influence the transfection efficiency of the cotransfected HIV molecular clone in the activity evaluation (section **2.5.3**). We use the Purelink HiPure plasmid mini-prep kit from Invitrogen.

Note 11: Align the sequencing results to the following sequence to confirm that the Rz is inserted properly and that there are no mutations from the PCR (the vector sequences are in bold):

5'-**TTCTGTATGAGACCACGGTACCTC**GGGCCAGCTAGTTT(Bs)(Bl)CAGGGTCCACC TCCTCGCGGT(RD)GGGCATCCGTTCGCGGATGGCTAAGGGACCCTTTCTAGCTGG**TT TTTGGAAAAGCTT**-3'.

Note 12: The non-radioactive cocktail contains NP40 at 1%. Exposure to 0.5% (v/v) NP-40 for 1 min is able to inactivate HIV in solution [33]. This step ensures that the virus is fully inactivated

before the samples are removed from the BL3 laboratory, and avoids using radioactivity in a BL3 laboratory.

Note 13: To avoid radioactive contamination of pipettes and the bench space, this and subsequent steps are done with filter tips. The radioactive cocktail is mixed in a 2 ml microcentrifuge tube (1250 µl for each 96 well plate) with a 1000 µl pipette, and added to each well of the 96 well plate using a single channel pipette.

2.7 REFERENCES

1. De Clercq, E (2010). Antiretroviral drugs. *Curr Opin Pharmacol* **10**: 507-515.
2. Tsibris, AM, and Hirsch, MS (2010). Antiretroviral therapy in the clinic. *J Virol* **84**: 5458-5464.
3. Taiwo, B, Hicks, C, and Eron, J (2010). Unmet therapeutic needs in the new era of combination antiretroviral therapy for HIV-1. *J Antimicrob Chemother* **65**: 1100-1107.
4. Scherer, LJ, and Rossi, JJ (2011). Ex vivo gene therapy for HIV-1 treatment. *Hum Mol Genet* **20**: R100-107.
5. Burnett, JC, and Rossi, JJ (2012). RNA-based therapeutics: current progress and future prospects. *Chem Biol* **19**: 60-71.
6. Serganov, A, and Patel, DJ (2007). Ribozymes, riboswitches and beyond: regulation of gene expression without proteins. *Nat Rev Genet* **8**: 776-790.
7. Haasnoot, J, and Berkhout, B (2009). Nucleic acids-based therapeutics in the battle against pathogenic viruses. *Handb Exp Pharmacol* **189**: 243-263.
8. Laine, S, Scarborough, RJ, Levesque, D, Didierlaurent, L, Soye, KJ, Mougel, M*, et al.* (2011). In vitro and in vivo cleavage of HIV-1 RNA by new SOFA-HDV ribozymes and their potential to inhibit viral replication. *RNA Biol* **8**.
9. Reyes-Darias, JA, Sánchez-Luque, FJ, and Berzal-Herranz, A (2008). Inhibition of HIV-1 replication by RNA-based strategies. *Curr HIV Res* **6**: 500-514.
10. Taylor, JM (2006). Hepatitis delta virus. *Virology* **344**: 71-76.
11. Bergeron, LJ, and Perreault, JP (2005). Target-dependent on/off switch increases ribozyme fidelity. *Nucleic Acids Res* **33**: 1240-1248.
12. Bergeron, LJ, Reymond, C, and Perreault, JP (2005). Functional characterization of the SOFA delta ribozyme. *RNA* **11**: 1858-1868.
13. Asif-Ullah, M, Lévesque, M, Robichaud, G, and Perreault, JP (2007). Development of ribozyme-based gene-inactivations; the example of the hepatitis delta virus ribozyme. *Curr Gene Ther* **7**: 205-216.

14. Lévesque, MV, Lévesque, D, Brière, FP, and Perreault, JP (2010). Investigating a new generation of ribozymes in order to target HCV. *PLoS One* **5**: e9627.
15. Motard, J, Rouxel, R, Paun, A, von Messling, V, Bisaillon, M, and Perreault, JP (2011). A novel ribozyme-based prophylaxis inhibits influenza A virus replication and protects from severe disease. *PLoS One* **6**: e27327.
16. Robichaud, GA, Perreault, JP, and Ouellette, RJ (2008). Development of an isoform-specific gene suppression system: the study of the human Pax-5B transcriptional element. *Nucleic Acids Res* **36**: 4609-4620.
17. Ben Aissa, M, April, MC, Bergeron, LJ, Perreault, JP, and Levesque, G (2012). Silencing of amyloid precursor protein expression using a new engineered delta ribozyme. *Int J Alzheimers Dis* **2012**: 947147.
18. D'Anjou, F, Routhier, S, Perreault, JP, Latil, A, Bonnel, D, Fournier, I*, et al.* (2011). Molecular Validation of PACE4 as a Target in Prostate Cancer. *Transl Oncol* **4**: 157-172.
19. Lévesque, MV, and Perreault, JP (2012). Target-induced SOFA-HDV ribozyme. *Methods Mol Biol* **848**: 369-384.
20. DeYoung, MB, and Hampel, A (1997). Computer analysis of the conservation and uniqueness of ribozyme-targeted HIV sequences. *Methods Mol Biol* **74**: 27-36.
21. Lee, SK, Dykxhoorn, DM, Kumar, P, Ranjbar, S, Song, E, Maliszewski, LE*, et al.* (2005). Lentiviral delivery of short hairpin RNAs protects CD4 T cells from multiple clades and primary isolates of HIV. *Blood* **106**: 818-826.
22. Waterhouse, AM, Procter, JB, Martin, DM, Clamp, M, and Barton, GJ (2009). Jalview Version 2--a multiple sequence alignment editor and analysis workbench. *Bioinformatics* **25**: 1189-1191.
23. Brummelkamp, TR, Bernards, R, and Agami, R (2002). A system for stable expression of short interfering RNAs in mammalian cells. *Science* **296**: 550-553.
24. Good, PD, Krikos, AJ, Li, SX, Bertrand, E, Lee, NS, Giver, L*, et al.* (1997). Expression of small, therapeutic RNAs in human cell nuclei. *Gene Ther* **4**: 45-54.
25. Puerta-Fernandez, E, Barroso-del Jesus, A, Romero-Lopez, C, Tapia, N, Martinez, MA, and Berzal-Herranz, A (2005). Inhibition of HIV-1 replication by RNA targeted against the LTR region. *AIDS* **19**: 863-870.
26. Unwalla, HJ, Li, H, Li, SY, Abad, D, and Rossi, JJ (2008). Use of a U16 snoRNA-containing ribozyme library to identify ribozyme targets in HIV-1. *Mol Ther* **16**: 1113-1119.
27. Chang, LJ, Liu, X, and He, J (2005). Lentiviral siRNAs targeting multiple highly conserved RNA sequences of human immunodeficiency virus type 1. *Gene Ther* **12**: 1133-1144.
28. Peden, KWC, and Martin, MA (1995). Virological and molecular genetic techniques for studies of established HIV isolates. In: Karn, J (ed). *HIV, a Practical Approach: Virology and Immunology*. IRL Press: Oxford. pp 21-45.
29. Clerzius, G, Gélinas, JF, Daher, A, Bonnet, M, Meurs, EF, and Gatignol, A (2009). ADAR1 interacts with PKR during human immunodeficiency virus infection of lymphocytes and contributes to viral replication. *J Virol* **83**: 10119-10128.
30. Altschul, SF, Madden, TL, Schäffer, AA, Zhang, J, Zhang, Z, Miller, W*, et al.* (1997). Gapped BLAST and PSI-BLAST: a new generation of protein database search programs. *Nucleic Acids Res* **25**: 3389-3402.

31. Lévesque, MV, Rouleau, SG, and Perreault, JP (2011). Selection of the most potent specific on/off adaptor-hepatitis delta virus ribozymes for use in gene targeting. *Nucleic Acid Ther* **21**: 241-252.
32. Lucier, JF, Bergeron, LJ, Brière, FP, Ouellette, R, Elela, SA, and Perreault, JP (2006). RiboSubstrates: a web application addressing the cleavage specificities of ribozymes in designated genomes. *BMC Bioinformatics* **7**: 480.
33. Butler, PJG (1995). Biological safety when working with HIV. In: Karn, J (ed). *HIV, a Practical Approach: Virology and Immunology*. IRL Press: Oxford. pp 1-12.

Chapter 3

A conserved target site in HIV-1 Gag RNA is accessible to inhibition by both an HDV ribozyme and a short hairpin RNA

This chapter was adapted from the following manuscript:

Scarborough RJ, Levesque MV, Boudrias-Dalle E, Chute IC, Daniels SM, Ouellette RJ, Perreault JP, and Gatignol A. 2014. "A Conserved Target Site in HIV-1 Gag RNA is Accessible to Inhibition by Both an HDV Ribozyme and a Short Hairpin RNA."
Mol Ther Nucleic Acids 3:e178.

3.1 PREFACE

Using the methods described in Chapter 2, this chapter presents data on the identification of a highly conserved target site in HIV-1 RNA that was accessible to both a SOFA-HDV ribozyme and an shRNA. Also presented are data used to characterise both molecules for potential off-target effects on human RNAs, effects against diverse viral strains and effects against viral replication in a T cell line.

Contribution of authors: Under the supervision of AG, RJS performed most of the experiments and wrote the manuscript. MVL performed northern blots for ribozyme expression levels (Figure 3.5 **b**) and designed and executed in vitro cleavage experiments (Figure 3.5 **c**). Micro-array experiments were designed by RJS, MVL and ICC under the supervision of AG, JPP and RJO. Data from the micro-arrays were generated by ICC (Figure 3.10) and analyzed by MVL (Figure 3.11). EBD assisted in the construction of SOFA-HDV ribozyme vectors under the supervision of RJS. All authors assisted in the review and revision of the manuscript.

3.2 ABSTRACT

Antisense-based molecules targeting HIV-1 RNA have the potential to be used as part of gene or drug therapy to treat HIV-1 infection. In this study, HIV-1 RNA was screened to identify more conserved and accessible target sites for ribozymes based on the hepatitis delta virus motif. Using a quantitative screen for effects on HIV-1 production we identified a ribozyme targeting a highly conserved site in the Gag coding sequence with improved inhibitory potential compared to our previously described candidates targeting the overlapping Tat/Rev coding sequence. We also demonstrate that this target site is highly accessible to short hairpin directed RNA interference, suggesting that it may be available for the binding of antisense RNAs with different modes of action. We provide evidence that this target site is structurally conserved in diverse viral strains and that it is sufficiently different from the human transcriptome to limit off-target effects from antisense therapies. We also show that the modified hepatitis delta virus ribozyme is more sensitive to a mismatch in its target site compared to the short hairpin RNA. Overall our results validate the potential of a new target site in HIV-1 RNA to be used for the development of antisense therapies.

3.3 INTRODUCTION

Over 30 small molecules are available for the treatment of Human Immunodeficiency Virus 1 (HIV-1) infection, targeting the viral enzymes reverse transcriptase (RT), protease and integrase, as well as the cellular entry co-receptor, CCR5 [1]. Although treatment of HIV-1 with combination small molecule therapy is effective in preventing acquired immune deficiency syndrome, it cannot eradicate the virus and is associated with a number of short- and long-term

side effects [2]. Alternative therapeutic strategies for long-term viral suppression with low adverse effects are needed and small RNAs represent a growing class of molecules with the potential to complement or replace current therapies. They are being evaluated for use in *ex vivo* gene therapy [3] and with advances that have been made in their systemic delivery [4], may soon be evaluated for use in combination drug therapy. Many small RNAs, including antisense oligonucleotides (ASONs), ribozymes (Rzs), decoys, aptamers, small nuclear (sn) RNAs, and small interfering (si) or short hairpin (sh) RNAs have been designed with diverse target sites in the HIV-1 replication cycle [5]. Antisense-based RNAs (ASONs, Rzs, snRNAs, sh/si RNAs) can be designed to target HIV-1 RNA, and several therapeutic candidates have been described.

Rzs targeting HIV-1 RNA have been made by modifying hammerhead, hairpin [6] and bacterial RNase P [7] motifs. The HDV Rz represents an alternative small Rz motif, that has evolved to function in human cells and has the potential to be used for the development of therapeutic Rzs [8]. To improve the specificity of the HDV Rz for its target RNA, the SOFA (Specific On/oFf Adaptor) module was engineered [9, 10] (Figure 3.1 **a**). Several SOFA-HDV-Rzs have been identified with the potential to target human [11, 12], viral [9, 13, 14] and bacterial [15] RNAs, including three Rzs that we have evaluated targeting the overlapping Tat/Rev coding sequence of HIV-1 RNA [16].

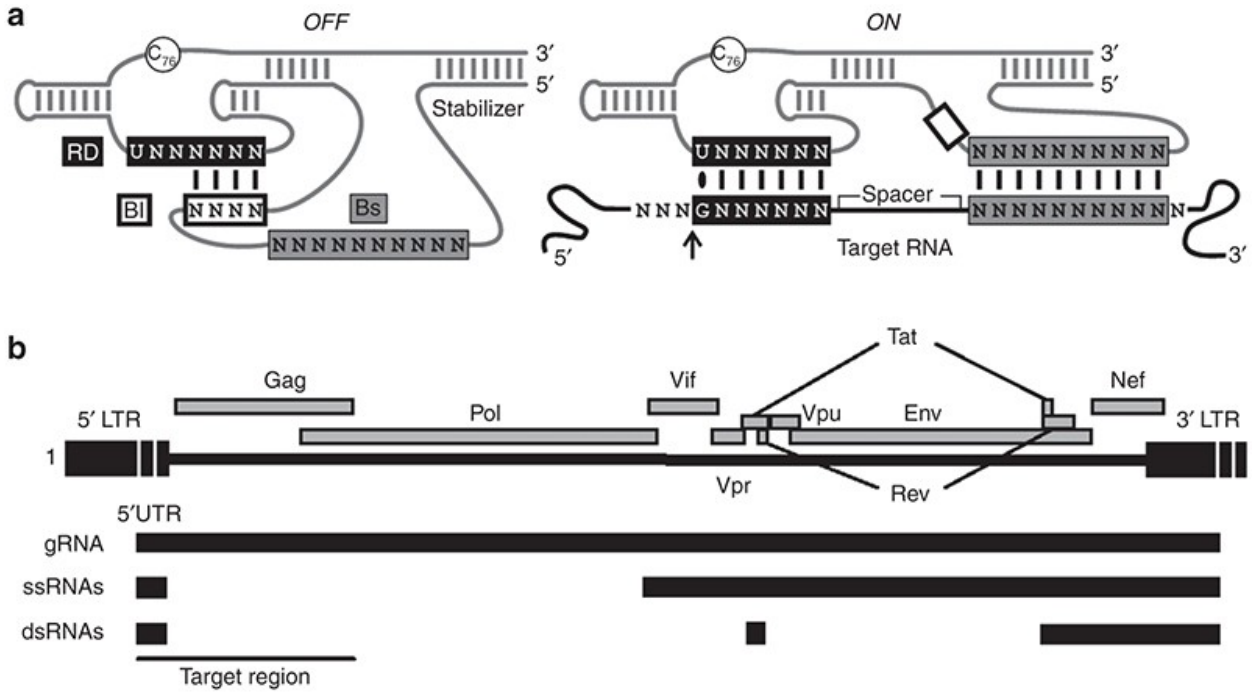

Figure 3.1. Schematic representation of the SOFA-HDV-Rz and the HIV-1 RNA region used to identify SOFA-HDV-Rz target sites.

a) The SOFA-HDV-Rz is illustrated in both its *OFF* and *ON* conformations. In the *OFF* conformation, the SOFA blocker (Bl) base pairs with the last 4 nts of the recognition domain (RD). When the SOFA biosensor (Bs) base pairs with a specific target sequence, the RD is released from the Bl sequence and binds at 3 to 5 nts upstream from the Bs binding site in the *ON* conformation. The first nt in the target site (n+1) must be a G, forming a wobble base pair with the RD U. The cleavage site is indicated with an arrow and the nt C_{76}, which can be mutated to disable the catalytic activity of the SOFA-HDV-Rz, is shown as a circle in the Rz backbone. **b)** The full length genomic (g), singly-spliced (ss) and doubly-spliced (ds) RNA species of HIV-1 are illustrated. Reading frames for all HIV-1 proteins are shown above the different RNAs and the 5' region, used to identify SOFA-HDV-Rz target sites, is underlined.

Optimal hammerhead Rz target sites in HIV-1 RNA have been identified using libraries of Rzs with randomized binding arms [17, 18] and a library of Rzs targeting highly conserved sequences [19]. Using different methods and datasets to estimate sequence conservation, sets of optimal siRNAs [20] or shRNAs [21, 22] have been identified and two of these studies have reported their conservation estimates in 19 to 21 nt frames [20, 22]. Estimates have also been reported at the nucleotide (nt) level to identify or characterize Rz [23], snRNA [24] and shRNA

[25] target sites. In this study we generated conservation estimates at the nt level to identify a set of optimal SOFA-HDV-Rzs target sites from the beginning of the 5' untranslated region (UTR) to the end of the Gag coding sequence (Figure 3.1 **b**). Out of 18 new SOFA-HDV-Rzs, one Rz targeting a novel site in the Gag coding sequence was particularly effective at reducing viral production. An shRNA targeting the same site was shown to be an extremely potent inhibitor of viral production and evidence that the identified target site is accessible to inhibition in diverse HIV-1 strains is provided.

3.4 RESULTS

3.4.1 Identification of SOFA-HDV-Rz target sites in HIV-1 RNA

HIV-1 sequence conservation was estimated to identify target sites that are relevant for the majority of HIV-1 strains. Estimates at the nt level were made using all complete sequences available in the LosAlamos National Laboratory (LANL) database (1850 at the time of analysis, subtype distribution shown in Figure 3.2). These estimates were used to identify highly conserved SOFA-HDV-Rz target sites (Figure 3.3 **a**) that were identical in HIV-1 strain NL4-3 (Figure 3.3 **b**). The Ribosubstrates informatics tool [26] was used to exclude SOFA-HDV-Rzs targeting 12 highly conserved and 19 moderately conserved regions in HIV-1 RNA, due to their potential to target human RNAs.

Consistent with previous studies [20, 22], several highly conserved target sites were identified in the 5'LTR U5 region within the 5'UTR (Figure 3.3 **c**). The Gag coding sequence had much lower overall conservation; however, four highly conserved and, with some exceptions to our

conservation criteria (Figure 3.3 **a**), nine moderately conserved target sites were identified in this region (Figure 3.3 **c**). Of the Rzs that we have previously evaluated targeting the Tat/Rev exon1 coding sequence of HIV-1 RNA [16], the target sites for Tat1 and Tev1 were highly and moderately conserved, respectively. Conservation exceptions and sequences of all target sites used in this study are illustrated, along with the DNA sequences of the corresponding SOFA-HDV-Rz variable regions, in Table 3.1.

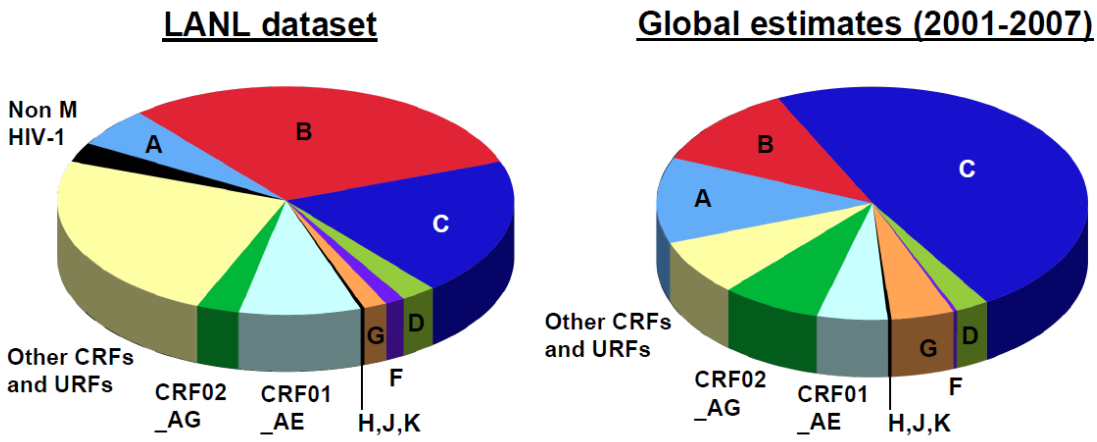

Figure 3.2. Subtype distribution of HIV-1 sequences used to calculate conservation estimates in comparison to global distribution estimates.

HIV-1 Group M subtypes A-D, F-H, J, K,circulating recombinant forms (CRFs) 01_AE and 02_AG, other CRFs and unique recombinant forms (URFs) and non M-group HIV-1 sequences are illustrated over or next to their proportional representation in the LANL dataset used to evaluate sequence conservation (left) and global estimates reproduced from manuscript reference # 44 (right).

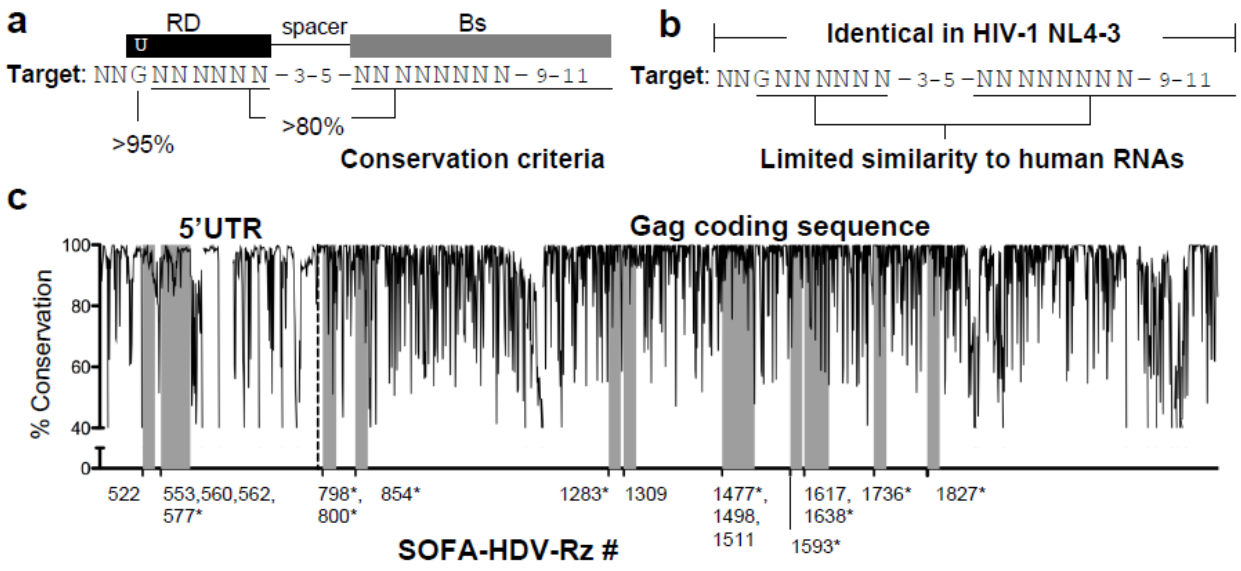

Figure 3.3. SOFA-HDV-Rz target site identification.

a) Criteria used to identify SOFA-HDV-Rz target sites in HIV-1 RNA based on our conservation estimates at the nt level are illustrated. The number of nts between the RD and the Bs (spacer, 3-5), and the length of the Bs (9-11), were adjusted to avoid poorly conserved positions or to reduce potential off-target effects on human RNAs. A spacer of 4 nt and Bs length of 10 nt were used as the default positioning. **b)** Target sites were excluded if they were not identical in HIV-1 NL4-3 or if the corresponding Rz had potential target sites in human RNAs using a cut-off score of 20 in the Ribosubstrates tool[26]. **c)** Sequence conservation estimates in the 5' region of HIV-1 RNA are shown for each nt position in HIV-1 NL4-3 with the selected Rz binding sites shaded in grey. SOFA-HDV-Rzs were named according to the first nt in their binding site. The dashed line represents the separation between the 5'UTR and Gag ORF. SOFA-HDV-Rz target sites that were moderately conserved, but did not meet our conservation criteria, are indicated with an asterisk (*).

Table 3.1. SOFA-HDV-Rz target sites and DNA coding sequences.

	HIV-1 NL4-3 target sites : 5'-3'[1]		SOFA-HDV-Rz DNA sequences : 5'-3'[2]		
Rz	RD	Bs	Bs	RD	Bl
HBV	-		GAGACAAGAA	AAACCAT	GTTT
Tat1	TAGATCCTA**ga**CTAGAGCCCTGGAA		CCAGGGCTCT	TAGGATT	CCTA
Tev1	CAGGAAGAAGCGGAGACA**g**CGACGA		GTCGCTGTCT	TTCTTCT	AGAA
522	AAGCCTCAATAAAGCTTGCCTTGAG		CAAGGCAAGC	TTGAGGT	TCAA
553	AAGTAGTGTGTGCCCGTCTGTTGTG		ACAACAGACGG	ACACTAT	GTGT
560	GTGTGCCCGTCTGTTGTGTGACTCT		AGTCACACAA	CGGGCAT	CCCG
562	GTGCCCGTCTGTTGTGTGACTCTGG		AGAGTCACAC	GACGGGT	CGTC
577	GTGACTCTGGTAACTAGAGATCCCT		GGATCTCTAG	CAGAGTT	TCTG
798	GCGAGAGCGTC**gg**TATTAAG**c**GGGG		CCGCTTAATA	CGCTCTT	AGCG
800	GAGAGCGTC**gg**TATTAAG**c**GGGGGA		CCGCTTAAT	GACGCTT	CGTC
854	AAGGCCAGGGGGAAAGAAA**c**A**a**TAT		ATTGTTTCTT	CCTGGCT	CAGG
1283	**C**AGCCCAGA**a**GTAATACCCATGTTT		ACATGGGTAT	TCTGGGT	CAGA
1309	CAGCATTATCAGA**a**GGAGCCACCCC		GGTGGCTCC	ATAATGT	TTAT
1477	G**a**GAACCAAGGGGAAGTGA**c**ATAGC		ATGTCACTTC	TTGGTTT	CCAA
1498	TAGCAGGAACTACTAGTACCCTTCA		AAGGGTACTA	TTCCTGT	GGAA
1511	TAGTACCCTTCA**g**GAACAAATAG**g**A		CTATTTGTTC	AGGGTAT	CCCT
1593	CTGGG**a**TTAAATAAAATAGTAAGAA		CTTACTATTT	TAATCCT	ATTA
1617	ATGTATAGCCCT**acc**AGCATT**c**TGG		CCAGAATGCTG	GCTATAT	TAGC
1638	**C**TGGACATAA**g**ACAAGG**a**CCAAA**g**G		CTTTGGTCCTT	TATGTCT	CATA
1736	TTGGATGACAGA**a**ACCTTG**t**TGGTC		CCAACAAGGT	GTCATCT	TGAC
1827	ATGATGACAGCATG**t**CAGGGAGTGG		ACTCCCTGAC	TGTCATT	GACA

[1] The target sites of SOFA-HDV-Rzs in HIV-1 NL4-3 are shown with the recognition domain (RD) and the biosensor (Bs) binding sites underlined. Nucleotide positions with less than 80% conservation according to our estimates are shown as bold lower case.

[2] The variable DNA sequences used to clone SOFA-HDV-Rzs into the psiRNA vector are shown for the RD, Bs and blocker (Bl) regions.

3.4.2 SOFA-HDV Rz screen for inhibition of HIV-1 production

The effect of each SOFA-HDV-Rz expressing plasmid on HIV-1 production was evaluated by co-transfection with HIV-1 molecular clone pNL4-3 in HEK293T cells, using conditions similar to those reported for other Rzs [7, 18, 27] and shRNAs [21, 22]. HIV-1 RT activity was measured to estimate the production of virus released into the medium of transfected cells and effects of Rzs were normalized to co-transfection of pNL4-3 with an empty Rz expression plasmid. An irrelevant Rz targeting Hepatitis B Virus RNA (SOFA-HDV-RzHBV, adapted from SOFA-δRz-303 [9]) was used as a negative control and previously described SOFA-HDV-Rzs Tat1 and Tev1 [16] were used as positive controls. Compared to SOFA-HDV-RzHBV, Rzs targeting both the 5'UTR and Gag coding sequences significantly inhibited viral production, with the top candidate (SOFA-HDV-Rz-1498) targeting the Gag coding sequence (Figure 3.4).

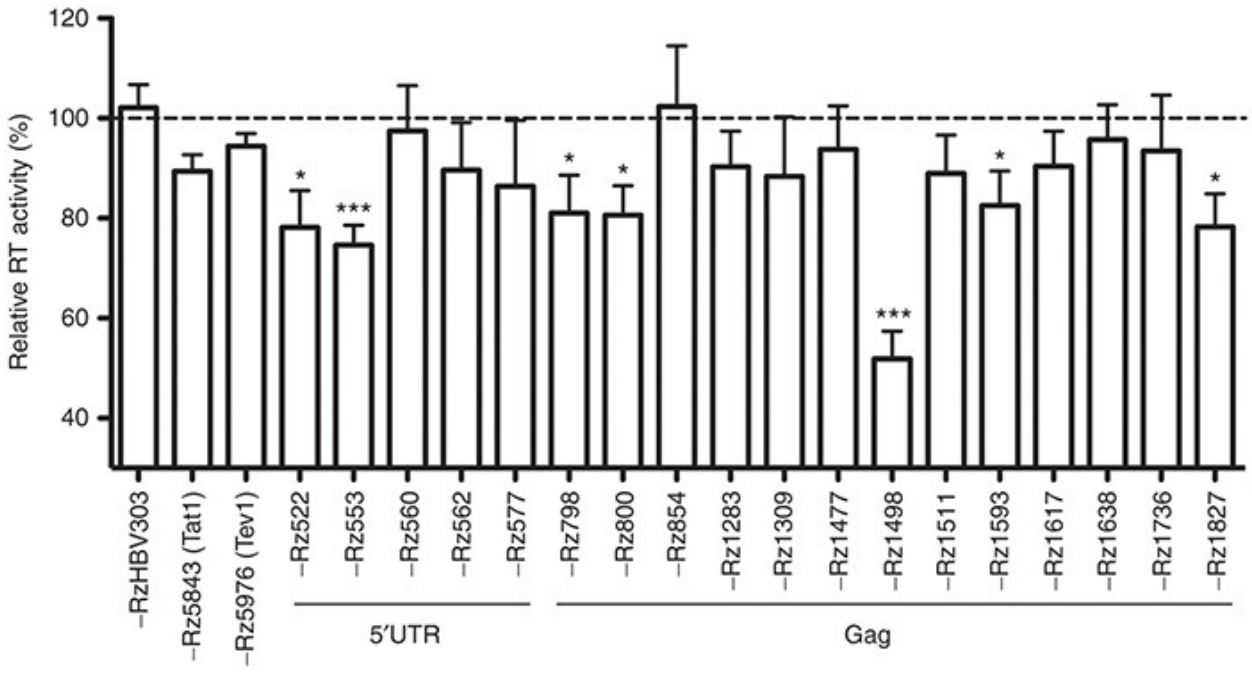

Figure 3.4. Inhibition of HIV-1 production by SOFA-HDV-Rzs.

HEK293T cells were seeded in 24 well plates and co-transfected with HIV-1 pNL4-3 plasmid DNA (75 ng) and one of the indicated psiRNA SOFA-HDV-Rz expression plasmids (750 ng). Viral production was estimated 48 h following transfection by measuring the activity of HIV-1 RT in culture supernatants. Each replicate was expressed as a percentage of the value obtained for co-transfection with the empty Rz expression plasmid tested in parallel (Relative RT activity). Rzs were evaluated in at least three independent experiments with one to three replicate transfections, data are expressed as the mean +/- standard error mean (SEM) (n=5-10). Graph Pad Prism was used to calculate P values for the effects of each HIV-1 specific SOFA-HDV-Rz compared to the irrelevant control (-RzHBV). Results from un-paired t-tests are shown above each SOFA-HDV-Rz that demonstrated a significant inhibition of viral production compared to the control (* $P<0.05$, ** $P<0.01$, *** $P<0.001$).

3.4.3 Antisense and mismatched variants of SOFA-HDV-Rz1498 are not effective inhibitors of HIV-1 production

To evaluate the antisense effect of SOFA-HDV-Rz1498, we generated an inactive variant (SOFA-HDV-Rz1498A76) in which a C to A mutation at position 76 in its backbone disables its cleaving capability [28] (Figure 3.5 **a**). SOFA-HDV-Rz1498A76 did not significantly inhibit HIV-1 production at similar expression levels to SOFA-HDV-Rz1498 (Figure 3.5 **b**), suggesting that Rz catalytic cleavage is primarily responsible for the effects of SOFA-HDV-Rz1498. No effect on the infectivity of virus from SOFA-HDV-Rz1498 expressing cells was observed (Figure 3.6), suggesting that the Rz reduces the amount of virus produced but does not affect the quality of the virions.

SOFA-HDV-Rz1498 variants with either a single or double mutation in their biosensor (Bs) sequence were also generated to evaluate the potential for SOFA-HDV-Rz1498 to tolerate mismatches with its target (SOFA-HDV-Rz1498Bs1 and SOFA-HDV-Rz1498Bs2, Figure 3.5 **a**). Neither variant inhibited HIV-1 production (Figure 3.5 **b**), suggesting that the effect of SOFA-HDV-Rz1498 is highly sensitive to mismatches with its target. The mismatched Rzs had similar *in vitro* cleavage rate constants (k_{obs}) with significantly reduced maximum cleavage (F_{max}) values (Figure 3.5 **c**), suggesting that part of their failure to inhibit HIV-1 production in cells is related to a reduced capacity to cleave their target.

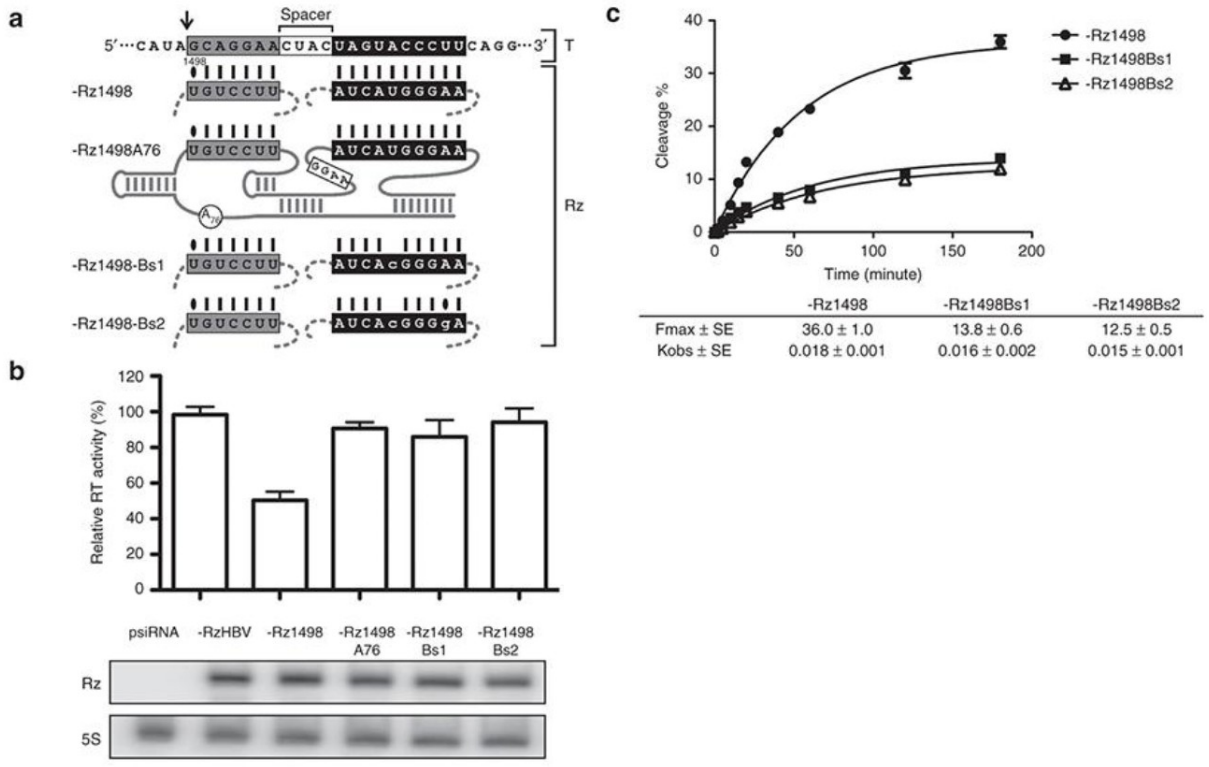

Figure 3.5. Effects of SOFA-HDV-Rz1498 variants on HIV-1 production.

a) Schematic representation of the SOFA-HDV-Rz1498 target site (T) and variants (Rz). SOFA-HDV-Rz1498A76 has a C to A mutation in the Rz backbone, -Rz1498Bs1 and -Rz1498Bs2 have 1 or 2 nt variants in the biosensor (Bs), indicated in lower case. **b)** Effects of each SOFA-HDV-Rz1498 variant on viral production in HEK293T cells were evaluated exactly as in Figure 3.4. Rzs were evaluated in at least three independent experiments with one to three replicate transfections (reported as mean +/- SEM, n=6-10). The relative expression of Rz and 5S RNA loading control for the different conditions are shown below for one of two independent experiments performed in HEK293T cells seeded in a 12 well plate and co-transfected with twice the amount of DNA used for the evaluation of viral production in 24 well plates. **c)** Single turnover *in vitro* cleavage activities for SOFA-HDV-Rz1498, -Rz1498Bs1 and -Rz1498Bs2 were determined at different incubation times with a small substrate RNA (Rz>>substrate). Cleavage % was measured by dividing cleaved products by cleaved + uncleaved products, quantified from bands on a gel. A nonlinear regression one phase exponential association equation with least squares (ordinary) fit was determined using Graph Pad Prism for the different Rzs. All data points represent two independent experiments and are reported as mean +/- SEM (n=2). The average rate constants (k_{obs}) and maximum cleavage values (F_{max}) for the SOFA-HDV-Rzs are reported in a table.

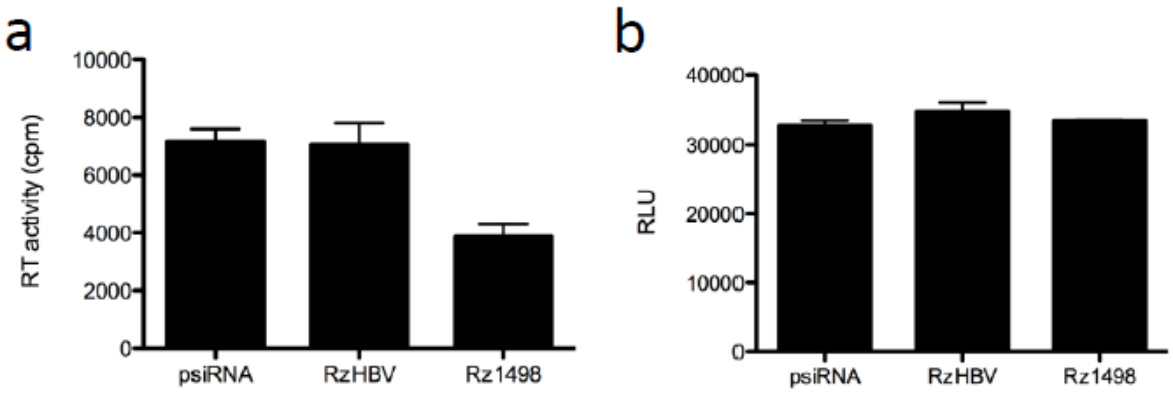

Figure 3.6. Effect of SOFA-HDV-Rz1498 on the quality of virions produced from co-transfected HEK293T cells.

a) HEK293T cells were seeded in 24 well plates and transfected exactly as in **Figure 3.4**. RT activity is expressed as counts per minute for cells transfected with the empty Rz expression plasmid (psiRNA), the irrelevant SOFA-HDV-RzHBV and SOFA-HDV-Rz1498 targeting HIV-1 RNA. **b**) Supernatants from A were normalized by volume to the same RT activity and used to infect TZM-bl cells seeded in 12 well plates 24 h prior to infection. 48 h after infection, intracellular luciferase activity was measured (expressed as relative luciferase units, RLU). Luciferase activity is proportional to the level of Tat protein produced from viral genomes that integrated into the TZM-bl genome following infection and is a measure of viral infectivity.

3.4.4 An shRNA targeting the 1498 site is a potent inhibitor of HIV-1 production and provides an additive effect in combination with SOFA-HDV-Rz1498

To evaluate the potential for other antisense molecules targeting the SOFA-HDV-Rz1498 target site to inhibit HIV-1 production, we designed shRNA1498. According to our conservation estimates, each nt in the shRNA1498 target site was conserved at >80% (Figure 3.7 **a**, Gag). Compared to a nonsense shRNA (shRNAns) as well as SOFA-HDV-Rz1498 and its controls, shRNA1498 provided a near complete inhibition of viral production (Figure 3.7 **b**). This inhibition correlated with a decrease in intracellular expression of the HIV-1 Gag polyprotein and one of its processing products, capsid (CA). Unexpectedly, the decrease in CA expression was much more pronounced for both the Rz and shRNA compared to their effects on Gag

expression. A similar effect was observed for shRNAs targeting sequences in the 5'UTR and tat/rev coding sequences of HIV-1 RNA (Figure 3.8), suggesting that it is not specific to an shRNA targeting the Gag 1498 sequence.

To compare the potency of shRNA1498 to other candidate shRNAs, we designed shRNA522 and shRNA553, modeled after previously characterized siRNAs [20] and shRNAs [22] targeting the 5'UTR (Figure 3.7 **a**, 5'UTR) and shRNA5983, modeled after a construct in clinical development targeting the Tat/Rev exon1 coding sequence [29] (Figure 3.7 **a**, Tat/Rev). All four shRNAs inhibited HIV-1 production (Figure 3.7 **c**). The potency of shRNA1498 was comparable to that of shRNA553 and shRNA5983, with 50% effective concentrations (EC50s) for shRNA plasmids below 5 ng of input DNA, whereas shRNA522 was much less potent with an EC50 value of 702 ng.

To evaluate the potential for shRNA1498 and shRNA5983 to be used in combination with SOFA-HDV-Rz1498, we co-transfected HEK293T cells with HIV-1 pNL4-3 and different combinations of Rzs and shRNAs (Figure 3.7 **d**). To quantify the effect of the combinations, we chose an input level of shRNA DNA that did not completely inhibit viral production in Figure 3.7 **c**. In combination with both shRNA1498 and shRNA5983, SOFA-HDV-Rz1498 provided an additional inhibition of HIV-1 production compared to the control Rz, SOFA-HDV-Rz-HBV. The level of inhibition was similar to its effect when co-transfected alone (50%) (Figure 3.7 **b**), suggesting that the Rz can provide an additive effect in combination with both an shRNA targeting the same site (shRNA1498) and an shRNA targeting a different site (shRNA5983).

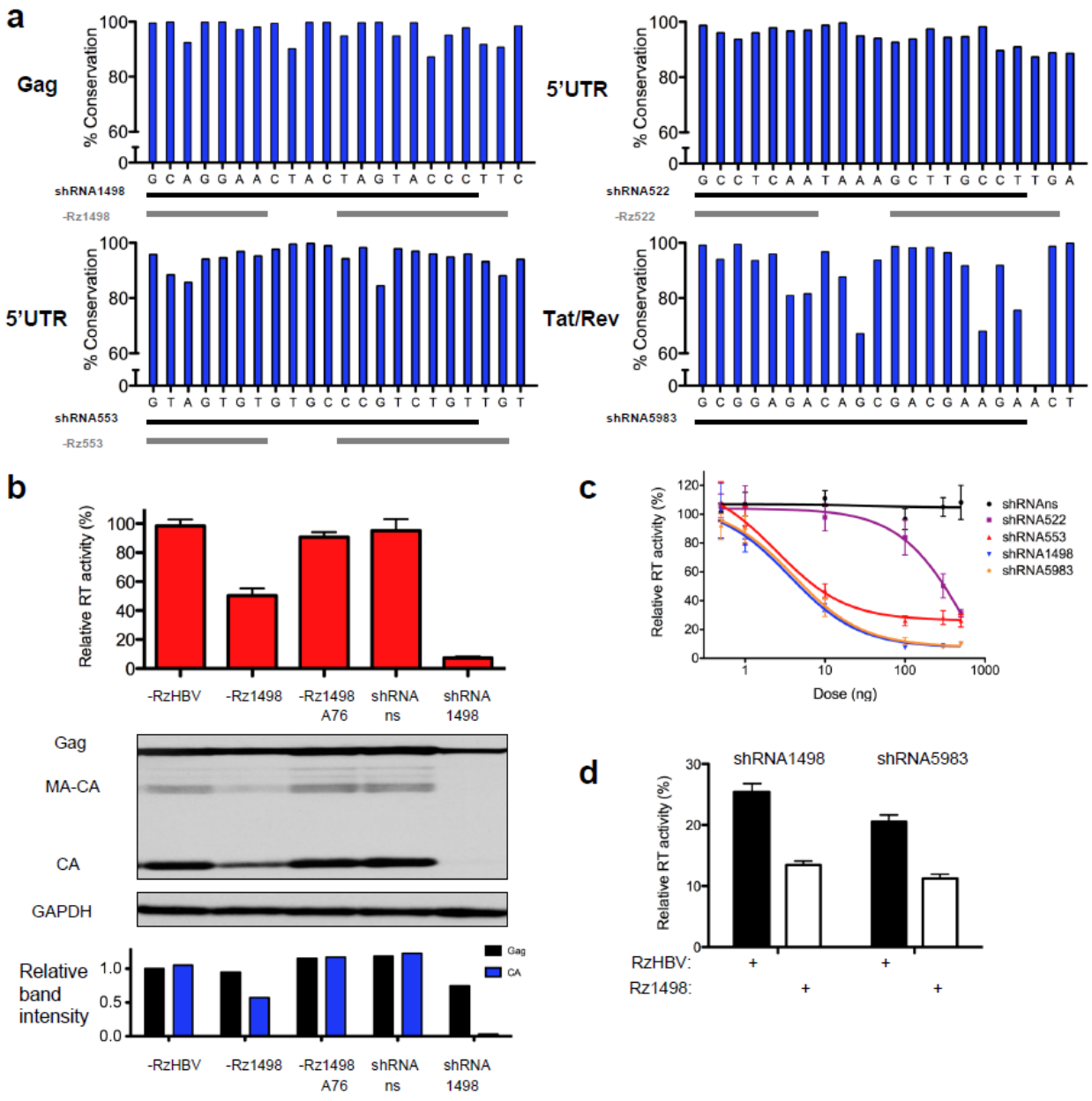

Figure 3.7. Effects of shRNA1498 on HIV-1 production (legend on following page).

Figure 3.7. Effects of shRNA1498 on HIV-1 production.

a) Sequences targeted by shRNA1498 and control shRNAs targeting HIV-1 RNA (shRNA522, shRNA553, and shRNA5983) are shown in relation to our conservation estimates at the nt level. **b)** Effects of shRNA1498 and a nonsense shRNA (shRNAns) on viral production in HEK293T cells were evaluated exactly as in Figure 3.4. Rzs and shRNAs were evaluated in at least three independent experiments with one to three replicate transfections (reported as mean +/- SEM, n=6-10). The relative intracellular expression of HIV-1 Gag polyprotein (GAG, p55), matrix-capsid intermediate (MA-CA, p39), and capsid (CA, p24) proteins as well as GAPDH loading control are shown below for one of two independent experiments performed in HEK293T cells seeded in a 12 well plate and co-transfected with twice the amount of DNA used for the evaluation of viral production. Relative band intensities for Gag and CA were calculated using Image J software and are expressed as a fraction of the intensity of Gag in the SOFA-HDV-RzHBV control lane. **c)** The potency of shRNAs was evaluated by co-transfecting HEK293T cells seeded in a 24 well plate with 100 ng of pNL4-3 DNA and 1-750 ng of shRNA expressing plasmids. For lower amounts of shRNA plasmid DNA (1-500 ng), co-transfections were topped up to 850 ng total DNA by the addition of an irrelevant plasmid (pBluescript SK+, Stratagene, La Jolla, CA). Relative RT activity measurements were log transformed and a nonlinear regression log(inhibitor) vs. response equation with least squares (ordinary) fit was determined using Graph Pad Prism for the different shRNAs. IC50 values from this equation are mentioned in the text. All data-points represent at least two independent experiments with 2-3 replicates and are reported as mean +/- SEM (n=4-8). **d)** Combinations of SOFA-HDV-Rz and shRNA expressing plasmids were evaluated in HEK293T cells seeded in 24 well plates and co-transfected with 100 ng pNL4-3, 10 ng of shRNA expressing plasmid and 1 µg of Rz expressing plasmid. Data were normalized to co-transfection of 100 ng pNL4-3 with 1 µg of the empty Rz/shRNA expression plasmid and are reported as the mean +/- SEM from two independent experiments performed in triplicate (n=6).

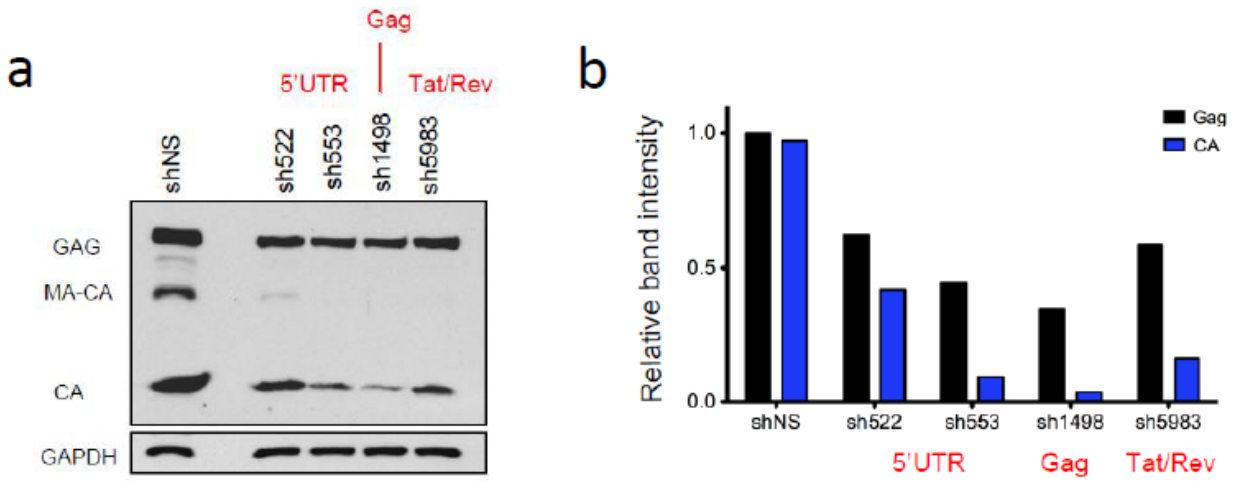

Figure 3.8. Gag and Capsid protein expression in cells co-transfected with HIV-1 pNL4-3 and different HIV-1 RNA specific shRNAs.

HEK293T cells were seeded in 12 well plates and co-transfected with HIV-1 pNL4-3 plasmid DNA (150 ng) and one of the indicated psiRNA short hairpin (sh) RNA expression plasmids (300 ng). A nonsense (NS) shRNA was used as a control (shRNAns) and shRNAs targeting the 5'UTR (shRNA522 and shRNA553), the Gag coding sequence (shRNA1498) and the overlapping tat/rev coding sequence (shRNA5983) of HIV-1 were evaluated. Cell lysates were obtained 48 h after co-transfection. **a**) The relative intracellular expression of HIV-1 Gag polyprotein (Gag, p55), matrix-capsid intermediate (MA-CA, p39), and capsid (CA, p24) proteins as well as GAPDH loading control are shown. **b**) Relative band intensities for Gag and CA were calculated using Image J software and are expressed as a fraction of the intensity of Gag in the shNS control lane.

3.4.5 SOFA-HDV-Rz1498 and shRNA1498 inhibit viral production from diverse HIV-1 strains

As the Gag 1498 target site was accessible to inhibition by both a Rz and an shRNA in HIV-1 strain NL4-3, we next evaluated whether this inhibition extended to diverse viral strains representing subtype B (Mal [30] and AD8 [31]), C (Indie-C1 [32] and MJ4 [33]), D (94UG114 [34]) and circulating recombinant form (CRF) 02_AG (97GH-AG1 [35]). SOFA-HDV-Rz1498 inhibited HIV-1 production from viral strains (Mal, AD8, MJ4 and 97GH-AG1) with nt variants in proximity to their target sites compared to NL4-3 (Figure 3.9), suggesting that the structure of the target site is equally accessible to the Rz in these strains. Consistent with results using SOFA-HDV-Rz binding site variants (Figure 3.5, -Bs1 and -Bs2), SOFA-HDV-Rz1498 did not inhibit HIV-1 production from the strains Indie-C1 and 94UG114, which harbor a single nt variant within their Bs binding sites (Figure 3.9). In contrast, shRNA1498 inhibited HIV-1 production from all strains suggesting that it can tolerate a single nt mismatch in its binding site at position 17 and can inhibit HIV-1 production in diverse strains.

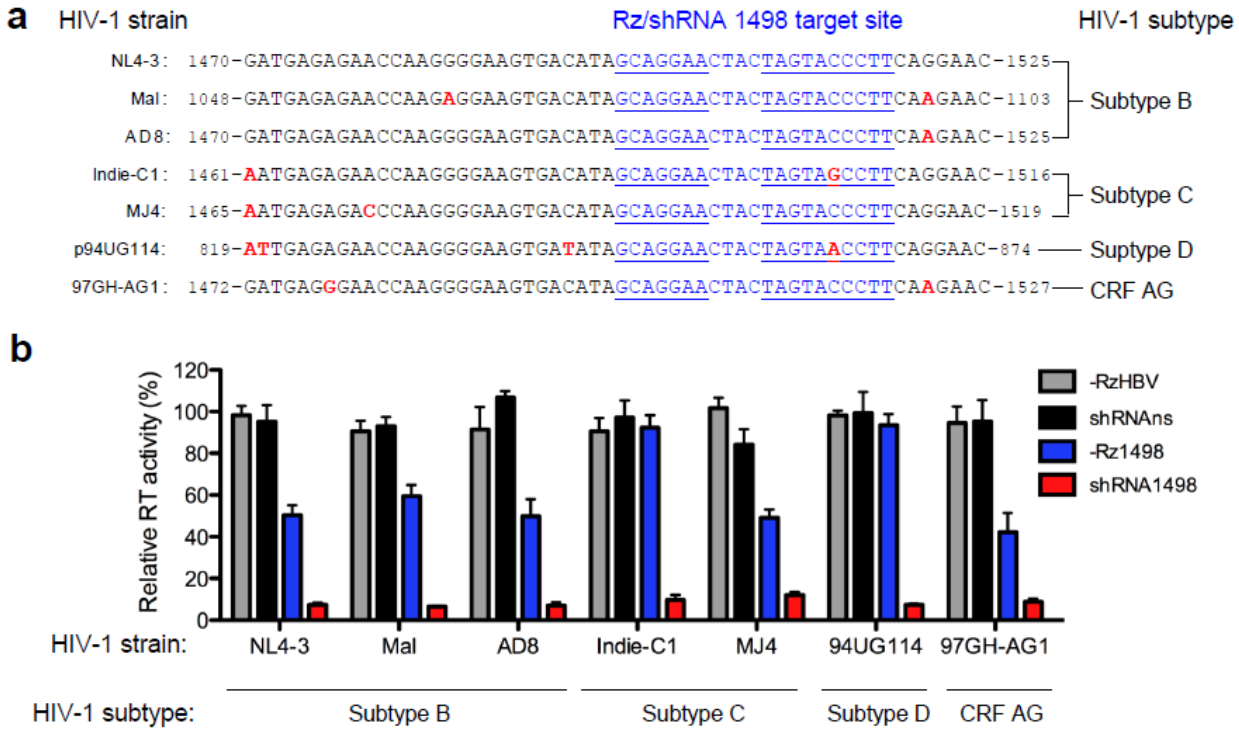

Figure 3.9. Inhibition of HIV-1 production from diverse viral strains by SOFA-HDV-Rz1498 and shRNA1498.

a) The sequence in and around the shRNA1498 and SOFA-HDV-Rz1498 target site is shown for HIV-1 NL4-3 (M19921), MAL (K03456), AD8 (AF004394), Indie-C1 (AB023804.1), MJ4 (AF321523), 94UG114 (U88824.1) and 97GH-AG1 (AB049811.1). The overlapping target site for shRNA1498 and SOFA-HDV-Rz1498 is highlighted in blue, with both the RD (7 nt) and Bs (10 nt) binding sites underlined. Nt variations compared to HIV-1 NL4-3 are highlighted in red and the start and end positions for each sequence are shown according to their annotation in Genbank. **b)** Effects of SOFA-HDV-Rz1498, shRNA1498 and their controls on HIV-1 production from different molecular clones in HEK293T cells were evaluated exactly as in Figure 3.4, with at least two independent experiments, each including two to three replicate transfections (reported as mean +/- SEM, n=4-10).

3.4.6 SOFA-HDV-Rz1498 and shRNA1498 have minimal off-target effects on human RNAs

The potential for both SOFA-HDV-Rz1498 and shRNA1498 to affect the expression of human mRNAs was next evaluated in HEK293T cells co-transfected with HIV-1 pNL4-3. Prior to gene expression profiling, the inhibition of viral production was confirmed for each condition (data not shown) and agreed with results presented in Figure 3.7 **b**. Microarray experiments were performed as triplicate dye swaps and the results were expressed as the log2 ratio of SOFA-HDV-Rz1498 or shRNA1498 compared to the empty vector co-transfected cells (Figure 3.10). All average log2 ratios were low (below 1.0) suggesting that both SOFA-HDV-Rz1498 and shRNA1498 can inhibit HIV-1 production with minimal effects on human mRNA expression. The log2 ratios for mRNAs with the greatest extent of up- or down- regulation are illustrated in Figure 3.11. Several of these mRNAs were found in both SOFA-HDV-Rz1498 and shRNA1498 conditions, suggesting that part of the observed changes may be target site specific.

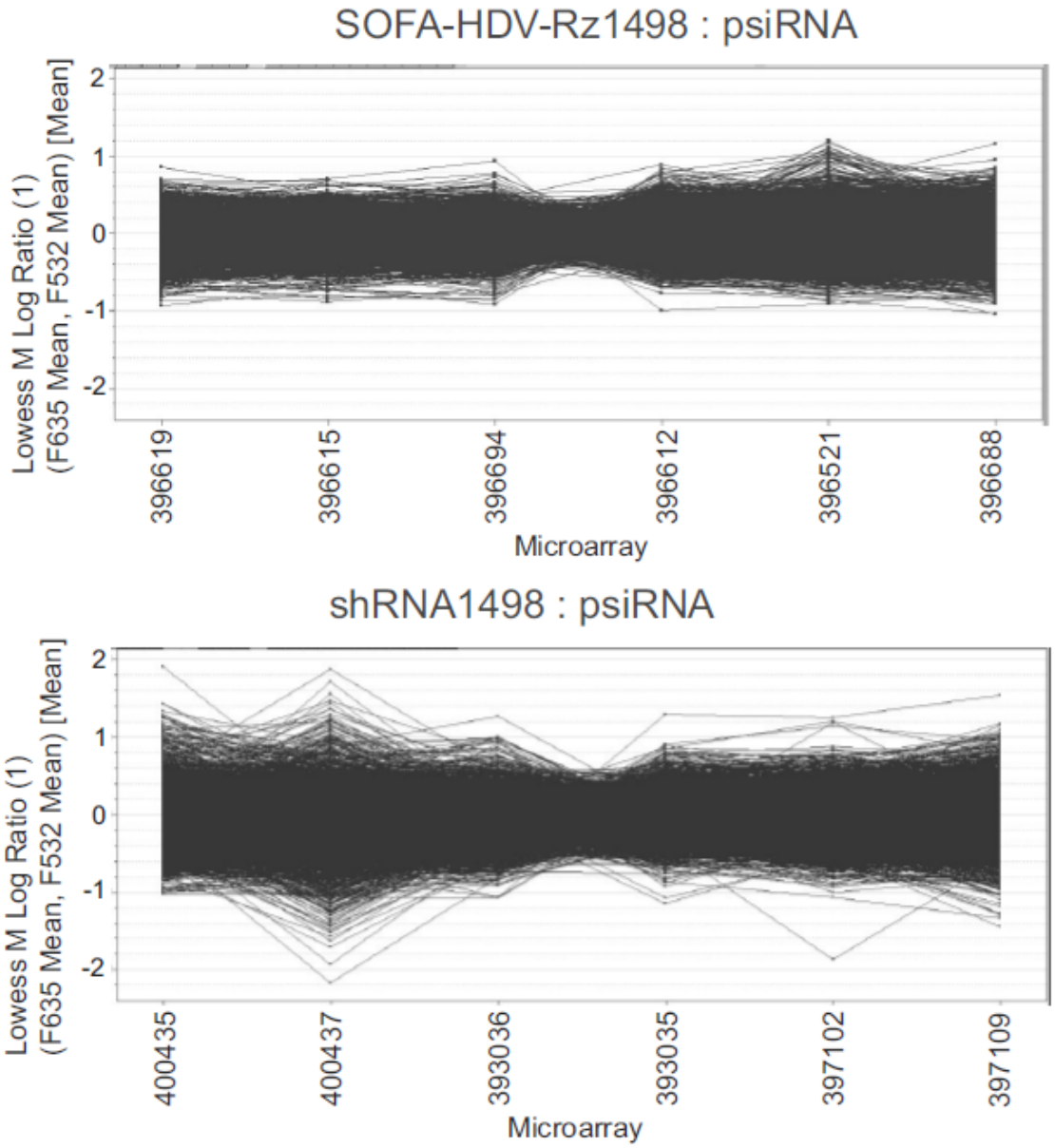

Figure 3.10. Change in mRNA expression ratios compared to a control vector for SOFA-HDV-Rz1498 and shRNA1498 transfected HEK293T cells as detected by microarray.

RNA extracts were obtained from HEK293T cells transfected with SOFA-HDV-Rz1498, shRNA1498 or the empty Rz/shRNA expression vector (psiRNA) and then analyzed using triplicate dye-swap microarray experiments. The results are expressed as Lowess log2 ratio plots comparing all detectable mRNA species from SOFA-HDV-Rz1498 or shRNA1498-transfected cells with those from empty vector transfected cells. Each individual line represents one detectable mRNA species and differences are reflected in the magnitude of change in log2 ratio between the triplicates on the left and right halves of each plot.

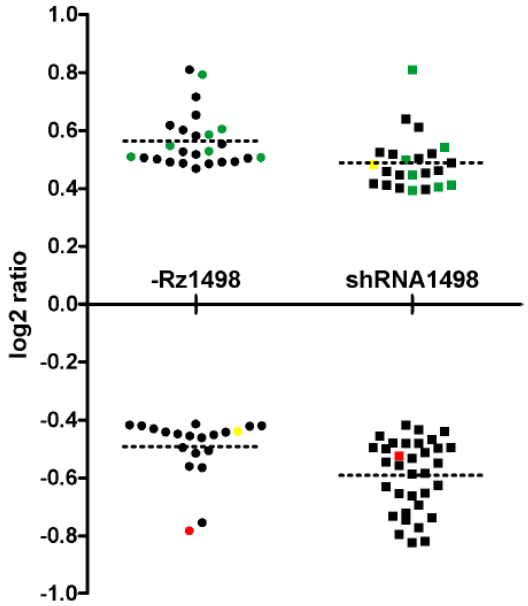

Figure 3.11. Gene expression changes in cells transfected with SOFA-HDV-Rz1498 and shRNA1498.

HEK293T cells were seeded in 12 well plates and co-transfected with HIV-1 pNL4-3 (150 ng) and either SOFA-HDV-Rz1498, shRNA1498 or the empty Rz/shRNA expression plasmid (1.5 µg). 48 h after transfection, total RNA was harvested and analyzed by micro-array. The log2 ratios of mRNAs with the greatest differential variation between SOFA-HDV-Rz1498 or shRNA1498 expressing cells and the empty expression vector expressing cells are shown. RNAs that were up- or down-regulated in both conditions are shown in green and red respectively. One gene that was down-regulated by SOFA-HDV-Rz1498 and up-regulated by shRNA1498 is shown in yellow. The horizontal dotted lines represent the average log2 ratios for the mRNAs with the greatest differential variation in each comparison.

3.4.7 SOFA-HDV-Rz1498 and shRNA1498 inhibit HIV-1 replication in a T lymphocyte cell line

To evaluate the potential for SOFA-HDV-Rz1498 and shRNA1498 to inhibit HIV-1 replication, we transfected Jurkat T cells with the same constructs used for their delivery to HEK293T cells and selected stably transfected cells in the presence of Zeocin. All cell lines had a similar distribution of GFP expression from the integrated plasmids and proliferated at similar levels (Figure 3.12). Following infection with HIV-1 NL4-3, both SOFA-HDV-Rz1498 and

shRNA1498 expressing cells had a lower level of viral replication compared to cells expressing the control molecules, SOFA-HDV-RzHBV and shRNAns (Figure 3.13). A moderate suppression of viral replication was also observed in cells expressing the catalytically inactive Rz (SOFA-HDV-Rz1498A76). These results suggest that in addition to its accessibility in HEK293T cells, the Gag 1498 target site is also accessible to inhibition by both a SOFA-HDV-Rz and an shRNA in a T lymphocytic cell line.

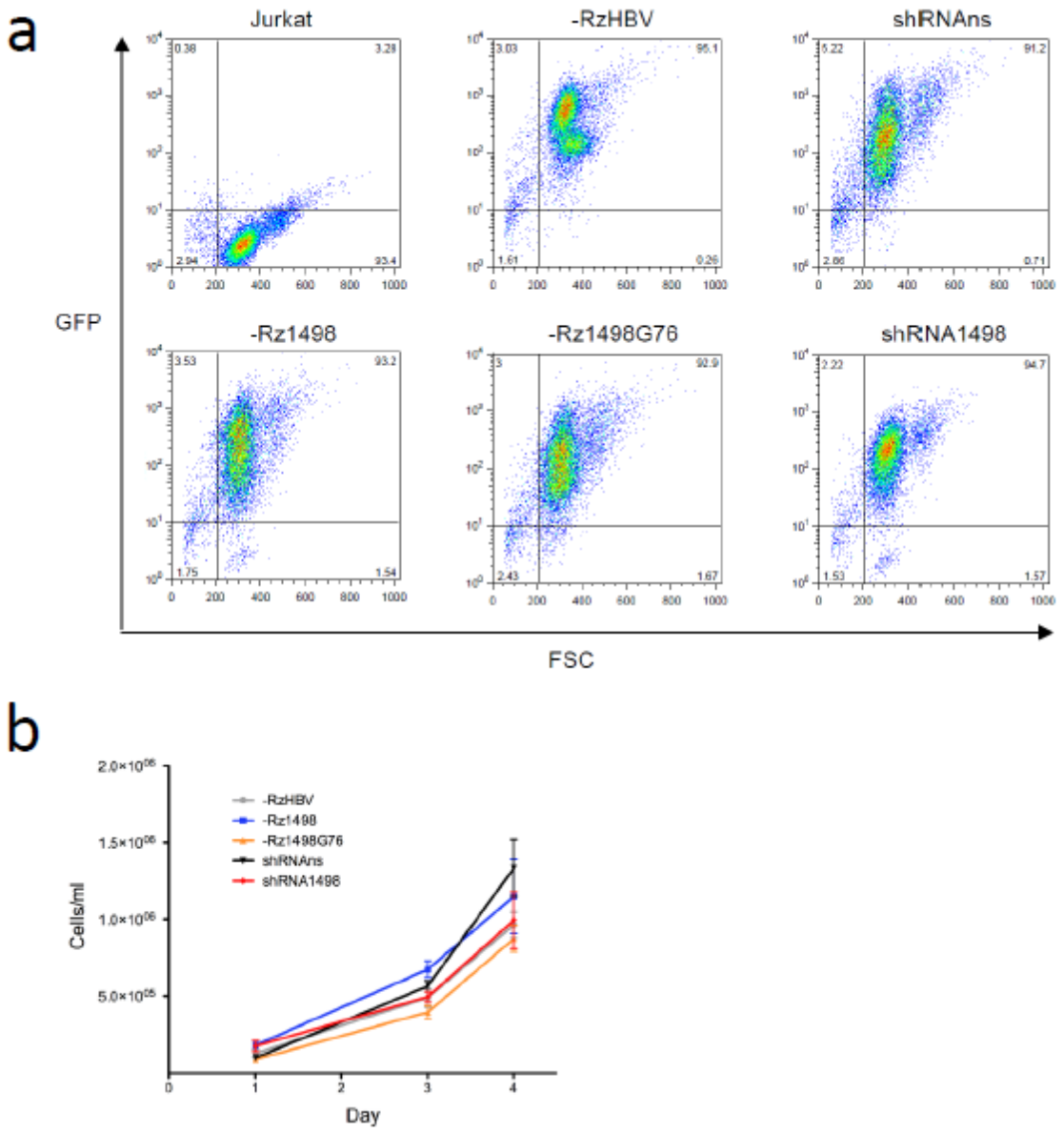

Figure 3.12. Stable Jurkat cell lines analysis.

a) 10,000 events are shown for the different cell lines, Green fluorescence levels versus Forward scatter (FSC) is plotted, showing the level of green fluorescent protein (GFP) expression and approximate cell size (FSC) for the different Jurkat cell lines. **b**) Live cell counts +/- SEM (n=2) out to four days after plating different cell lines at 1.0×10^5 cells/mL.

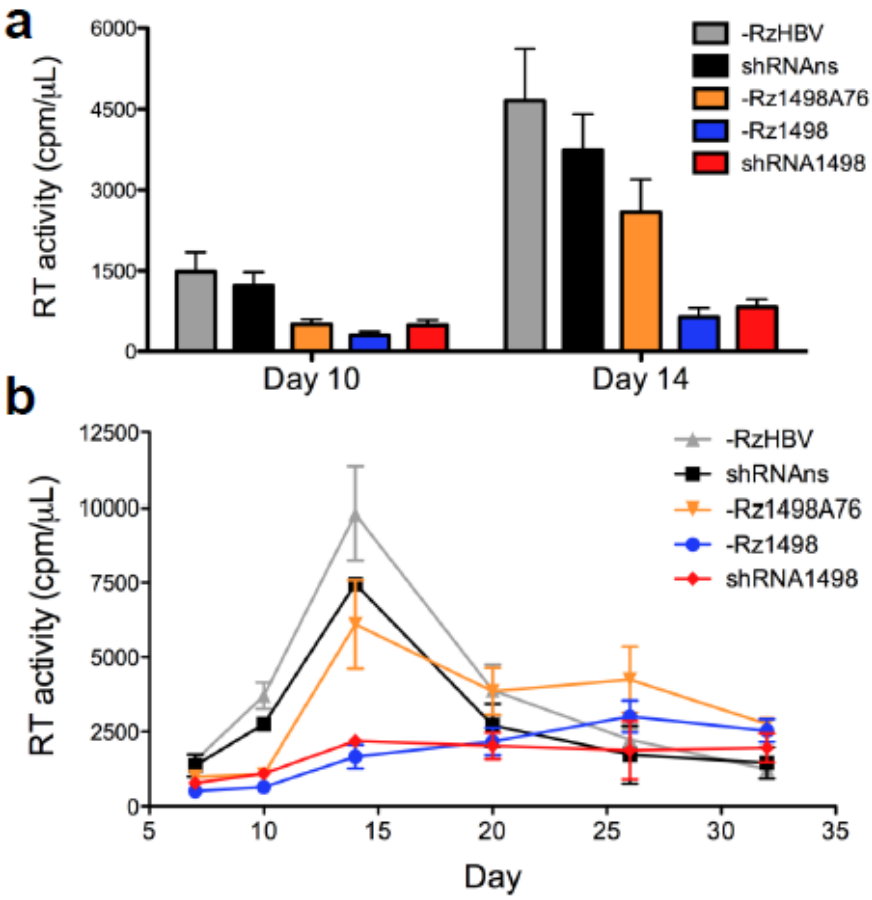

Figure 3.13. Inhibition of HIV-1 replication by SOFA-HDV-Rz1498 and shRNA1498.

a) Jurkat T cells stably transfected with the indicated SOFA-HDV-Rzs and shRNAs were infected with HIV-1 NL4-3. The average RT activity (cpm/µL) in culture supernatants across four independent infections performed in triplicate (n=12) is shown for days 10 and 14 following infection. **b)** Time course of a representative infection (n=3) followed out to 32 days post infection.

3.5 DISCUSSION

Rzs targeting HIV-1 RNA were among the first gene therapy agents tested in a clinical setting [36], and the only agent tested in a phase II vector controlled trial [37]. While no toxicity has been observed in this study, the moderate effect reported emphasizes the need to find more inhibitory molecules for use in gene therapy. Approaches that have been described to identify new Rz candidates include the use of i) RNA Polymerase III (Pol III) promoters to achieve higher levels of expression [38, 39], ii) cellular screens to identify optimal target sites [18, 19], iii) chimeric Rzs to enhance antiviral effects [18, 27, 40, 41], and iv) alternative motifs such as modified RNase P and HDV Rzs [7, 16]. In this study we screened SOFA-HDV-Rzs, expressed from the RNA Pol III H1 promoter, targeting the 5'UTR and Gag coding sequence of HIV-1 RNA for effects on viral production. Several candidate Rzs with the potential to target a broad range of HIV-1 strains were identified (Figure 3.3) and one of these (SOFA-HDV-Rz1498) was a particularly effective inhibitor of HIV-1 production (Figure 3.4). In agreement with other Rz screens [17-19], where only a small number of Rzs out of a library of candidates were effective, the majority of SOFA-HDV-Rzs evaluated did not strongly inhibit HIV-1 production. One explanation for this could be that Rzs may be particularly sensitive to the accessibility of their target sites and that most target sites in HIV-1 RNA do not permit Rzs to bind and form the appropriate structure required for catalysis. Other explanations include a failure of most Rzs to fold correctly or to localize with their target RNA.

According to the secondary structure published for the full length genomic RNA of HIV-1 NL4-3 [42], the target site we identified in the Gag coding sequence lies predominantly in a 27 nt single-stranded loop enumerated 1033 to 1059 based on its position in NL4-3 HIV-1 RNA (1487

to 1513 in NL4-3 DNA). In addition to being accessible to inhibition by a SOFA-HDV-Rz, the 1498 target site was also accessible to an shRNA, with similar potency in an HIV-1 production assay compared to previously described shRNA candidates (Figure 3.7 **c**). Although both SOFA-HDV-Rz1498 and shRNA1498 target the same site, our results suggested that they could be used together to inhibit viral production with an additive effect comparable to the combination of SOFA-HDV-Rz1498 with shRNA5983 targeting a different site (Figure 3.7 **d**). These results are compatible with SOFA-HDV-Rz1498 and shRNA1498 acting in different cellular compartments to provide a non-redundant effect on HIV-1 production. Consistent with this, Rzs expressed from the RNA Pol III promoter U6 were shown to localize predominantly in the nucleus [38], while shRNAs are exported to the cytoplasm through the exportin 5-dependent pathway.

For both SOFA-HDV-Rz1498 and shRNA1498, the inhibition of intracellular CA expression was more apparent than inhibition of Gag (Figure 3.7 **b**) and a similar effect was observed for shRNAs targeting the 5'UTR and overlapping tat/rev reading frame (Figure 3.8). It is possible that in these experiments both Rzs and shRNAs inhibit intracellular Gag processing to the CA protein, a mechanism that has been described as contributing to the inhibition of HIV-1 production provided by modified U1 snRNAs [43]. Another possibility is that intracellular Gag is more stable compared to CA in these experiments, making the effect on CA expression more apparent at the sampling time evaluated. Further studies will be required to evaluate whether this effect is reproducible in different cell types and experimental conditions and determine whether it could be a contributing mechanism to the inhibition of viral production provided by Rzs and shRNAs targeting HIV-1 RNA.

An important consideration for the design of therapies targeting HIV-1 is that they target the majority of HIV-1 circulating strains. According to our estimates, the target site for both SOFA-HDV-Rz-1498 and shRNA1498 was highly conserved at the nt level (Figure 3.7 **a**, Gag). The LANL dataset we used to generate our estimates was made up of 1850 complete HIV-1 sequences, compared to 170 and 495 in earlier studies that used this dataset to identify shRNA [21] or siRNA [20] target sites, respectively. A comparison of the subtype distribution between the LANL dataset we used and global estimates [44] (Figure 3.2) suggests that HIV-1 subtype C is under-represented in the LANL dataset while subtype B, unique recombinant forms (URFs) and CRFs other than AG or AE are all over-represented. While not exactly representative of the global distribution, the LANL dataset includes all published HIV-1 sequences with representatives from all major subtypes and circulating recombinant forms and can easily be used to generate conservation estimates at the nt level for the identification of antisense target sites [45]. In addition to being highly conserved across the different sequences available in the LANL database, our results suggest that the 1498 target site may also have a conserved structure, as the effects of shRNA1498 were similar against diverse viral strains with sequence variation within and around the target site (Figure 3.9).

Another important consideration for the design of antisense molecules targeting HIV-1 RNA is their potential to target cellular RNAs with complementary target sites. While target sites can be compared to the human genome, it is not always possible to predict off-target effects, as many antisense technologies do not require perfectly matched target sites. In agreement with *in vitro* studies [9, 10], a single nt mismatch in SOFA-HDV-Rz1498 (Figure 3.5) or its binding site (strain Indie-C1 and 94UG114, Figure 3.9) greatly affected its ability to inhibit HIV-1

production. In contrast, an imperfectly matched snoRNA linked hammerhead Rz targeting HIV-1 RNA was an effective inhibitor of HIV-1 production [18] and several shRNAs have been shown to tolerate single and even double mismatches in HIV-1 RNA [25, 46]. Consistent with previous results [25], a single nt mismatch at position 17 did not affect the inhibition of viral production provided by shRNA1498 (strain Indie-C1 and 94UG114, Figure 3.9) suggesting that SOFA-HDV-Rzs are more sensitive to mismatches in their target sites compared to shRNAs. While this sensitivity would be beneficial in terms of limiting off-target effects, it is a liability for targeting a broader range of HIV-1 circulating strains and would render SOFA-HDV-Rzs more sensitive to the emergence of resistant virus in a therapeutic setting. At levels where both SOFA-HDV-Rz1498 and shRNA1498 inhibited HIV-1 production, only small changes in gene expression were observed (Figure 3.10, Figure 3.11), suggesting that their target site may be sufficiently different from human RNA sequences to avoid major off-target effects on human mRNAs. Combined with its potency and effects on diverse HIV-1 strains, in addition to our predictions for sequence conservation, these results suggest that shRNA1498 has the potential to be used safely and effectively against a broad range of HIV-1 circulating strains in a therapeutic setting. Future studies to directly compare the safety and efficacy of shRNA1498 to other shRNA candidates in more relevant cell lines and HIV-1 infection models are planned.

Although SOFA-HDV-Rz1498 was more effective than our previously designed candidates targeting the Tat/Rev region of HIV-1 RNA it reached only a 50% inhibition of viral production in co-transfection assays compared to an almost complete inhibition at much lower levels by shRNA1498 (Figure 3.7 **b,c**). In contrast, it showed a similar potential to support a sustained inhibition of viral replication in Jurkat T cells (Figure 3.13), suggesting a long-term persistence

of its effects in an infection model. Improvements in the design or expression of SOFA-HDV-Rz1498 may further increase its efficacy and modifications to render it less sensitive to mutations in its target site are being considered. Overall, our results suggest that both SOFA-HDV-Rz-1498 and shRNA1498 could be further developed for expression in a gene therapy setting or by direct delivery with newly developed methods [4] as RNA drugs.

3.6 MATERIALS AND METHODS

3.6.1 *In silico* identification of SOFA-HDV-Rz target sites

The use of the LANL dataset to estimate sequence conservation at the nt level has been previously described [45]. Briefly, a multiple sequence alignment of all complete HIV-1 sequences were downloaded from the LANL database using the QuickAlign tool and a consensus sequence with % conservation at each position was generated using Jalview sequence editor [47] and exported to Microsoft Excel. Several positions in the consensus sequence were represented in only a small number of sequences and positions that occurred in less than 10% of the sequences were removed from the raw data to facilitate target site selection. Highly conserved target sites were selected based on criteria illustrated in Figure 3.3 **a**. Nucleotide BLAST [48] was then used to align target sites to HIV-1 NL4-3 (M19921) and Ribosubstrates software (www.riboclub.org/ribosubstrates) was used to evaluate the potential for the corresponding SOFA-HDV-Rzs to target human RNAs as previously described [26]. Briefly, the software identifies potential target sites for SOFA-HDV-Rzs in a cDNA database allowing for variations in the length of the spacer sequence and biosensor (Figure 3.1 **a**). Perfectly matched target sites are assigned a value of 0, and the score increases by 10 for each wobble base pair and

by 100 for each mismatch. We set a value of 20 as the cut-off for potential off-target effects, representing at least two wobble base pairs between a SOFA-HDV-Rz targeting HIV-1 RNA and a potential target site in any human RNA.

3.6.2 Plasmid construction

All SOFA-HDV Rzs and shRNAs were expressed from the human RNaseP H1 promoter in the vector psiRNA-H1GFP::Zeo (InvivoGen, San Diego, CA). SOFA-HDV-Rz inserts were generated using an overlapping PCR strategy [11, 14, 28] and shRNA inserts were generated by annealing complementary oligonucleotides. Sequences for shRNA522 and shRNA553 inserts were obtained from a previous study [22] and using an identical design, shRNAns (non-sense, adapted from siControl [20]), shRNA5983 (adapted from sh1 [49]) and shRNA1498 inserts were designed. Detailed methods are provided below.

SOFA-HDV-Rz inserts were generated by PCR using DNA primers A and B (2 μM), C and D (25 nM):

A: 5'-TATAAGTTCTGTATGAGTTCACG**GAAGAC**CGACCT↓CGGGCCAGCTAGTTT-3'

B: 5'-CAACAACAGTGTTCGGATGAACTGATGCTAT**GAAGAC**TCCAAA↓AACCAGCT AGAAAGGGTC-3'

C: 5'-CCAGCTAGAAAGGGTCCCTTAgCCATCCGCGAACGGATGCCC-3'

D: 5'-TAATACGACTCACTATAGGGCCAGCTAGTTT(Bs)(Bl)CAGGGTCCACCTCCTCG CGGT(RD)GGGCATCCGTTCGCG-3'

Primers A and B include *Bbs*I recognition sites (bold, cut site indicated with an arrow), C and D contain a common reverse and specific forward ribozyme sequence respectively (overlapping sequences underlined). The nucleotide in primer C that was mutated to produce a catalytically inactivate SOFA-HDV Rz is shown as lower case (G to T mutation in this study). Variable Bs, Bl and RD sequences in primer D are shown in Table 3.1 for each SOFA-HDV-Rz evaluated.

shRNA inserts were generated by annealing complementary sense (S) and antisense (AS) oligonucleotides (1.25 μM each in 75 mM NaCl, 40 μL, 2 min at 80 °C, cooled to 37 °C):

shRNA522 S:

5'-ACCTCGCCTCAATAAAGCTTGCCTTC**CTCGAG**CAAGGCAAGCTTTATTGAGGCTT-3'

shRNA522 AS:

5'-CAAAAAGCCTCAATAAAGCTTGCCTTG**CTCGAG**GAAGGCAAGCTTTATTGAGGCG-3'

shRNA553 S:

5'-ACCTCGTAGTGTGTGCCCGTCTGTTC**CTCGAG**CAACAGACGGGCACACACTACTT-3'

shRNA553 AS:

5'-CAAAAAGTAGTGTGTGCCCGTCTGTTG**CTCGAG**GAACAGACGGGCACACACTACG-3'

shRNAns S:

5'-ACCTCGTACCGCACGTCATTCGTATC**CTCGAG**CATACGAATGACGTGCGGTACTT-3'

shRNAns AS:

5'-CAAAAAGTACCGCACGTCATTCGTATG**CTCGAG**GATACGAATGACGTGCGGTACG-3'

shRNA5983 S:

5'-ACCTCGCGGAGACAGCGACGAAGAGG**CTCGAG**GCTCTTCGTCGCTGTCTCCGCTT-3'

shRNA5983 AS:

5'-CAAAAAGCGGAGACAGCGACGAAGAGC**CTCGAG**CCTCTTCGTCGCTGTCTCCGCG-3'

shRNA1498 S:

5’-ACCTCGCAGGAACTACTAGTACCCTA**CTCGAG**AAGGGTACTAGTAGTTCCTGCTT-3’

shRNA1498 AS:

5’- CAAAAAGCAGGAACTACTAGTACCCTT**CTCGAG**TAGGGTACTAGTAGTTCCTGCG-3’

The nucleotides flanking the core loop sequence (bold) for the HIV-1 specific shRNA522, shRNA553, shRNA5983 and shRNA1498 are complementary to the 21st nt of their target site in case of differential processing as previously described [22]. *Bbs* I cut site overhangs in the complementary oligonucleotides are underlined.

SOFA-HDV-Rz and shRNA inserts were ligated into *Bbs* I (Thermo Fischer Scientific, Waltham, MA) digested psiRNA-H1GFP::Zeo (InvivoGen, San Diego, CA) expression plasmid. All constructs were confirmed by sequencing using a primer located in the H1 promoter: 5’-TCTACGGGGTCTGACGC-3’

3.6.3 Transfections

Co-transfections of HIV-1 molecular clones with Rz or shRNA expressing plasmids were performed in either 24 or 12 well plate formats as indicated in the figure legends. HEK293T cells were maintained in Dulbecco’s modified Eagle’s medium with high glucose (Hyclone, Logan, UT) supplemented with 10% fetal bovine serum (Hyclone, Logan, UT), 50 U/mL Penicillin and 50 μg/mL Streptomycin (Life Tech., Carlsbad, CA). 24 h prior to transfection, HEK293T cells were plated at 2×10^5 cells/mL and transfections were carried out using using TransIT reagent (Mirus, Madison, WI) according to the manufacturer's instructions. Viral production was

estimated 48 h following transfection by measuring HIV-1 RT activity in the culture supernatant. To account for differences in viral production between experiments, replicates for each construct evaluated were performed in parallel with the empty vector psiRNA-H1GFP::Zeo and all data are expressed as a percentage of viral production in the empty vector co-transfected cells (Relative RT activity). For each Rz or shRNA construct evaluated we also included the irrelevant control SOFA-HDV-Rz-HBV or the nonsense control shRNAns, respectively.

3.6.4 Rz expression in HEK293T cells

Total RNA extracts were harvested from transfected cells using Trizol reagent (Life Tech., Carlsbad, CA) according to the manufacturer's instructions. 10 µg of total RNA was resolved on an 8% denaturing polyacrylamide gel, transferred to a nylon membrane (Amersham Hybond-N+, GE Healthcare, Little Chalfont, UK) and UV cross-linked. Membranes were incubated with ProbeSOFA followed by Probe5S and visualized using a Phosphor screen. Probe sequences, labelling and details on the northern blot conditions are provided below.

Probe labeling and sequences: 5 pmol of the oligonucleotide ProbeSOFA or 10 pmol of the oligonucleotide Probe5S were 5'-end labeled by incubation for 1 h at 37 °C with 3 U of T4 polynucleotide kinase (Affymetrix, Santa Clara, CA) and 3.2 pmol of [γ-^{32}P]ATP (6000 Ci/mmol; Perkin Elmer, Waltham, MA). The quantity of [γ-^{32}P]ATP was doubled for the ProbeSOFA labeling reaction. The labeled oligonucleotides were purified with ProbeQuant^{tm} G50 Micro Colums (GE Healthcare, Little Chalfont, UK) and used directly for the northern blot, their sequences were:

ProbeSOFA: 5'-GAAAGGGTCCCTTAGCCATCCGCGAACGGATGCCC-3'

Probe5S: 5'-AAAGCCTACAGCACCCGGTATTCCC-3'

Northern blot conditions: Total RNA samples were dissolved in RNAse-free water and quantified (Nanvovue, Roche, Basel, Switzerland). For each condition, 10 µg of total RNA mixed with 2 volumes of loading buffer was resolved on 8% denaturing PAGE. The RNA was then transferred (90 min, 4 °C, 200 mA) to a nylon membrane (Amersham Hybond-N+, GE Healthcare, Little Chalfont, UK) in 0.5× TBE using a Trans-blot cell (Bio-Rad, Hercules, CA). Membranes were UV crosslinked prior to pre-hybridization at 42 °C in CHURC buffer (1% (W/V) BSA, 1 mM EDTA, 500 mM phosphate buffer and 7% (W/V) SDS). After 2 to 4 h, the radio-labeled ProbeSOFA was added, and the membranes were hybridized at 42 °C overnight. Before analysis, the membranes were washed twice, 5 min each, in wash buffer #1 (2× SSC, 0.1% SDS) and twice, 15 min each, in wash buffer #2 (0.1× SSC, 0.1% SDS), all at 42 °C. The results were visualized using a Phosphor Screen. For the Probe5S hybridization, the membranes were stripped by incubation in wash #2 at 80 °C for 20 min to remove the ProbeSOFA. Only 5 to 10% of the labeled Probe5S was used for the hybridization of one membrane.

3.6.5 *In vitro* SOFA-HDV-Rz cleavage assay

Single-turnover conditions (Rz>>substrate) were used to evaluate the catalytic activity of SOFA-HDV-Rzs as previously described [28]. Briefly, a trace amount of 5'-end-labeled substrate (< 1 nM) was incubated at 37 °C with a final concentration of 100 nM of the selected SOFA-HDV-Rz. The cleavage reactions were initiated by the addition of $MgCl_2$ and samples were taken at

different time intervals and stopped with loading buffer. Recovered samples were resolved on a 20% denaturing polyacrylamide gel, visualized using a Phosphor Screen and quantified using ImageQuant software (Molecular Dynamics, Sunnyvale, CA). The control reaction was performed in the absence of Rzs (replaced by water) and its last time interval sample was used to subtract the background. For each time point, the percentage of cleavage was calculated (cleaved product counts over cleaved + uncleaved products counts). The k_{obs} and F_{max} were then calculated using GraphPad Prism 5 for each Rz. The rate of cleavage (k_{obs}) was obtained by fitting the data to the equation $F_t = F_{max} (1\text{-}e^{-kt})$, where F_t is the percentage of cleavage at time *t*, F_{max} is the maximum percent cleavage and *k* is the rate constant (k_{obs}). Details on the DNA templates used for *in vitro* transcription, RNA synthesis and labelling are provided in below.

DNA templates for *in vitro* transcription: SOFA-HDV-Rz DNA templates were generated through a PCR-based strategy with DNA primers C and D used to construct SOFA-HDV-Rz inserts. The SOFA-HDV-Rz sense primer (D) provided the T7 RNA polymerase promoter needed for subsequent *in vitro* transcription. The fully double-stranded DNA sequences were produced using *Pwo* DNA polymerase (Roche, Basel, Switzerland). Similarly, the substrate DNA template was produced by a combination of two complementary oligonucleotides, subA and subB:

subA:

5'-taatacgactcactata**GGGCATAGCAGGAACTACTAGTACCCTT**GGGTCGGCAGGG

TCCACCTCC-3'

subB:

5'-GGGTCCCTTAGCCATGCGAAGCCGCATGCCCAGGTCGGACCGCGAGGAGGTGG

ACCCTGCCGACCC-3'

subA contained the T7 RNA polymerase promoter (lower case) at its 5'-end and part of a *cis*-acting HDV ribozyme (underlined sequence) at its 3'end. The subB primer is complementary (underlined sequence) to the forward primer and completes the *cis*-acting HDV ribozyme. The *cis*-acting HDV ribozyme permits the production of a precise 3'-end as described in Supplementary reference [50]. The final RNA substrate, SubMin1498, corresponds to the sequence in bold. All PCR reactions were ethanol precipitated prior to *in vitro* transcription.

RNA synthesis for *in vitro* transcription: The SOFA-HDV-Rz and the substrate RNA were synthesized by run-off transcriptions as described previously [28]. Briefly, transcriptions were performed in the presence of purified T7 RNA polymerase (10 μg), pyrophosphatase (0.01 U, Roche, Basel, Switzerland) and PCR product (2 to 5 μM) in a buffer containing 80 mM HEPES-KOH (pH 7.5), 24 mM $MgCl_2$, 2 mM spermidine, 40 mM DTT and 5 mM of each NTP in a final volume of 100 μL at 37 °C for 2 h. The reaction mixtures were then treated with RQ1 DNase (Promega, Madison, WI) at 37 °C for 20 min. After phenol/chloroform extraction the RNAs were ethanol precipitated. The pellets were dissolved in equal volumes of ultrapure water and loading buffer (95% formamide, 10 mM EDTA [pH 8.0], 0.025% xylene cyanol and 0.025% bromophenol blue). The samples were then fractionated through either 8% or 20% denaturing polyacrylamide gels (PAGE, 19:1 ratio of acrylamide to bisacrylamide) in buffer containing 45 mM Tris-borate (pH 7.5), 8 M urea, and 2 mM EDTA. The RNA products were visualized by ultraviolet (UV) shadowing. The bands corresponding to the correct sizes for both the SOFA-HDV-Rzs and the substrate were cut out of the gel and the RNAs eluted overnight at 4 °C in elution buffer (500 mM ammonium acetate, 10 mM EDTA, 0.1% SDS). The samples were again

ethanol precipitated, washed, dried and dissolved in ultrapure water. The RNA was quantified by absorbance at 260 nm and diluted to the desired concentration (Rz 1 μM and Substrate 5 μM).

RNA and Probes Labelling: The RNA substrate used in cleavage reactions was 5'-end labeled as described previously [28]. Briefly, the purified RNA substrate was dephosphorylated by mixing 50 pmol of RNA with 1 U of Antarctic phosphatase (New England Biolabs, Ipswich, MA) in a final volume of 10 μL containing the buffer provided with the enzyme, and then incubated for 30 min at 37 °C. Incubation at 65 °C for 8 min was used to inactivate the enzyme. The 5'-end labeling reaction was performed with 5 pmol of dephosphorylated RNAs that were incubated for 1 h at 37 °C with 3 U of T4 polynucleotide kinase (Affymetrix, Santa Clara, CA) and 3.2 pmol of [γ-^{32}P]ATP (6000 Ci/mmol; Perkin Elmer, Waltham, MA) in the reaction buffer provided with the enzyme. The reactions were stopped by the addition of two volumes of loading buffer prior to fractionation by 20% denaturing PAGE. The RNAs were detected by autoradiography, cut out of the gel and eluted as described in RNA synthesis for *in vitro* transcription.

3.6.6 HIV-1 protein expression in HEK293T cells

The detection of HIV-1 protein expression using an HIV-1 p24 antibody in HEK293T cells has been previously described [51]. Briefly, 100 μg of total protein was resolved on a 10% denaturing poly-acrylamide gel and transferred to a Hybond ECL nitrocellulose membrane (GE Healthcare, Little Chalfont, United Kingdom). Membranes were incubated first with anti-HIVp24 (183-H12-5C) followed by anti-GAPDH (sc-32233, Santa Cruz Biotechnology, Dallas,

TX), bands were visualized using ECL (GE Healthcare, Little Chalfont, United Kingdom). The relative intensity of bands were calculated using Image J densitometry software (Version 1.48, National Institutes of Health, USA). Data are expressed as Gag or CA band intensities relative to the intensity of the Gag band in the control SOFA-HDV-RzHBV or shRNAns lanes.

3.6.7 Gene expression profiling in HEK293T cells

Gene expression levels relative to control transfections were analyzed by human gene expression microarrays (ACRI proprietary slides). Total RNA extracts were harvested from transfected cells using Trizol reagent (Life Tech., Carlsbad, CA) according to the manufacturer's instructions and purified using an RNeasy column (Qiagen). Quality of total RNA samples was assessed using the Experion bioanalyzer system with RNA Stdsens chips and associated reagents (Bio-Rad, Hercules, CA). All RNA used in these experiments had an RNA Quality Index (RQI) value greater than nine. 1 μg of each total RNA sample was amplified using the Amino Allyl MessageAmp II aRNA amplification kit and subsequently labeled with AlexaFluor 555 or 647 (Life Tech., Carlsbad, CA). Quantity and quality of amplified aRNA was assessed using a Nanodrop spectrophotometer and the Experion bioanalyzer. Samples were compared in triplicate dye swap experiments, with 1.5 μg of each labeled, fragmented aRNA (3 μg total per slide) hybridized to proprietary human cDNA microarray slides. These arrays consist of roughly 35000 spots, representing roughly 17000 different 50-mer oligonucleotides spotted in duplicate on Nexterion-E epoxy microarray slides (Schott, Mainz, Germany).

Hybridizations were performed in Ambion SlideHyb #2 buffer (Life Tech., Carlsbad, CA) at 42 °C for 16 h using the automated TECAN 4800 Hybridization station (TECAN). Following hybridization, slides were scanned at 10 μm resolution using an Axon GenePix 4200AL scanner (Molecular Devices, Sunnyvale, CA) and gridded using SpotReader (Niles Scientific). Fine tuning of spot rejection was subsequently done by visual inspection of the gridded image and of a scatter plot of M = log(532/635) versus A = log(532) + log(635), special attention being paid to outliers. A GPR file was generated that was subsequently processed to flag spots with a signal to noise ratio of less than 5.

Analysis was done with Acuity 4.0 (Axon Instruments, Sunnyvale, CA). The data was normalized using Lowess and is expressed as the log2 ratio of SOFA-HDV-Rz or shRNA1498 transfected cells compared to the empty vector (psiRNA) transfected cells.

3.6.8 HIV-1 infection assay

Stable Jurkat T lymphocytes were generated by electroporation of psiRNA constructs followed by selection with Zeocin (InvivoGen, San Diego, CA). The relative expression of psiRNA constructs in the stable cell populations was estimated by measuring GFP expression from the integrated vector with a FACS Calibur flow cytometer (BD Biosciences, San Jose, CA), and proliferation was determined by counting live cells by Trypan blue (Wisent, St Bruno, Canada) exclusion using a hemocytometer. Prior to infection, SOFA-HDV-Rz or shRNA expressing cells were plated in 6 well plates at 2×10^5 cells per well. Viral replication was monitored by measuring RT activity in culture supernatants at various days post infection. Jurkat T cells were

maintained in Roswell Park Memorial Institute 1640 (Hyclone, Logan, UT) supplemented with 10% heat inactivated (55°C, 30min) fetal bovine serum (Hyclone, Logan, UT), 50 U/mL Penicillin and 50 μg/mL Streptomycin (Life Tech., Carlsbad, CA). Selection and HIV-1 infection conditions are provided below.

Generation and characterization of stable Jurkat T cells: 1×10^6 Jurkat T cells were electroporated at 250 mV for 10 msec (GenePulserII, Bio-rad, Hercules, CA) with 15 μg of psiRNA plasmids and cultured in 5 mL RPMI overnight. Cells were transferred to 20 mL culture media containing 600 μg/mL Zeocin (InvivoGen, San Diego, CA) and cultured for 4 weeks with selection media changed every 3-4 days. Cells were split at various times during the selection to maintain a high cell density in the first 2 weeks of selection, and a low cell density in the last 2 weeks of selection. At the end of the selection period cells were frozen, or cultured for an additional day in the absence of Zeocin prior to infection with HIV-1 virions. The expression of GFP in the different cell populations was determined using a FACS Calibur flow cytometer (BD Biosciences, San Jose, CA) and data analysis was performed using FlowJo Version 8.7 (Tree Star, St Ashland, OR). Cell proliferation was determined by plating cells at 1×10^5 cells/mL in a 6 well plate followed by counting live cells diluted in Trypan blue (Wisent, St Bruno, Canada) with a hemocytometer. Duplicate wells were counted for each cell line out to four days.

Virus infection: A 20 mL culture of HEK293T cells was transfected with 20 μg of HIV-1 pNL4-3 plasmid DNA. The supernatant was harvested 48 h later, cleared of cell debris by centrifugation, and stored at -80 °C in 1 mL aliquots. SOFA-HDV-Rz and shRNA expressing

Jurkat T cells were plated in 6 well plates at 2×10^5 cells/ well and infected with the HEK293T cell supernatant corresponding to 6×10^5 cpm equivalent of HIV-1 RT activity per well. Viral replication was monitored by measuring RT activity in the culture supernatants at various days post infection. All infections were performed in triplicate wells, cells were split twice a week.

3.6.9 HIV-1 RT assay

The HIV-1 RT assay used in this study was performed as previously described ([45]). Briefly, 5 ul of supernatant was incubated with a polyadenylic acid template (Roche, Basel, Switzerland), an oligo dT primer (Life Tech., Carlsbad, CA) and [^{32}P]-dTTP (3,000 Ci/mmol, Perkin Elmer, Waltham, MA) for 2 h at 37°C in 50 µl total reaction mixture. 5 µl of the reaction mixture was then spotted onto Diethylaminoethyl (DEAE) filter mat (Perkin Elmer, Waltham, MA) and washed five times in 2X SSC buffer, followed by two washes in 95% ethanol to remove [^{32}P]-dTTP not incorporated into the poly dT RT product. Counts per minute (cpm) were calculated for each sample using a microplate scintillation counter (Microbeta TriLux, Perkin Elmer,) and are proportional to the amount of HIV-1 RT enzyme present in the reaction mixture.

3.7 References

1. De Clercq, E (2010). Antiretroviral drugs. *Curr Opin Pharmacol* **10**: 507-515.
2. Le Douce, V, Janossy, A, Hallay, H, Ali, S, Riclet, R, Rohr, O*, et al.* (2012). Achieving a cure for HIV infection: do we have reasons to be optimistic? *J Antimicrob Chemother* **67**: 1063-1074.
3. Scherer, LJ, and Rossi, JJ (2011). Ex vivo gene therapy for HIV-1 treatment. *Hum Mol Genet* **20**: R100-107.
4. Burnett, JC, and Rossi, JJ (2012). RNA-based therapeutics: current progress and future prospects. *Chem Biol* **19**: 60-71.

5. Haasnoot, J, and Berkhout, B (2009). Nucleic acids-based therapeutics in the battle against pathogenic viruses. *Handb Exp Pharmacol* **189**: 243-263.
6. Rossi, JJ (2000). Ribozyme therapy for HIV infection. *Adv Drug Deliv Rev* **44**: 71-78.
7. Zeng, W, Chen, YC, Bai, Y, Trang, P, Vu, GP, Lu, S*, et al.* (2012). Effective Inhibition of Human Immunodeficiency Virus 1 Replication by Engineered RNase P Ribozyme. *PLoS One* **7**: e51855.
8. Asif-Ullah, M, Lévesque, M, Robichaud, G, and Perreault, JP (2007). Development of ribozyme-based gene-inactivations; the example of the hepatitis delta virus ribozyme. *Curr Gene Ther* **7**: 205-216.
9. Bergeron, LJ, and Perreault, JP (2005). Target-dependent on/off switch increases ribozyme fidelity. *Nucleic Acids Res* **33**: 1240-1248.
10. Bergeron, LJ, Reymond, C, and Perreault, JP (2005). Functional characterization of the SOFA delta ribozyme. *RNA* **11**: 1858-1868.
11. Robichaud, GA, Perreault, JP, and Ouellette, RJ (2008). Development of an isoform-specific gene suppression system: the study of the human Pax-5B transcriptional element. *Nucleic Acids Res* **36**: 4609-4620.
12. D'Anjou, F, Routhier, S, Perreault, JP, Latil, A, Bonnel, D, Fournier, I*, et al.* (2011). Molecular Validation of PACE4 as a Target in Prostate Cancer. *Transl Oncol* **4**: 157-172.
13. Lévesque, MV, Lévesque, D, Brière, FP, and Perreault, JP (2010). Investigating a new generation of ribozymes in order to target HCV. *PLoS One* **5**: e9627.
14. Motard, J, Rouxel, R, Paun, A, von Messling, V, Bisaillon, M, and Perreault, JP (2011). A novel ribozyme-based prophylaxis inhibits influenza A virus replication and protects from severe disease. *PLoS One* **6**: e27327.
15. Fiola, K, Perreault, JP, and Cousineau, B (2006). Gene targeting in the Gram-Positive bacterium Lactococcus lactis, using various delta ribozymes. *Appl Environ Microbiol* **72**: 869-879.
16. Lainé, S, Scarborough, RJ, Lévesque, D, Didierlaurent, L, Soye, KJ, Mougel, M*, et al.* (2011). In vitro and in vivo cleavage of HIV-1 RNA by new SOFA-HDV ribozymes and their potential to inhibit viral replication. *RNA Biol* **8**: 343-353.
17. Bramlage, B, Luzi, E, and Eckstein, F (2000). HIV-1 LTR as a target for synthetic ribozyme-mediated inhibition of gene expression: site selection and inhibition in cell culture. *Nucleic Acids Res* **28**: 4059-4067.
18. Unwalla, HJ, Li, H, Li, SY, Abad, D, and Rossi, JJ (2008). Use of a U16 snoRNA-containing ribozyme library to identify ribozyme targets in HIV-1. *Mol Ther* **16**: 1113-1119.
19. Müller-Kuller, T, Capalbo, G, Klebba, C, Engels, JW, and Klein, SA (2009). Identification and characterization of a highly efficient anti-HIV pol hammerhead ribozyme. *Oligonucleotides* **19**: 265-272.
20. Naito, Y, Nohtomi, K, Onogi, T, Uenishi, R, Ui-Tei, K, Saigo, K*, et al.* (2007). Optimal design and validation of antiviral siRNA for targeting HIV-1. *Retrovirology* **4**: 80.
21. ter Brake, O, Konstantinova, P, Ceylan, M, and Berkhout, B (2006). Silencing of HIV-1 with RNA interference: a multiple shRNA approach. *Mol Ther* **14**: 883-892.
22. McIntyre, GJ, Groneman, JL, Yu, YH, Jaramillo, A, Shen, S, and Applegate, TL (2009). 96 shRNAs designed for maximal coverage of HIV-1 variants. *Retrovirology* **6**: 55.

23. DeYoung, MB, and Hampel, A (1997). Computer analysis of the conservation and uniqueness of ribozyme-targeted HIV sequences. *Methods Mol Biol* **74**: 27-36.
24. Sajic, R, Lee, K, Asai, K, Sakac, D, Branch, DR, Upton, C*, et al.* (2007). Use of modified U1 snRNAs to inhibit HIV-1 replication. *Nucleic Acids Res* **35**: 247-255.
25. Lee, SK, Dykxhoorn, DM, Kumar, P, Ranjbar, S, Song, E, Maliszewski, LE*, et al.* (2005). Lentiviral delivery of short hairpin RNAs protects CD4 T cells from multiple clades and primary isolates of HIV. *Blood* **106**: 818-826.
26. Lucier, JF, Bergeron, LJ, Brière, FP, Ouellette, R, Elela, SA, and Perreault, JP (2006). RiboSubstrates: a web application addressing the cleavage specificities of ribozymes in designated genomes. *BMC Bioinformatics* **7**: 480.
27. Sánchez-Luque, FJ, Reyes-Darias, JA, Puerta-Fernández, E, and Berzal-Herranz, A (2010). Inhibition of HIV-1 replication and dimerization interference by dual inhibitory RNAs. *Molecules* **15**: 4757-4772.
28. Lévesque, MV, and Perreault, JP (2012). Target-induced SOFA-HDV ribozyme. *Methods Mol Biol* **848**: 369-384.
29. DiGiusto, DL, Krishnan, A, Li, L, Li, H, Li, S, Rao, A*, et al.* (2010). RNA-based gene therapy for HIV with lentiviral vector-modified CD34(+) cells in patients undergoing transplantation for AIDS-related lymphoma. *Sci Transl Med* **2**: 36ra43.
30. Peden, K, Emerman, M, and Montagnier, L (1991). Changes in growth properties on passage in tissue culture of viruses derived from infectious molecular clones of HIV-1LAI, HIV-1MAL, and HIV-1ELI. *Virology* **185**: 661-672.
31. Theodore, TS, Englund, G, Buckler-White, A, Buckler, CE, Martin, MA, and Peden, KW (1996). Construction and characterization of a stable full-length macrophage-tropic HIV type 1 molecular clone that directs the production of high titers of progeny virions. *AIDS Res Hum Retroviruses* **12**: 191-194.
32. Mochizuki, N, Otsuka, N, Matsuo, K, Shiino, T, Kojima, A, Kurata, T*, et al.* (1999). An infectious DNA clone of HIV type 1 subtype C. *AIDS Res Hum Retroviruses* **15**: 1321-1324.
33. Ndung'u, T, Renjifo, B, and Essex, M (2001). Construction and analysis of an infectious human Immunodeficiency virus type 1 subtype C molecular clone. *J Virol* **75**: 4964-4972.
34. Gao, F, Robertson, DL, Carruthers, CD, Morrison, SG, Jian, B, Chen, Y*, et al.* (1998). A comprehensive panel of near-full-length clones and reference sequences for non-subtype B isolates of human immunodeficiency virus type 1. *J Virol* **72**: 5680-5698.
35. Kusagawa, S, Takebe, Y, Yang, R, Motomura, K, Ampofo, W, Brandful, J*, et al.* (2001). Isolation and characterization of a full-length molecular DNA clone of Ghanaian HIV type 1 intersubtype A/G recombinant CRF02_AG, which is replication competent in a restricted host range. *AIDS Res Hum Retroviruses* **17**: 649-655.
36. Rossi, JJ, June, CH, and Kohn, DB (2007). Genetic therapies against HIV. *Nat Biotechnol* **25**: 1444-1454.
37. Mitsuyasu, RT, Merigan, TC, Carr, A, Zack, JA, Winters, MA, Workman, C*, et al.* (2009). Phase 2 gene therapy trial of an anti-HIV ribozyme in autologous CD34+ cells. *Nature medicine* **15**: 285-292.
38. Good, PD, Krikos, AJ, Li, SX, Bertrand, E, Lee, NS, Giver, L*, et al.* (1997). Expression of small, therapeutic RNAs in human cell nuclei. *Gene Ther* **4**: 45-54.

39. Puerta-Fernandez, E, Barroso-del Jesus, A, Romero-Lopez, C, Tapia, N, Martinez, MA, and Berzal-Herranz, A (2005). Inhibition of HIV-1 replication by RNA targeted against the LTR region. *AIDS* **19**: 863-870.
40. Chang, Z, Westaway, S, Li, S, Zaia, JA, Rossi, JJ, and Scherer, LJ (2002). Enhanced expression and HIV-1 inhibition of chimeric tRNA(Lys3)-ribozymes under dual U6 snRNA and tRNA promoters. *Mol Ther* **6**: 481-489.
41. Michienzi, A, Cagnon, L, Bahner, I, and Rossi, JJ (2000). Ribozyme-mediated inhibition of HIV 1 suggests nucleolar trafficking of HIV-1 RNA. *Proc Natl Acad Sci U S A* **97**: 8955-8960.
42. Watts, JM, Dang, KK, Gorelick, RJ, Leonard, CW, Bess, JW, Jr., Swanstrom, R*, et al.* (2009). Architecture and secondary structure of an entire HIV-1 RNA genome. *Nature* **460**: 711-716.
43. Mandal, D, Feng, Z, and Stoltzfus, CM (2010). Excessive RNA splicing and inhibition of HIV-1 replication induced by modified U1 small nuclear RNAs. *J Virol* **84**: 12790-12800.
44. Hemelaar, J, Gouws, E, Ghys, PD, and Osmanov, S (2011). Global trends in molecular epidemiology of HIV-1 during 2000-2007. *AIDS* **25**: 679-689.
45. Scarborough, RJ, Lévesque, MV, Perreault, JP, and Gatignol, A (2014). Design and Evaluation of Clinically Relevant SOFA-HDV Ribozymes Targeting HIV RNA. *Methods Mol Biol* **1103**: 31-43.
46. Sabariegos, R, Giménez-Barcons, M, Tàpia, N, Clotet, B, and Martínez, MA (2006). Sequence homology required by human immunodeficiency virus type 1 to escape from short interfering RNAs. *J Virol* **80**: 571-577.
47. Waterhouse, AM, Procter, JB, Martin, DM, Clamp, M, and Barton, GJ (2009). Jalview Version 2--a multiple sequence alignment editor and analysis workbench. *Bioinformatics* **25**: 1189-1191.
48. Altschul, SF, Madden, TL, Schäffer, AA, Zhang, J, Zhang, Z, Miller, W*, et al.* (1997). Gapped BLAST and PSI-BLAST: a new generation of protein database search programs. *Nucleic Acids Res* **25**: 3389-3402.
49. Li, MJ, Kim, J, Li, S, Zaia, J, Yee, JK, Anderson, J*, et al.* (2005). Long-term inhibition of HIV-1 infection in primary hematopoietic cells by lentiviral vector delivery of a triple combination of anti-HIV shRNA, anti-CCR5 ribozyme, and a nucleolar-localizing TAR decoy. *Mol Ther* **12**: 900-909.
50. Avis, JM, Conn, GL, and Walker, SC (2012). Cis-acting ribozymes for the production of RNA in vitro transcripts with defined 5' and 3' ends. *Methods Mol Biol* **941**: 83-98.
51. Clerzius, G, Shaw, E, Daher, A, Burugu, S, Gelinas, JF, Ear, T*, et al.* (2013). The PKR activator, PACT, becomes a PKR inhibitor during HIV-1 replication. *Retrovirology* **10**: 96.

Chapter 4

Effective inhibition of HIV-1 production by shRNAs and siRNAs targeting a highly conserved site in HIV-1 Gag RNA is optimized by evaluating alternative length formats.

This chapter was adapted from the following manuscript:

Scarborough RJ, Adams KL, Daher A, and Gatignol A. 2015. "Effective inhibition of HIV-1 production by shRNAs and siRNAs targeting a highly conserved site in HIV-1 Gag RNA is optimized by evaluating alternative length formats."
Antimicrob Agents Chemother. Jun 15. pii: AAC.00949-15. [Epub ahead of print]

4.1 Preface

This chapter presents data on siRNAs and shRNAs modeled after the shRNA identified in Chapter 3 for further development as potential drug and gene therapies, respectively. Data on the effects of different nts in the 3' overhangs of intended siRNA and shRNA antisense strands is provided. The effects on the length of different siRNAs and shRNAs is also presented and potential immune stimulation is evaluated for different siRNAs.

Contribution of authors: Under the supervision of AG, RJS designed most of the experiments and wrote the manuscript. Under the supervision of RJS and AD, KLA assisted in the generation of shRNA constructs as well as their efficacy evaluation. KLA also set up and performed cell viability experiments (Figure 4.3 and Figure 4.4). All authors assisted in the review and revision of the manuscript.

4.2 ABSTRACT

We have previously identified a target site in HIV-1 RNA that was particularly accessible to a ribozyme as well as a short hairpin RNA (shRNA). To design small interfering RNAs (siRNAs) targeting this site, we evaluated the effects of siRNAs with different lengths on HIV-1 production. The potency and efficacy of these siRNAs was dependent on the length of their intended sense strand with a similar trend for both symmetrical and asymmetrical formats. Although a typical canonical format with a 21-nucleotide sense strand was effective at inhibiting HIV-1 production, Dicer substrate siRNAs (dsiRNAs) with the longest lengths (27 to 29 nucleotides) were the most effective. Induction of double stranded RNA immune responses and effects on cell viability could not be detected in cells transfected with different siRNAs, suggesting that the differences observed were not related to indirect effects on HIV-1 production. For the corresponding shRNA designs, a different trend in potency and efficacy against HIV-1 production was observed with the most effective shRNAs having stem lengths from 20 to 27 base pairs. Our results highlight the importance of evaluating different designs to identify the best siRNA and shRNA format for any particular target site and provide a set of highly effective molecules for further development as drug and gene therapies for HIV-1 infection.

4.3 INTRODUCTION

RNA interference (RNAi) is a highly conserved process by which small double-stranded RNAs (dsRNAs) use cellular proteins to degrade or repress a complementary target RNA. First described in 1998 [1], RNAi plays major roles in both cellular defence against pathogenic RNAs and post-transcriptional gene regulation in diverse eukaryotic cells [2]. In human cells, the endonuclease Dicer, in complex with the TAR RNA binding protein (TRBP), cleaves precursor micro RNAs (pre-miRNAs) into mature miRNAs, which associate with the RNA induced silencing complex (RISC) [3]. One of the miRNA strands, called the guide or antisense strand, then directs the RISC to a complementary target in an mRNA where it can repress translation or target the mRNA for degradation. Human Dicer can also cleave complementary dsRNAs into small interfering RNAs (siRNAs) of 21 to 23 nucleotides [4, 5] that can direct the RISC protein Argonaute 2 (Ago2) to cleave a specific target RNA sequence. These Dicer products are often called canonical siRNAs and can be delivered to mammalian cells to elicit an effective and specific RNAi response [6, 7]. Over 22 synthetic siRNAs have entered clinical trials targeting both human and viral RNAs [8, 9], and the potential to use siRNAs to treat HIV-1 infection has been validated in preclinical mouse models using different delivery strategies [10-12].

Several non-canonical siRNAs have been designed with various nt modifications and different structural formats (reviewed in [13]). In 2005 it was shown that longer siRNAs, that can serve as substrates for the Dicer enzyme, were up to 100 times more potent compared to their sequence matched canonical formats [14]. These siRNAs are called Dicer substrate siRNAs (dsiRNAs) and a common design includes a 25 nucleotide (nt) sense strand and 27 nt antisense strand with a blunt end and two DNA modifications at the 3' end of the sense strand (25D/27 format) [15].

This format helps direct Dicer to process the desired canonical siRNA product [16, 17] and results in better RISC assembly and more loading of the antisense strand into Ago proteins compared to canonical designs [18]. Although several reports have observed superior efficacy of dsiRNAs compared to canonical siRNAs, one study reported no major difference in efficacy between a large set of molecules and provided evidence that dsiRNAs have greater effects on cell viability [19]. In another study, dsiRNAs were shown to have major effects on cell viability in DU145, MCF7 and HeLa S3 cells in comparison to canonical designs [20]. In addition to dsiRNAs, several effective siRNAs with shorter lengths compared to canonical designs have been described [21-23], and the optimal length and format of therapeutic siRNAs remains an area of debate and ongoing research.

In addition to the preclinical development of siRNAs targeting HIV-1 replication for use as drug therapies, several genes expressing short hairpin RNA (shRNA) precursors of siRNAs have been developed for use as gene therapies (reviewed in [24-26]). shRNA transcripts are composed of two complementary strands that form a stem, separated by a short sequence that forms a loop. They are similar in structure to pre-miRNAs, except that the intended antisense strand is perfectly complementary to both its target RNA and the corresponding sense strand in the shRNA stem [27]. shRNAs are typically expressed from RNA polymerase III type 3 promoters, which allow for a defined transcript with two to four uridines at the 3' end from the polymerase termination signal [28, 29]. These transcripts are exported from the nucleus by the pre-miRNA transporter Exportin 5 and processed by Dicer to yield 21-23 nt siRNAs. Variations in shRNA design such as different loop sequences and lengths have demonstrated that alternative structural formats can have marked effects on the efficacy of an shRNA (reviewed in [27]). Similar to

conflicting reports regarding the optimal length of therapeutic siRNAs, some studies have reported that longer shRNAs are more effective gene silencers [30-32], while others have reported that shorter shRNAs are superior [33]. In a study evaluating shRNAs with different stem lengths targeting several sites in HIV-1 RNA, McIntyre et al. concluded that there is no fixed correlation between stem length and suppressive activity [34], suggesting that empirical data is necessary to identify the optimal format for any particular target site.

We have previously screened HIV-1 RNA for conserved ribozyme target sites [35, 36] based on the specific on/off adaptor (SOFA) Hepatitis delta virus (HDV) ribozyme motif [37-39]. A target site in the Gag coding sequence was identified that was highly conserved and accessible to both a ribozyme and an shRNA [36]. We named this target site Gag 1498 based on its starting position in HIV-1 NL4-3 DNA (Genbank: M19921). Our results suggested that an shRNA targeting this site had similar therapeutic potential compared to an shRNA targeting a site in the Tat/Rev coding sequence starting at position 5983, that has advanced to clinical trials for HIV-1 gene therapy [40] (ClinicalTrials.gov NCT-01961063). In this study we evaluated the antiviral effects of several different siRNAs and shRNAs targeting the Gag 1498 site to identify the most effective formats for further development. Our results show that for the Gag 1498 target site, 27-29 nt long dsiRNAs have superior HIV-1 inhibitory effects compared to the typical 25 nt dsiRNA format and that they have an increased potency and efficacy over the canonical siRNA format. We also demonstrate that this increase is not due to effects on cell viability or induction of dsRNA immune responses. Finally, we show that siRNAs and shRNAs targeting the same sequence in HIV-1 RNA follow a different length dependent trend for potency and efficacy against HIV-1 production. Overall, our results provide a set of effective siRNAs and shRNAs

targeting the Gag1498 site for further therapeutic development and highlight the importance of obtaining empirical data to identify the optimal length format for a particular target site.

4.4 RESULTS

4.4.1 dsiRNAs targeting the Gag 1498 site are effective inhibitors of HIV-1 production

To evaluate whether siRNAs targeting the Gag 1498 site described in our previous study [36] could provide effective inhibition of HIV-1 production, we designed two dsiRNAs (si1498-25D/27 and si1498-27/29D). dsiRNAs were named according to the lengths of their intended sense and antisense strands with a D to indicate the strand with two DNA modifications at its 3' end (Figure 4.1 **a**, left). si1498-25D/27 followed previously described design principles for dsiRNAs [15], while si1498-27/29D followed a design used for a dsiRNA targeting a sequence in HIV-1 starting at position 5983 in the overlapping Tat/Rev coding sequence of HIV-1 RNA [10]. Design matched siRNAs targeting the Tat/Rev coding sequence (si5983-25D/27 and si5983-27/29D) were used as positive controls (Figure 4.1 **a**, left). The effects of siRNAs on HIV-1 production were evaluated by co-transfection of HEK293T cells with HIV-1 molecular clone pNL4-3 and different concentrations of siRNAs. HIV-1 production was estimated by measuring the activity of the HIV-1 RT enzyme in culture supernatants and data were expressed as a percentage of RT activity in cells co-transfected with a nonsense siRNA (siNS-25D/27). All siRNAs dose dependently inhibited HIV-1 production (Figure 4.1 **b**). While both si5983 designs had similar effects on viral production, the longer si1498-27/29D format was more effective compared to the si1498-25D/27 format, representing the typical dsiRNA design.

To evaluate the effects of dsiRNA designs that more closely resemble the expected transcription products for shRNAs, si1498-25/27 and si1498-27/29 were designed with two uridines at the 3' end of their intended antisense strands and no DNA modifications (Figure 4.1 **a**, right). The potency and efficacy of si1498-25/27 and si1498-27/29 were indistinguishable from the modified designs (si1498-25D/27 and si1498-27/29D) (Figure 4.1 **c**), suggesting that the identity of nts in the 3' antisense strand overhang and DNA base modifications are not important determinants for inhibition of HIV-1 production. Rather, the effects of both the modified and unmodified designs were dependent on the siRNA length, with si1498-27/29 and si1498-27/29D providing more effective inhibition of HIV-1 production compared to si1498-25/27 and si1498-25D/27 (Figure 4.1 **c**). As dsiRNA designs with uridines in the 3' antisense strand overhang and no DNA modifications were effective inhibitors of HIV-1 production, this format was used to compare the effects of length on HIV-1 production for different siRNAs targeting the Gag 1498 site.

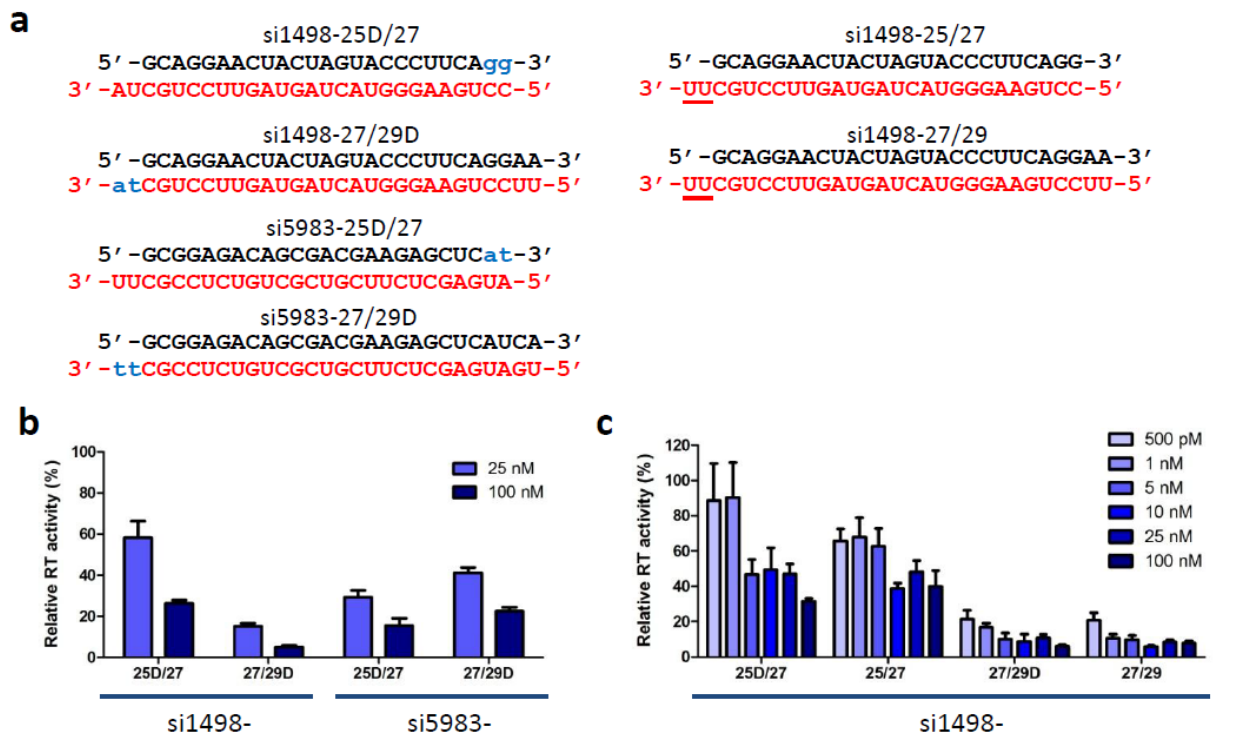

Figure 4.1. Inhibition of HIV-1 production by different Dicer substrate siRNA (dsiRNA) designs targeting the Gag 1498 and Tat/Rev 5983 sites in HIV-1 strain NL4-3.

a) Sequences of the different dsiRNA designs targeting the Gag 1498 and Tat/Rev 5983 sites in HIV-1 RNA. The intended sense strands are on top in black and the intended antisense strands are on the bottom in red. DNA nucleotide modifications are illustrated in blue using lower case letters. **b) Comparison between dsiRNAs 1498 and 5983 effects on HIV-1 production.** HEK293T cells were co-transfected with HIV-1 pNL4-3 plasmid DNA (100 ng) and one of the indicated dsiRNAs at 25 or 100 nM. 48 h after co-transfection, supernatants were harvested and the activity of HIV-1 RT was determined. Data were expressed as a percentage of the value obtained for co-transfection with a nonsense siRNA (siNS-25D/27) tested in parallel, shown as relative RT activity. **c) Influence of length and modifications of dsiRNAs 1498 effects on HIV-1 production.** HEK293T cells were co-transfected with HIV-1 pNL4-3 plasmid DNA (100ng) and one of the indicated dsiRNAs at 500 pM to 100 nM. Relative RT activity was determined as in (b). For each concentration of dsiRNA tested, at least two independent experiments with two to three replicate transfections were performed, data are expressed as the mean +/- standard error of the mean (SEM) (n=4-6).

4.4.2 dsiRNAs targeting the Gag 1498 site with sense strand lengths of at least 27 nucleotides provide improved inhibition of HIV-1 production compared to a canonical design.

The typical canonical siRNA design is symmetrical with two 3' nt overhangs on each strand, while the recommended dsiRNA design is asymmetrical with a blunt end at the 3' nt of its intended sense strand [15] (Figure 4.1 **a**). To compare the effects of length on siRNAs targeting the Gag 1498 site, a set of symmetrical and asymmetrical siRNAs were designed with intended sense strand lengths of 17 to 29 nts (Figure 4.2 **a**). Antisense strands were designed to be complementary to the target sequence along their entire lengths except for the terminal uridine in their 3' overhang. The trend in potency and efficacy for siRNAs targeting the Gag 1498 site was similar for both symmetrical and asymmetrical designs and depended on the length of their intended sense strand (Figure 4.2 **b,c**). Most siRNAs provided a dose dependent inhibition of HIV-1 production; however, siRNAs with sense strand lengths of 17 and 20 nts had low to no efficacy at the concentrations tested. The most effective siRNAs had sense strand lengths of 27 and 29 nts and these molecules provided both the greatest potency and efficacy against HIV-1 production.

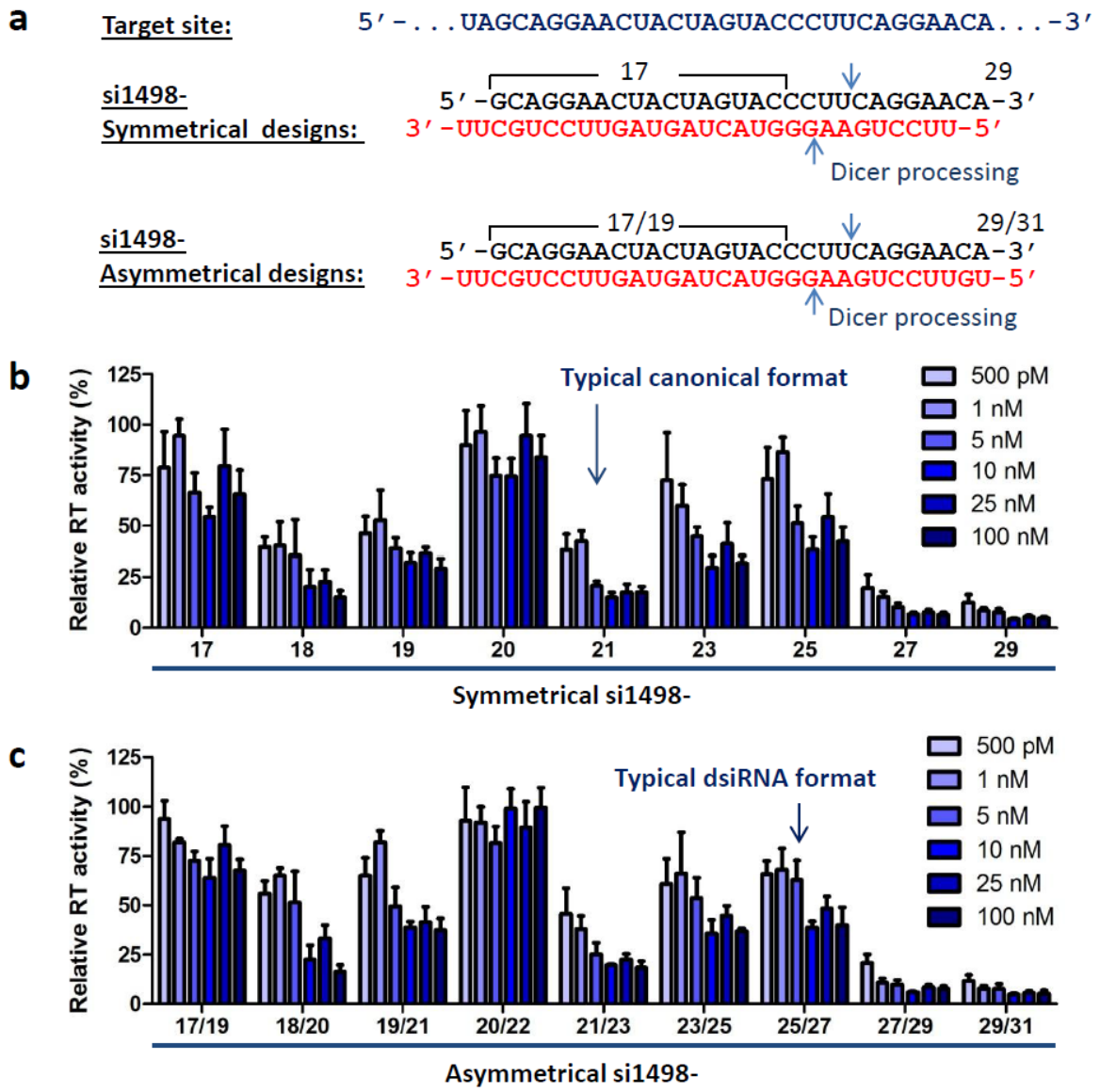

Figure 4.2. Symmetrical and asymmetrical siRNAs with sense strand lengths of 27 and 29 nts targeting the Gag 1498 site are more effective inhibitors of HIV-1 production compared to a canonical design.

a) Symmetrical and asymmetrical designs for siRNAs with different lengths targeting the Gag 1498 site. The intended sense strands are on top in black and the intended antisense strands are on the bottom in red. The sequences for si1498 -29 and -29/31 are shown and the position of si1498 -17 and -17/19 are illustrated within the longer siRNAs. Expected sites of Dicer processing for longer siRNAs are illustrated with blue arrows. **b) and c) Effects of si1498 length and symmetry on HIV-1 production.** HEK293T cells were co-transfected with HIV-1 pNL4-3 plasmid DNA (100ng) and one of the indicated symmetrical (**b**) or asymmetrical (**c**) dsiRNAs at 500 pM to 100 nM. Relative RT activity was determined as in Figure 4.1 **b**. For each concentration of dsiRNA tested, at least two independent experiments with two to three replicate transfections were performed, data are expressed as the mean +/- SEM (n=4-6).

4.4.3 si1498 length variants do not affect cell viability or induce dsRNA immune responses in HEK293T cells

A major concern for the development of siRNA therapeutics is their potential to stimulate dsRNA immune responses as this can both confound the interpretation of experimental results and limit their potential for development as therapeutics (reviewed in [41]). To determine whether the increase in efficacy and potency observed for longer siRNAs targeting the Gag1498 site was related to toxicity in HEK293T cells, we evaluated the potential for different effective siRNAs to affect cell viability. siRNAs were transfected into HEK293T cells at 100 nM and their effects were compared to mock transfected cells and cells transfected with a low molecular weight (200 to 1000 base pairs) long dsRNA control (poly(I:C)). Cell viability was estimated using a standard MTT colorimetric assay and data were expressed as relative MTT metabolism compared to mock transfected cells (Figure 4.3 **a**). A minor decrease in cell viability compared to mock transfected cells was apparent for the long dsRNA control, poly(I:C). However, it was only statistically significant at the higher concentration tested (200 µg/mL). No significant differences in cell viability between mock transfected and siRNA transfected cells were observed.

In the absence of effects on cell viability, activation of dsRNA immune responses has the potential to inhibit HIV-1 production and confound the interpretation of experimental results [41]. To evaluate the potential for si1498 length variants to activate the dsRNA immune sensors PKR and TLR-3, we next measured levels of phosphorylated PKR and IRF3 (a downstream response to TLR-3 activation) in transfected HEK293T cells. The expression of the interferon stimulated gene ADAR1 p150 was also evaluated to compare potential induction of interferon

responses (Figure 4.3 **b**). In conditions where transfection with the long dsRNA control (poly(I:C)) induced phosphorylation of both PKR and IRF3 as well as expression of ADAR1 p150, no significant effects could be observed in cells transfected with si1498 variants. These results suggest that the differences in anti-HIV-1 effects observed for the si1498 variants in Figure 4.2 were related to differences in RNA silencing as opposed to off-target effects on cell viability, dsRNA immune sensor activation or interferon stimulated gene expression.

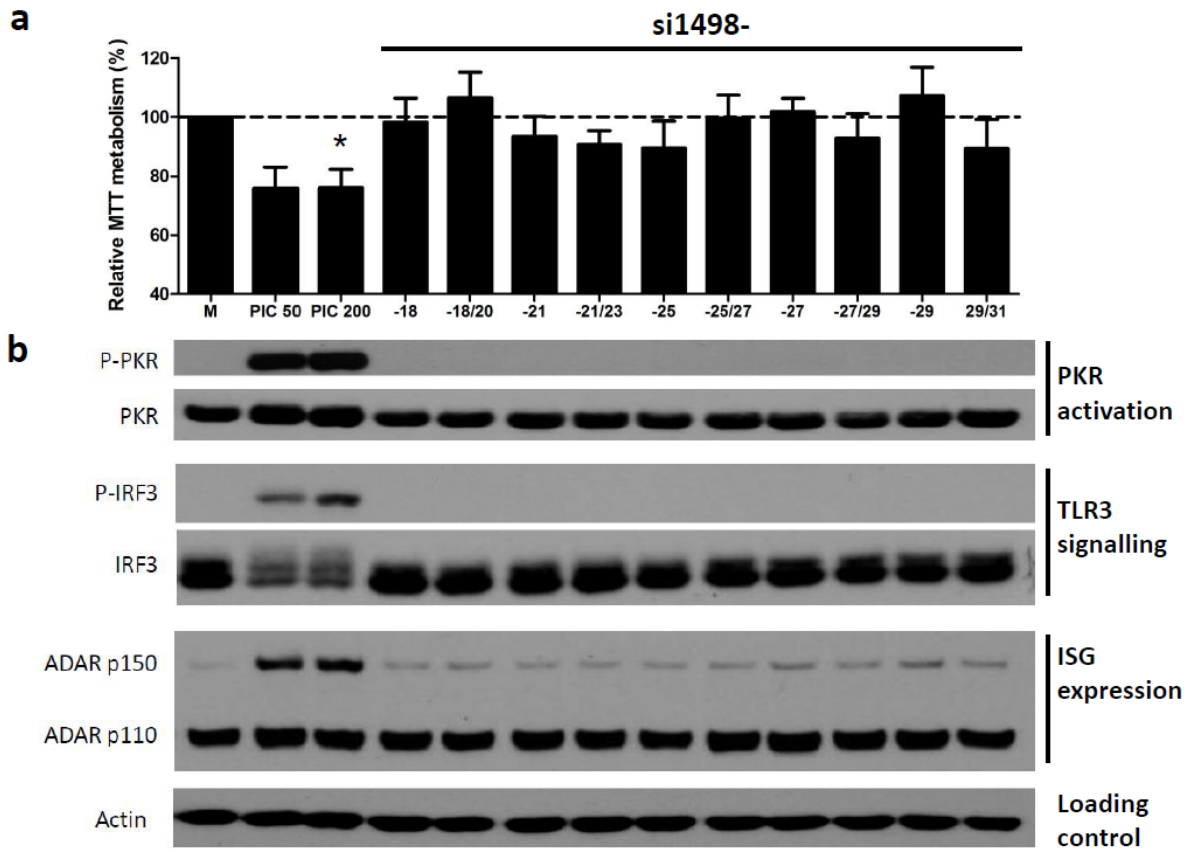

Figure 4.3. si1498 variants do not affect cell viability, dsRNA immune sensor activation or interferon gene stimulation in HEK293T cells.

a) Effects of si1498 variants on cell viability. HEK293T cells were mock (M) transfected, transfected with 50 or 200 µg/mL poly(I:C) (PIC 50 and PIC 200) or transfected with 100 nM of the indicated si1498 variants. Cell viability was estimated by measuring the metabolism of MTT 48 h following transfection. Data are expressed as relative MTT metabolism compared to mock transfected cells tested in parallel. Three independent experiments with two to three replicate transfections were performed, data are expressed as the mean +/- SEM (n=7). Results from un-paired Student t-tests are shown above each condition that demonstrated a significant decrease compared to the mock transfected condition (*P < 0.05, **P < 0.01, ***P < 0.001). **b) Effects of si1498 variants on dsRNA responses.** HEK293T cells were transfected as in (**a**) and 48 h after transfection cell lysates were blotted for expression of phosphorylated PKR and IRF3 (P-PKR and P-IRF3), total PKR and IRF3, ADAR p110 and p150 and actin.

4.4.4 si1498 length variants have minor effects on cell viability and dsRNA immune responses in MCF7 cells

It has been suggested that the length threshold for dsRNA immune responses is cell type dependent and reductions in cell viability for dsiRNAs (25/27 format) compared to canonical siRNAs has been observed in MCF7, DU145, HeLa S3 [20] and HeLa SS6 cells [19]. For si1498 length variants, cell viability was assessed in MCF7 cells (Figure 4.4 **a**). In comparison to HEK293T cells (Figure 4.3 **a**), MCF7 cells were slightly more sensitive to the toxic effects of poly(I:C) and minor decreases in cell viability were observed in siRNA transfected cells with significant decreases observed for si1498-21/23 and si1498-27/29 variants. While activation of PKR and TLR-3 were not detected in MCF7 cells transfected with si1498 variants, minor effects on the expression of the ISG, ADAR p150 were observed in some conditions (Figure 4.4 **b**). As longer siRNAs did not elicit more pronounced effects on cell viability or ADAR p150 expression compared to shorter siRNAs, these results provide evidence that the more effective longer siRNAs do not have greater potential to illicit innate immune responses in different cell types. Experiments in additional cell types are planned to confirm that the longer siRNAs have an equal potential to be used safely in a therapeutic setting compared to shorter siRNAs.

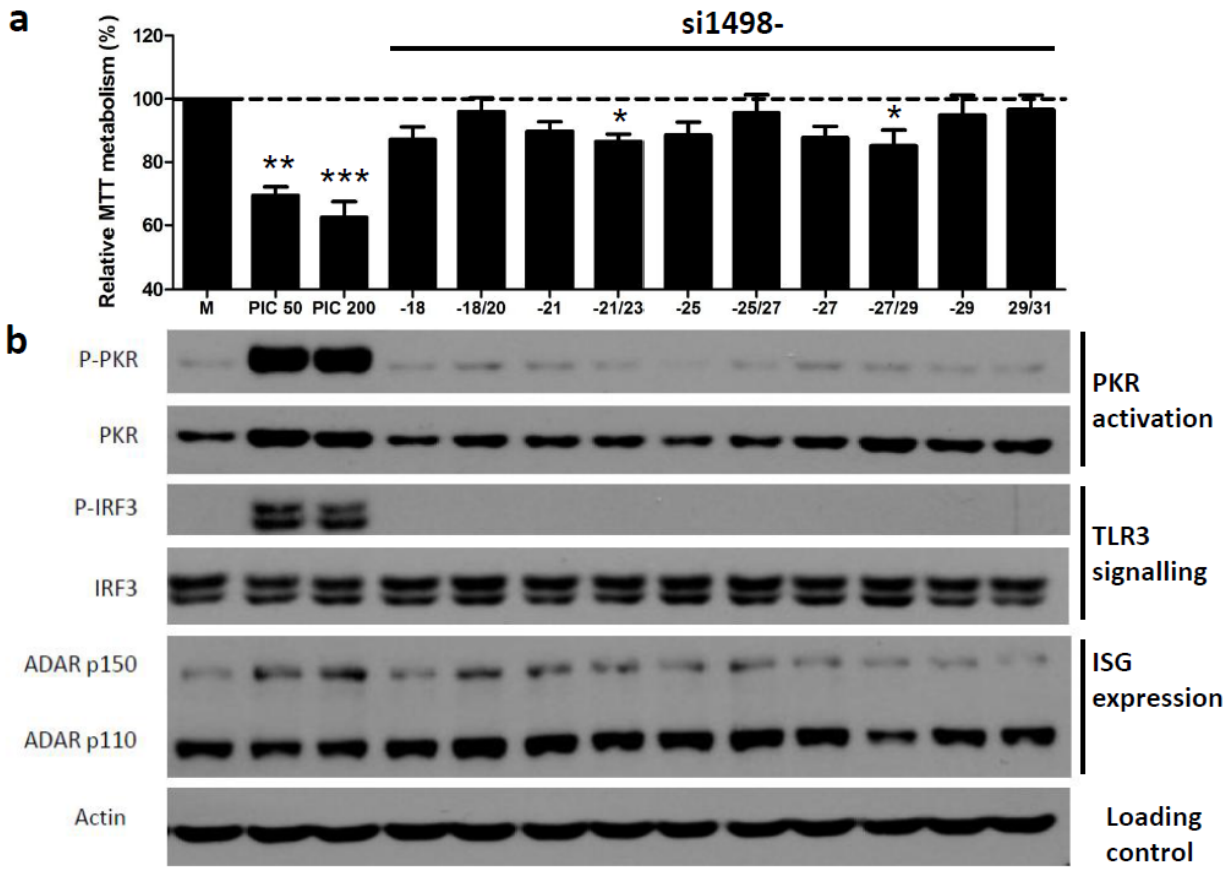

Figure 4.4. si1498 variants have moderate to no effects on cell viability, dsRNA immune sensor activation and interferon gene stimulation in MCF7 cells.

a) Effects of si1498 variants on cell viability. MCF7 cells were mock (M) transfected, transfected with 50 or 200 µg/mL poly(I:C) (PIC 50 and PIC 200) or transfected with 100 nM of the indicated si1498 variants. Cell viability was estimated by measuring the metabolism of MTT 48 h following transfection. Data are expressed as relative MTT metabolism compared to mock transfected cells tested in parallel. Three independent experiments with two to three replicate transfections were performed, data are expressed as the mean +/- SEM (n=7). Results from un-paired Student t-tests are shown above each condition that demonstrated a significant decrease compared to the mock transfected condition (*P < 0.05, **P < 0.01, ***P < 0.001). **b) Effects of si1498 variants on dsRNA responses.** MCF7 cells were transfected as in (**a**) and 48 h after transfection cell lysates were blotted for expression of phosphorylated PKR and IRF3 (P-PKR and P-IRF3), total PKR and IRF3, ADAR p110 and p150 and actin.

4.4.5 shRNAs targeting the Gag 1498 site with hairpin stems of 20 to 27 base pairs provide the most effective inhibition of HIV-1 production

The shRNA targeting the Gag 1498 site in HIV-1 RNA identified in our previous study (shRNA1498) [36] had a 20 base pair stem with two to four uridines at its 3' end from the RNA Pol III H1 promoter termination signal (named sh1498-20 in this study). To determine whether the effects of sh1498-20 (Figure 4.5 **a**, top) could be improved by introducing target matched nts at its 3' antisense overhang, we designed sh1498-20-3'c (Figure 4.5 **a**, bottom). Consistent with results comparing siRNAs with perfectly (si1498-25D/27 and si1498-27/29D) and imperfectly (si1498-25/27 and si1498-27/29) matched antisense strand 3' nt overhangs (Figure 4.1 **c**), the efficacy and potency of the two shRNAs against HIV-1 production was nearly identical (Figure 4.5 **b**). As the addition of perfectly matched nts did not improve the effects of sh1498-20, the original format with imperfectly matched nts in the 3' overhang was used to compare the effects of sh1498 variants with different stem lengths on HIV-1 production.

To determine the optimal stem length for different shRNAs targeting the Gag 1498 site, a set of shRNAs were designed based on sh1498-20 with stem lengths of 17 to 29 base pairs (Figure 4.5 **c**). The loop sequence followed a previously described format of eight nts, where the nt N is complementary to the target site [42]. In contrast to results for siRNAs (Figure 4.2), shRNAs with stem lengths below 20 base pairs were not effective inhibitors of HIV-1 production (Figure 4.5 **b**). Beyond 20 base pairs, a trend towards decreasing potency and efficacy was observed as the stem length was increased to 29 base pairs.

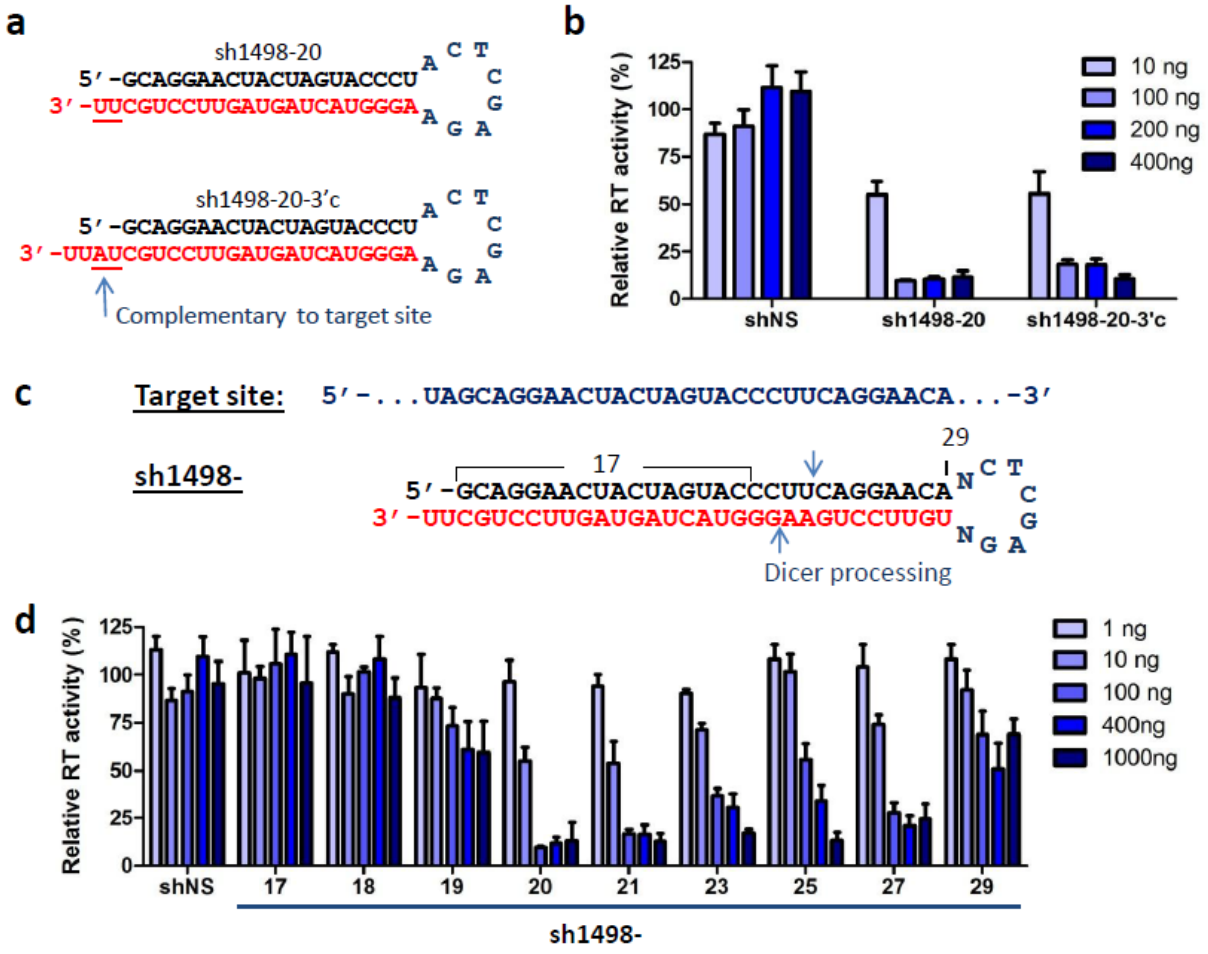

Figure 4.5. Effects of sh1498 on HIV-1 production, with and without target complementary nts in the 3' overhang.

a) Schematic representation of sh1498-20 with a 3' complementary antisense overhang (sh1498-20-3'c). The sh1498 design used in our previous study [36] and the modified sh1498-20-3'c with nts in its 3' antisense overhang complementary to the target RNA are illustrated. **b) Effects of sh1498-20 and sh1498-20-3'c on HIV-1 production.** HEK293T cells were co-transfected with 100 ng of pNL4-3 DNA and 10-400 ng of shRNA expressing plasmids. Relative RT activity is expressed as a percentage of the value obtained for co-transfection with an empty shRNA expression vector tested in parallel. Each concentration of the different shRNAs was evaluated in at least two independent experiments with two to three replicate transfections, data are expressed as the mean +/- SEM (n=4-6). **c) Schematic representation of sh1498 length variants.** The intended sense strand is on top in black and the intended antisense strand is on the bottom in red. The sequence for sh1498-29 is shown and the position of sh1498-17 is illustrated within the longer shRNA. Expected sites of Dicer processing for longer shRNAs are illustrated with blue arrows. For each length variant, the nucleotide N was complementary to the next position in the target site. **d) Effects of sh1498 length variants on HIV-1 production.** shRNAs were evaluated for effects on HIV-1 production as in (**b**). For each concentration of shRNA at least two independent experiments were performed with two to three replicates, data are expressed as the mean +/- SEM (n=4-6).

4.5 Discussion

HIV-1 RNA represents an attractive target for the therapeutic development of siRNAs or shRNAs and over 750 molecules have been designed with diverse target sites [43]. A primary consideration for the design of these molecules is that their target sequence is highly represented in HIV-1 infected populations and that it is accessible enough to allow for the development of effective siRNA or shRNA molecules. Results from our previous study suggested that a novel target site in the Gag coding sequence of HIV-1 RNA was highly conserved across circulating HIV-1 strains, accessible in diverse viral strains and that an shRNA (shRNA1498) targeting it was an effective inhibitor of viral production with low potential to affect human mRNA expression [36]. In this study, our aim was to determine the optimal format for siRNAs and shRNAs targeting this site for further development as drug or gene therapies, respectively.

The first study to demonstrate gene silencing by siRNAs in mammalian cells used a canonical format (-21) with two thymidine residues on the 3' overhang of each strand (-21tt) [6]. The optimal format of the overhangs was shown to be dependent on their length (2 nts), rather than their identity (target matched, RNA or DNA nts) [44], and the -21tt format became the industry standard for gene silencing studies. For therapeutic development, several nt modifications at specific internal positions have been shown to enhance the stability of siRNAs without affecting their RNAi activity [45, 46]. A comprehensive analysis of modifications to the 3' overhang in the antisense strand of canonical siRNAs showed that, although similar in short-term gene silencing, target matched RNA nts were superior to thymidine residues in these positions [47] and similar results have been observed for dsiRNAs [17]. Our results comparing si1498 variants (Figure 4.1 **a,c**) and sh1498 variants (Figure 4.5 **a,b**) with different nts in the 3' overhang of the antisense

strands suggested that the identity of nts in these positions are not important determinants for effective gene silencing. However, small differences may have been missed on account of the short time course of the experiments (48 h) and future studies to determine the optimal identity of nts in these positions are planned.

Although symmetrical siRNAs are commonly used, Sano et al. showed that asymmetrical siRNAs with blunt end modifications at the 3' end of the sense strand can improve selection of the intended antisense strand by the RISC [48]. It was also demonstrated that for dsiRNAs, the blunt end format at the 3' end of the sense strand enhances Dicer processing to yield a more homogeneous population of intended siRNA products [16]. Our results for both shorter and longer siRNAs targeting the Gag 1498 site, showed that blunt end modifications do not affect their potency or efficacy against HIV-1 production, and that instead, their inhibitory effects were dependent only on the length of their sense strands (Figure 4.2). As with effects of the nt identity in the 3' antisense overhang, benefits of the blunt end modification may have been missed due to the short time course of the experiments.

Our results are consistent with previous observations [14, 16, 18] suggesting that longer siRNAs that can act as substrates for the Dicer enzyme are superior to their sequence matched canonical formats (si1498-21) (Figure 4.2). It has been postulated, that by engaging the Dicer complex, dsiRNAs can more efficiently enter into effective RISC complexes [14] and optimal design principles for dsiRNAs have been described [15]. Our results suggest that for the Gag 1498 target site, the standard dsiRNA format (si1498-25/27) may not be long enough to engage Dicer and observe an increase in gene silencing over the canonical format (si1498-21). As several

studies have reported highly effective -25/27 dsiRNA formats and only one target site was evaluated in this study, we cannot make conclusions on the frequency of sequences that would benefit from longer -27/29 and -29/31 dsiRNA formats. However, our results suggest that conflicting conclusions reported by Foster et al., showing no benefit of dsiRNAs in gene silencing [19], may have been a result of the -25/27 format used, rather than the dsiRNA concept itself. For the Gag 1498 target site, our results demonstrate that dsiRNAs with a sense strand length of at least 27 nts provide the greatest potency and efficacy against HIV-1 production compared to shorter siRNAs. We also provide evidence that the potency and efficacy of different siRNA length variants was not related to differential effects on cell viability, activation of immune sensors or expression of an interferon stimulated gene (Figure 4.3 and Figure 4.4).

Studies have shown that lower thermodynamic stability (less G/C content) at the 5' end of the intended antisense strand of a canonical siRNA can improve gene silencing by enhancing its selection over the sense strand into effective RISC complexes [49, 50]. We cannot exclude therefore, that the increased effectiveness of longer siRNAs in our study was due to the generation of additional siRNA Dicer products with better thermodynamic properties compared to the intended canonical format. While further studies will be required to elucidate the mechanism behind the observed differences in HIV-1 inhibition, it has been shown that the predominant Dicer product of dsiRNAs with an asymmetrical format is the intended canonical siRNA [16]. Based on this observation we can suggest that at least for the asymmetrical siRNAs evaluated (Figure 4.2 **c**), the increased effects observed for the longer siRNAs was related to recruitment of the Dicer complex as opposed to the production of improved Dicer products.

As shRNAs already engage Dicer to cleave off their loop sequences, an increase in stem length would not be expected to provide the benefit of recruiting the Dicer complex proposed for longer siRNAs. In agreement, McIntyre et al. showed that for different target sites, no correlation existed between stem length and gene silencing effects [34]. For shRNAs targeting the Gag 1498 site, a stem length of at least 20 base pairs was required to achieve an efficacious effect against HIV-1 production and as the stem length was increased, the potency and efficacy of shRNAs showed a decreasing trend (Figure 4.5 **c,d**). Our results also show that for the Gag1498 target site, there was little correlation in anti-HIV-1 effects between siRNA sense strand lengths (**Fig. 2**) and shRNA stem lengths (Figure 4.5 **c,d**).

The use of shRNAs targeting HIV-1 RNA is currently being evaluated in clinical trials for cell transplant therapy [40] (ClinicalTrials.gov NCT-01961063), and the potential to use siRNAs in drug therapy has been evaluated in preclinical mouse models [10-12]. In both approaches, combinations of effective molecules will be required to control HIV-1 replication and prevent the development of resistant virus. In this study we have identified several optimized candidates targeting a highly conserved and accessible site in HIV-1 RNA for use in combination RNA gene or drug therapy. Our results also support the concept that longer dsiRNAs are more effective compared to canonical siRNAs and highlight the importance of evaluating different siRNA and shRNA lengths to identify the optimal therapeutic format for any particular target site.

4.6 MATERIALS AND METHODS

4.6.1 siRNA sequences and construction of shRNA vectors

All siRNAs used in this study were purchased from GE Dharmacon (Lafayette, CO). The sequences for sense and antisense strands are provided in Table 4.1. Sequences for si5983-27/29D were obtained from a published sequence called Site I (tat/rev) 27 mer [10] and the nonsense siRNA, siNS-25D/27, was adapted from a previous nonsense siRNA called siControl [51]. All shRNAs were expressed from the human RNase P H1 promoter in the vector psiRNA-H1GFP::Zeo (InvivoGen, San Diego, CA). sh1498-20 and shNS were from our previous study (shRNA1498 and shRNAns, respectively) [36]. New shRNA inserts were generated by annealing complementary sense and antisense oligonucleotides at 1.25 μM each in 40 μL of 75 mM NaCl for 2 min at 80 °C, followed by slowly decreasing the temperature to 37 °C. All oligonucleotides were purchased from Life technologies (Carlsbad, CA). Sequences for sense and antisense strands are provided in Table 4.2. Inserts were ligated into Bbs1 digested psiRNA-H1GFP::Zeo and correct insertion into the vector was confirmed by sequencing using a primer located upstream in the vector: 5'-TCTACGGGGTCTGACGC-3'.

Table 4.1 Sense and antisense sequences for siRNAs

siRNA	5'-3' Sense (S) and 3'-5' Antisense (AS) strands
siNS-25D/27: S	5′-GUACCGCACGUCAUUCGUAUCCUat-3'
AS	3′-UUCAUGGCGUGCAGUAAGCAUAGGAUA-5'
si5983-25D/27: S	5′-GCGGAGACAGCGACGAAGAGCUCat-3'
AS	3′-UUCGCCUCUGUCGCUGCUUCUCGAGUA-5'
si5983-27/29D: S	5′-GCGGAGACAGCGACGAAGAGCUCAUCA-3'
AS	3′-ttCGCCUCUGUCGCUGCUUCUCGAGUAGU-5'
si1498-25D/27: S	5′-GCAGGAACUACUAGUACCCUUCAgg-3'
AS	3′-AUCGUCCUUGAUGAUCAUGGGAAGUCC-5'
si1498-27/29D: S	5′-GCAGGAACUACUAGUACCCUUCAGGAA-3'
AS	3′-atCGUCCUUGAUGAUCAUGGGAAGUCCUU-5'
si1498-17/19: S	5'-GCAGGAACUACUAGUAC-3'
AS	3'-UUCGUCCUUGAUGAUCAUG-5'
si1498-18/20: S	5'-GCAGGAACUACUAGUACC-3'
AS	3'-UUCGUCCUUGAUGAUCAUGG-5'
si1498-19/21: S	5'-GCAGGAACUACUAGUACCC-3'
AS	3'-UUCGUCCUUGAUGAUCAUGGG-5'
si1498-20/22: S	5'-GCAGGAACUACUAGUACCCU-3'
AS	3'-UUCGUCCUUGAUGAUCAUGGGA-5'
si1498-21/23: S	5'-GCAGGAACUACUAGUACCCUU-3'
AS	3'-UUCGUCCUUGAUGAUCAUGGGAA-5'
si1498-23/25: S	5'-GCAGGAACUACUAGUACCCUUCA-3'
AS	3'-UUCGUCCUUGAUGAUCAUGGGAAGU-5'
si1498-25/27: S	5'-GCAGGAACUACUAGUACCCUUCAGG-3'
	3'-UUCGUCCUUGAUGAUCAUGGGAAGUCC-5'
si1498-27/29: S	5'-GCAGGAACUACUAGUACCCUUCAGGAA-3'
AS	3'-UUCGUCCUUGAUGAUCAUGGGAAGUCCUU-5'
si1498-17: S	5'-GCAGGAACUACUAGUAC-3'
AS	3'-UUCGUCCUUGAUGAUCA-5'
si1498-18: S	5'-GCAGGAACUACUAGUACC-3'
AS	3'-UUCGUCCUUGAUGAUCAU-5'
si1498-19: S	5'-GCAGGAACUACUAGUACCC-3'
AS	3'-UUCGUCCUUGAUGAUCAUG-5'
si1498-20: S	5'-GCAGGAACUACUAGUACCCU-3'
AS	3'-UUCGUCCUUGAUGAUCAUGG-5'
si1498-21: S	5'-GCAGGAACUACUAGUACCCUU-3'
AS	3'-UUCGUCCUUGAUGAUCAUGGG-5'
si1498-23: S	5'-GCAGGAACUACUAGUACCCUUCA-3'
AS	3'-UUCGUCCUUGAUGAUCAUGGGAA-5'
si1498-25: S	5'-GCAGGAACUACUAGUACCCUUCAGG-3'
AS	3'-UUCGUCCUUGAUGAUCAUGGGAAGU-5'
si1498-27: S	5'-GCAGGAACUACUAGUACCCUUCAGGAA-3'
AS	3'-UUCGUCCUUGAUGAUCAUGGGAAGUCC-5'
si1498-29: S	5'-GCAGGAACUACUAGUACCCUUCAGGAACA-3'
AS	3'-UUCGUCCUUGAUGAUCAUGGGAAGUCCUU-5'

Table 4.2 Sequences of shRNA coding oligonucleotides

shRNA	S and AS oligonucleotides for inserts (5' to 3')
sh1498-17: S	ACCTCGCAGGAACTACTAGTACGCTCGAGGGTACTAGTAGTTCCTGCTT
sh1498-17: AS	CAAAAAGCAGGAACTACTAGTACCCTCGAGCGTACTAGTAGTTCCTGCG
sh1498-18: S	ACCTCGCAGGAACTACTAGTACCGCTCGAGGGGTACTAGTAGTTCCTGCTT
sh1498-18: AS	CAAAAAGCAGGAACTACTAGTACCCCTCGAGCGGTACTAGTAGTTCCTGCG
sh1498-19: S	ACCTCGCAGGAACTACTAGTACCCACTCGAGAGGGTACTAGTAGTTCCTGCTT
sh1498-19-AS:	CAAAAAGCAGGAACTACTAGTACCCTCTCGAGTGGGTACTAGTAGTTCCTGCG
sh1498-20-3'c: S	ACCTCGCAGGAACTACTAGTACCCTACTCGAGAAGGGTACTAGTAGTTCCTGCATT
sh1498-20-3'c: AS	CAAAAATGCAGGAACTACTAGTACCCTTCTCGAGTAGGGTACTAGTAGTTCCTGCG
sh1498-21: S	ACCTCGCAGGAACTACTAGTACCCTTGCTCGAGGAAGGGTACTAGTAGTTCCTGCTT
sh1498-21: AS	CAAAAAGCAGGAACTACTAGTACCCTTCCTCGAGCAAGGGTACTAGTAGTTCCTGCG
sh1498-23: S	ACCTCGCAGGAACTACTAGTACCCTTCACCTCGAGCTGAAGGGTACTAGTAGTTCCTGCTT
sh1498-23: AS	CAAAAAGCAGGAACTACTAGTACCCTTCAGCTCGAGGTGAAGGGTACTAGTAGTTCCTGCG
sh1498-25: S	ACCTCGCAGGAACTACTAGTACCCTTCAGGTCTCGAGTCCTGAAGGGTACTAGTAGTTCCTGCTT
sh1498-25: AS	CAAAAAGCAGGAACTACTAGTACCCTTCAGGACTCGAGACCTGAAGGGTACTAGTAGTTCCTGCG
sh1498-27: S	ACCTCGCAGGAACTACTAGTACCCTTCAGGAAGCTCGAGGTTCCTGAAGGGTACTAGTAGTTCCTGCTT
sh1498-27: AS	CAAAAAGCAGGAACTACTAGTACCCTTCAGGAACCTCGAGCTTCCTGAAGGGTACTAGTAGTTCCTGCG
sh1498-29: S	ACCTCGCAGGAACTACTAGTACCCTTCAGGAACATCTCGAGTTGTTCCTGAAGGGTACTAGTAGTTCCTGCTT
sh1498-29: AS	CAAAAAGCAGGAACTACTAGTACCCTTCAGGAACAACTCGAGATGTTCCTGAAGGGTACTAGTAGTTCCTGCG

4.6.2 Cells and transfections

HEK293T and MCF7 cells (ATCC, Manassas, VA) were maintained in Dulbecco's modified Eagle's medium with high glucose (Hyclone, Logan, UT) supplemented with 10% fetal bovine serum (Hyclone, Logan, UT), 50 U/mL Penicillin and 50 μg/mL Streptomycin (Life technologies, Carlsbad, CA). Co-transfection of cells with HIV-1 molecular clone pNL4-3 and siRNAs or shRNA expressing plasmids were performed in 24 well plates seeded 24 h prior to co-transfection at 1×10^5 cells per well. Transfection with siRNAs was performed with 1.5 μL of Dharmafect 1 (Dharmacon, Lafayette, CO) and transfection with shRNAs was performed with 1.5 μL of TransIT (Mirus, Madison, WI), according to the manufacturer's instructions. For co-transfection with shRNAs, an equal amount of DNA was used by topping up lower dose transfections with an irrelevant plasmid (Bluescript SK+, Stratagene, La Jolla, CA).

For cell viability and protein expression assays, cells were seeded 24 h prior to transfection in 96 and 12 well plates, respectively. HEK293T and MCF7 cells were plated at 2×10^5 cells/mL and transfected with siRNAs or low molecular weight polyinosinic-polycytidylic acid (poly(I:C) LMW, InvivoGen, San Diego, CA), using 0.4 μL (96 well plate) or 3 μL (12 well plate) of Dharmafect 1 (Dharmacon, Lafayette, CO). For all transfection experiments, assays were performed 48 h after transfection.

4.6.3 HIV-1 production assay

The HIV-1 RT assay used in this study was performed as previously described (Chapter 2, [35]). Briefly, 5 ul of supernatant was incubated with a polyadenylic acid template (Roche, Basel,

Switzerland), an oligo dT primer (Life Tech., Carlsbad, CA) and [^{32}P]-dTTP (3,000 Ci/mmol, Perkin Elmer, Waltham, MA) for 2 h at 37°C in 50 µl total reaction mixture. 5 µl of the reaction mixture was then spotted onto Diethylaminoethyl (DEAE) filter mat (Perkin Elmer, Waltham, MA) and washed five times in 2X SSC buffer, followed by two washes in 95% ethanol to remove [^{32}P]-dTTP not incorporated into the poly dT RT product. Counts per minute (cpm) were calculated for each sample using a microplate scintillation counter (Microbeta TriLux, Perkin Elmer,) and are proportional to the amount of HIV-1 RT enzyme present in the reaction mixture.

4.6.4 Cell viability assay

Cell viability was estimated by measuring the metabolism of MTT (3-(4,5-dimethylthiazol-2-yl)-2,5-diphenyltetrazolium bromide tetrazolium) (Sigma-Aldrich, St. Louis, MO) in cell cultures, as previously described [52]. Briefly, cells were incubated for 3 h at 37 °C with MTT, followed by the addition of acidified isopropanol to solubilize the blue crystals formed due to the conversion of MTT to Formazan by cellular enzymes. Plates were then incubated for 2 h at room temperature and read at 570 nm using a Benchmark Plus microplate spectrophotometer (BioRad, Hercules, CA). To evaluate statistical significance, values for RNA transfected cells were compared to mock transfected cells using unpaired Student t-tests (Microsoft Excel).

4.6.5 Protein expression assay

Cell lysates were obtained 48 h after co-transfection in lysis buffer containing anti-proteases and anti-phosphatases (Roche, Basel, Switzerland). 75 µg of total protein was resolved on a 10% denaturing polyacrylamide gel and transferred to a Hybond ECL nitrocellulose membrane (GE

Healthcare, Little Chalfont, UK) as previously described [53]. Membranes were incubated first with anti-protein kinase R (PKR) (phospho-T446) E120 (Abcam, Cambridge, UK), anti-IRF3 (phospho S396) 4D4G (Cell Signalling, Danvers, MA) and anti-ADAR1 (from Dr. BL Bass) at a 1/1000 dilution. Membranes were stripped by incubation with Re-Blot Plus Strong (Millipore, Billerica, MA) for 10 min and then incubated with anti-PKR 71-10 (from Dr. A. Hovanessian) at a 1/500 dilution, anti-IRF3 D614C (Cell Signalling, Danvers, MA) at a 1/1000 dilution and anti-actin C4 (Millipore, Billerica, MA) at a 1/5000 dilution. Following primary antibody incubation, membranes were incubated with anti-mouse or anti-rabbit IgG-horseradish peroxidase (GE Healthcare, Little Chalfont, UK) at a 1/5000 dilution for 2 h. Bands were visualized with ECL (GE Healthcare, Little Chalfont, UK).

4.7 References

1. Fire, A, Xu, S, Montgomery, MK, Kostas, SA, Driver, SE, and Mello, CC (1998). Potent and specific genetic interference by double-stranded RNA in Caenorhabditis elegans. *Nature* **391**: 806-811.
2. Daniels, SM, and Gatignol, A (2012). The multiple functions of TRBP, at the hub of cell responses to viruses, stress, and cancer. *Microbiology and molecular biology reviews : MMBR* **76**: 652-666.
3. Daniels, SM, Melendez-Pena, CE, Scarborough, RJ, Daher, A, Christensen, HS, El Far, M*, et al.* (2009). Characterization of the TRBP domain required for dicer interaction and function in RNA interference. *BMC Mol Biol* **10**: 38.
4. Provost, P, Dishart, D, Doucet, J, Frendewey, D, Samuelsson, B, and Radmark, O (2002). Ribonuclease activity and RNA binding of recombinant human Dicer. *Embo j* **21**: 5864-5874.
5. Zhang, H, Kolb, FA, Brondani, V, Billy, E, and Filipowicz, W (2002). Human Dicer preferentially cleaves dsRNAs at their termini without a requirement for ATP. *Embo j* **21**: 5875-5885.
6. Elbashir, SM, Harborth, J, Lendeckel, W, Yalcin, A, Weber, K, and Tuschl, T (2001). Duplexes of 21-nucleotide RNAs mediate RNA interference in cultured mammalian cells. *Nature* **411**: 494-498.

7. Caplen, NJ, Parrish, S, Imani, F, Fire, A, and Morgan, RA (2001). Specific inhibition of gene expression by small double-stranded RNAs in invertebrate and vertebrate systems. *Proc Natl Acad Sci U S A* **98**: 9742-9747.
8. Kanasty, R, Dorkin, JR, Vegas, A, and Anderson, D (2013). Delivery materials for siRNA therapeutics. *Nature materials* **12**: 967-977.
9. Burnett, JC, and Rossi, JJ (2012). RNA-based therapeutics: current progress and future prospects. *Chem Biol* **19**: 60-71.
10. Zhou, J, Neff, CP, Liu, X, Zhang, J, Li, H, Smith, DD*, et al.* (2011). Systemic administration of combinatorial dsiRNAs via nanoparticles efficiently suppresses HIV-1 infection in humanized mice. *Mol Ther* **19**: 2228-2238.
11. Zhou, J, Neff, CP, Swiderski, P, Li, H, Smith, DD, Aboellail, T*, et al.* (2013). Functional in vivo delivery of multiplexed anti-HIV-1 siRNAs via a chemically synthesized aptamer with a sticky bridge. *Mol Ther* **21**: 192-200.
12. Kumar, P, Ban, HS, Kim, SS, Wu, H, Pearson, T, Greiner, DL*, et al.* (2008). T cell-specific siRNA delivery suppresses HIV-1 infection in humanized mice. *Cell* **134**: 577-586.
13. Snead, NM, and Rossi, JJ (2012). RNA interference trigger variants: getting the most out of RNA for RNA interference-based therapeutics. *Nucleic Acid Ther* **22**: 139-146.
14. Kim, DH, Behlke, MA, Rose, SD, Chang, MS, Choi, S, and Rossi, JJ (2005). Synthetic dsRNA Dicer substrates enhance RNAi potency and efficacy. *Nat Biotechnol* **23**: 222-226.
15. Amarzguioui, M, Lundberg, P, Cantin, E, Hagstrom, J, Behlke, MA, and Rossi, JJ (2006). Rational design and in vitro and in vivo delivery of Dicer substrate siRNA. *Nature protocols* **1**: 508-517.
16. Rose, SD, Kim, DH, Amarzguioui, M, Heidel, JD, Collingwood, MA, Davis, ME*, et al.* (2005). Functional polarity is introduced by Dicer processing of short substrate RNAs. *Nucleic Acids Res* **33**: 4140-4156.
17. Zhou, J, Song, MS, Jacobi, AM, Behlke, MA, Wu, X, and Rossi, JJ (2012). Deep Sequencing Analyses of DsiRNAs Reveal the Influence of 3' Terminal Overhangs on Dicing Polarity, Strand Selectivity, and RNA Editing of siRNAs. *Mol Ther Nucleic Acids* **1**: e17.
18. Snead, NM, Wu, X, Li, A, Cui, Q, Sakurai, K, Burnett, JC*, et al.* (2013). Molecular basis for improved gene silencing by Dicer substrate interfering RNA compared with other siRNA variants. *Nucleic Acids Res* **41**: 6209-6221.
19. Foster, DJ, Barros, S, Duncan, R, Shaikh, S, Cantley, W, Dell, A*, et al.* (2012). Comprehensive evaluation of canonical versus Dicer-substrate siRNA in vitro and in vivo. *Rna* **18**: 557-568.
20. Reynolds, A, Anderson, EM, Vermeulen, A, Fedorov, Y, Robinson, K, Leake, D*, et al.* (2006). Induction of the interferon response by siRNA is cell type- and duplex length-dependent. *Rna* **12**: 988-993.
21. Chu, CY, and Rana, TM (2008). Potent RNAi by short RNA triggers. *Rna* **14**: 1714-1719.
22. Sun, X, Rogoff, HA, and Li, CJ (2008). Asymmetric RNA duplexes mediate RNA interference in mammalian cells. *Nat Biotechnol* **26**: 1379-1382.

23. Chang, CI, Yoo, JW, Hong, SW, Lee, SE, Kang, HS, Sun, X*, et al.* (2009). Asymmetric shorter-duplex siRNA structures trigger efficient gene silencing with reduced nonspecific effects. *Mol Ther* **17**: 725-732.
24. Eekels, JJ, and Berkhout, B (2011). Toward a durable treatment of HIV-1 infection using RNA interference. *Prog Mol Biol Transl Sci* **102**: 141-163.
25. Hoxie, JA, and June, CH (2012). Novel cell and gene therapies for HIV. *Cold Spring Harb Perspect Med* **2**: a007179.
26. Bennett, MS, and Akkina, R (2013). Gene therapy strategies for HIV/AIDS: preclinical modeling in humanized mice. *Viruses* **5**: 3119-3141.
27. Lambeth, LS, and Smith, CA (2013). Short hairpin RNA-mediated gene silencing. *Methods Mol Biol* **942**: 205-232.
28. Brummelkamp, TR, Bernards, R, and Agami, R (2002). A system for stable expression of short interfering RNAs in mammalian cells. *Science* **296**: 550-553.
29. Scarborough, RJ, and Gatignol, A (2015). HIV and Ribozymes. *Adv Exp Med Biol* **848**: 97-116.
30. Siolas, D, Lerner, C, Burchard, J, Ge, W, Linsley, PS, Paddison, PJ*, et al.* (2005). Synthetic shRNAs as potent RNAi triggers. *Nat Biotechnol* **23**: 227-231.
31. Yu, JY, Taylor, J, DeRuiter, SL, Vojtek, AB, and Turner, DL (2003). Simultaneous inhibition of GSK3alpha and GSK3beta using hairpin siRNA expression vectors. *Mol Ther* **7**: 228-236.
32. Paddison, PJ, Caudy, AA, Bernstein, E, Hannon, GJ, and Conklin, DS (2002). Short hairpin RNAs (shRNAs) induce sequence-specific silencing in mammalian cells. *Genes Dev* **16**: 948-958.
33. Miyagishi, M, Sumimoto, H, Miyoshi, H, Kawakami, Y, and Taira, K (2004). Optimization of an siRNA-expression system with an improved hairpin and its significant suppressive effects in mammalian cells. *J Gene Med* **6**: 715-723.
34. McIntyre, GJ, Yu, YH, Lomas, M, and Fanning, GC (2011). The effects of stem length and core placement on shRNA activity. *BMC Mol Biol* **12**: 34.
35. Scarborough, RJ, Lévesque, MV, Perreault, JP, and Gatignol, A (2014). Design and Evaluation of Clinically Relevant SOFA-HDV Ribozymes Targeting HIV RNA. *Methods Mol Biol* **1103**: 31-43.
36. Scarborough, RJ, Levesque, MV, Boudrias-Dalle, E, Chute, IC, Daniels, SM, Ouellette, RJ*, et al.* (2014). A Conserved Target Site in HIV-1 Gag RNA is Accessible to Inhibition by Both an HDV Ribozyme and a Short Hairpin RNA. *Mol Ther Nucleic Acids* **3**: e178.
37. Bergeron, LJ, and Perreault, JP (2005). Target-dependent on/off switch increases ribozyme fidelity. *Nucleic Acids Res* **33**: 1240-1248.
38. Bergeron, LJ, Reymond, C, and Perreault, JP (2005). Functional characterization of the SOFA delta ribozyme. *RNA* **11**: 1858-1868.
39. Lainé, S, Scarborough, RJ, Lévesque, D, Didierlaurent, L, Soye, KJ, Mougel, M*, et al.* (2011). In vitro and in vivo cleavage of HIV-1 RNA by new SOFA-HDV ribozymes and their potential to inhibit viral replication. *RNA Biol* **8**: 343-353.
40. DiGiusto, DL, Krishnan, A, Li, L, Li, H, Li, S, Rao, A*, et al.* (2010). RNA-based gene therapy for HIV with lentiviral vector-modified CD34(+) cells in patients undergoing transplantation for AIDS-related lymphoma. *Sci Transl Med* **2**: 36ra43.

41. Whitehead, KA, Dahlman, JE, Langer, RS, and Anderson, DG (2011). Silencing or stimulation? siRNA delivery and the immune system. *Annual review of chemical and biomolecular engineering* **2**: 77-96.
42. McIntyre, GJ, Groneman, JL, Yu, YH, Jaramillo, A, Shen, S, and Applegate, TL (2009). 96 shRNAs designed for maximal coverage of HIV-1 variants. *Retrovirology* **6**: 55.
43. Tyagi, A, Ahmed, F, Thakur, N, Sharma, A, Raghava, GP, and Kumar, M (2011). HIVsirDB: a database of HIV inhibiting siRNAs. *PLoS One* **6**: e25917.
44. Elbashir, SM, Martinez, J, Patkaniowska, A, Lendeckel, W, and Tuschl, T (2001). Functional anatomy of siRNAs for mediating efficient RNAi in Drosophila melanogaster embryo lysate. *Embo j* **20**: 6877-6888.
45. Czauderna, F, Fechtner, M, Dames, S, Aygun, H, Klippel, A, Pronk, GJ*, et al.* (2003). Structural variations and stabilising modifications of synthetic siRNAs in mammalian cells. *Nucleic Acids Res* **31**: 2705-2716.
46. Amarzguioui, M, Holen, T, Babaie, E, and Prydz, H (2003). Tolerance for mutations and chemical modifications in a siRNA. *Nucleic Acids Res* **31**: 589-595.
47. Strapps, WR, Pickering, V, Muiru, GT, Rice, J, Orsborn, S, Polisky, BA*, et al.* (2010). The siRNA sequence and guide strand overhangs are determinants of in vivo duration of silencing. *Nucleic Acids Res* **38**: 4788-4797.
48. Sano, M, Sierant, M, Miyagishi, M, Nakanishi, M, Takagi, Y, and Sutou, S (2008). Effect of asymmetric terminal structures of short RNA duplexes on the RNA interference activity and strand selection. *Nucleic Acids Res* **36**: 5812-5821.
49. Khvorova, A, Reynolds, A, and Jayasena, SD (2003). Functional siRNAs and miRNAs exhibit strand bias. *Cell* **115**: 209-216.
50. Schwarz, DS, Hutvagner, G, Du, T, Xu, Z, Aronin, N, and Zamore, PD (2003). Asymmetry in the assembly of the RNAi enzyme complex. *Cell* **115**: 199-208.
51. Naito, Y, Nohtomi, K, Onogi, T, Uenishi, R, Ui-Tei, K, Saigo, K*, et al.* (2007). Optimal design and validation of antiviral siRNA for targeting HIV-1. *Retrovirology* **4**: 80.
52. Riss, TL, Moravec, RA, Niles, AL, Benink, HA, Worzella, TJ, and Minor, L (2004). Cell Viability Assays. In: Sittampalam, GS*, et al.* (eds). *Assay Guidance Manual*: Bethesda MD.
53. Clerzius, G, Shaw, E, Daher, A, Burugu, S, Gelinas, JF, Ear, T*, et al.* (2013). The PKR activator, PACT, becomes a PKR inhibitor during HIV-1 replication. *Retrovirology* **10**: 96.

Chapter 5

DISCUSSION

5.1 Towards an HIV cure

Members of the International AIDS Society have issued several strategies to reach a sterilizing or a functional cure for HIV infection [1]. One strategy that has received a lot of attention is referred to as the "shock and kill" approach. The aim of this approach is to activate HIV expression in latently infected cells and make those cells susceptible to clearance by the immune system and/or the pathological effects of HIV replication in the presence of suppressive drug therapy [2]. Although this approach has the potential to eliminate HIV from an infected person, and thereby provide a sterilizing cure, several clinical trials conducted over the past two decades have so far failed to identify a successful treatment regimen. Newer strategies include a combination of compounds designed to activate HIV expression in latent cells [3] and stimulation of HIV specific cytotoxic T lymphocyte responses to help clear the activated cells [4]. A better understanding of the mechanisms of viral latency and HIV persistence in different reservoirs should also lead to the identification of novel approaches to HIV elimination; however, whether these new approaches will be successful remains to be determined.

In the absence of a sterilizing cure, a few examples of individuals attaining a functional cure have been reported. One example is the "Mississippi baby", who was treated within 30 hours after birth, stopped treatment after two and a half years, and remained free of HIV for 28 months [5]. Another example is the VISCONTI cohort of 14 individuals who initiated therapy during primary infection and were able to sustain long-term control of HIV replication after therapy was stopped [6]. While these examples demonstrate that early treatment can lead to a functional cure, most HIV transmissions are not identified early enough for this approach to work and it cannot be applied to those who are already infected. The only confirmed functional cure of someone

with an established HIV infection is that of the Berlin patient, who received a cell transplant from a donor with natural resistance to HIV replication. Making this approach available to all infected individuals represents a very promising strategy towards reaching an HIV functional cure and the molecules that we have identified and characterized in this work represent potentially useful tools for future clinical trials.

5.2 Lessons from cell transplant studies for HIV-1 infection

Although proof-of-concept for HIV-1 resistant HSC transplant was provided with the unique set of circumstances that lead to a confirmed functional cure for the Berlin patient [7], the limited availability of potential donors makes this approach inaccessible to the majority of HIV-1 infected individuals. In addition to receiving an allogeneic HSC transplant from a donor with the HIV-1 resistant homozygous CCR5Δ32 genotype, the Berlin patient also underwent an intense conditioning regimen including total body irradiation, immune suppression and $CD3^+$ T cell depletion [8]. Hopes that a similar treatment regimen without HIV-1 resistant cells could be used to attain a functional cure were provided by two patients treated in Boston, who were able to control HIV-1 replication in the absence of therapy following an allogeneic HSC transplant [9]. However, both patients eventually experienced viral rebound, suggesting that the transplant of HIV-1 resistant cells was the major determinant in the functional cure attained by the Berlin patient.

The current approach to translate the case of the Berlin patient into an acceptable clinical protocol for all HIV-1 infected individuals is to use an autologous HSC transplant with gene-

modified cells. For this approach to be successful, the gene-modified cells must efficiently engraft and repopulate the immune system. Results from the only vector controlled phase II clinical trial estimated that following HSC transplant, less than 5 % of total HSCs were gene-modified and that gene-modified cells decreased over time [10]. These results suggest that some form of conditioning regimen will be required to make space for gene-modified HSCs, and the identification of safe and effective procedures to accomplish this represents a major challenge for the development of gene-modified autologous HSC transplant clinical protocols [11].

Ongoing clinical trials of gene-modified cell transplant include Sangamo BioScience's SB728-T (ClinicalTrials.gov NCT-01044654), and Calimmune's Cal-1 (ClinicalTrials.gov NCT-01734850). SB728-T consists of autologous $CD4^+$ enriched T cells modified with a Zinc finger nuclease (ZFN) at a locus in the CCR5 gene. The goal is to phenotypically mimic the HIV-1 resistant homozygous CCR5Δ32 genotype of cells transplanted into the Berlin patient. While efficacy and long-term safety have not yet been demonstrated, a preliminary clinical trial suggested that this approach was both safe and feasible [12]. An advantage of the ZFN approach is that it does not require the permanent expression of a foreign gene to generate HIV-1 resistance; however, even if it can be shown to be safe and efficacious, this therapy approach would only apply to HIV-1 infected individuals harbouring exclusively R5 virus. Cal-1 consists of autologous $CD4^+$ enriched T cells and HSCs transduced with a lentiviral vector expressing an shRNA targeting the CCR5 mRNA and a membrane anchored gp41 C peptide inhibitor of viral fusion. Such an approach could conceivably be effective against both R5 and X4 viruses as the peptide inhibitor can prevent the entry of both strains. However, a concern for the use of peptide

inhibitors is that they may be processed and presented to the adaptive immune system, which could result in clearance of the gene modified cells and lead to chronic immune activation [13].

While several completed and ongoing clinical trials have demonstrated the feasibility and safety of autologous HSC or $CD4^+$ T cell transplant for use in HIV-1 therapy, a broadly applicable efficacious approach has not yet been identified. In addition to advances in the clinical protocols, results from different studies suggest that better antiviral genes are needed to realize the potential for cell transplant to be used in HIV-1 therapy. Our general objective was to identify and characterize new ribozymes and siRNAs targeting HIV-1 RNA for development as antiviral genes. The following two sections discuss our results in relation to other studies and provide perspectives for these classes of antivirals in HIV-1 therapy.

5.3 Perspectives for ribozymes targeting HIV-1 RNA for HIV-1 therapy

Ribozymes targeting HIV-1 RNA were among the first antiviral genes tested in clinical studies, and remain the only agent tested in a phase II, vector-controlled trial for HIV-1 infection [10]. Although the failure to observe a significant antiviral effect in the phase II trial can partially be attributed to suboptimal engraftment of ribozyme expressing HSCs, the results also suggested that the ribozyme itself was not very active. The ribozyme used, called RRz2 in preclinical studies and OZ-1 as part of the murine retroviral vector (MMLV) used for its delivery in the clinic, was a hammerhead (HH) ribozyme targeting the overlapping tat/vpr coding sequence of HIV-1 RNA. One explanation for the weak antiviral activity of RRz2/OZ-1 could be related to the choice of the RNA Pol II MMLV LTR promoter to drive its expression in transplanted cells.

Evidence that greater stability and expression can be attained using RNA Pol III promoters was provided in the first clinical study comparing two individuals receiving ribozyme-expressing $CD4^+$ T cells [14, 15]; however, all other ribozymes that have been evaluated in clinical trials have been expressed from RNA Pol II promoters. In direct cell culture comparisons, Yu et al. showed that a Hairpin (Hp) ribozyme was a better inhibitor of viral replication when expressed from the RNA Pol III VA1 promoter compared to the MMLV LTR promoter and Puerta-Fernandez et al. demonstrated that ribozymes expressed from the RNA Pol III U6 promoter were more active compared to those expressed from both RNA Pol III $tRNA^{val}$ and RNA Pol II CMV promoters [16]. In our studies, we used the RNA Pol III H1 promoter to evaluate the effects of SOFA-HDV ribozymes on HIV-1 production in cell culture. Like the U6 promoter, the H1 promoter can be used to express therapeutic RNAs with minimal unintended RNA appended during transcription. These promoters have been extremely useful for the development of potent therapeutic shRNAs [17] and are likely to be the promoters of choice for future clinical trials evaluating ribozymes that target HIV-1 RNA. Further comparisons of the SOFA-HDV ribozyme identified in this thesis expressed from different RNA Pol III promoters will help establish which promoter is optimal for its expression and activity.

Another limitation that may have contributed to the low activity observed for RRz/OZ-1 is that HH ribozymes targeting HIV-1 RNA in general are weak inhibitors of HIV-1 replication. Indeed, using a quantitative co-transfection assay, Good et al. directly compared the effects of HH and Hp ribozymes expressed from the U6 promoter to Rev-binding RNAs expressed from the same promoter and showed that, compared to the Rev-binding RNAs, the inhibition provided by the ribozymes was quite modest [18]. To improve upon the activity of HH and Hp ribozymes,

several RNA conjugates have been explored. So far, the best results have been obtained for two U16 snoRNA-linked HH ribozymes targeting the 5'UTR and Pol coding sequence of HIV-1 RNA, identified from a large scale screen for accessible target sites in HIV-1 RNA [19]. It was proposed that the improvement of activity over previous ribozymes was a result of their localization to the nucleolus through the U16 snoRNA conjugation; however, protection of the ribozymes from exonuclease degradation may also have contributed to the high activity observed for these ribozymes. In addition to the effects of the conjugation, the identification of optimal target sites for these ribozymes with the use of a large-scale screen ensured that the target sites in HIV-1 RNA were highly accessible to their effects, and these two U16 snoRNA-linked ribozymes represent the top candidates for clinical evaluation.

In the methods and results presented in Chapters 2 and 3, we evaluated the potential for SOFA-HDV ribozymes targeting HIV-1 RNA to be developed as alternatives to HH and Hp ribozymes for HIV-1 therapy. The SOFA-HDV ribozyme was designed to improve the specificity of trans-cleaving ribozymes based on the HDV ribozyme motif, which binds to its target RNA with only seven base pairs [20, 21]. In addition to the 7 nt ribozyme domain, the SOFA module has an antisense domain called the biosensor and a short sequence called the blocker sequence, which is complementary to the ribozyme domain. In the absence of its target RNA, the ribozyme domain is inactivated through binding to the blocker domain and the high specificity of SOFA-HDV ribozyme catalysis has been demonstrated in vitro [22, 23]. A theoretical advantage of the SOFA-HDV ribozyme over HH and Hp ribozymes is that it is derived from a ribozyme that has evolved to function in human cells. Another potential advantage is that, in contrast to HH and Hp ribozymes, the SOFA-HDV ribozyme is double-stranded at its 5' and 3' ends, making it more

resistant to exonuclease degradation.

Previous results from our lab showed that SOFA-HDV ribozymes targeting the overlapping tat/rev coding sequence of HIV-1 RNA could be used to cleave HIV-1 RNA in vitro and inhibit HIV-1 production in cell culture [24]. Similar to results reported for HH and Hp ribozymes [18], the inhibition of HIV-1 production provided by the SOFA-HDV ribozymes was modest and they were not more active compared to their antisense controls. We postulated that, by evaluating a library of SOFA-HDV ribozyme candidates with different target sites in HIV-1 RNA, we could identify target sites that were accessible to SOFA-HDV ribozyme cleavage in cell culture. Out of 13 ribozymes targeting highly conserved target sites in the 5' UTR and Gag coding sequence of HIV-1 RNA, we identified one target site that was particularly accessible to a SOFA-HDV ribozyme (Figure 3.4) and had activity superior to its antisense control (Figure 3.5). The methods we developed to screen SOFA-HDV ribozymes described in Chapter 2 were similar to those used by Unwalla et al. to characterize the antiviral activity of the highly active U16 snoRNA-linked HH ribozymes targeting the 5'UTR and Pol coding sequence of HIV-1 RNA [19]. Although we could not observe as potent an activity for the SOFA-HDV ribozyme targeting the Gag coding sequence of HIV-1 RNA, its activity was superior to previously described unconjugated HH and Hp ribozymes and its ability to provide long term inhibition of HIV-1 replication in a T cell model (Figure 3.13) suggests that it may be an ideal ribozyme candidate for further development.

The ability of ribozymes to cleave their target RNA without the assistance of cellular proteins makes them excellent candidates for therapeutic development [25]. Data from clinical trials

conducted to date have so far suggested that anti-HIV-1 ribozymes can be expressed safely in patients undergoing both $CD4^+$ T cell transplant [26, 27] and HSC transplant [10, 28-30]. Results from different studies, including the work presented in this thesis, suggest that more active candidates can be designed with different promoter strategies, RNA conjugations, ribozyme motifs and screens for highly accessible target sites. Over the past several years major advances have been made in the use of humanized mouse models to evaluate both the safety and efficacy of candidate antiviral genes for $CD4^+$ T cell and HSC transplant clinical studies [31]. Although several new ribozyme candidates targeting HIV-1 RNA have been identified, they have not yet been evaluated in these models and further studies will be required to determine whether they can compete with other classes of antiviral genes for use in HIV-1 cell transplant therapy. The SOFA-HDV ribozyme we identified targeting the Gag coding sequence of HIV-1 RNA had good activity in cell culture compared to other candidates and appears to be stable and effective in long-term cell culture. Improvements in its design and expression may further enhance its clinical potential and it represents a promising candidate for gene therapy.

5.4 Perspectives for sh/siRNAs targeting HIV-1 RNA for HIV-1 therapy

Although the development of therapeutic sh/siRNAs targeting HIV-1 RNA began over a decade after the first ribozyme targeting HIV-1 RNA was published, the number of molecules reported in the literature has far exceeded that of ribozymes with over 750 sh/siRNAs evaluated in cell culture [32]. By using the cellular RNAi machinery, sh/siRNAs can provide a potent inhibition of gene expression and have been shown to have IC50 values of about 100-fold less than target matched ribozymes and antisense oligonucleotides [33]. Given their excellent efficacy profile,

several shRNAs have been evaluated in mouse models of HIV-1 cell transplant [34-38] and an shRNA targeting the tat/rev coding sequence of HIV-1 RNA has advanced to a clinical trial in combination with a CCR5 mRNA targeting ribozyme and a TAR decoy of the HIV-1 Tat protein [30]. A single lentiviral vector expressing three shRNAs targeting highly conserved sites in HIV-1 RNA was shown in long term cell culture to provide a durable inhibition of HIV-1 replication without the development of resistant virus [39], and this combination was recently shown to be safe and efficacious in a mouse model [34]. Among antiviral genes, shRNAs targeting HIV-1 RNA represent one of the most promising agents for use in cell transplant therapy and the identification of safe molecules with highly conserved and accessible target sites represents an important direction towards their use in effective therapeutic approaches.

An important consideration towards the selection of optimal shRNA target sites is that they are highly conserved across the majority of circulating HIV-1 strains. In the first study to use this criterion to identify shRNA target sites, ter Brake et al. calculated sequence conservation using 495 HIV-1 sequences, and identified 19 highly conserved regions in HIV-1 RNA [39]. Out of 86 shRNAs targeting these regions, about one in four was classified as active and out of these active candidates four were shown to provide long-term inhibition of HIV-1 replication in T cell lines [40, 41]. Three of these candidates were identified as safe in a mouse model of HSC transplant and have been proposed as an ideal combination for HIV-1 cell transplant therapy [34]. Using additional sequences to calculate conservation of shRNA target sites in HIV-1 RNA, McIntryre et al. proposed a new list of 96 candidate shRNAs for use in HIV-1 therapy, ranked by their sequence conservation and activity against HIV-1 production [42]. Although the top candidates evaluated in this study have not yet been directly compared in long term HIV-1 replication

studies or humanized mouse models, their results suggest that shRNA target sites with better sequence conservation compared to those identified in the ter Brake et al. study can be identified using more HIV-1 sequences to generate conservation estimates.

In Chapter 2, methods to calculate sequence conservation at the nt level are described. Using 1850 HIV-1 sequences with representatives from all major HIV-1 subtypes and CRFs a set of highly conserved SOFA-HDV ribozyme target sites were identified and evaluated in Chapter 3. Building on previously described methods [43, 44], the procedures we developed provide numerical data on the estimated conservation of each nt in HIV-1 RNA and can be used to eliminate potential antisense target sites that have a significant number of nt insertions in known HIV-1 sequences. Compared to previous studies that have screened HIV-1 RNA in 20 to 23 nt windows [39, 42, 45], these methods permit the comparison of potential target sites based on different nt positions in the target site. Since the SOFA-HDV ribozyme binds its target site in two adjacent regions, these methods were ideal for the identification of highly conserved SOFA-HDV ribozyme target sites. With reports that mismatches at certain nt positions in an shRNA target site differentially affect their activity [44, 46], these methods may also be ideal for future screens to identify shRNA target sites with optimal conservation.

In addition to high sequence conservation, it is also important that an shRNA target site is highly accessible. Results from our ribozyme screen suggested that a highly conserved target site in the Gag coding sequence of HIV-1 RNA was particularly accessible to a SOFA-HDV ribozyme (Figure 3.4) and we demonstrated that a potent shRNA could be designed targeting this sequence (Figure 3.7). According to our sequence conservation estimates at the nt level, this target site had

better conservation compared to the candidate currently in clinical trials targeting the tat/rev coding sequence of HIV-1 RNA [30] and had similar conservation to two target sites in the 5'UTR of HIV-1 RNA, identified among the top candidates reported in the McIntyre et al. study [42]. Our results also showed that, although the efficacy of the two shRNAs targeting the 5'UTR was similar, only one of these was able to provide a potent inhibition of HIV-1 production (Figure 3.7). These results highlight a limitation of previous screens, which used only one concentration of inhibitor to determine shRNA activity and did not consider the potency of the different candidates proposed [39, 42, 45]. Interestingly, the shRNA candidate targeting the 5'UTR, which we showed was highly potent, targets a site in close proximity to one of two target sites identified in a large-scale screen for snoRNA-linked HH ribozymes [19]. Results from this screen as well as our ribozyme screen suggest that highly accessible target sites in HIV-1 RNA are rare and that many of the shRNAs identified with high sequence conservation in previous screens may not have sufficient potency to permit their use at safe therapeutic levels.

To further characterise the potential for the shRNA candidate and ribozyme identified in our studies to be used safely in HIV-1 therapy, we evaluated their effects on mRNA expression in human cells. In agreement with our bioinformatics approach to eliminate target sites with similarities to sequences in the human transcriptome using the RiboSubstrates software [47], we did not identify any major changes in mRNA levels that could be attributed to either the ribozyme or shRNA (Figure 3.10). Since it has been shown that HIV-1 RNA can escape from si/shRNA inhibition by adopting a different structure [48], we also evaluated whether the structure of the target site we identified was conserved in diverse viral strains. Since the shRNA candidate was equally active in strains from diverse HIV-1 subtypes (Figure 3.9), our results

suggest that, in addition to its high sequence conservation, the target site we identified may also be structurally conserved. Together with its ability to provide a long-term inhibition of HIV-1 replication in a T cell model (Figure 3.13), our results suggest that the shRNA candidate we identified has a great potential to be used safely and effectively in combination gene therapy for HIV-1 infection and studies in mouse models are planned.

Advances in non-viral delivery methods have resulted in more than 50 RNA-based therapeutics entering clinical trials [49]. Although there has not yet been a clinical trial for HIV-1 infection, exogenous delivery of siRNAs to HIV-1 infected mice has been achieved [37, 38]. With recent advances in RNA delivery technologies [50-52], an oral formulation for siRNAs could conceivably be identified, opening up the field for a new class of antivirals to be used in cART. In Chapter 4, we designed several siRNAs targeting the attractive shRNA target site characterised in Chapter 3. Our results provided additional evidence that longer siRNAs that can serve as substrates for Dicer cleavage (Dicer substrate siRNAs, dsiRNAs) are more effective compared to their shorter siRNA counterparts [53-55]. We also showed that for our target site, a commonly used dsiRNA design was not long enough to observe an increase in siRNA potency. Our results highlight the importance of using empirical data to identify the best siRNA and shRNA format for further therapeutic development against a particular target site and could explain the failure of one study to demonstrate the superior potency of the dsiRNA design [56]. The results also demonstrate that shRNAs with 20-23 base pair stems and siRNAs with 27 to 29 nt sense strands are the optimal formats for further development of RNAi molecules targeting the identified site in the Gag coding sequence for use in gene or drug therapy, respectively.

5.5 Conclusions

Small RNAs have a great potential to be used for the treatment of HIV-1 infection as antiviral genes for cell transplant or as exogenously delivered agents for cART. HIV-1 RNA is an attractive target for the development of small RNAs such as ribozymes and shRNAs for development as highly specific therapeutics with a low potential to disturb cellular pathways. Both the structure and sequence diversity of HIV-1 RNA make it difficult to identify target sites for these classes of molecules and the work presented in this thesis describes the identification of an attractive antisense target site as well as the characterisation of a ribozyme and different shRNAs and siRNAs targeting it. In addition to identifying candidates for HIV-1 therapy the work presented has made several contributions to scientific knowledge and has added to the body of literature available on the development of RNA therapeutics specifically for HIV-1 and in general.

First, we described novel methods to calculate sequence conservation in HIV-1 RNA, which could be extremely useful for the design of new antisense candidates and could also be adapted for the design of molecules targeting other viral infections with significant degrees of sequence diversity in their genomes. Second, we show that the high sensitivity of the SOFA-HDV ribozyme to mismatches in its target site observed in vitro can also be observed in cell culture. These results contribute to our understanding of SOFA-HDV ribozyme mechanisms and support their further development as highly specific gene knockdown tools and therapeutic molecules. Third, we provide evidence that part of the mechanism responsible for an inhibition of HIV-1 production by shRNAs and ribozymes targeting HIV-1 RNA is related to an inhibition of intracellular Gag processing. These results could form the basis for additional studies exploring

mechanisms of antisense molecules targeting HIV-1 RNA to provide a better understanding of their effects and methods to enhance their activities. Fourth, our results highlight the importance of shRNA stem length and siRNA sense strand length on the activity of therapeutic sh/siRNAs and demonstrate that empirical data can be used to identify the best formats for therapeutic development.

To further develop the molecules identified in this thesis, we applied for and received proof of principle I funding from the Canadian Institutes of Health Research (CIHR) and submitted a full international co-operation treaty patent application to cover the intellectual property generated. Data obtained on our molecules suggest that they are among the top candidates for combination gene therapy and we have had discussions with researchers at different companies and academic institutions to test their efficacy and safety in combination with other molecules. The hope is that these studies will identify the optimal combination gene therapy approach for HIV-1 infection and ultimately lead to a safe and effective functional cure.

5.6 References

1. Deeks, SG, Autran, B, Berkhout, B, Benkirane, M, Cairns, S, Chomont, N, *et al.* (2012). Towards an HIV cure: a global scientific strategy. *Nat Rev Immunol* **12**: 607-614.
2. Xing, S, and Siliciano, RF (2013). Targeting HIV latency: pharmacologic strategies toward eradication. *Drug discovery today* **18**: 541-551.
3. Archin, NM, and Margolis, DM (2014). Emerging strategies to deplete the HIV reservoir. *Current opinion in infectious diseases* **27**: 29-35.
4. Shan, L, Deng, K, Shroff, NS, Durand, CM, Rabi, SA, Yang, HC, *et al.* (2012). Stimulation of HIV-1-specific cytolytic T lymphocytes facilitates elimination of latent viral reservoir after virus reactivation. *Immunity* **36**: 491-501.
5. Persaud, D, Gay, H, Ziemniak, C, Chen, YH, Piatak, M, Jr., Chun, TW, *et al.* (2013). Absence of detectable HIV-1 viremia after treatment cessation in an infant. *The New England journal of medicine* **369**: 1828-1835.

6. Saez-Cirion, A, Bacchus, C, Hocqueloux, L, Avettand-Fenoel, V, Girault, I, Lecuroux, C*, et al.* (2013). Post-treatment HIV-1 controllers with a long-term virological remission after the interruption of early initiated antiretroviral therapy ANRS VISCONTI Study. *PLoS pathogens* **9**: e1003211.
7. Yukl, SA, Boritz, E, Busch, M, Bentsen, C, Chun, TW, Douek, D*, et al.* (2013). Challenges in detecting HIV persistence during potentially curative interventions: a study of the Berlin patient. *PLoS pathogens* **9**: e1003347.
8. Younan, P, Kowalski, J, and Kiem, HP (2014). Genetically modified hematopoietic stem cell transplantation for HIV-1-infected patients: can we achieve a cure? *Mol Ther* **22**: 257-264.
9. Cannon, PM, Kohn, DB, and Kiem, HP (2014). HIV eradication--from Berlin to Boston. *Nat Biotechnol* **32**: 315-316.
10. Mitsuyasu, RT, Merigan, TC, Carr, A, Zack, JA, Winters, MA, Workman, C*, et al.* (2009). Phase 2 gene therapy trial of an anti-HIV ribozyme in autologous CD34+ cells. *Nature medicine* **15**: 285-292.
11. DiGiusto, DL, Stan, R, Krishnan, A, Li, H, Rossi, JJ, and Zaia, JA (2013). Development of hematopoietic stem cell based gene therapy for HIV-1 infection: considerations for proof of concept studies and translation to standard medical practice. *Viruses* **5**: 2898-2919.
12. Tebas, P, Stein, D, Tang, WW, Frank, I, Wang, SQ, Lee, G*, et al.* (2014). Gene editing of CCR5 in autologous CD4 T cells of persons infected with HIV. *The New England journal of medicine* **370**: 901-910.
13. Hoxie, JA, and June, CH (2012). Novel cell and gene therapies for HIV. *Cold Spring Harb Perspect Med* **2**: a007179.
14. Wong-Staal, F, Poeschla, EM, and Looney, DJ (1998). A controlled, Phase 1 clinical trial to evaluate the safety and effects in HIV-1 infected humans of autologous lymphocytes transduced with a ribozyme that cleaves HIV-1 RNA. *Hum Gene Ther* **9**: 2407-2425.
15. Kruger, M, Beger, C, and Wong-Staal, F (1999). Use of ribozymes to inhibit gene expression. *Methods Enzymol* **306**: 207-225.
16. Puerta-Fernandez, E, Barroso-del Jesus, A, Romero-Lopez, C, Tapia, N, Martinez, MA, and Berzal-Herranz, A (2005). Inhibition of HIV-1 replication by RNA targeted against the LTR region. *AIDS* **19**: 863-870.
17. Brummelkamp, TR, Bernards, R, and Agami, R (2002). A system for stable expression of short interfering RNAs in mammalian cells. *Science* **296**: 550-553.
18. Good, PD, Krikos, AJ, Li, SX, Bertrand, E, Lee, NS, Giver, L*, et al.* (1997). Expression of small, therapeutic RNAs in human cell nuclei. *Gene Ther* **4**: 45-54.
19. Unwalla, HJ, Li, H, Li, SY, Abad, D, and Rossi, JJ (2008). Use of a U16 snoRNA-containing ribozyme library to identify ribozyme targets in HIV-1. *Mol Ther* **16**: 1113-1119.
20. Bergeron, LJ, and Perreault, JP (2005). Target-dependent on/off switch increases ribozyme fidelity. *Nucleic Acids Res* **33**: 1240-1248.
21. Bergeron, LJ, Reymond, C, and Perreault, JP (2005). Functional characterization of the SOFA delta ribozyme. *RNA* **11**: 1858-1868.

22. Lévesque, MV, Rouleau, SG, and Perreault, JP (2011). Selection of the most potent specific on/off adaptor-hepatitis delta virus ribozymes for use in gene targeting. *Nucleic Acid Ther* **21**: 241-252.
23. Lévesque, MV, and Perreault, JP (2012). Target-induced SOFA-HDV ribozyme. *Methods Mol Biol* **848**: 369-384.
24. Lainé, S, Scarborough, RJ, Lévesque, D, Didierlaurent, L, Soye, KJ, Mougel, M*, et al.* (2011). In vitro and in vivo cleavage of HIV-1 RNA by new SOFA-HDV ribozymes and their potential to inhibit viral replication. *RNA Biol* **8**: 343-353.
25. Mulhbacher, J, St-Pierre, P, and Lafontaine, DA (2010). Therapeutic applications of ribozymes and riboswitches. *Curr Opin Pharmacol* **10**: 551-556.
26. Buchschacher, GL, Jr., and Wong-Staal, F (2001). Approaches to gene therapy for human immunodeficiency virus infection. *Hum Gene Ther* **12**: 1013-1019.
27. Macpherson, JL, Boyd, MP, Arndt, AJ, Todd, AV, Fanning, GC, Ely, JA*, et al.* (2005). Long-term survival and concomitant gene expression of ribozyme-transduced CD4+ T-lymphocytes in HIV-infected patients. *J Gene Med* **7**: 552-564.
28. Michienzi, A, Castanotto, D, Lee, N, Li, S, Zaia, JA, and Rossi, JJ (2003). RNA-mediated inhibition of HIV in a gene therapy setting. *Ann N Y Acad Sci* **1002**: 63-71.
29. Amado, RG, Mitsuyasu, RT, Rosenblatt, JD, Ngok, FK, Bakker, A, Cole, S*, et al.* (2004). Anti-human immunodeficiency virus hematopoietic progenitor cell-delivered ribozyme in a phase I study: myeloid and lymphoid reconstitution in human immunodeficiency virus type-1-infected patients. *Hum Gene Ther* **15**: 251-262.
30. DiGiusto, DL, Krishnan, A, Li, L, Li, H, Li, S, Rao, A*, et al.* (2010). RNA-based gene therapy for HIV with lentiviral vector-modified CD34(+) cells in patients undergoing transplantation for AIDS-related lymphoma. *Sci Transl Med* **2**: 36ra43.
31. Bennett, MS, and Akkina, R (2013). Gene therapy strategies for HIV/AIDS: preclinical modeling in humanized mice. *Viruses* **5**: 3119-3141.
32. Tyagi, A, Ahmed, F, Thakur, N, Sharma, A, Raghava, GP, and Kumar, M (2011). HIVsirDB: a database of HIV inhibiting siRNAs. *PLoS One* **6**: e25917.
33. Miyagishi, M, Hayashi, M, and Taira, K (2003). Comparison of the suppressive effects of antisense oligonucleotides and siRNAs directed against the same targets in mammalian cells. *Antisense Nucleic Acid Drug Dev* **13**: 1-7.
34. Centlivre, M, Legrand, N, Klamer, S, Liu, YP, Jasmijn von Eije, K, Bohne, M*, et al.* (2013). Preclinical in vivo evaluation of the safety of a multi-shRNA-based gene therapy against HIV-1. *Mol Ther Nucleic Acids* **2**: e120.
35. Ringpis, GE, Shimizu, S, Arokium, H, Camba-Colon, J, Carroll, MV, Cortado, R*, et al.* (2012). Engineering HIV-1-resistant T-cells from short-hairpin RNA-expressing hematopoietic stem/progenitor cells in humanized BLT mice. *PLoS One* **7**: e53492.
36. Anderson, J, Li, MJ, Palmer, B, Remling, L, Li, S, Yam, P*, et al.* (2007). Safety and efficacy of a lentiviral vector containing three anti-HIV genes--CCR5 ribozyme, tat-rev siRNA, and TAR decoy--in SCID-hu mouse-derived T cells. *Mol Ther* **15**: 1182-1188.
37. Zhou, J, Neff, CP, Liu, X, Zhang, J, Li, H, Smith, DD*, et al.* (2011). Systemic administration of combinatorial dsiRNAs via nanoparticles efficiently suppresses HIV-1 infection in humanized mice. *Mol Ther* **19**: 2228-2238.

38. Zhou, J, Neff, CP, Swiderski, P, Li, H, Smith, DD, Aboellail, T*, et al.* (2013). Functional in vivo delivery of multiplexed anti-HIV-1 siRNAs via a chemically synthesized aptamer with a sticky bridge. *Mol Ther* **21**: 192-200.
39. ter Brake, O, Konstantinova, P, Ceylan, M, and Berkhout, B (2006). Silencing of HIV-1 with RNA interference: a multiple shRNA approach. *Mol Ther* **14**: 883-892.
40. von Eije, KJ, ter Brake, O, and Berkhout, B (2009). Stringent testing identifies highly potent and escape-proof anti-HIV short hairpin RNAs. *J Gene Med* **11**: 459-467.
41. von Eije, KJ, ter Brake, O, and Berkhout, B (2008). Human immunodeficiency virus type 1 escape is restricted when conserved genome sequences are targeted by RNA interference. *J Virol* **82**: 2895-2903.
42. McIntyre, GJ, Groneman, JL, Yu, YH, Jaramillo, A, Shen, S, and Applegate, TL (2009). 96 shRNAs designed for maximal coverage of HIV-1 variants. *Retrovirology* **6**: 55.
43. DeYoung, MB, and Hampel, A (1997). Computer analysis of the conservation and uniqueness of ribozyme-targeted HIV sequences. *Methods Mol Biol* **74**: 27-36.
44. Lee, SK, Dykxhoorn, DM, Kumar, P, Ranjbar, S, Song, E, Maliszewski, LE*, et al.* (2005). Lentiviral delivery of short hairpin RNAs protects CD4 T cells from multiple clades and primary isolates of HIV. *Blood* **106**: 818-826.
45. Naito, Y, Nohtomi, K, Onogi, T, Uenishi, R, Ui-Tei, K, Saigo, K*, et al.* (2007). Optimal design and validation of antiviral siRNA for targeting HIV-1. *Retrovirology* **4**: 80.
46. Sabariegos, R, Giménez-Barcons, M, Tàpia, N, Clotet, B, and Martínez, MA (2006). Sequence homology required by human immunodeficiency virus type 1 to escape from short interfering RNAs. *J Virol* **80**: 571-577.
47. Lucier, JF, Bergeron, LJ, Brière, FP, Ouellette, R, Elela, SA, and Perreault, JP (2006). RiboSubstrates: a web application addressing the cleavage specificities of ribozymes in designated genomes. *BMC Bioinformatics* **7**: 480.
48. Westerhout, EM, Ooms, M, Vink, M, Das, AT, and Berkhout, B (2005). HIV-1 can escape from RNA interference by evolving an alternative structure in its RNA genome. *Nucleic Acids Res* **33**: 796-804.
49. Burnett, JC, and Rossi, JJ (2012). RNA-based therapeutics: current progress and future prospects. *Chem Biol* **19**: 60-71.
50. Zhou, J, Shum, KT, Burnett, JC, and Rossi, JJ (2013). Nanoparticle-Based Delivery of RNAi Therapeutics: Progress and Challenges. *Pharmaceuticals (Basel)* **6**: 85-107.
51. Costa, PM, Cardoso, AL, Mendonca, LS, Serani, A, Custodia, C, Conceicao, M*, et al.* (2013). Tumor-targeted Chlorotoxin-coupled Nanoparticles for Nucleic Acid Delivery to Glioblastoma Cells: A Promising System for Glioblastoma Treatment. *Mol Ther Nucleic Acids* **2**: e100.
52. Kim, T, Afonin, KA, Viard, M, Koyfman, AY, Sparks, S, Heldman, E*, et al.* (2013). In Silico, In Vitro, and In Vivo Studies Indicate the Potential Use of Bolaamphiphiles for Therapeutic siRNAs Delivery. *Mol Ther Nucleic Acids* **2**: e80.
53. Kim, DH, Behlke, MA, Rose, SD, Chang, MS, Choi, S, and Rossi, JJ (2005). Synthetic dsRNA Dicer substrates enhance RNAi potency and efficacy. *Nat Biotechnol* **23**: 222-226.
54. Rose, SD, Kim, DH, Amarzguioui, M, Heidel, JD, Collingwood, MA, Davis, ME*, et al.* (2005). Functional polarity is introduced by Dicer processing of short substrate RNAs. *Nucleic Acids Res* **33**: 4140-4156.

55. Snead, NM, Wu, X, Li, A, Cui, Q, Sakurai, K, Burnett, JC*, et al.* (2013). Molecular basis for improved gene silencing by Dicer substrate interfering RNA compared with other siRNA variants. *Nucleic Acids Res* **41**: 6209-6221.
56. Foster, DJ, Barros, S, Duncan, R, Shaikh, S, Cantley, W, Dell, A*, et al.* (2012). Comprehensive evaluation of canonical versus Dicer-substrate siRNA in vitro and in vivo. *Rna* **18**: 557-568.